Distribution Agreement

In presenting this thesis or dissertation as a partial fulfillment of the requirements for an advanced degree from Emory University, I hereby grant to Emory University and its agents the non-exclusive license to archive, make accessible, and display my thesis or dissertation in whole or in part in all forms of media, now or hereafter known, including display on the world wide web. I understand that I may select some access restrictions as part of the online submission of this thesis or dissertation. I retain all ownership rights to the copyright of the thesis or dissertation. I also retain the right to use in future works (such as articles or books) all or part of this thesis or dissertation.

Signature:

_____ _____

Elizabeth Grace H. Veatch Date

The Zooarchaeology and Taphonomy of Small Mammal Remains at Liang Bua, Flores, Indonesia

By

Elizabeth Grace H. Veatch
Doctor of Philosophy

Anthropology

Jessica C. Thompson, Ph.D.
Advisor

Melvin Konner, Ph.D.
Committee Member

Dietrich Stout, Ph.D.
Committee Member

Matthew W. Tocheri, Ph.D.
Committee Member

Accepted:

Lisa A. Tedesco, Ph.D.
Dean of the James T. Laney School of Graduate Studies

Date

The Zooarchaeology and Taphonomy of Small Mammal Remains at Liang Bua, Flores, Indonesia

By

Elizabeth Grace H. Veatch
B.A., University of Colorado at Boulder, CO, 2010
M.A., The George Washington University, DC, 2014

Advisor: Jessica C. Thompson, Ph.D.

An abstract of
a dissertation submitted to the Faculty of the
James T. Laney School of Graduate Studies of Emory University
in partial fulfillment of the requirements for the degree of
Doctor of Philosophy
in Anthropology
2021

Abstract

The Zooarchaeology and Taphonomy of Small Mammal Remains at Liang Bua, Flores, Indonesia
By Elizabeth Grace H. Veatch

The role of small mammals as a dietary resource for non-modern humans remains unclear. Depending on the method of capture, small mammals are generally considered uneconomical for hominins to pursue given their small body sizes and the estimated amount of effort required to obtain them. Conversely, small mammals are perceived as a profitable and accessible dietary resource for modern humans due to the development of more-complex technology (traps, snares, nets, etc.). This dissertation focuses on the small mammal assemblage from Liang Bua, an archaeological cave site on the Indonesian island of Flores, to gauge how an anatomically archaic hominin species (*Homo floresiensis*) and modern humans (*Homo sapiens*) obtained and consumed rodents of various body sizes (~50 – 3500 g).

Using taphonomy, ethnoarchaeology, and stable isotope analyses to test how small mammal subsistence strategies varied between these two hominin species and also between two modern human subsistence lifestyles (foraging and agriculture), this dissertation aims to: (1) determine the relative proportion of small mammal remains at Liang Bua accumulated by hominin versus non-hominin agents; (2) evaluate how local hunting and consumption of small mammals manifest as bone surface modifications to aid in taphonomic identifications from archaeological remains; and (3) identify the habitat preferences of these small mammals to gauge the ecological habitats from which the various accumulating agents (e.g., hominins, raptors, etc.) were selecting their prey.

This dissertation is composed of seven chapters, including an introduction to the context and questions addressed in this dissertation (chapter 1); background to paleoanthropological research at Liang Bua (chapter 2); theoretical review and considerations for interpreting small mammal zooarchaeological assemblages (chapter 3); ethnoarchaeological and experimental studies involving human and avian subjects that help identify taphonomic limitations for small mammal analyses (chapter 4); carbon and oxygen stable isotopic analyses on small mammal subfossil samples from Liang Bua to gauge paleoecological settings and changes through time (chapter 5); a taphonomic and zooarchaeological study using the abundant murine fossil assemblage at Liang Bua to gauge how and the degree to which *H. floresiensis* and *H. sapiens* consumed murines during different temporal and ecological contexts (chapter 6); and the conclusions, which highlight the results of the dissertation and their importance for understanding the contribution of small mammals in hominin diets at Liang Bua (chapter 7).

The Zooarchaeology and Taphonomy of Small Mammal Remains at Liang Bua, Flores, Indonesia

By

Elizabeth Grace H. Veatch
B.A., University of Colorado at Boulder, CO, 2010
M.A., The George Washington University, DC, 2014

Advisor: Jessica C. Thompson, Ph.D.

A dissertation submitted to the Faculty of the
James T. Laney School of Graduate Studies of Emory University
in partial fulfillment of the requirements for the degree of
Doctor of Philosophy
in Anthropology
2021

Acknowledgments

I would like to express my deepest appreciation to my committee for their invaluable guidance and insightful suggestions that greatly improved the writing and work presented in this dissertation. I also would like to extend my sincerest thanks and appreciation towards my advisor, Jessica Thompson, whose expertise was crucial in developing the methodology and overall approach to the dissertation. I am also grateful to Dietrich Stout and Melvin Konner for their continuous support and encouragement throughout my graduate career at Emory University.

I am also extremely grateful to committee member and mentor Matt Tocheri for his unwavering support over the years. His thoughtful advice, encouragement, and belief in my abilities was instrumental in completing this work. Special thanks also to Kristofer Helgen for his support and mentorship, as well as the endless discussions on murine evolution, systematics, and behavior.

I also wish to extend my gratitude to the institutions and research teams that made the research presented in this dissertation possible. Thank you to I Made Geria, E. Wahyu Saptomo, and Jatmiko from Pusat Penelitian Arkeologi Nasional (Arkenas) in Jakarta, Indonesia, and Thomas Sutikna (University of Wollongong) for their support and access to archaeological material for study and analysis. Thank you to Joe Mendelson and the Zoo Atlanta staff for allowing access to avian and reptilian animals for conducting experimental taphonomic studies. Thank you to Tosha Dupras from the University of Central Florida for your guidance, expertise, and contribution of sample preparation for stable isotope analysis. Finally, thank you to all members of the Liang Bua research team for your support, discussions, and encouragement throughout this process, including Thomas Sutikna, Jatmiko, E. Wahyu Saptomo, I Made Agus Julianto, Nico Alamsyah, Sekar Rizqy Amallia Ramadhani, Bert Roberts, Zenobia Jacobs, Sam Lin, and many others who have contributed to Liang Bua scholarship. Special thanks to Rokus Due Awe (deceased)

for his work in identifying and curating the hundreds of thousands of faunal skeletal elements and for his time spent handwriting thousands of bag labels. His unwavering efforts were fundamental for this and all future research on the Liang Bua faunal collections.

Saya ucapkan terimakasih kepada anggota tim ekskavasi Liang Bua dari Teras, Bere Barat, Bere, dan Golo Manuk, khususnya kepada Kamelus Nampung dan Stanis Mbembak yang telah berbagi semangat dan pengetahuannya tentang berburu tikus. *I am extremely grateful to members of the Liang Bua excavation team from Teras, Bere, and Golo Manuk, with special thanks to Kamelus Nampung and Stanis Mbembak for sharing their enthusiasm for and knowledge on rat hunting.*

I would also like to extend my deepest gratitude to Hanneke Meijer, Rebecca Biermann Gürbüz, Paige Madison, and Kate McGrath for their unconditional friendship and encouragement. Special thanks to Hanneke Meijer for her edits and suggestions, as well as her guidance and mentorship over the years. Thank you for being an outstanding female academic role model and for introducing me to Indonesian culture back in 2015. Thank you to Paige Madison for your incredible insight into the history of paleoanthropology and sharing in the many adventures abroad over the years. Thank you to Rebecca Biermann Gürbüz and Kate McGrath for the endless intellectual discussions on paleoanthropology and late night brainstorming of future research projects.

Thank you to Emory University's Department of Anthropology staff, faculty members (current and former), and graduate student body (current and former) for their guidance and support. Thank you also to Yale University's Department of Anthropology for allowing me to be part of their academic family during the final stages of my graduate career.

I would also like to thank the granting agencies that directly funded this dissertation research, including the National Geographic Society Early Career Grant (EC-

214R-18), National Science Foundation (1830816), Wenner-Gren Foundation, and the Philanthropic Educational Organization (PEO) Scholar Award.

Special thanks to the food service and food delivery industry for providing much needed sustenance during the final stages of writing this dissertation while in a global pandemic.

Dedication

To Gigi, mom, and dad for their unconditional love and support.

Contents

List of Figures

List of Tables

Chapter 1

Dissertation Introduction

"Enak sekali" (*Very delicious*) remarked one participant as he chewed on the bones of a giant rat. The night before, a group of villagers from the small Manggarai hamlet of Teras (Flores, Indonesia) had hunted for small wild animals and were now enjoying the fruit of their hunt. Several animals had been caught that night, including a giant rat (called "betu" in the Manggarai language) and a young macaque that were currently roasting over an open fire pit. On Flores, hunting betu and other smaller animals forms a small part of a diet comprising mainly of agricultural and domesticated resources. While rat hunting is mostly considered a leisurely activity today—"hanya untuk bersenang-senang" (*Just for fun*)—hunting and consuming rats may have more ancient roots on the island of Flores.

For what may be perceived to some as an odd dietary choice, rat comprises a large proportion of meat consumption in many agricultural and rural communities of South and Southeast Asia, including in Indonesia (Harrison et al., 2016). This behavior is often practiced in the form of pest control where farmers will opportunistically kill and consume rodents that forage in agricultural rice fields (Fiedler, 1990; Suwannarong and Chapman, 2014; Suwannarong et al., 2015). In addition, foraging communities, such as the Adi of northern India and Bofi from Central African

Republic, regularly consume rats, such as various *Rattus* sp. in India and the giant pouched rats (*Cricetomys gambianus*) in Central Africa, respectively (Landt, 2007; Meyer-Rochow et al., 2015). While rat consumption is observed worldwide among urban, rural, and foraging communities (Andrade and Fernández, 2017; Estioko-Griffin and Griffin, 1981; Landt, 2004; Yellen, 1991b,a), its origin and occurrence within the diets of other hominin species remains unknown.

Hominin diets and small mammals

Diet in all organisms is mediated through both biological adaptations and foraging behaviors. In humans, the use of innovative technologies to acquire dietary resources has been of anthropological interest since Darwin asserted that early humans used stone tools to hunt large game (Darwin, 1871). Scholarship centered on "meat-eating" has since been used to explain the evolution of large brains, technology, and complex social systems using energetic models and optimal foraging theory (Smith et al., 1983; Kurland and Beckerman, 1985; Shipman, 1986; Stanford, 1996; Clark, 2011; Thompson et al., 2019; Pobiner, 2020). The combination of tool use with the targeting of large prey and subsequent food-sharing practices, for example, forms part of a complex behavioral repertoire used to satisfy both the caloric and nutritional needs of earlier hominin populations while also building social cohesion and complexity (Rayne et al., 2013).

Due to the body sizes of large mammals and the relatively high preservation rates of their skeletal remains, an understandable focus on these taxa has been fundamental in investigations of the evolution of hominin diets (Kaplan et al., 2009; Speth, 2010). For example, the earliest physical evidence of large mammal consumption by ancient hominins extends back to at least ~2.6 Ma (million years ago) and possibly back to 3.4 Ma in East Africa (McPherron et al., 2010; Domínguez-Rodrigo et al., 2005) and is theorized to have contributed to significant changes in hominin biological and

behavioral evolution. These changes involve life history, technological innovations, and social coordination and cooperation that would have increased access to the food energy necessary for a relatively large brain while concomitantly resulting in a reduction of the gastrointestinal tract (Thompson et al., 2019; Kaplan et al., 2009; Anton et al., 2014; Aiello and Wheeler, 1995). Termed the human niche (Fuentes, 2015; Kaplan et al., 2000) and the human predatory pattern (Thompson et al., 2019), increasing evidence suggests that regular exploitation of large game by ~2.0 Ma was likely one of several interrelated adaptations creating a recursive effect on evolution within the genus *Homo* (Anton et al., 2014; Kaplan et al., 2009; Ferraro et al., 2013). Exploitation of marine and aquatic resources at 1.95 Ma at Koobi Fora, Kenya (Braun et al., 2010), and small terrestrial mammals at 1.73 Ma at Oldupai Gorge, Tanzania (Fernandez-Jalvo et al., 1999) further suggests that the calorie and nutrient-rich diets of early *Homo* in eastern Africa required diverse and flexible foraging strategies necessary for maintaining an increasingly complex ecological, biological, and social niche.

The incorporation of small mammals specifically—defined as any mammalian taxa weighing less than 5 kg (Brain, 1981; Andrews, 1990)—within hominin diets is largely considered uneconomical and has traditionally been viewed as a sign of environmental stress, depression, or instability (see review in Zeder (2012)). As a byproduct of popular diet breadth models deriving from optimal foraging theory and behavioral ecology, Paleolithic foragers aiming to maximize caloric intake are expected to collect high ranking resources, such as ungulates and other larger-bodied prey items, to balance energetic foraging returns (Kurland and Beckerman, 1985; Pyke, 1984; Burger et al., 2005). Depending on the abundance, distribution, and profitability of prey items based on hunting technology, smaller animals may be considered a valuable resource, but rarely in the presence of other large-bodied animals or when procured individually as this strategy is considered energetically costly (Lupo and Schmitt,

2005). This interpretation has largely been supported by a relative increase in small fast prey items (e.g., leporids, birds, etc.) at Upper Paleolithic sites (beginning ~40,000 years ago) in regions like Spain and the eastern Mediterranean during periods of environmental fluctuations when food availability was likely low (Smith et al., 1983; Winterhalder and Kennett, 2006; Hawkes and O'Connell, 1992). The procurement of large quantities of smaller difficult-to-catch prey items in the past suggested a variety of behavioral and cultural circumstances, including potential use of biodegradable traps or snares (Wadley, 2010; Hoffecker and Hoffecker, 2017; Dewar et al., 2006), demographic pressures, and/or climatic shifts (Stiner et al., 1999; Stiner, 2001, 2002).

Due to this expanding diet breadth to include smaller prey items within Upper Paleolithic sites, large quantities of small mammals tends to be associated with modern human technology, subsistence patterns, and foraging strategies: "modern humans appear to have quickly developed new practices of subsistence ... that required the investment of additional effort to out compete the indigenous Neanderthals by extracting more calories from their environment" (187) (Conard et al., 2013). It was therefore interpreted that capturing large quantities of small mammals required advanced cognitive abilities not present in hominins other than *H. sapiens*, and that the presence of small mammal remains within archaeological contexts reflected a certain biocultural and technological capability by the hominins responsible for their procurement (Wynn and Coolidge, 2008).

Recent taphonomic studies on leporid (rabbits and hares) remains spanning the Middle Paleolithic from the western Mediterranean region suggest that *Homo* sp. also incorporated small and fast prey items in addition to ungulates during substantial periods of environmental fluctuations (Morin et al., 2019; Blasco et al., 2019; Serra and Peris, 2008; Cochard et al., 2012). A considerable underestimation of consuming leporids, birds and other smaller animals by Middle Paleolithic hominins challenged the perception of a narrow diet for Neanderthals, along with the social and technological

implications, while also raising important issues regarding variation in diet breadth prior to the Upper Paleolithic. For example, varying degrees of leporid consumption at Gran Dolina TD10–1 and Bolomor Cave suggests that early Neanderthals were (1) engaging in highly plastic foraging techniques to accommodate for fluctuating environmental and occupational densities and (2) knowledgeable of the environment and had an objective understanding of animal prey behavior (Blasco et al., 2013). However, the degree of small mammal exploitation in the Middle Paleolithic dwarfs in comparison to the densities of leporid remains in the Upper Paleolithic, and thus, small mammal exploitation by Neanderthals may more adequately reflect population densities and/or foraging patterns rather than evidence of complex cognition or environmental stress (Morin et al., 2019).

The incorporation of small animals within the diets of other Pleistocene hominin groups are even less well known. At Zhoukoudian locality 1 dated to ~0.78 Ma in China, large amounts of charred rodent material recovered in deposits associated with dense *H. erectus* occupations suggests that small mammals may have been hunted in addition to large game, such as young rhinoceroses and large megacerine deer (Shen et al., 2009; Aigner, 1981). While taphonomic studies at African *H. erectus* sites demonstrate regular exploitation of meat and marrow from larger herbivores (Monahan, 1996; Pickering and Carlson, 2004; Pobiner et al., 2008; Domínguez-Rodrigo et al., 2009b; Pante, 2013), it's unclear how African, as well as Asian and Southeast Asian *H. erectus*, incorporated small mammals as part of their diet and the circumstances under which smaller animals were or were not exploited.

Interestingly, hominin subsistence strategies involving small mammals have been paradoxically posited as both a hallmark of modern human (or at least relatively complex) behavior (Stiner et al., 1999; Stiner, 2002) as well as a common dietary resource during earlier stages of hominin evolution (Stanford, 1996, 2012). The former position argues that small mammals only became a higher ranked resource during the

Upper Paleolithic when the use of traps and other technologies began to outweigh the energetic costs required to capture small, fast prey (as discussed above) (Stiner et al., 1999, 2001; Wadley, 2010; Hoffecker and Hoffecker, 2017). This evidence also suggests that modern humans were probably driven to exploit small game to reduce niche overlap with competitors, such as Neanderthals and hyenas (Hoffecker, 2009).

Conversely, small-brained hominins may also have been adept at acquiring small game (Stanford, 1996, 2012; Domínguez-Rodrigo and Pickering, 2017). In some chimpanzee populations, cooperative hunting and meat-eating are observed and these behaviors are interpreted by some as synapomorphic traits between humans and chimpanzees that were likely part of the adaptive strategies of early hominins (Stanford, 2012). Assuming that early hominins such as *Ardipithecus* shared a similar behavioral ecology as that of living chimpanzees (Stanford (2012) but see Sayers et al. (2012)), this model suggests that early hominins were already skilled at hunting small prey prior to the development of traps and snares found otherwise only in "modern" technologies. These competing ideas posit two very different prey ranking structures for small mammals. Either small mammals are only energetically profitable after the development of complex technologies and social coordination associated with advanced cognition, or acquiring small prey has been profitable for early hominins since prior to the splitting of the *Pan–Homo* clade.

Understanding the energetic benefit from acquiring small game is challenging, in part because the ecological variation observed within this broad category results in potentially quite different search and capture strategies (Lupo and Schmitt, 2002, 2005). For example, Yellen (1991b,a) ethnoarchaeological studies of small mammal hunting among the !Kung San show hunters employing various foraging strategies (e.g., by hand, run down, ambush) and hunting technologies (e.g., stick, traps, snares, bow and arrow) to target small mammalian prey based on the behavioral ecology of the animal (also observed in Central African Bofi and Aka forest foragers, see Lupo and Schmitt

(2005)). This variety in strategy and technique is probably because, as a resource group, small mammals are extremely diverse both taxonomically and behaviorally and they inhabit a wide range of ecological habitats (Andrews, 1990). Traditionally, taxonomic variation within small mammal assemblages is used for reconstructing past habitats of animals preserved at archaeological or paleontological sites (Reed, 2003); but because of variation in habitat preferences, predator evasion strategies, and activity patterns, small mammal assemblages also have under-exploited potential to reveal that other hominins also used diverse acquisition strategies to capture small mammals (Lupo and Schmitt, 2005). Although this suggests a long history of small mammal consumption by hominins, targeted research is needed to understand the contribution of these prey to the diets of various hominin taxa, as well as the behavioral and possibly technological skills or anatomical adaptations necessary to successfully target small prey.

The relatively little evidence for small mammal consumption by non-Upper Paleolithic hominins is likely due to a combination of taphonomic, research, recovery, and recognition biases that influence our understanding of hominin subsistence behaviors. Unfortunately, a paucity of archaeological sites with clear evidence of small game consumption by one or multiple hominin groups has limited opportunities to test the circumstances for which small mammal consumption may have been profitable by other hominins, especially in comparison to *H. sapiens*, until now.

An abundant small mammal assemblage with approximately 223,000 identified small mammal specimens recovered from archaeological excavations at Liang Bua (Sutikna et al., 2018) offers a unique opportunity to directly test if and how *H. sapiens* and *H. floresiensis* incorporated small mammals into their respective diets. Located on the oceanic island of Flores along the eastern Indonesian archipelago (Figure 1.1), Liang Bua preserves evidence of three distinct periods of hominin activity during the past ~190 thousand years (ka): the small-brained and small-bodied *H.*

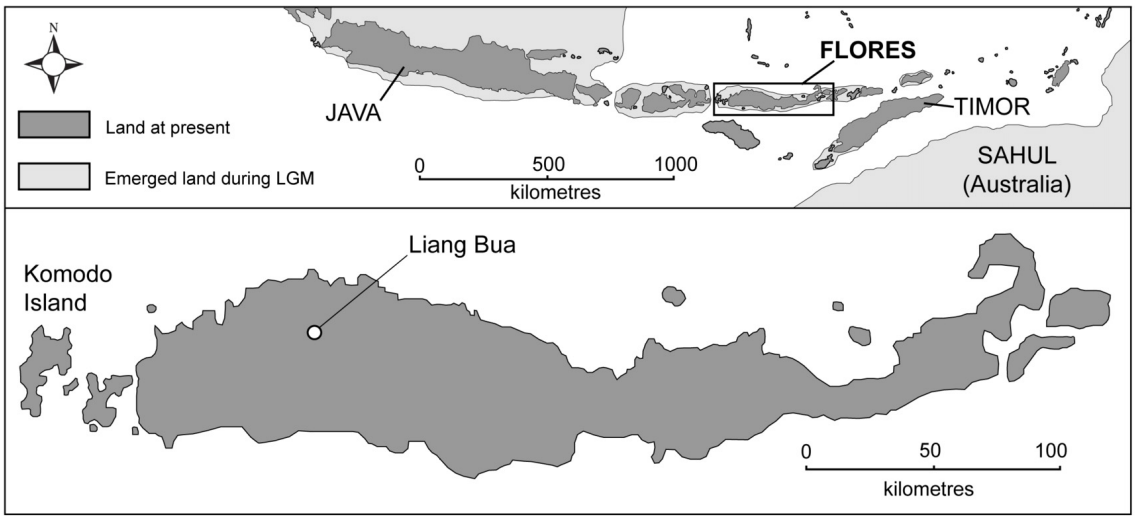

Figure 1.1: *Above*. The location of Flores island along the Indonesian archipelago in Island Southeast Asia. *Below*. The location of Liang Bua on the island of Flores.

floresiensis (~190 – 50 ka), foraging *H. sapiens* (~46 – 3 ka), and agriculturalists (~3 ka to present day) (Brown et al., 2004; Morwood et al., 2005; Sutikna et al., 2018; Sutikna, 2016; Sutikna et al., 2016). These three distinct temporal intervals are used to test hypotheses about hominin behavior as it relates to small mammal exploitation between two hominin species (*H. floresiensis* and *H. sapiens*) and among two subsistence strategies (foraging and agriculturalism). By combining ethnoarchaeological, experimental, geochemical, and taphonomic data and analyses, this dissertation investigates if, how, and the degree to which hominins at Liang Bua incorporated small mammals into their diets within the past ~190 ka interval.

1.1 Goals and Aims of the Dissertation

The goals of this dissertation are oriented around the question of small mammal accumulation and utilization by *H. sapiens* and *H. floresiensis* at Liang Bua, as well as to expand upon observational and experimental taphonomic studies of human and avian agents. Thus, the succeeding chapters described below address the following questions:

1. How can theoretical frameworks like niche construction theory contribute to our understanding of hominin foraging behaviors?

2. What are the defining features that distinguish between human and avian agents within a small mammal faunal assemblage?

3. Are the murine rodent skeletal remains from the Middle to Late Pleistocene and Holocene deposits at Liang Bua the result of human or avian agents, or a mixture of both?

4. How do the foraging strategies employed by *H. floresiensis* (~190 –60 ka) and *H. sapiens* (~18 ka –present) compare with one another and how do any similarities or differences in behavior relate to the specific environmental and ecological contexts of these temporal intervals?

Using a combination of theoretical (Chapter 3), experimental (Chapter 4), paleoecological (Chapter 5), and zooarchaeological (Chapter 6) approaches, the following hypotheses on small mammal accumulation by *H. sapiens*, *H. floresiensis*, and avian predators are tested under the assumption that hominins rank small mammals based on body size to meet their foraging goal of reducing net energetic costs while acquiring as many calories as possible:

Null hypothesis: *All small mammal remains were the result of natural deaths.* Several of the Flores murine species will frequently burrow, spending a significant amount of time underground (Musser, 1981). Support for this null hypothesis would result in an absence of bone modification by raptors and/or hominins and would suggest that the small mammal assemblage was deposited by processes independent of predatory activity.

Alternative hypothesis 1: *All small mammal remains at Liang Bua were accumulated through avian predators.* The most common agents of small mammal accumulations in cave environments are roosting raptors (e.g., owls) that frequently deposit pellets containing digested bone (Andrews, 1990). This process creates specific

taphonomic features on the bone surface in the form of gastric etching, fragmentation patterns, and enamel erosion, that distinguishes these bones from those accumulated by other agents, such as hominins (Andrews, 1990; Landt, 2007). Failure to reject this hypothesis would suggest (1) that the rats around Liang Bua were too low ranked for hominins to expend energy acquiring and/or processing them, or (2) hominins were exploiting an ecological and/or cultural niche that did not involve subsiding on small terrestrial mammals at Liang Bua. Identifying taphonomic signatures of hominin activity (e.g., cutmarks, human tooth marks, and fragmentation from butchery) within the Liang Bua murine assemblage will result in rejection of this alternative hypothesis and support for one or more of the alternatives listed below.

Alternative hypothesis 2 (~190 – 60 ka): *Under this alternative hypothesis,* H. floresiensis *incorporated high ranking small mammals (i.e., giant rats) into their diets using simple technology in order to reduce niche overlap with other scavenging predators.* Evidence that small murines were incorporated into their diet would suggest that *H. floresiensis* engaged in more complex behavior in order to capture small, fast prey (See Wadley (2010)). While the large-bodied herbivore *Stegodon florensis insularis* (a likely grazer) was available to *H. floresiensis* during this temporal interval, competition with other scavenging predators (i.e., Komodo dragons, giant marabou storks, and vultures) for this resource, which may have been highly ranked because of its large body size, was likely high and risky. This would likely cause pressure for *H. floresiensis* to expand prey choice and diet breadth to include giant-sized murines like the forest-dwelling *Papagomys*, especially ones larger in body mass (e.g., ~1–2 kg). Incorporating these animals into their diet would also suggest that *H. floresiensis* exploited forested environments in addition to grasslands (in pursuit of *Stegodon*). In the absence of fire, *H. floresiensis* most likely processed small mammals through a series of skinning and disarticulating activities that are likely to leave distinctive marks on the bone surface.

Alternative hypothesis 3 (~18 – 3 ka): *Modern human foragers incorporated rats of various body sizes into their diet using technologies unavailable to* H. floresiensis. In the absence of any higher ranked sources of animal protein available to modern human foragers during this time (i.e., *Stegodon* or introduced, non-endemic mammals), all previous ranks for rats surrounding Liang Bua would be raised. The disappearance of giant marabou storks and vultures at ~50 ka also suggests minimal competition for these food items (i.e., only owls and potentially Komodo dragons). This would most likely result in a broad diet containing a variety of rodent taxa representing diverse habitats. To be made profitable enough for capture, foragers potentially utilized other advanced technologies (i.e., nets and traps/snares) to lower search and handling costs of small murines (Wadley, 2010). This would result in a greater abundance and diversification of small mammals during this time interval. While the complexity of stone artifacts is comparable to those associated with *H. floresiensis*, the change in raw material preferences suggests a potential change in resource use that might affect how foragers foraged on the landscape (Sutikna, 2016; Sutikna et al., 2018). The clear presence of intentional fire-use at ~41 ka and after also suggests that foragers were further reducing processing costs (Morley et al., 2017).

Alternative hypothesis 4 (~3 ka to present): *As agricultural practices emerged, agriculturalists continued to incorporate higher ranking giant murines into their diet but at a lower frequency compared to foragers.* During this time interval, modern humans had access to other higher-ranked resources (e.g., introduced mammals such as pigs, macaques, porcupines, and civets) and alternative subsistence pathways (e.g., agriculture) that would have reduced the demand for hunting endemic small mammals (van den Bergh et al., 2009; Sutikna et al., 2020; Lin et al., 2020). Moreover, the stone artifact assemblage shows a marked decline in the use and production of stone artifacts signaling a shift in human occupation and use of the cave to elsewhere on the landscape for food production and management (Lin et al., 2020). The presence

of adzes could also indicate other biodegradable technologies used for farming and/or hunting techniques that would lower the cost to capture endemic rats (Moore et al., 2009; Sutikna, 2016). Thus, this broadening of the diet using domesticated resources is predicted to result in an exclusion of low ranking endemic small-bodied murines and fewer high ranked large-bodied murines. Processing behaviors would also likely include fire-use to reduce handling costs.

1.1.1 Chapter Summaries

Dissertation structure: This dissertation is written in a four paper format with the intention of submitting each paper to a peer-reviewed journal. In addition to these free standing chapters, a separate introduction, background, and conclusion chapter to the dissertation are included to provide context and implications for hominin foraging behavior at Liang Bua.

Chapter 2 provides a background to archaeological research at Liang Bua, including a brief history of the hominin and faunal activity recorded at the site that establishes the archaeological and temporal context for this research. An overview of the phylogenetic, morphological, and behavioral debates surrounding *H. floresiensis* is discussed to provide context for the research questions, results, and interpretations. The faunal and temporal record are also discussed in detail to provide a background to the current understanding of zooarchaeology at Liang Bua, with a particular focus on the rats of Flores. Finally, a brief discussion regarding the possible dietary behaviors of *H. floresiensis* is provided as a prelude to the research presented in this dissertation.

Chapter 3 provides a theoretical overview of the most frequently used theorems for interpreting human foraging behavior in the archaeological record. Optimal foraging theory (OFT) and niche-construction theory (NCT) are specifically contrasted against one another to argue in favor of a more nuanced approach to interpreting

faunal data. An agent-based decision model utilizing features of both OFT and NCT is presented and tested using Liang Bua as a case example. This paper was published by the journal *Evolutionary Anthropology* as part of a special issue on the Extended Evolutionary Synthesis in Archaeology. Erik Ringen and Megan Beney from Emory University, USA, and Jatmiko from Pusat Penelitian Arkeologi Nasional, Indonesia contributed to the paper as co-authors.

Chapter 4 presents one ethnoarchaeological study and one observational study, both of which involve the consumption of small mammals by humans and/or avian agents to provide a comparative basis for evaluating the taphonomy of small mammal remains from archaeological sites. The ethnoarchaeological study involves individuals from Teras (Flores, Indonesia) who voluntarily provided the bones of small animals after they were butchered and processed to explore how anthropogenic traces are recorded on rats and other small mammals from Flores. The observational study involves a controlled feeding experiment where rats of various body sizes were fed to eagle owls (*Bubo lacteus*), king vultures (*Sarcoramphus papa*), and Lappet-faced vultures (*Torgos tracheliotos*) to test whether prey body size affects the taphonomic signature of the predator. A taphonomic analysis on both experimental assemblages was conducted to assist in differentiating avian from human consumption when diagnostic evidence, such as signs of digestion or cutmarks, is absent.

Chapter 5 focuses on exploring the paleoecology of different stratigraphic units using $\delta^{13}C$ and $\delta^{18}O$ stable isotopes from carbonate to determine the local ecological context at Liang Bua through time. A previous paleoecological study using the relative abundance of murine body sizes suggested that Liang Bua was exposed to more-open landscapes from ~190 – 60 ka while *H. sapiens* were exposed to more-forested environments (Veatch et al., 2019). This study tests this hypothesis by reconstructing the diets of murine fauna at Liang Bua at different temporal intervals to understand (1) the dietary preferences of murine species at Liang Bua, and (2)

the availability of local resources. Results from this study are used in combination with taphonomic results from Chapter 6 to interpret hominin foraging behavior and environmental exploitation by hominins at Liang Bua.

Chapter 6 is a comprehensive taphonomic and zooarchaeological study using murine skeletal remains to explore how and the extent to which hominins incorporated small mammals into their diets at Liang Bua. Standard taphonomic data, including skeletal element patterns, breakage and fragmentation patterns, and bone surface modifications were collected and analyzed according to stratigraphic unit, murine species, and murine body sizes. Post-depositional data were also collected to control for damage caused by non-predatory processes. The results are used to estimate the relative contribution of predatory agents responsible for the murine faunal assemblage at Liang Bua and to compare the foraging patterns on the small mammal community by *H. floresiensis*, foraging *H. sapiens*, and agriculturalists.

Chapter 7 concludes the dissertation with a discussion on the results presented in chapters 3 through 6. The diets of *H. sapiens* and *H. floresiensis* involving small mammals at Liang Bua are further discussed with implications for the role of small mammals as a dietary resource, and the importance of small mammal zooarchaeological research to the study of hominin evolution.

Chapter 2

Hobbit Holes: A Review of *Homo floresiensis* and Liang Bua Research

Liang Bua is an archaeological limestone cave site located on the island of Flores along the Indonesian archipelago (Figure 2.1). The site contains deep and complex stratified deposits with stone artifacts and faunal remains that date to within the past ~190 ka (thousand years) ago (Sutikna et al., 2016; Roberts et al., 2009). Initial excavations were conducted by Fr. Theodor Verhoeven, Ph.D., in 1965 and revealed several Neolithic modern human burials with grave goods in the western part of the cave (Morwood et al., 2009). Continued excavations by Professor Raden Soejono, an Indonesian archaeologist and former Director of the National Research Centre for Archaeology in Indonesia (Pusat Penelitian Arkeoologi Nasional, or Arkenas for short) during the late 1970s and 1980s recovered additional modern human burials with grave goods and sampled a sequence of matereial culture and faunal remains that extended back as far as the early Holocene (Morwood et al., 2009). Liang Bua was clearly a promising and important location for Indonesian pre-history that could

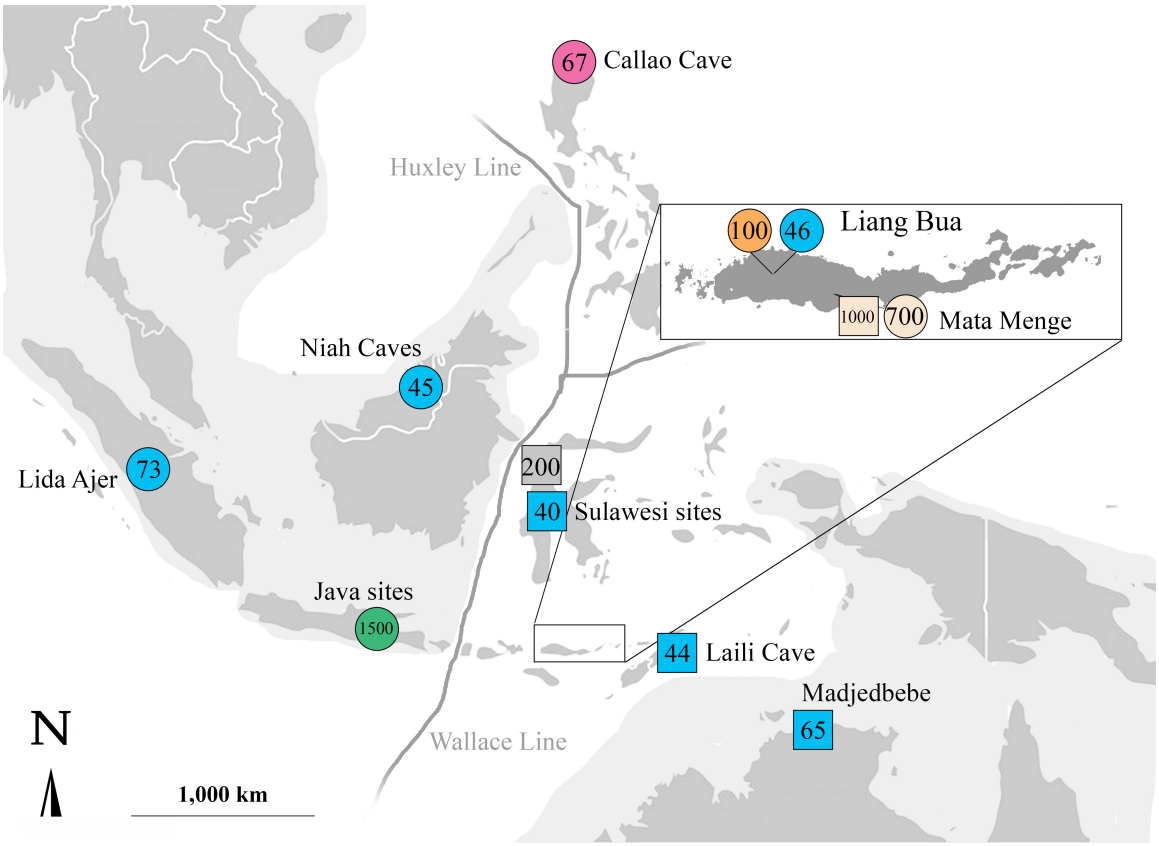

Figure 2.1: Dates for the earliest known localities of archaic *Homo* and *H. sapiens* in Southeast Asia represented by skeletal (circles) and behavioral (squares) evidence. Blue = *H. sapiens*; green = *H. erectus*; orange = *H. floresiensis*; light orange = *H. floresiensis*–like; pink = *H. luzonensis*; grey = unknown archaic *Homo*. Estimated date range in thousand years (ka).

also provide critical, and potentially significant, insight for understanding human migrations in the region.

To better understand how modern humans migrated across Island Southeast Asia (ISEA), Professors Mike Morwood from the University of New England collaborated with Soejono in the early 2000s on a project focused on the archaeological and paleontological records on Java and Flores—islands that fall west and east of the biogeographical barrier known as the Wallace Line, respectively (Figure 2.1). Both islands contain rich faunal records from Early and Middle Pleistocene deposits that would reveal how oceanic barriers affected human and animal migrations in the past. What was not expected was to unearth a distant human relative who inhabited the island

long before the arrival of modern humans.

Laying roughly six meters beneath the surface of the cave floor, the partial skeleton now known as "LB1" (Liang Bua 1) was first uncovered on September 2nd, 2003. Initially believed to be the remains of a young child, Indonesian excavators and archaeologists carefully removed the surrounding sediment to reveal a partial skeleton of an adult with a surprising combination of traits unseen in any previously known hominin taxon. Commonly known as "The Hobbit", LB1 became the holotype of a new species called *Homo floresiensis* that was announced to the world in 2004 (Brown et al., 2004; Morwood et al., 2004) and sparked the beginning of a new age of human evolutionary discoveries.

2.1 A most Excellent and Audacious Hobbit

Homo floresiensis broadly resembles other small-bodied hominins from the Early Pleistocene of Africa, but with a unique combination of archaic (Jungers et al., 2009b; Gordon et al., 2008; Jungers et al., 2009a; Baab and Mcnulty, 2009; Kaifu et al., 2011, 2015b,a; Kubo et al., 2013; Larson et al., 2007, 2009; Orr et al., 2013; Tocheri et al., 2007) and derived morphologies (Falk et al., 2005a; Brown and Maeda, 2009; Kaifu et al., 2011, 2015a,b) . This combination of traits, along with the temporal and geographic context of the discovery, have been used to support three working hypotheses to explain the ancestry of *H. floresiensis* and its phylogenetic relationship to other hominin taxa. These include (1) *H. floresiensis* evolved as an island-dwarfed descendant of Asian *H. erectus* (Kaifu et al., 2011, 2015b,a; Gordon et al., 2008; Lyras et al., 2009); (2) *H. floresiensis* evolved as a descendant of a small-bodied and small-brained species of early *Homo* (*Homo* cf. *habilis*) (Falk et al., 2005a; Morwood et al., 2005; Dembo et al., 2015; Argue et al., 2017; Jungers et al., 2009a,b; Argue et al., 2006; Brown and Maeda, 2009; Baab and Mcnulty, 2009; Gordon et al., 2008; Argue

et al., 2009); or (3) the skeletal material attributed to this species represents modern humans with some form of undiagnosed pathology and/or derive from a population of short-statured modern humans (Henneberg and Thorne, 2004; Jacob et al., 2006; Henneberg et al., 2014). Without doubt, the unexpected morphology and context of *H. floresiensis* challenged longstanding paradigms of human evolution in Southeast Asia.

2.1.1 A Morphological Debate

Published in the journal *Nature* on October 28th, 2004, a portion of the partial skeleton known as LB1 was first described with a surprisingly small cranial capacity (380 cm^3) and short stature (106 cm) resembling the smallest of the australopith skeletons from Africa (Brown et al., 2004; Morwood et al., 2004). The relatively short tibia showed an oval cross-section with thick cortical walls that, together, were outside the range of *Homo* and resembled those from chimpanzees (Brown et al., 2004). Yet, the pelvic and femoral elements shared similar morphologies with other bipedal hominins, such as a short and wide iliac blade and a relatively long femoral neck and a developed intertrochanteric crest that more closely resembled obligate bipedalism (Brown et al., 2004). Moreover, the facial features showed substantially reduced prognathism and facial height, with similar postcanine tooth sizes indicative of the genus *Homo* (Brown et al., 2004). Thus, despite its small body and brain size and other archaic morphologies, LB1 was assigned to the genus *Homo* due to its facial and dental proportions as well as reduced masticatory apparatus in relative size and function, all of which share greater similarity to *Homo* compared to australopiths.

The small body and brain size observed in LB1 were not initially considered phylogenetically relevant due to the evolutionary pressures frequently observed in insular environments (Brown et al., 2004). Known as the "island rule", a trend in mammalian body sizes on islands have been observed in response to a series of ecological pressures

unique to island biota (Foster, 1964; Van Valen, 1973). Evolutionary pressures acting on impoverished faunal communities with an absence of (or fewer) predators reduces interspecific competition that affects the maximum rates a population is able to grow (Sondaar, 1977; Heaney, 1978; Lomolino, 1985, 2005; Raia and Meiri, 2006). This can result in either a reduction (dwarfism) or expansion (gigantism) in body size. Critics of the "island rule" caution against its generality and found there are clade-specific patterns where mammalian carnivores, heteromyid rodents, and artiodactyls tend to evolve smaller body sizes on islands and murid rodents can grow larger (Meiri, 2007; Meiri et al., 2008), while lizards, turtles, and other clades fail to conform to the "island rule" (Itescu et al., 2014). Meiri et al. (2008) also highlights methodological inconsistencies in testing the "island rule" where approximations for animal body size vary, such as body length, weight, and skull size, as well as a failure for considering variables such as island area, carnivore frequency, and trophic level to predict observed animal body size reduction (Welch, 2009; van der Geer, 2020). Interestingly, there are no reports of pleisiomorphic (or archaic) traits emerging as a consequence of island dwarfism or gigantism (Bromham and Cardillo, 2007; Lomolino, 2005, 1985; Lomolino et al., 2006; van der Geer, 2020; van der Geer et al., 2016). Nonetheless, the absence of any early *Homo* other than *H. erectus* in Asia gave credence to the possibility that *H. floresiensis* was the result of a founding *H. erectus* population that dwarfed over time on Flores instead of belonging to a potentially more ancient hominin relic lineage (Brown et al., 2004).

As excavations at Liang Bua continued, Indonesian archaeologists uncovered the upper limbs bones belonging to LB1 from an adjacent Sector (XI), along with an additional mandible (LB6/1) and postcranial elements from other individuals (Morwood et al., 2005). Surprisingly, the relative proportions of the humerus and femur were almost identical to those of AL288-1 (*Australopithecus afarensis*). However, the lower dentition observed in the second mandible was consistent with that of LB1, de-

spite the peculiar morphology of the lower 3rd premolars, was overall very *Homo*-like (Morwood et al., 2005). The resulting gross combination of primitive and derived morphological features across the entire skeleton indicated that *H. floresiensis* was a legitimate taxon, but its ancestry remained opaque with similarities to both *H. erectus* and other early *Homo* sp. strongly represented. Moreover, the estimated relative body proportions brought doubt on the plausibility of *H. floresiensis* merely being a scaled-down version of *H. erectus* (Morwood et al., 2005). Since, there have been a number of additional comparative studies of *H. floresiensis* that support the taxonomic diagnosis but do not necessarily resolve the debate over the species' ancestry, including analyses of the endocast and cranium (Falk et al., 2005a,b; Baab and Mcnulty, 2009), the wrist (Tocheri et al., 2007; Orr et al., 2013), shoulder (Larson et al., 2007), and foot (Jungers et al., 2009a), as well as the postcranial skeleton overall (Jungers et al., 2009a, Larson et al., 2009).

Soon after the discovery was announced, an alternative viewpoint arguing for a pathological or developmental abnormality as an explanation for the peculiar features of LB1 emerged and attempted to refute claims of a new archaic hominin species. Henneberg and Thorne (2004) was the first to challenge *H. floresiensis* as a species arguing that several dimensions of the skull and facial features were within the range of modern humans who have secondary microcephaly—a developmental disorder. Several other studies have argued in favor of additional pathologies or growth disorders, including Laron syndrome (Hershkovitz et al., 2007), endemic cretinism (iodine deficiency disorder) (Obendorf et al., 2008), and most recently Down syndrome (Henneberg et al., 2014). Collectively, these studies have continued to claim a pathological explanation for the surprisingly small cranium and body size of LB1, all while mostly ignoring the postcranial evidence from LB1 and other individuals recovered from Liang Bua (Brown et al., 2004; Morwood et al., 2004, 2005). In response, criticisms of these proposed pathological and genetic disorders have been intense (Argue et al., 2006,

2009; Lyras et al., 2009; Kaifu et al., 2009; Argue et al., 2017; Falk et al., 2007, 2009; Balzeau and Charlier, 2016; Jungers et al., 2009a; Aiello, 2010; Brown, 2012; Baab et al., 2013, 2016; Van Heteren, 2013) and have failed to find support for such claims.

Homo erectus is known to have inhabited the island of Java from ~1.45 Ma to ~108 ka (Morwood et al., 2003; Rizal et al., 2020). Given the geographical proximity to Flores, craniometric and dentognathic comparisons were made between Javanese *H. erectus* and *H. floreisensis* to assess their relationships. Kaifu et al. (2011, 2015b,a) found support for the hypothesis that *H. floresiensis* evolved from Javanese *H. erectus* through island dwarfism based on derived features shared between these taxa but not with *H. habilis*. However, without sufficient postcranial elements confidently associated with *H. erectus* in Southeast Asia (Antón, 2003), the only possible comparison between *H. floresiensis* and Asian *H. erectus*-grade forms can be made using cranial and dental characteristics. Other studies centered on other anatomical regions of the skeleton, including the (virtual) endocast (Falk et al., 2005a,b), cranium (Baab and Mcnulty, 2009), mandibles and mandibular teeth (Brown and Maeda, 2009), shoulder joint (Larson et al., 2007), cranial shape (Gordon et al., 2008), wrist (Tocheri et al., 2007; Orr et al., 2013), and pelvis, upper and lower limbs (Larson et al., 2009; Jungers et al., 2009b,a) found greater support for more archaic ancestry suggesting either a close relationship with *H. habilis*/*H. rudolfensis* or early forms of *Homo erectus* as seen in the Dmanisi hominins. Moreover, Falk et al. (2005a) concluded that while the external brain anatomy of LB1 shared many features with Asian *H. erectus*, the well-convoluted brain shape failed to support an allometrically scaled down version of a *H. erectus* brain shape and structure, and thus, challenged the idea that the cranial features observed in *H. floresiensis* are the result of island dwarfism. Interestingly, cladistic studies incorporating a combination of cranial, dental, and sometimes postcranial metric and non-metric features as well (Argue et al., 2006, 2009; Dembo et al., 2015; Argue et al., 2017) have repeatedly concluded that *H. floresiensis* is more

similar to non-*erectus* early forms of the *Homo* lineage, rejecting support for a close phylogenetic relationship with Asian *H. erectus* and *H. sapiens* (Argue et al., 2017). While island dwarfing from an isolated *H. erectus* population is certainly a possibility, this process would require both the re-emergence of pleisomorphic traits and the convergence of derived dental traits (such as reduced post-canine molar size) with *H. sapiens* (Stringer, 2014), which again are processes that have not been observed in other dwarfed species (Lomolino, 1985, 2005; Lomolino et al., 2006).

Another argument put forth by Jacob et al. (2006) claimed that LB1 derives from an earlier population of pygmy *H. sapiens* on Flores in combination with pathological abnormalities. Specifically, Jacob et al. (2006) refers to the ancestors of a living group of undefined pygmy families from the village of Wae Mulu, one of numerous villages ~1 km from Liang Bua. Described as the Rampasasa pygmies, Jacob et al. (2006) reports a combined sex average stature of 1.46 m across 35 males and 41 females. Problematic methodological claims of reduced cranial capacities, absence of a true chin, and short-stature observed in select individuals from Wae Mulu, as well as facial asymmetry in LB1 (interpreted by "doubling [a photograph of the skull] at the midline and mirrored") forms an unusual basis for challenging *H. floresiensis* as a new hominin species (Jacob et al., 2006). Moreover, genome-wide sequences of individuals from Wae Mulu failed to find any support for archaic admixture that might indicate an ancestral relationship with *H. floresiensis* but did find a genetic basis for short stature in select individuals (Tucci et al., 2018); however, at the population level, including sampling individuals over 1.6 m tall across Flores, remains untested. Nonetheless, a hominin with a height estimate of 106 cm is still considerably shorter than any known "dwarfed" or pygmy human populations (Brown et al., 2004).

The unprecedented discovery of *H. floresiensis* challenged the established human evolution paradigm that left many scientists questioning its authenticity (Bednarik, 2009; Barham et al., 2004). Prior to the discovery of *H. floresiensis*, it was believed

that *H. erectus* first emigrated out of Africa (Morwood et al., 2003), crossed sea barriers (Bednarik, 2003), and was responsible for the Early Pleistocene stone artifacts found on Flores (van den Bergh et al., 1996; Morwood et al., 1998). Globally at this time, hominin brain size was also slowly increasing from ~609 cc (*H. habilis sensu stricto*) to ~929 cc (*H. erectus sensu lato*), and ~1,373 cc (*H. neanderthalensis*), as well as an autapomorphic shift in body proportions (Du et al., 2018; Pearce et al., 2013; Holliday, 2012). It's no wonder that the discovery of a short-statured and small-brained hominin during the Late Pleistocene with relatively long arms and feet, and a primitive wrist was heavily scrutinized. Myths of the Ebu-Gogo (forest-dwelling ape-like woman) from the Ngada region of Flores also tempted scientists to draw a connection between facts, legend, and oral-histories, an appealing temptation to explain such an enigmatic hominin (Madison, 2020). However, since the discovery of *H. floresiensis*, other non-*H. erectus*-grade hominins have now been found in the Phillippines (*H. luzonensis*) and in South Africa (*H. naledi*) contemporaneous with *H. sapiens*, *H. neanderthalensis*, and Denisovans revealing a complex interwoven tapestry of hominin lineages (Détroit et al., 2019; Tocheri, 2019; Berger et al., 2015; Hawks et al., 2017). Discoveries like *H. floresiensis* are therefore a reminder that the study of human evolution involves a gradual accumulation of knowledge, including slow and collaborative work involving anatomy, taphonomy, archaeology, geology, genomics, primatology, systematics, and others, that continuously refines and improves our understanding of hominin evolution.

2.2 The stratigraphic, faunal, and paleoenvironmental record at Liang Bua

Although *H. floresiensis* remains were initially thought to be as recent as 18 – 13 ka, subsequent excavations at Liang Bua (2007 – present) have generated substantially

more stratigraphic and chronological information that was available at the time of discovery (Sutikna et al., 2016). These new details led to a revision of the previously estimated temporal ranges for *H. floresiensis* as well as a refined faunal and archaeological sequence at Liang Bua (Morley et al., 2017; Sutikna et al., 2016; Sutikna, 2016; Sutikna et al., 2018; Veatch et al., 2019). In brief, *H. floresiensis* remains are buried deep within a pedestal of stratified deposits (>50 ka), the northern face of which was eroded away and subsequently covered by younger sediments during the past ~30 ka (Sutikna et al., 2016). Based on a combination of radiocarbon (^{14}C), infrared stimulated luminescence (IRSL), thermoluminescence (TL), uranium-series (234U/230Th) for both bone (including *H. floresiensis* individuals) and speleothem, and argon-argon (40Ar/39Ar) dating techniques, all *H. floresiensis* skeletal remains are ~100 – 60 ka and stone artifacts attributed to this taxon are ~190 – 50 ka (Sutikna et al., 2016).

Overall, the distribution of faunal and cultural remains at Liang Bua is now broadly distinguished by three main temporal periods divided into a total of 8 stratigraphic units and 5 subunits (Morley et al., 2017; Sutikna, 2016; Sutikna et al., 2016, 2018) These include: ~190 – 50 ka (Units 1A, 1B, 2) associated with skeletal and behavioral evidence of *H. floresiensis*; ~46 – 5 ka (Units 4, 5, 6, 8A) associated with *H. sapiens* foragers; ~5 – 3 ka (Unit 8B) a transitional *H. sapiens* populations adopting a more sedentary lifestyle; and ~3 ka – present (Unit 8C) associated with *H. sapiens* farmers. The boundaries for these units are defined by eight volcanic tephras (T1 – T8) while the subunits are defined by major changes in either the stratigraphy (Units 1A and 1B) or faunal abundances (Units 8A and 8B) as well as the appearance of pottery (Units 8B and 8C) (Sutikna et al., 2018). A summary of dating methods, faunal distributions, and paleoenvironmental data for each unit is described below.

Unit 1A: ~190 – 120 ka. The oldest date of ~190 ka from Liang Bua derives from a bleached TL sample (LBC-36) taken at roughly 2.9 m depth from the top

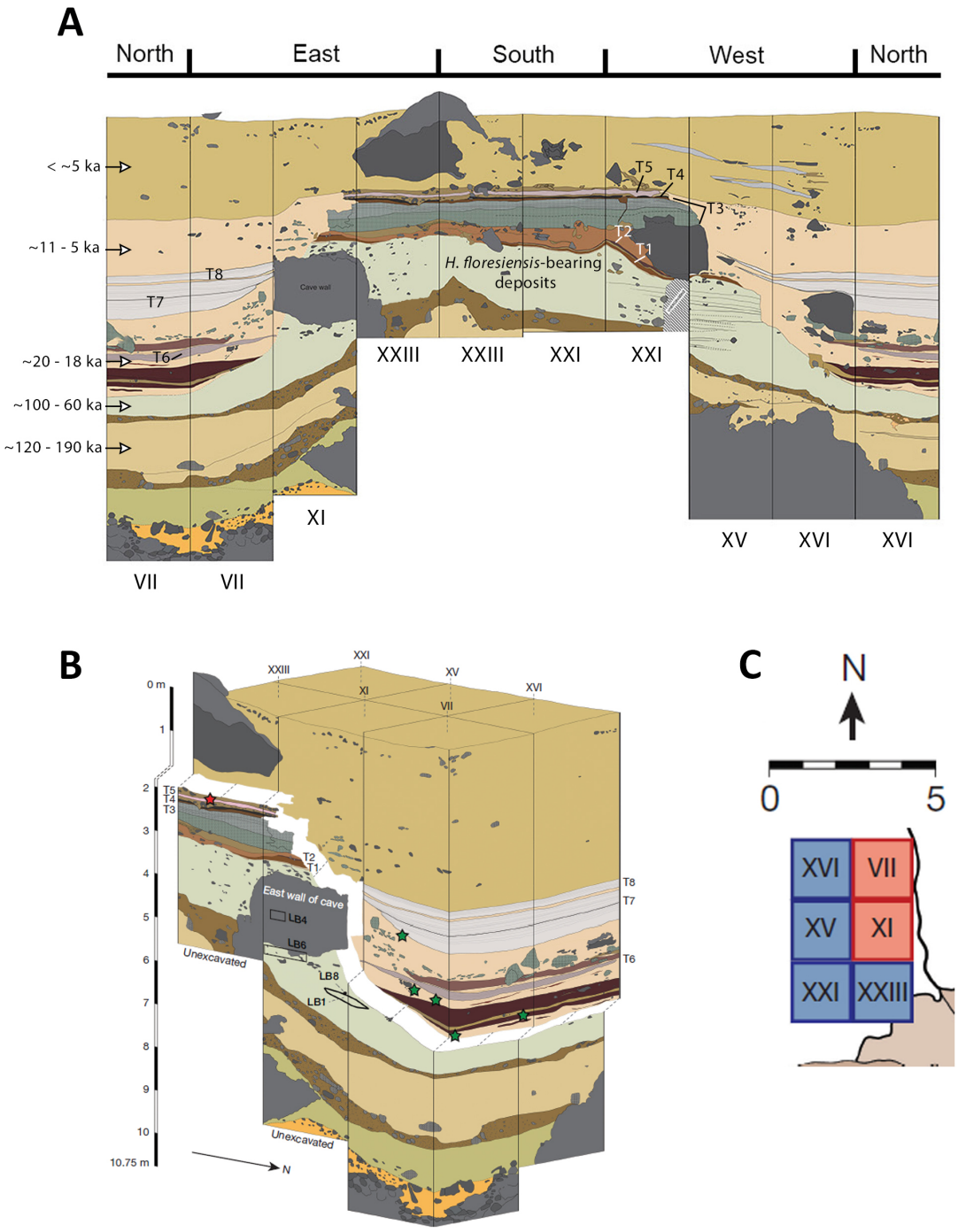

Figure 2.2: Stratigraphic excavation drawings of Sectors VII, XI, XXIII, XXI, XV, and XVI at Liang Bua from (Sutikna et al., 2016). (A) Volcanic tephras 1 – 8 are denoted along with age ranges for sedimentary layers from Sutikna et al. (2016, 2018); (B) 3D view of excavated sectors along the eastern wall of the cave from (Sutikna et al., 2016); (C) Plan view with red sectors excavated in 2003 – 2004 and blue sectors excavated between 2009 and 2012.

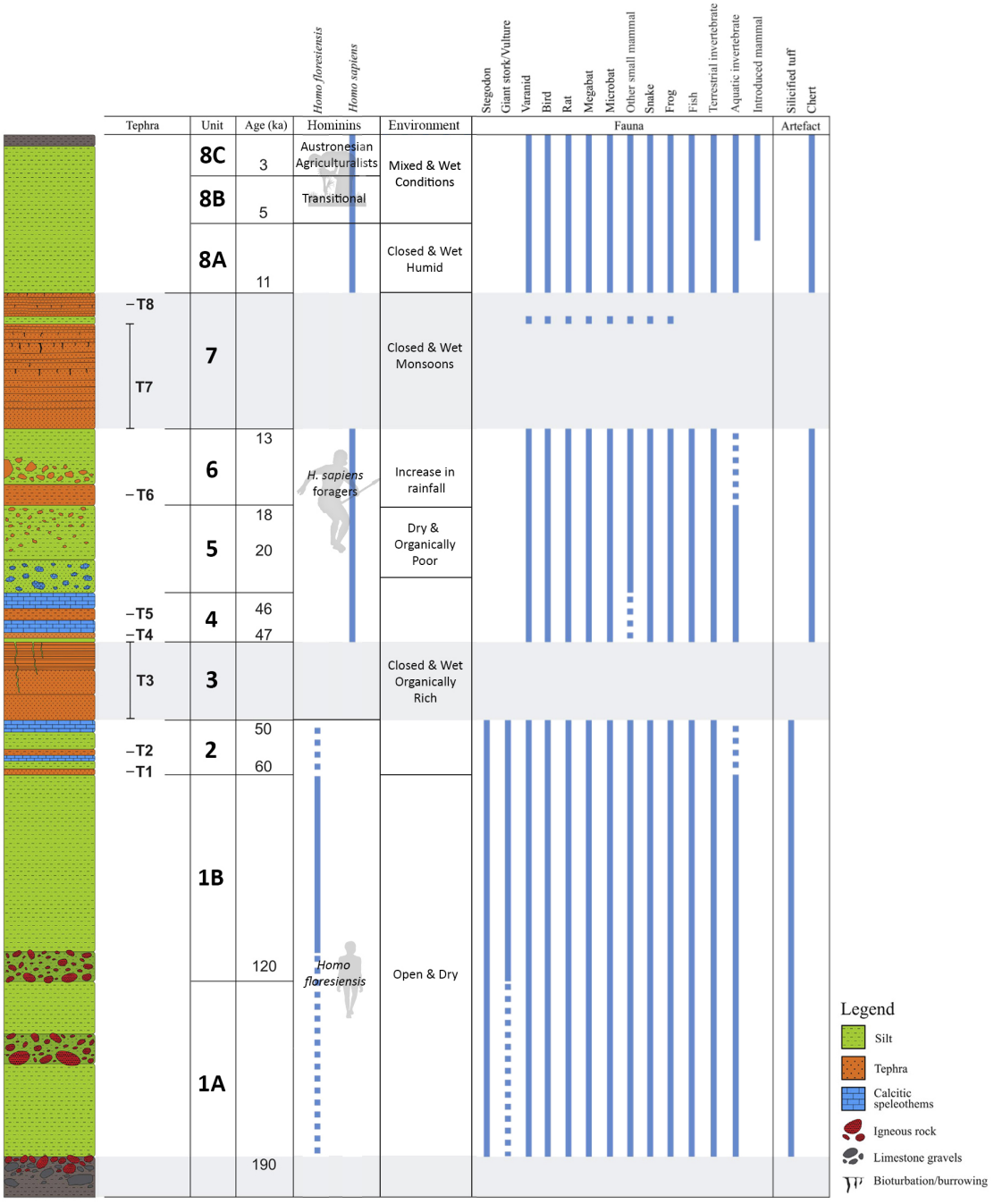

Figure 2.3: Summary of stratigraphic interpretations, environment, and faunal abundances at Liang Bua modified from Sutikna et al. (2018). Environmental interpretations are from Westaway et al. (2009a,b); Veatch et al. (2019).

of the conglomerate deposit at the rear of the cave (Westaway et al., 2007a; Roberts et al., 2009). A subsequent gravel-rich layer immediately underlies the *H. floresiensis*-bearing sediments and is dated to ~120 ka (113 +/- 9 and 128 +/- 17 ka based on TL and IRSL dating methods, respectively) (Sutikna et al., 2016). This stratigraphic unit contains stone artifacts made of primarily silicified tuff (70%) and is currently the oldest behavioral evdience attributed to *H. floresiensis* at Liang Bua (Sutikna et al., 2016, 2018). Murine rodents (i.e., rats) dominate the relative abundance of faunal elements (93.6 %) with a majority representing open-habitat adapted species (i.e., rats of medium and large body sizes), with some *Stegodon* (1.6%), frog (1.5%), bird (0.6%), Megabat (0.9%), and reptiles (0.3%) also represented (Sutikna et al., 2018; Veatch et al., 2019).

Unit 1B: ~120 – 60 ka. This unit occurs immediately above the ~120-ka-old gravel-rich layer and extends until (and includes) T1 and T2, which are dated to ~60 ka based on a combination of 40Ar/39Ar, uranium-series, and luminescence methods (Sutikna et al., 2016). It contains all of the skeletal elements attributed thus far to *H. floresiensis*. In addition to *H. floresiensis*, Unit 1B also contains skeletal elements belonging to four other animals larger than ~3 kg, including a dwarfed proboscidean (*Stegodon florensis insularis*), marabou stork (*Leptoptilos robustus*), vulture (*Trigonoceps* sp.), and Komodo dragon (*Varanus komodoensis*) (Meijer and Due, 2010; Meijer et al., 2013; van den Bergh et al., 2008, 2009; Hocknull et al., 2009). Smaller animals (under roughly 3 – 4 kg) like rats (86.5 %), bats (2.67 %), frogs (1.53 %), birds (1 %), fish (0.21 %), and snakes (0.15 %) are also present in this unit. Similar to Unit 1A, Unit 1B likely represents a more-open environment due to the large representation of open-habitat adapted murines (Veatch et al., 2019).

Unit 2: ~60 – 50 ka. This unit occurs immediately above T2 and extends until the base of T3, a 0.75 m thick volcaniclastic mass flow deposit (Sutikna et al., 2018). Flowstone directly underlying T3 in Sector XII near the middle of the cave was

also dated to 49.6 +/- 0.5 kya using uranium-series methods (Sutikna et al., 2016). Unit 2 may represent a shift in the local environment from more-open grasslands in Units 1A and 1B to more-closed and forested environments after ~60 ka based on a significant decrease in more-open habitat adapted murines and an increase in more-closed habitat adapted murines (Veatch et al., 2019). Stone tools attributed to *H. floresiensis* as well as remains of *Stegodon*, giant marabou stork, and vulture are also present in this unit (Sutikna et al., 2016, 2018).

Unit 3: ~50 – 47 ka. This unit represents the entirety of T3, within which very few findings were recovered (Sutikna et al., 2018). These findings were most likely reworked into the unit as T3 was emplaced or subsequent to its initial deposition (Sutikna et al., 2018).

Unit 4: ~47 – 46 ka. This unit includes all sediments above T3 up until and including the flowstone that immediately overlies T5 (Sutikna et al., 2018). Three flowstone samples within this unit yielded a uranium-series weighted mean age of 46 +/- 0.5 ka and a charcoal sample recovered at 1.89 m on the top surface of T5 in Sector XXIII yielded an age of ~46 thousand calibrated radiocarbon years before present (ka cal. BP) (Sutikna et al., 2016). Artifacts recovered from this unit show a substantial change in raw material proportions compared to Unit 2 (e.g., silicified tuff decreased from 64.5% to 36.8% wheras chert increased to 56.1% from 12.9%—and this change has been interpreted as a possible behavioral signature for *H. sapiens* activity at the site (Sutikna et al., 2018). In addition, two isolated hominin teeth—a left maxillary 3rd premolar and a right mandibular 2nd molar—are morphologically similar in shape to those of modern humans, supporting this behavioral interpretation (Sutikna et al., 2016; Sutikna, 2016). Also, the relative abundance of shell (mostly freshwater with some marine mollusks) increases to 2.9% compared to 0.01% in Unit 2, and may also indicate modern human activity (Sutikna et al., 2018). Although a few *Stegodon* remains occur in the unit, the relative abundances in this and subsequent

units suggest that these have been eroded and reworked from Units 1 and 2 into these younger deposits. With the exception of murines, the relative abundances of all other vertebrate fauna also increase to 20.99% compared to 9.09% in Unit 2 (Sutikna et al., 2018). Paleoenvironmental data from speleothem records indicate a closed woodland environment with montane forests between ~49 and 39 ka that may partially explain the increase in other vertebrate faunas (Westaway et al., 2009c).

Unit 5: ~46 – 18 ka. This unit includes all sediments above the T5-capping flowstone up to and including T6 (Sutikna et al., 2018). The upper age estimate for this unit is based on two charcoal samples from Sector VII recovered at 575 and 588 cm depth that yielded ages of 18.0 and 18.5 ka cal. BP, respectively—these are the same samples used to erroneously date LB1 to ~18 ka (Morwood et al., 2004; Sutikna et al., 2018). Within the temporal duration of this unit, the environment changes from primarily wet and forested to more dry and organically poor (Westaway et al., 2009c). Faunal compositions in Unit 5 suggest that the environment was still relatively closed with a majority of close-habitat adapted murines represented (Veatch et al., 2019), along with a steady increase of other non-murine fauna (Sutikna et al., 2018). The earliest documented instances of controlled fire-use at Liang Bua occurs within this unit at ~41 –38 and ~34 –31 ka cal. BP in Sector XXIV (Morley et al., 2017).

Units 6: ~18 – 13 ka. This unit includes all sediments above T6 extending until immediately beneath T7 (Sutikna et al., 2018). The upper age estimate for this unit is based on a charcoal sample from Sector VII recovered at 463 cm depth that yielded an age of 13.0 ka cal. BP (Sutikna et al., 2018). Similar to Unit 5, Unit 6 shows a steady decline in the relative abundances of murines while non-murine fauna, such as frogs, snakes, megabats, and microbats, increase (Sutikna et al., 2018). Westaway et al. (2009b,a) describes environmental conditions associated with Units 6 and 7 that involve an increase in rainfall and closed-canopy conditions (Westaway et al., 2009a).

Unit 7: ~13 – 12 ka. This unit represents the entirety of T7 and T8 along with

a thin sedimentary layer that lies between them (Sutikna et al., 2018). The upper age estimate for this unit is based on a charcoal sample from Sector XXVI recovered at 395 cm depth that yielded an age of 12.1 ka cal. BP (Sutikna et al., 2018).

Unit 8A ~12 – 5 ka. Unit 8A consists of sediments accumulated immediately above T8 and extending until evidence of the Neolithic transition beginning at ~5 ka in the form of a massive shell midden (Sutikna et al., 2018). The first appearance of pig (most likely *Sus celebensis*, the Sulawesi warty pig), an introduced large mammal, occurs in this unit at ~7 ka (Sutikna et al., 2018; van den Bergh et al., 2009) along with a noticeable increase in frog (12.7% from 3.2%) and megabats (7.9% from 4.8%) compared to Unit 7 (Sutikna et al., 2018). These changes are consistent with paleoenvironmental data suggesting a transition to wetter and more organically-rich environments with the re-expansion of rainforests and returning monsoons, all of which are consequences of the Younger Dryas in the tropical Pacific (Sutikna et al., 2018; Westaway et al., 2009a; Cheng et al., 2020).

Unit 8B ~5 – 3 ka. This unit is defined by sediments dated between ~5 and 3 ka and includes a large and dense shell midden (Sutikna et al., 2018; Julianto et al., 2020). In this unit, significant increases in the relative abundances of fish (1.2% from 0.58%), frogs (22.4% from 12.69%) and varanid reptiles (1.4% from 1.04%) occur in comparison to the previous unit (Sutikna et al., 2018). Other introduced mammals also appear for the first time during this temporal interval, including Javanese porcupines (*Hystrix javanica*), Eurasian pigs (*Sus scrofa*), long-tailed macaques (*Macaca fascicularis*), and masked palm civets (*Paradoxurus hermaphroditus*) (van den Bergh et al., 2009; Sutikna et al., 2018, 2020; Evans et al., 2020). Most notably, aquatic and terrestrial invertebrates significantly increase from <1% in previous units to ~20% in relation to all other faunal groups (Sutikna et al., 2018). This, along with an increase in other faunal groups, likely represents a peak of resource intensification prior to the introduction of farming.

Unit 8C: ~3 ka – present. The most recent stratigraphic layers are represented by Unit 8C and are defined by the presence of pottery and farming practices (Sutikna et al., 2018). Relative abundances of fish (0.7% from 1.2%), frog (10.7% from 22.4%), megabat (3.2% from 6.3%), microbat (6.5% from 8.1%), and varanids (0.5% from 1.4%) also noticeably decrease within this unit while murines increase (71.4% from 55.4%) for the first time since Unit 2—an indication of either an environmental change to more-open habitats, wide-spread clearing of vegetation for agricultural purposes, or both (Sutikna et al., 2018). Murine rodents also show a significant increase in the relative abundances of more-open habitat adapted species compared to the previous units (Veatch et al., 2019). In addition, birds (1.1% from 0.8%), introduced large mammals (5.2% from 3.1%)—including pigs, porcupines, civets, macaques, as well as deer (*Rusa* sp.), dog (*Canis familiaris*), bovid (*Bos* sp.), and horse (*Equus* sp.)—and other small mammals (0.3% from 0.1%) noticeably increase in relative abundances (van den Bergh et al., 2009; Sutikna et al., 2018). Intentional burials with grave goods (e.g., pottery, polished adzes, pig tusks) also characterize the unit (Sutikna et al., 2018). Altogether, changes in the faunal and stone artifact assemblages in this unit suggest that modern humans utilized the cave and its landscape differently than in previous units (Sutikna et al., 2018).

2.3 Hominin diets at Liang Bua

The behavior of *H. floresiensis* was initially interpreted as revealing a surprisingly complex repertoire for a small-brained hominin (Morwood et al., 2004). Skeletal remains of this species recovered from Sector IV were found alongside multiple fragments of juvenile *Stegodon* and a dense concentration of stone artifacts that were initially described to include blades, micro-blades, points, and perforators interpreted as "big game" hunting technology (Morwood et al., 2004). However, further detailed study

of this artifact assemblage revealed it was broadly similar to Oldowan-like or Mode 1 technology found throughout the Old World (Moore et al., 2009). Moreover, early claims that *H. floresiensis* used fire (Morwood et al., 2004, 2005) have not been supported and is most likely the result of *H. sapiens* activity at the site, but this requires further investigation (Morley et al., 2017; Sutikna et al., 2018). The association of *H. floresiensis* with *Stegodon*, giant marabou storks, vultures, and Komodo dragons, and their collective disappearance after ~50 ka suggests that some sort of interdependence existed among these taxa perhaps with a shared preference for more-open landscapes (Veatch et al., 2019). It is certainly likely that *H. floresiensis* incorporated *Stegodon* into their diets to some extent, as evidencee by possible cutmarks reported on two *Stegodon* fragments (van den Bergh et al., 2009), but whether they acquired access through hunting or scavenging remains unclear. Similarly, whether *H. floresiensis* incorporated other animals into their diets, such as murines (i.e., rats) and chiropterans (i.e., bats), and exploited other ecological niches has yet to be considered.

From the time modern humans first appear in the stratigraphic record (~46 ka) and until the onset of farming (~3 ka) at Liang Bua (Sutikna, 2016; Sutikna et al., 2016; Morley et al., 2017), the primary sources of mammalian protein available to these foraging populations would have been limited to murines and chiropterans. The increased relative abundance of other resources at ~11 ka (such as frog at 12.7%) and ~5 ka (such as aquatic invertebrates at 19.8%) suggests a possible increase in diet breadth and resource exploitation prior to the adoption of agriculture ~3 ka (Sutikna et al., 2018). However, without a taphonomic approach to understanding the relationship between hominins and other faunal groups at Liang Bua, the extent of which humans and other predators, such as owls and eagles, contributed to these faunal accumulations remains unclear.

At ~3 ka at Liang Bua, agriculture and several non-endemic mammals (e.g., pigs, macaques, porcupines, civets, etc.) were introduced but the extent to which endemic

fauna were incorporated as dietary resources remains unknown (van den Bergh et al., 2009; Sutikna et al., 2018). Notably, rats and bats still comprise ~68% of the total faunal assemblage at Liang Bua during this most recent temporal interval, compared to ~86% throughout the remaining ~187 ka stratigraphic sequence (Sutikna et al., 2018; van den Bergh et al., 2009). Making up ~78 % of the total faunal assemblage (Sutikna et al., 2016), the rats at Liang Bua in particular are both taxonomically and ecologically diverse ranging in body masses up to ~3 kg (Musser, 1981). Thus, understanding the relative contribution of murines into the diets of both *H. floresiensis* and *H. sapiens* by differentiating avian from hominin accumulation would expand our understanding of the environmental and biological circumstances under which hominins chose to exploit small mammals.

Chapter 3

Using Niche Construction Theory to Generate Testable Foraging Hypotheses at Liang Bua

E. Grace Veatch[1,2], Erik J. Ringen[1], Megan Beney Kilgore[1], Jatmiko[3]

[1] Department of Anthropology, Emory University, USA [2] Department of Anthropology, Yale University, USA [3] Pusat Penelitian Arkeologi Nasional, Jakarta, Indonesia

Citation: Veatch, E.G., Ringen, E.J., Kilgore, M.B., Jatmiko, 2021. Using niche construction theory to generate testable foraging hypotheses at Liang Bua. *Evolutionary Anthropology* 30, 8–16. https://doi.org/10.1002/evan.2188416.

3.1 Abstract

Niche construction theory (NCT) has emerged as a promising theoretical tool for interpreting zooarchaeological material. However, its juxtaposition against more established frameworks like optimal foraging theory (OFT) has raised important criticism around the testability of NCT for interpreting hominin foraging behavior. Here, we

present an optimization foraging model with NCT features designed to consider the destructive realities of the archaeological record after providing a brief review of OFT and NCT. Our model was designed to consider a foragers decision to exploit an environment given predation risk, mortality, and payoff ratios between different ecologies, like more-open or more-forested environments. We then discuss how the model can be used with zooarchaeological data for inferring environmental exploitation by a primitive hominin, *Homo floresiensis*, from the island of Flores in Southeast Asia. Our example demonstrates that NCT can be used in combination with OFT principles to generate testable foraging hypotheses suitable for zooarchaeological research.

3.2 Introduction

Understanding the evolutionary outcomes of hominin dietary and foraging behavior is central to paleoanthropological research (Aiello and Wheeler, 1995; Anton et al., 2014; Pobiner, 2020; Thompson et al., 2019). Decades of zooarchaeological analyses suggests that 2-3 million years ago our hominin ancestors began to rely on consuming fatty and calorically dense nutrients from hunting and/or scavenging big game using advanced cognitive, social, and technical abilities (Domínguez-Rodrigo, 2002; Domínguez-Rodrigo and Pickering, 2017; Pobiner, 2020; Thompson et al., 2019). Theoretical frameworks such as middle range theory (Binford, 1981; Gifford-Gonzalez, 1989, 1991) and optimal foraging theory (OFT)(Codding and Bird, 2015; Jones and Hurley, 2017; Macarthur and Pianka, 1966; Smith et al., 1983) have refined our interpretations of hominin-butchery assemblages by guiding inferences for hominin foraging processes (accumulating food) from their static derivatives (cut marked bone). More recently, niche construction theory (NCT) has entered the literature as a promising theoretical tool for archaeology (Gremillion et al., 2014; Laland et al., 2000; Murray et al., 2020; Shennan, 2004; VanPool and VanPool, 2003). However, its juxtapo-

sition against more established theoretical frameworks, such as OFT, highlights its difficulty in testing NCT in zooarchaeological contexts (Stiner and Kuhn, 2016). Here, we explore the literature surrounding the debate on the utility of OFT and NCT and provide an integrated optimization foraging model to generate foraging hypotheses for *H. floresiensis*, an extinct human relative from Liang Bua, Flores, Indonesia.

3.3 OFT and NCT within zooarchaeology

Within archaeological scholarship, NCT is often critiqued against optimal foraging theory (OFT), which falls under the broader human behavioral ecology umbrella (Codding and Bird, 2015; Gremillion, 2002). Critical reviews of and between OFT and NCT within archaeology are extensive (Jones and Hurley, 2017; Pyke, 1984; Smith et al., 1983; Winterhalder and Smith, 2000; Zeder, 2012) and often include statements of exclusivity, but their methodological toolkits overlap and both approaches offer benefits for interpreting hominin subsistence practices (Riede, 2019; Stiner and Kuhn, 2016). Nevertheless, the two approaches may be better suited for different kinds of inquiry, depending on the temporal and spatial resolution of an assemblage(s) (i.e., the degree to which material is attributable to specific actions in the past) (Binford, 1981), as well as the research goals of the investigator (Gremillion et al., 2014; Mohlenhoff et al., 2015; Stiner and Kuhn, 2016). Specifically, OFT may be better suited for investigating short term adaptation whereas NCT emphasizes longer time-scales of co-evolution (Stiner and Kuhn, 2016).

3.3.1 Optimal foraging theory (OFT)

OFT applies the concepts of optimization and evolutionary theory to the study of human behavior by generating formal predictive models of how organisms behave while searching for food, (Macarthur and Pianka, 1966) and is frequently applied

to zooarchaeological assemblages to interpret species representation, skeletal element abundances, and fragmentation patterns of accumulated vertebrate fauna (Codding and Bird, 2015; Gremillion, 2002; Henshilwood and Marean, 2003; Jones and Hurley, 2017; Lupo, 2007; Marean and Cleghorn, 2003; Smith et al., 1983). This theoretical framework operates under several core assumptions, including: (1) behavior while foraging affects fitness; (2) foraging behavior is heritable (but not necessarily genetically fixed; this can include gene-by-environment interactions and learning); (3) relationships between foraging behavior and fitness is known; (4) the evolution of foraging behavior is unaffected by genetic constraints; (5) a foragers anatomical or technological features are known and "fixed"; and (6) foragers aim to maximize expected fitness (Pyke, 1984). While there are numerous predictive models available under OFT (e.g. diet breadth, prey choice, patch choice, marginal value theorem, etc.), the most commonly used in zooarchaeology are diet breadth models (Kelly, 1995; Stephens and Krebs, 1986; Winterhalder and Smith, 2000).

Diet breadth models within zooarchaeology assume that foragers will preferentially collect higher ranked resources that yield greater net return rates compared to lower ranked ones as they are encountered within a homogenous landscape (Lupo, 2007). High net return rates can include a combination of low search and handling time for smaller returns (e.g., small prey items with a large and predictable distribution) or high search and handling times for large returns (e.g., large and risky prey items). The resulting combination of prey items that were of greatest profitability given environmental and behavioral contexts can be interpreted as diet breadth – fewer and higher rank types in the diet indicate resource abundance while greater and lower rank types indicates resource depletion (Stephens and Krebs, 1986). This is assuming that a foragers goal was to maximize caloric intake – a goal that is frequently assumed in human OFT models in lieu of other foraging goals, such as balancing diet, taste preference, or social stigmas (Hawkes et al., 1991; Machovsky-Capuska et al., 2016).

In doing so, many models have created a false notion that body-size based abundance indices reflects foraging efficiency—known as the body-size proxy (Bird et al., 2009; Broughton et al., 2011; Haws and Hockett, 2004; Jones, 2016).

Testing hypotheses generated from OFT models comes with a unique set of challenges (Gremillion, 2002). Because of the cumulative nature of the archaeological record and the indirect means of reconstructing paleoenvironments, parameters such as prey availability, abundance, heterogeneity, and distribution, are not always known (Broughton et al., 2010; Jones and Hurley, 2017) or cannot be represented accurately using modern analogs (Faith et al., 2019). One way to overcome this challenge is to apply parameter values estimated from modern human foraging societies, such as search and handling times and energetic returns for individual prey items (Bettinger et al., 2015; Hill et al., 1987). But even when such approximations are possible, the destructive nature of archaeological assemblages often fail to reliably reflect the culmination of foraging events, particularly for small animals (Lyman and Lyman, 2003; Yellen, 1991b,a). In addressing these taphonomic realities, a more nuanced approach that utilizes a broader ecological framework may be better suited for interpreting hominin subsistence behaviors within a particular environment.

3.4 Niche construction theory (NCT)

NCT places an emphasis on how organisms, through their actions and/or behavior, change their own selective environments and act as co-directors of evolution (Laland et al., 2015; Laland and O'Brien, 2010; O'brien and Bentley, 2020; O'Brien and Laland, 2012; Zeder, 2015). Actions such as environmental modification are expected to serve as an additional source of non-genetic inheritance for organisms that engage in niche constructive behaviors because they directly affect resource availability for themselves, other members of their species, and other conspecific organisms in their

environment over generations ("ecological inheritance") (Laland et al., 2015). Any traits created through these processes are now considered evolutionarily significant under the Extended Evolutionary Synthesis (EES) (Laland et al., 2014, 2015). In this view, the environment does not merely 'pose the problem' and organisms 'posit solutions', but the decision to modify can be a cultural or behavioral response to an unsuitable habitat where selection then favors those that modify to survive (Laland and O'Brien, 2010).

The evolutionary "success" of *Homo sapiens* has been dependent upon our species' ability to not only modify its environment, but to transfer knowledge from one generation to the next (Fuentes, 2015; Fuentes et al., 2010; Laland and O'Brien, 2010). By accumulating culture through high-fidelity social learning and cooperation, humans are able to directly influence the selective environments of future generations (Boyd et al., 2011; Fuentes, 2014, 2017; Kaplan et al., 2009; Laland et al., 2016; Laland and O'Brien, 2010). For example, habitual fire-use opened a new dietary niche for Middle and Late Pleistocene hominins that left broad-scale effects on the environment as well as future generations (Riede, 2019; Wrangham, 2009). Fire management also became an important social tool for fostering imaginative phenomena like story-telling, dancing, and singing, while also reinforcing cooperation and trust by conveying social networks and group identity (Fuentes, 2014; Wiessner, 2014). Additionally, the development of stone tools opened a new niche for early hominins to exploit resources in an environment that might have otherwise been unavailable to them (Anton et al., 2014). By simultaneously constructing, improving, maintaining, and teaching future generations how to use and develop stone artifacts, this early form of culture likely had a substantial impact on subsequent hominin evolution than natural selection alone (Laland et al., 2015; Laland and O'Brien, 2010).

The main critique of NCT is its tautological approach to interpreting archaeological phenomena (Codding and Bird, 2015; Stiner and Kuhn, 2016). A theoretical tool

is meant to provide a logical basis, or concept, that is supported through rigorous hypothesis-testing of observed phenomena (Gremillion, 2002). For some, NCT fails to accomplish this and provides, instead, merely a post-hoc explanatory approach for describing changes in human behavior Stiner and Kuhn (2016). Other proposed limitations of NCT are a matter of scale for measuring behavioral phenomenon, where NCT is more suitable for interpreting the effects of emergent phenomena across generations (Lyman and Lyman, 2003). Regardless, any theoretical tool that is used to explain past human subsistence behavior is limited by the survival of material culture and the destruction from taphonomic processses (Marean and Cleghorn, 2003).

Stiner and Kuhn (2016) originally argued that OFT and NCT can complement each other in interpreting archaeological phenomena: "Integrating research on niche construction in humans with testable individual (agent) decision models really can provide us with some of the tools we desperately need for understanding complex coevolutionary processes." (182). We extend their argument by presenting an integrated decision-based foraging model designed with NCT concepts to generate testable hypotheses relevant for archaeological research.

Finally, animal body size has been central to discussions of OFT and NCT applications due to the emergence of small game exploitation in the Mediterranean Basin that defined the Broad-Spectrum Revolution (Haws and Hockett, 2004; Stiner, 2002; Zeder, 2012, 2015). In order to avoid body size proxy, we chose the Indonesian archaeological site of Liang Bua as an alternative location for discussing hominin diets where small and large game are each readily available. In addition, the stratigraphic resolution at Liang Bua is reasonably high, at which features from both OFT and NCT can be concomitantly applied.

3.5 Theoretical applications at Liang Bua

Liang Bua is a Middle to Late Pleistocene and Holocene archaeological cave site located on the Indonesian island of Flores (Figure 3.1) and is better known as the discovery site of *Homo floresiensis* (Brown et al., 2004; Morwood et al., 2004, 2005). Skeletal evidence of this taxon (100 – 60 ka) was recovered alongside four other animals larger than ~3 kg— *Stegodon* (*Stegodon florensis insularis*), giant marabou stork (*Leptoptilos robustus*), vulture (*Trigonoceps* sp.), and Komodo dragon (*Varanus komodoensis*) from deposits ranging from ~190 – 50 ka (Table 3.1) (Sutikna et al., 2018). Previous paleoecological reconstructions suggest that Liang Bua was exposed to more-open terrain from ~190 – 60 ka before shifting to more-closed environments at ~60 ka (Veatch et al., 2019; Westaway et al., 2009b). The abrupt disappearance of all five of these larger animals from the Liang Bua stratigraphic sequence, including *H. floresiensis*, at ~60 ka suggests a type of ecological relationship existed among these taxa (e.g., a sole herbivore surrounded by a scavenging guild) preferring the more-open savanna ecosystems (Sutikna, 2016; Sutikna et al., 2016; Veatch et al., 2019).

The most abundant animal at Liang Bua are murine rodents (rats), which comprise 75% of the total faunal assemblage (Sutikna et al., 2018). They are taxonomically and ecologically diverse, with at least eight endemic species (four extant, four extinct) ranging in average body size from 50 g to 2,500 g and specializing in either more-open or more-forested habitats (Table 3.1) (Musser, 1981; van den Bergh et al., 2009; Veatch et al., 2019).

The diet of *H. floresiensis* likely consisted of some combination of animal (vertebrates and invertebrates) and plant matter. On Flores, the only terrestrial mammalian prey available to *H. floresiensis* would have been *Stegodon* and rats (Veatch et al., 2019). *Stegodon* in particular would have been a significant source of fatty nutrients for *H. floresiensis* (Thompson et al., 2019) but the degree to which ho-

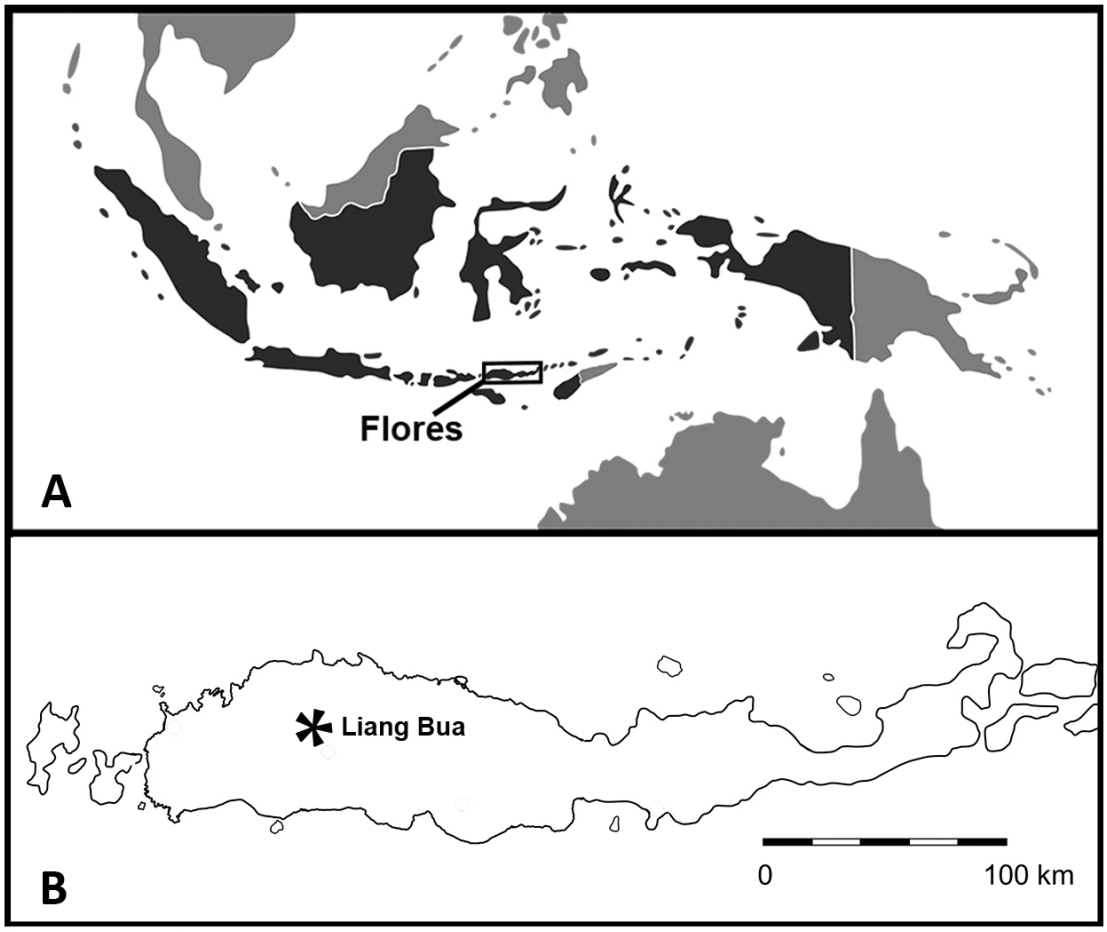

Figure 3.1: Map showing the location of Flores within island Southeast Asia (above) and the location of Liang Bua on Flores (below). Modified from Veatch et al. (2019)

Table 3.1: Summary of Liang Bua fauna by body size and habitat type

Taxon	**Classification**	**Body Mass (g)a**	**Murine Body Sizea**	**Habitat Type**
Papagomys armandvillei	Murine	1200–2500	Giant	Closed
Papagomys theodorverhoeveni	Murine	600–1600	Huge	Closed
Spelaeomys florensis	Murine	600–1600	Huge	Closed
Paulamys naso	Murine	100–200	Medium	Closed
Rattus hainaldi	Murine	40–100	Small	Closed
Hooijeromys nusatenggara	Murine	300–600	Large	Open
Komodomys rintjanus	Murine	100–200	Medium	Open
Stegodon florensis insularis	Proboscidean	569,000b	N/A	Open
Leptoptilos robustus	Stork	16,000c	N/A	Open
Trigonoceps sp.	Vulture	3,000d	N/A	Open
Varanus komodoensis	Varanid	70,000e	N/A	Open

a Murine body size estimates and categories summarized from Veatch et al. (2019)
b Body size estimated from a regression based on limb bone length(van der Geer et al., 2016)
c Body weight estimated from the tibiotarsus recovered from Liang Bua(Meijer & Due, 2010)
d Body weight estimated from skeletal remains at Liang Bua(Meijer et al., 2015)
e Body weight averaged from living Komodo dragons on Flores(McNab & Auffenberg, 1976)

minins were hunting individuals and/or scavenging carrion is still unknown. Either way, competition with scavenging birds and Komodo dragons in an open environment would have put *H. floresiensis* under greater predation risk than in a forested one (i.e., hunting rats). There are a number of scenarios that can be modeled given their encounter and success rates, the encounter rates of competing predators, their means of obtaining *Stegodon* meat (hunting and/or scavenging), and the order of access with other competing scavengers – but all of these values are unknown and/or unattainable. An alternative way to model the foraging behavior of *H. floresiensis* is to consider the basic types of environments available to them, the relative payoffs provided by each habitat type, and a means to estimate why (i.e., what form of niche construction) hominins would behave under these circumstances.

3.5.1 Hominin NCT Foraging Model

Odling-Smee et al. (2003) originally proposed two binary forms of niche construction resulting in four behavioral categories with relevance to archaeology (Table 3.2) (Laland and O'Brien, 2010). The first two categories are ways in which organisms

change the selection pressures between themselves and the environment: perturbation and relocation. The former occurs when organisms physically change aspects of their currently inhabited environment, while the latter occurs when organisms choose to migrate to other locations exposing themselves and future generations to different environments. The other two forms of niche construction focus on whether organisms initiate (inceptive) or respond (counteractive) to a change in their environment (Riede, 2019).

Table 3.2: Categorization of niche constructing behaviors modified from Laland and O'Brien (2010) and Odling-Smee et al. (2003) with examples reflecting behaviors observed in the Paleolithic.

	Perturbation	**Relocation**
Inceptive	Organisms initiate a change in their selective environment by physically modifying their surroundings, *e.g., stone tool production*	Organisms expose themselves to a novel selective environment by moving to or growing into a new place, *e.g., invasion of new habitat*
Counteractive	Organisms counteract a prior change in the environment by physically modifying their surroundings, *e.g., fire management*	Organisms respond to a change in the environment by moving to or growing into a more suitable place, *e.g., migration due to climate change*

Counteractive relocation (moving to a different, presumably more suitable environment due to climate change) is one form of niche construction relevant to Liang Bua. Given the shifting availability of prey species from more-open to more-closed environments at 60 ka, *H. floresiensis* would have either (1) migrated in response to changing foraging returns, or (2) remained in the region and adapted to a different environment. In OFT, the decision to leave an environment (or 'patch') where returns diminish over time due to depletion by the forager is often represented using the Patch Choice Model (i.e., Charnov's Marginal Value Theorem) (Charnov, 1976). In contrast, we are interested in (1) how tradeoffs between foraging returns and predation risk affected hominin behavior, and (2) how foragers respond to long-term (years or generations) exogenous change in the abundance of high-value prey species. Optimal foraging in this scenario may involve counteractively relocating to a more favorable environment, depending on the degree of both ecological change and mor-

tality risk. Here, we present a model based on first-principles broad enough to apply data attainable for zooarchaeological research (i.e., omitting handling times, travel time, patch heterogeneity, predator encounter rates, etc.) (Figure 3.2). We make the following modeling assumptions:

- At each time t, foragers choose to exploit either an open or forest environment. Both types of environment are equally available and accessible.

- The payoff from forest foraging, characterized by small- and giant-body sized murines, is a constant $x(Forest) = 1$ assuming the greater reproductive rates of murines (more K-selected) compared with *Stegodon* (more r-selected).

- The payoff from open foraging, characterized by *Stegodon* and medium- to large-body sized murines is a variable p (for example, $p = 2$ implies that the open environment has twice the payoff as the forest environment). The pay-off ratio between the two environments is constant when the open habitat is not depleted over time ($\delta = 1$).

- After making their decision, foragers are subject to a stochastic survival event (N). μ is the background mortality rate, which is *extrinsic*, or independent of the foraging decision. μ can be estimated from comparative datasets (see Table 3.3). If the forager chooses to exploit an open environment, they incur some additional mortality risk θ due to predation. Predation risk is a common feature in non-human OFT models but is often omitted when applied to humans (Gilliam and Fraser, 1987; Verdolin, 2006). θ and μ are additive.

- Individuals that survive at the end of time t repeat the decision problem indefinitely until their death.

- Open environments may be subject to depletion over time (which is exogenous, i.e., not dependent on the foraging decision), as represented by the payoff mod-

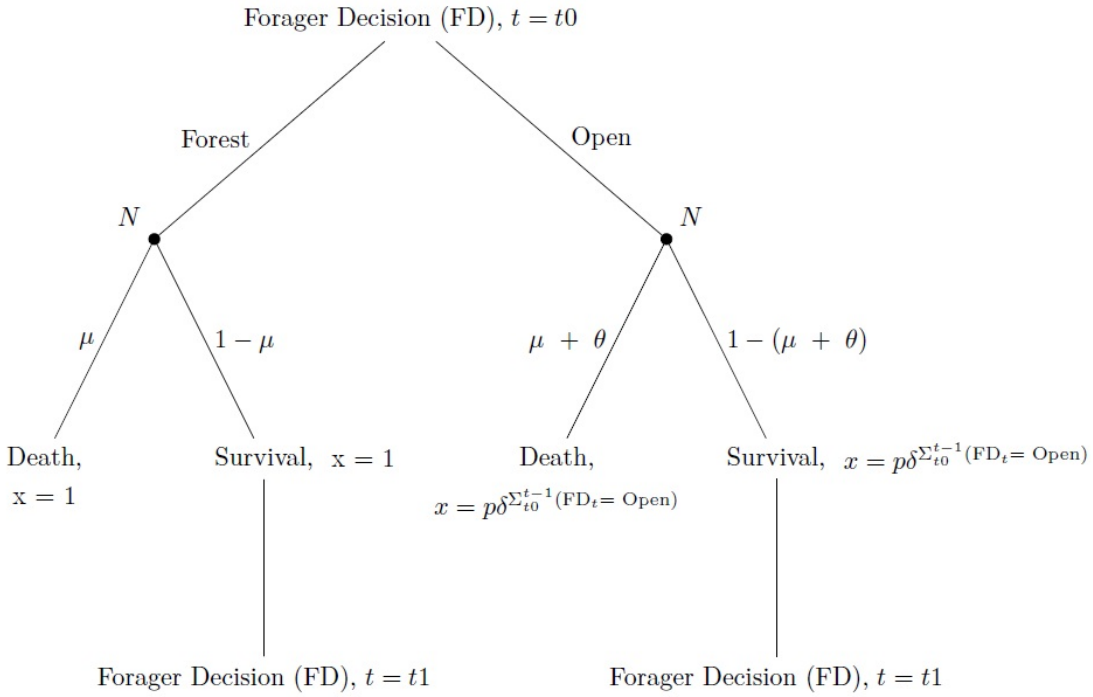

Figure 3.2: Decision tree representation of the foraging model. t = start time. N = stochastic survival event. μ = background mortality rate. θ = additional mortality rate incurred in open environments due to predation risk.

ifier $0 < \delta \leq 1$. This can be thought of as over predation by other predators like Komodo Dragons that reduce the availability of *Stegodon* for hominins, or exogenous climate change. The payoff for open foraging thus varies with time: $x(Open, t) = p\delta^t$.

Table 3.3: Description of model parameters

Model Parameter	Description	Empirical Data Sources	Citation Example
p	Payoff ratio of open/forest foraging	Zooarchaeological and taphonomical data	Roberts et al. (2015b)
μ	Background mortality rate	Comparative analyses, i.e., phylogenetic regression of primate adult mortality rate conditional on body size.	Bronikowski et al. (2002, 2011); Purvis et al. (2003)
θ	Predation rate in open patches	Comparative analyses of hunter-gatherer and/or primate predation rates given similar ecological contexts	Hill and Dunbar (1998); Isbell (1994); Stanford (2002)

The long-run expectations of forest and open foraging strategies are conditional on both resource value and mortality risk. Following the geometric distribution, expected time until death is:

$$E[t_{Death}|FD = Forest] = \frac{1}{\mu} \tag{3.1}$$

$$E[t_{Death}|FD = Open] = \frac{1}{\mu + \theta} \tag{3.2}$$

Now consider the pure strategy of exclusive forest foraging, $S_{Forest} : FD_t = \text{Open}$ for all t in $[t_0, t_\infty]$. Because the payoff from forest foraging is always 1, $E[S_{Forest}] = E[t_{Death}|FD = Forest] * 1 = 1/\mu$. The pure strategy of exclusive open foraging is defined as $S_{Open} : FD_t = \text{Open}$ for all t in $[t_0, t_\infty]$. Thus,

$$E[S_{Open}] = p\frac{1 - \delta^{\frac{1}{\mu + \theta}}}{1 - \delta} \tag{3.3}$$

We calculated the conditions in which open foraging has a higher expected payoff than forest foraging, given different values of μ (background mortality rate) and δ (depletion rate of large prey), as visualized in Figure 3.3.

Thus far, we have only considered pure strategies (i.e., always forest or always open). When $\delta = 1$, the pure strategies are unimprovable by mixing between forest and open because the ratio of mortality to payoff is constant for all time steps. However, when $\delta < 1$, S_{Open} can be improved by adopting a more flexible strategy where the forager initially exploits in open environments and then switches at some time $t\phi$ to forest—similar to the patch choice OFT model. Once again, in niche construction terms, this is an example of *counteractive relocation*. For $\delta < 1$, we can define this optimal switching threshold as the number of time periods to pursue open foraging before switching to exclusive forest foraging.

$$t_\phi = log_\delta \frac{\mu + \theta}{\mu p} \tag{3.4}$$

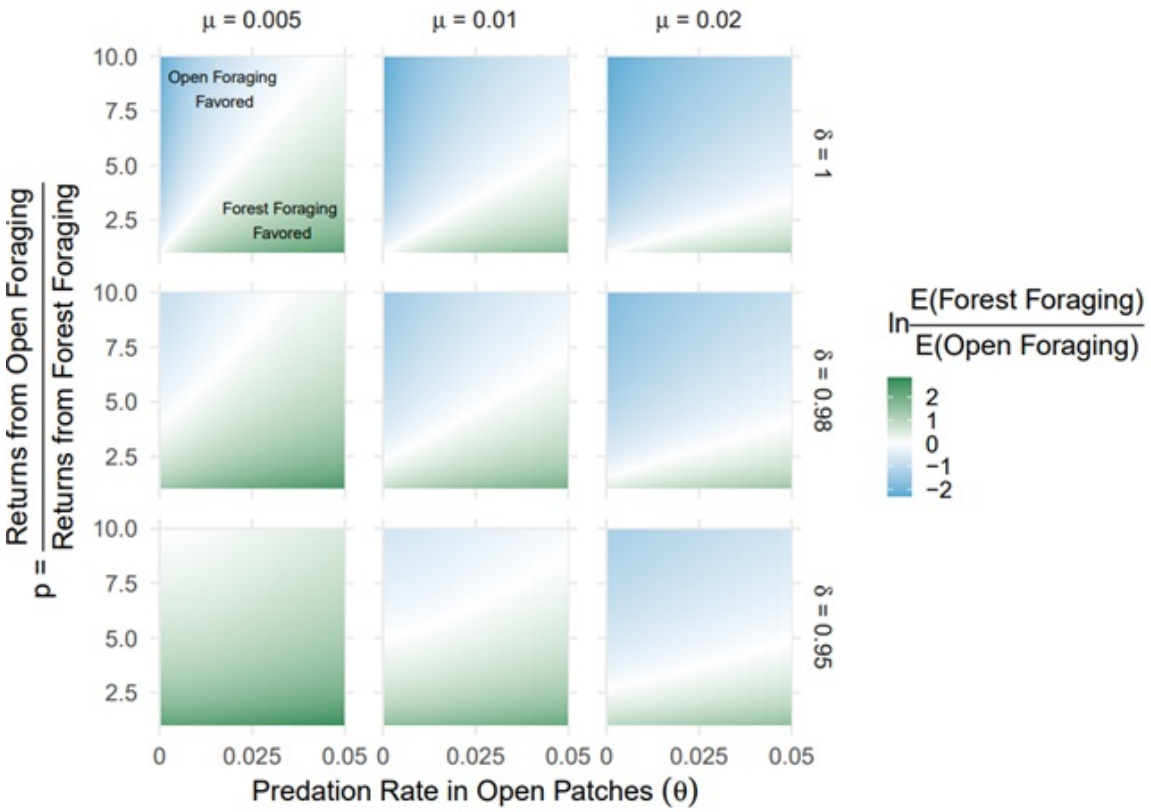

Figure 3.3: Model simulations showing proportion of mixed-habitat foraging (Natural log of $E[S_{Forest}]$ / $E[S_{Open}]$) for given values of μ (background mortality rate), θ (additional mortality rate incurred in open environments due to predation risk), p (payoff for open foraging), and δ (diminishing return in open environments). Blue indicates open foraging favored and green indicates forest foraging favored.

$$S_{CounteractiveRelocation} : FD_t = \text{Open for all } t \text{ in } [t_0, t_\phi], FD_t = \text{Forest for all } t \text{ in } [t_\phi, t_\infty] \tag{3.5}$$

Figure 3.4 Illustrates the mechanics of the counteractive relocation strategy across different levels of open-habitat depletion (δ), holding constant $p = 2$, $\mu = 0.02$, and $\theta = 0.01$.

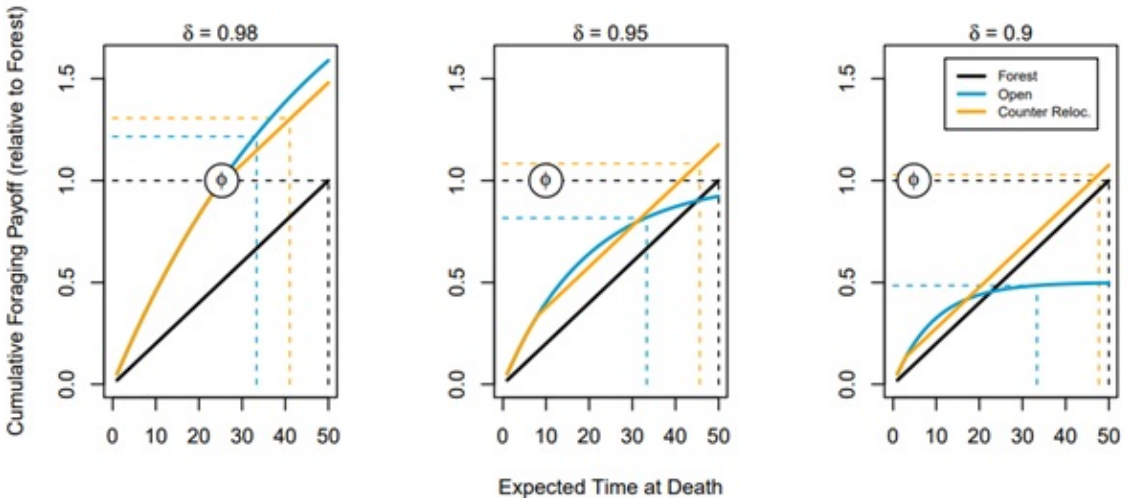

Figure 3.4: Foraging payoffs over time from pure open foraging S_{Open} and counteractive relocation $S_{CounteractiveRelocation}$, relative to the constant payoffs from forest foraging (represented by the solid black line). ϕ is the time when $S_{CounteractiveRelocation}$ switches from open to forest environments. Vertical dashed lines denote expected time at death for each strategy, horizontal dashed lines represent expected payoff at time of death. We hold constant $p = 2$, $\mu = 0.02$, and $\theta = 0.01$.

3.5.2 Model Results and Discussion

Assuming technologies remain static (i.e., no fire-use, stone tool innovation, etc.) and given the composition of assemblages under different ecological scenarios, we can hypothesize how *H. floresiensis* will forage within their environment and why.

When open habitats are more abundant and predation risk is low, we expect assemblages to reflect a pure open habitat foraging strategy. For example (see Figure 3.3), foraging in an open environment is profitable when large game is abundant ($\delta = 1$) and background mortality rates are highest ($\mu = 0.02$). If large game becomes depleted ($\delta = 0.95$), an open environment may still be a more suitable niche to exploit given the same mortality rate. Note that we interpret μ as annual mortality rate, 0.02 is typical for modern human foragers (Gurven and Kaplan, 2007; Hewlett, 1991). When mortality rate is high, foraging in an open environment maximizes payoffs even when under relatively high rates of predation. For a smaller-bodied hominin like *H. floresiensis*, background mortality rates may have been even higher, favoring more

risky foraging strategies. Therefore, if *H. floresiensis* favors a more-open habitat foraging strategy (i.e., hunting predominantly *Stegodon* and open-habitat adapted murines), we could hypothesize (1) that competition with or risk of predation by Komodo dragons was low, and (2) background mortality rates were potentially high.

If background mortality rates are low, we expect assemblages to reflect a pure closed-habitat foraging strategy, regardless of open-habitat resource availability. According to our model, foraging in a forested environment is profitable when open environmental resources are low ($\delta = 0.95$) or unavailable, and background mortality rates are low ($\mu = 0.01$ and 0.005). In this scenario, we can interpret that forested environments are a steady and reliable food source for a stable population of *H. floresiensis*. Therefore, if the archaeological record reflects a greater proportion of close-habitat foraging when more-open environments were available, we could interpret that *H. floresiensis* favored a low-risk foraging strategy.

If the ratio between open-habitat and forest-habitat resource availability changes, we expect assemblages to reflect a mixed-habitat foraging strategy. According to our model, this is more likely to occur when open habitat resources are depleted ($\delta = 0.95$ or lower) and the open habitats are only modestly more profitable than forest habitats. In other words, as open environments become unavailable (i.e., climate change and/or predator-driven prey depletion), we would predict *H. floresiensis* to follow the more-open environments (counteractive relocation) while also exploiting the more stable forested resources.

The model highlights the importance of understanding ecological factors impacting hominin behavior, such as predation risk and habitat depletion. Like all models, there is an innate simplicity to how these scenarios are generated with limitations in reflecting real life situations. The archaeological record, for example, will rarely show a "pure" foraging strategy, but these models help to better understand how hominins could react under certain circumstances, and why. While we focused on modeling

counteractive relocation, other models containing perturbational niche construction could provide additional insight into the ecological conditions of hominin behaviors, especially for modern humans. Overall, modeling hominin foraging behaviors is an extremely complex endeavor and is unlikely to reflect every decision made, but there is still value in quantitatively interrogating our assumptions about the costs and benefits of different hominin foraging strategies over time.

3.6 Conclusion

It is imperative that theoretical frameworks provide a means for generating testable hypotheses. In contrast to the more frequently used agent based OFT models, NCT has been critiqued as being a post-hoc explanatory tool, and thus, uninstructive for testing niche constructive behaviors in the past (Stiner and Kuhn, 2016). Here, we provided an example of an integrated NCT decision-based model for hominin resource exploitation suitable for archaeological research. We demonstrate how NCT and OFT principles can generate several foraging scenarios for *H. floresiensis* that can be directly tested using zooarchaeological data. By considering what ecologies are available to *H. floresiensis* we can thereby predict where individuals will forage while considering various rates of mortality, predation, and habitat depletion. While few applications of NCT involve non-modern human hominins, we hope to have provided a tool to explore these more simple forms of niche construction for more ancient hominins, and how we may attempt to uncover the complexity of hominin behavior.

3.7 Acknowledgements

Thank you to John Murray, Robert Benitez, and Michael J. O'Brien for organizing this special issue on the extended evolutionary synthesis in archaeology, and for the invitation to contribute. We also thank Jessica Thompson, Matthew Tocheri, and Re-

becca Biermann Gürbüz for their comments and suggestions, as well as the insightful and constructive comments from our reviewers that greatly improved this paper. Special thanks to Jessica Thompson and Matthew Tocheri for their guidance, support, and discussions that inspired this paper. Special thanks to Thomas Sutikna, Wahyu Saptomo, Jatmiko, and members of the Liang Bua excavation team for welcoming my contribution and their continued support.

3.8 References

Aiello, L. C., Wheeler, P. (1995). The Expensive-Tissue Hypothesis: The Brain and the Digestive System in Human and Primate Evolution. *Current Anthropology*, 36(2), 199–221.

Anton, S. C., Potts, R., Aiello, L. C. (2014). Evolution of early *Homo*: An integrated biological perspective. *Science*, 345, 1236828.

Bettinger, R. L., Garvey, R., Tushingham, S. (2015). Hunter-Gatherers: Archaeological and Evolutionary Theory (J. Eerkens (ed.); Second Edi). Springer Science+Business Media.

Binford, L. R. (1981). Bones: Ancient Men and Modern Myths. Academic Press.

Bird, D. W., Bird, R. B., Codding, B. F. (2009). In Pursuit of Mobile Prey: Martu Hunting Strategies and Archaeofaunal Interpretation. *American Antiquity*, 74(1), 3–29.

Boyd, R., Richerson, P. J., Henrich, J. (2011). The cultural niche: Why social learning is essential for human adaptation. *Proceedings of the National Academy of Sciences*, 108, 10918–10925.

Bronikowski, A. M., Alberts, S. C., Altmann, J., Packer, C., Dee Carey, K., Tatar, M., Wachter, K. W. (2002). The aging baboon: Comparative demography in a non-human primate. *PNAS*, 99(14), 9591–9595.

Bronikowski, A. M., Altmann, J., Brockman, D. K., Cords, M., Fedigan, L. M., Pusey, A., Stoinski, T., Morris, W. F., Strier, K. B., Alberts, S. C. (2011). Aging in the natural world: Comparative data reveal similar mortality patterns across primates. *Science*, 331(6022), 1325–1328.

Broughton, J. M. (2010). Prey spatial structure and behavior affect archaeological tests of optimal foraging models: Examples from the Emeryville Shellmound vertebrate fauna. *World Archaeology*, 34(1), 60–83.

Broughton, J. M., Cannon, M. D., Bayham, F. E., Byers, D. A. (2011). Prey body size and ranking in zooarchaeology: Theory, empirical evidence, and applications from the northern Great Basin. *American Antiquity*, 76(3), 403–428.

Brown, P., Sutikna, T., Morwood, M. J., Soejono, R. P., Jatmiko, Saptomo, E. W., Due, R. A. (2004). A new small-bodied hominin from the Late Pleistocene of Flores, Indonesia. *Nature*, 431(7012), 1055–1061.

Charnov, E. (1976). Optimal foraging: The marginal value theorem. *Theoretical Population Biology*, 9(2), 129–136.

Codding, B. F., Bird, D. W. (2015). Behavioral ecology and the future of archaeological science. *Journal of Archaeological Science*, 56, 9–20.

Domínguez-Rodrigo, M. (2002). Hunting and scavenging by early humans: the state of the debate. *Journal of World Prehistory*, 16(1), 1–54.

Domínguez-Rodrigo, M., Pickering, T. R. (2017). The meat of the matter: an evolutionary perspective on human carnivory. *Azania: Archaeological Research in Africa*, 52(1), 4–32.

Faith, J. T., Rowan, J., Du, A. (2019). Early hominins evolved within non-analog ecosystems. *PNAS*, 116(43), 21478–21483.

Fuentes, Agustin. (2014). The extended evolutionary synthesis, ethnography, and the human niche toward an integrated anthropology. *Current Anthropology*, 57(13), S13–S26.

Fuentes, Agustín. (2015). Integrative Anthropology and the Human Niche: Toward a Contemporary Approach to Human Evolution. *American Anthropologist*, 117(2), 302–315.

Fuentes, Agustín. (2017). The creative spark: How imagination made humans exceptional. Dutton.

Fuentes, Agustín, Wyczalkowski, M. A., MacKinnon, K. C. (2010). Niche construction through cooperation: A nonlinear dynamics contribution to modeling facets of the evolutionary history in the genus *Homo*. *Current Anthropology*, 51(3), 435–444.

Gifford-Gonzalez, D. (1989). Overview - Modern Analogues: Developing an Interpretive Framework. In R. Bonnichsen M. H. Sorg (Eds.), Bone Modification (pp. 43–52). Center for the Study of the First Americans.

Gifford-Gonzalez, D. (1991). Bones are not enough: Analogues, knowledge, and interpretive strategies in zooarchaeology. *Journal of Anthropological Archaeology*, 10(3), 215–254.

Gilliam, J. F., Fraser, D. F. (1987). Habitat Selection Under Predation Hazard: Test of a Model with Foraging Minnows. *Ecology*, 68(6), 1856–1862.

Gremillion, K. J. (2002). Foraging theory and hypothesis testing in archaeology: An exploration of methodological problems and solutions. *Journal of Anthropological Archaeology*, 21, 142–164.

Gremillion, K. J., Barton, L., Piperno, D. R. (2014). Particularism and the retreat from theory in the archaeology of agricultural origins. *PNAS*, 111(17), 6171–6177.

Gurven, M., Kaplan, H. S. (2007). Longevity among hunter-gatherers: A cross-cultural examination. *Population and Development Review*, 33(2), 321–365.

Hawkes, K. (1991). Showing off: Tests of an hypothesis about men's foraging goals. *Ethology and Sociobiology*, 12, 29–54.

Haws, J. A., Hockett, B. S. (2004). Theoretical perspectives on the dietary role of small animals in human evolution. In J.-P. Brugal J. Desse (Eds.), Petits Animaux

et Societe s Humaines (pp. 173–184). APDCA.

Henshilwood, C. S., Marean, C. W. (2003). The Origin of Modern Human Behavior: Critique of the models and their test implications. *Current Anthropology*, 44(5), 627–651.

Hewlett, B. (1991). Demography and childcare in preindustrial societies. *Journal of Anthropological Research*, 47(1), 1–37.

Hill, K., Kaplan, H., Hawkes, K., Hurtado, A. M. (1987). Foraging decisions among Ache hunter-gatherers: New data and implications for optimal foraging models. *Ethology and Sociobiology*, 8(1), 1–36.

Hill, R. A., Dunbar, R. I. M. (1998). An Evaluation of the Roles of Predation Rate and Predation Risk as Selective Pressures on. *Behaviour*, 135(4), 411–430.

Isbell, L. A. (1994). Predation on primates: Ecological patterns and evolutionary consequences. *Evolutionary Anthropology*, 3(2), 61–71.

Jones, E. L. (2016). In search of the Broad-Spectrum Revolution in Paleolithic Southwest Europe. Springer Briefs in Archaeology.

Jones, E. L., Hurley, D. A. (2017). Beyond depression? A review of the optimal foraging theory literature in zooarchaeology and archaeobotany. *Ethnobiology Letters*, 8(1), 35–42.

Kaplan, H. S., Hooper, P. L., Gurven, M. (2009). The evolutionary and ecological roots of human social organization. *Philosophical Transactions of the Royal Society B*, 364(1533), 3289–3299.

Kelly, R. (1995). The foraging spectrum: Diversity in hunter-gatherer lifeways. Cambridge University Press.

Laland, K., Matthews, B., Feldman, M. W. (2016). An introduction to niche construction theory. *Evolutionary Ecology*, 30, 191–202.

Laland, K. N., O'Brien, M. J. (2010). Niche construction theory and archaeology. *Journal of Archaeological Method and Theory*, 17(4), 303–322.

Laland, K. N., Odling-Smee, J., Feldman, M. W. (2000). Niche construction, biological evolution, and cultural change. *Behavioral and Brain Sciences*, 23, 131–175.

Laland, K. N., Uller, T., Feldman, M. W., Sterelny, K., Müller, G. B., Moczek, A., Jablonka, E., Odling-Smee, J. (2015). The extended evolutionary synthesis: its structure, assumptions and predictions. *Proceedings of the Royal Society B: Biological Sciences*, 282, 20151019.

Laland, K., Uller, T., Feldman, M., Sterelny, K., Muller, G. B., Moczek, A., Jablonka, E., Odling-Smee, J. (2014). Does evolutionary theory need a rethink? *Nature*, 514, 161–164.

Lupo, K. D. (2007). Evolutionary foraging models in zooarchaeological analysis: Recent applications and future challenges. *Journal of Archaeological Research*, 15(2), 143–189.

Lyman, R. L. (2003). The influence of time averaging and space averaging on the application of foraging theory in zooarchaeology. *Journal of Archaeological Science*, 30, 595–610.

Macarthur, R. H., Pianka, E. R. (1966). On optimal use of a patchy environment. *The American Naturalist*, 100(916), 603–609.

Machovsky-Capuska, G. E., Coogan, S. C. P., Simpson, S. J., Raubenheimer, D. (2016). Motive for killing: What drives prey choice in wild predators? *Ethology*, 122(9), 703–711.

Marean, C. W., Cleghorn, N. (2003). Large mammal skeletal element transport: Applying foraging theory in a complex taphonomic system. *Journal of Taphonomy*, 1(1), 15–42.

McNab, B. K., Auffenberg, W. (1976). The effect of large body size on the temperature regulation of the komodo dragon, *Varanus komodoensis*. *Comparative Biochemistry and Physiology*, 55A, 345–350.

Meijer, H. J. M., Due, R. A. (2010). A new species of giant marabou stork (Aves:

Ciconiiformes) from the Pleistocene of Liang Bua, Flores (Indonesia). *Zoological Journal of the Linnean Society*, 160, 707–724.

Meijer, H. J. M., Tocheri, M. W., Due, R. A., Sutikna, T., Saptomo, E. W., James, H. F. (2015). Continental-style avian extinctions on an oceanic island. *Palaeogeography, Palaeoclimatology, Palaeoecology*, 429, 163–170.

Mohlenhoff, K. A., Coltrain, J. B., Codding, B. F. (2015). Optimal foraging theory and niche-construction theory do not stand in opposition. *PNAS*, 112(24), E3093.

Morwood, M. J., Brown, P., Jatmiko, Sutikna, T., Saptomo, E. W., Westaway, K. E., Due, R. A., Roberts, R. G., Maeda, T., Wasisto, S., Djubiantono, T. (2005). Further evidence for small-bodied hominins from the Late Pleistocene of Flores, Indonesia. *Nature*, 437(7061), 1012–1017.

Morwood, M. J., Soejono, R. P., Roberts, R. G., Sutikna, T., Turney, C. S. M., Westaway, K. E., Rink, W. J., Zhao, J. -x., van den Bergh, G. D., Rokus Awe Due, Hobbs, D. R., Moore, M. W., Bird, M. I., Fifield, L. K. (2004). Archaeology and age of a new hominin from Flores in eastern Indonesia. *Nature*, 431(7012), 1087–1091.

Murray, J. K., Benitez, R. A., O'Brien, M. J. (2020). The extended evolutionary synthesis and human origins: Archaeological perspectives. *Evolutionary Anthropology*, 1–4.

Musser, G. G. (1981). The giant rat of Flores and its relative east of Borneo and Bali. In Bulletin of the American Museum of Natural History (Vol. 169, Issue 2).

O'Brien, M. J., Bentley, R. A. (2020). Genes, culture, and the human niche: An overview. *Evolutionary Anthropology*, 1–10.

O'Brien, M. J., Laland, K. N. (2012). Genes, culture, and agriculture an example of human niche construction. *Current Anthropology*, 53(4), 434–470.

Odling-Smee, F. J., Laland, K. N., Feldman, M. W. (2003). Niche construction. The neglected process in evolution. Princeton University Press.

Pobiner, B. L. (2020). The zooarchaeology and paleoecology of early hominin scavenging. *Evolutionary Anthropology*, 29(2), 68–82.

Purvis, A., Webster, A. J., Agapow, P. M., Jones, K. E., Isaac, N. J. (2003). Primate life histories and phylogeny. In Primate Life Histories and Socioecology (pp. 25–40). University of Chicago Press.

Pyke, G. H. (1984). Optimal foraging theory: a critical review. *Annual Review of Ecology, Evolution and Systematic*, 15(1984), 523–575.

Riede, F. (2019). Niche construction theory and human biocultural evolution. In A. M. Prentiss (Ed.), Handbook of Evolutionary Research in Archaeology (pp. 337–358). Springer Nature Switzerland.

Roberts, P., Perera, N., Wedage, O., Deraniyagala, S., Perera, J., Eregama, S., Gledhill, A., Petraglia, M. D., Lee-Thorp, J. A. (2015). Direct evidnce for human reliance on rainforest resources in late Pleistocene Sri Lanka. *Science*, 347(6227), 1246–1250.

Shennan, S. (2004). An evolutionary perspective on agency in archaeology. In A. Gardner (Ed.), Agency Uncovered: Archaeological perspectives on social agency, power, and being human (pp. 19–32). UCL Press.

Smith, E. A. (1983). Anthropological Applications of Optimal Foraging Theory: A Critical Review. *Current Anthropology*, 24(5), 625–651.

Smith, E. A., Bettinger, R. L., Bishop, C. A., Blundell, V., Cashdan, E., Casimir, M. J., Christenson, A. L., Cox, B., Dyson-Hudson, R., Hayden, B., Richerson, P. J., Abella Roth, E., Simms, S. R., Stini, W. A. A., Roth, E. A., Simms, S. R., Stini, W. A. A., Abella Roth, E., Simms, S. R., Stini, W. A. A. (1983). Anthropological applications of optimal foraging theory: A critical review. *Current Anthropology*, 24(5), 625–651.

Stanford, C. B. (2002). Avoiding Predators: Expectations and evidence in primate antipredator behavior. *International Journal of Primatology*, 23(4), 741–757.

Stephens, D. W., Krebs, J. R. (1986). Foraging Theory (J. R. Krebs T. Clutton-Brock (eds.)). Princeton University Press.

Stiner, M. C., Kuhn, S. L. (2016). Are we missing the "sweet spot" between optimality theory and niche construction theory in archaeology? *Journal of Anthropological Archaeology*, 44, 177–184.

Stiner, M. C., Munro, N. D. (2002). Approaches to prehistoric diet breadth, demography, and prey ranking systems in time and space. *Journal of Archaeological Method and Theory*, 9(2), 181–214.

Sutikna, T., Tocheri, M. W., Faith, J. T., Jatmiko, Due Awe, R., Meijer, H. J. M., Wahyu Saptomo, E., Roberts, R. G. (2018). The spatio-temporal distribution of archaeological and faunal finds at Liang Bua (Flores, Indonesia) in light of the revised chronology for *Homo floresiensis*. *Journal of Human Evolution*, 124, 52–74.

Sutikna, T., Tocheri, M. W., Morwood, M. J., Saptomo, W. E., Jatmiko, Awe, R. D., Wasisto, S., Westaway, K. E., Aubert, M., Li, B., Zhao, J., Storey, M., Alloway, B. V., Morley, M. W., Meijer, H. J. M., van den Bergh, G. D., Grun, R., Dosseto, A., Brumm, A., ... Roberts, R. G. (2016). Revised stratigraphy and chronology for *Homo floresiensis* at Liang Bua in Indonesia. *Nature*, 532(7599), 366–369.

Thompson, J. C., Carvalho, S., Marean, C. W., Alemseged, Z. (2019). Origins of the Human Predatory Pattern The Transition to Large-Animal Exploitation by Early Hominins. *Current Anthropology*, 60(1), 1–23.

Van den Bergh, G. D., Meijer, H. J. M., Due Awe, R., Morwood, M. J., Szabó, K., van den Hoek Ostende, L. W. W., Sutikna, T., Saptomo, E. W., Piper, P. J., Dobney, K. M., Due, R. A., Morwood, M. J., Szabo, K., van den Hoek Ostende, L. W. W., Sutikna, T., Saptomo, E. W., Piper, P. J., Dobney, K. M., Due Awe, R., ... Dobney, K. M. (2009). The Liang Bua faunal remains: a 95 k.yr. sequence from Flores, East Indonesia. *Journal of Human Evolution*, 57(5), 527–537.

van der Geer, A. A. E., van den Bergh, G. D., Lyras, G. A., Prasetyo, U. W.,

Due, R. A., Setiyabudi, E., Drinia, H. (2016). The effect of area and isolation on insular dwarf proboscideans. *Journal of Biogeography*, 43(8), 1656–1666.

VanPool, T. L., VanPool, C. S. (2003). Agency and evolution: The role of intended and unintended consequences of action. In T. L. VanPool C. S. VanPool (Eds.), Essential tensions in archaeological Methods and Theory (pp. 89–114). University of Utah Press.

Veatch, E. G., Tocheri, M. W., Sutikna, T., McGrath, K., Wahyu Saptomo, E., Jatmiko, Helgen, K. M. (2019). Temporal shifts in the distribution of murine rodent body size classes at Liang Bua (Flores, Indonesia) reveal new insights into the paleoecology of *Homo floresiensis* and associated fauna. *Journal of Human Evolution*, 130, 45–60.

Verdolin, J. L. (2006). Meta-analysis of foraging and predation risk trade-offs in terrestrial systems. *Behav Ecol Sociobiol*, 60, 457–464.

Westaway, K. E., Morwood, M. J., Sutikna, T., Moore, M. W., Rokus, A. D., Van Den Bergh, G. D., Roberts, R. G., Saptomo, E. W. (2009). Homo floresiensis and the late Pleistocene environments of eastern Indonesia: defining the nature of the relationship. *Quaternary Science Reviews*, 28, 2897–2912.

Wiessner, P. W. (2014). Embers of society: Firelight talk among the Ju/'hoansi Bushmen. *PNAS*, 111(39), 14027–14035.

Winterhalder, B., Smith, E. A. (2000). Analyzing adaptive strategies: Human behavioral ecology at twenty-five. *Evolutionary Anthropology*, 9(2), 51–72.

Wrangham, R. W. (2009). Catching fire: how cooking made us human. Basic Books.

Yellen, J. E. (1991a). Small mammals:!Kung San utilization and the production of faunal assemblages. *Journal of Anthropological Archaeology*, 10, 1–26.

Yellen, J. E. (1991b). Small Mammals: Post-discard Patterning of!Kung San Fauna Remains. *Journal of Anthropological Archaeology*, 10, 152–192.

Zeder, M. A. (2012). The broad spectrum revolution at 40: Resource diversity, intensification, and an alternative to optimal foraging explanations. *Journal of Anthropological Archaeology*, 31(3), 241–264.

Zeder, M. A. (2015). Reply to Mohlenhoff et al.: Human behavioral ecology needs a rethink that niche-construction theory can provide. *PNAS*, 112(24), E3094.

Chapter 4

The Effects of Small Mammal Prey Body Size on the Taphonomy and Zooarchaeology for Human and Avian Agents

4.1 Introduction

Small mammal fossil assemblages are typically the product of long-term avian habitation in locations such as caves or rock shelters where pellets and discarded animal remains accumulate over time (Andrews, 1990). As small mammals have smaller home ranges and are adapted to specific ecological niches (Reed, 2003), the relative abundances of small mammals can provide critical ecological information about the past (Fernandez-Jalvo, 1995; Fernández-Jalvo and Andrews, 2011; Louchart et al., 2009; Stoetzel et al., 2011; Lopez, 2020), such as habitat structure, productivity, predation, and distances between similar habitats (Avenant, 2000; Nel et al., 2016). Perhaps more accurately, these assemblages tend to reflect the diets and behaviors of

predatory birds who forage in specific habitats before regurgitating pellets (Andrews, 1990). Reconstructing the taxonomic composition and taphonomic damage caused by hunting and consuming small mammals by avian predators therefore provides an indication as to the most frequently exploited habitat and the type of raptor responsible for the assemblage.

More recently, the role of smaller animals as a dietary resource for modern humans and ancient hominins is receiving greater attention and has been documented as far back as 1.75 million years ago at Oldupai Gorge (Fernandez-Jalvo et al., 1999). Evidence for small prey exploitation by *Homo erectus* (Lebreton et al., 2017), Neanderthals (Brown et al., 2011; Hardy et al., 2013; Morin et al., 2019), and modern humans (Real, 2020; Andrade and Fernández, 2017; Sathe, 2017) suggests a long history of consuming smaller mammals. However, discussion surrounding the utility of small mammal exploitation is heavily centered on the Upper Paleolithic faunal assemblages in Eurasia where interpretations for an increased abundance of leporid remains as a dietary expansion due to resource depletion and/or environmental changes are debated (Cochard et al., 2012; Fa et al., 2013; Lloveras et al., 2011; Stiner, 2009; Stiner et al., 2009, 2000; Tortosa et al., 2002; Zeder, 2012). In this view, smaller animals are used as signals for foraging efficiency, a perspective that has and continues to be challenged due to evidence of small game exploitation in the Middle (Broughton et al., 2011; Haws and Hockett, 2004; Morin et al., 2019) and Lower Paleolithic of Eurasia (Lebreton et al., 2017). Analyzing small mammal assemblages also has the potential to reveal information about paleodemography (Stiner et al., 2001; Stiner, 2009; Stiner et al., 1999; Stiner, 2002), population mobility and landscape use (Hockett and Haws, 2002; Stiner et al., 1999), site occupation intensity (Hockett and Haws, 2002; Lupo and Schmitt, 2005; Stiner, 2013), division of labor (Bird et al., 2005a), socioeconomic status (Schmitt and Lupo, 2008), environmental and economic stress (Lupo, 2007), technological complexity (Wadley, 2010; Jones, 2006), and the tran-

sition to domesticated resources (Munro, 2004). The challenge in analyzing small mammal bone assemblages is confidently attributing the bone accumulators given the potential for multiple agents, including avian, human, and other carnivore, or possibly from intrusive deposition.

Assessing the accumulator for small mammal bone assemblages requires identifying the taphonomic signature of different predators (Andrews, 1990). Unfortunately, there is a lack of actualistic and observational studies involving diverse predators and prey species (Armstrong, 2016). The majority of experiments involve leporids and primates as prey and raptors and mammalian carnivores as predators, respectively (Armstrong and Avery, 2014; Pobiner et al., 2007; Álvarez et al., 2012; Domínguez-Solera and Domínguez-Rodrigo, 2011; Lloveras et al., 2010, 2012a,b). Observational studies of small mammal hunting also tend to focus on foraging returns and hunting strategies (Ugan, 2005; Yellen, 1991a) with few documenting the taphonomic variation of skinning, disarticulating, and defleshing small animals (Lloveras et al., 2009). Moreover, the criteria established by these and other studies to characterize predator taphonomic signatures are highly variable, with some raptor studies reporting low levels of bone damage (Bochenski et al., 2009; Hockett, 1996) and others reporting extensive bone modification (Andrews, 1990; Lloveras et al., 2008b; Cruz-Uribe and Klein, 1998). To overcome this problem, some studies have attempted to analyze the feeding behavior of various predators through controlled feeding experiments (Armstrong, 2016, 2015; Comay and Dayan, 2018) to better understand how the range of prey skeletal morphologies, body sizes, and other characteristics affect the taphonomic profile of small mammals.

Originally defined by Brain (1981), small mammals have typically been referred to any mammalian species weighing less than 5 kg. This extraordinary broad category contains animals of diverse body plans, sizes, and behaviors that live in a range of habitats and environments, all of which contribute to predator acquisition strategies

and feeding behaviors. This, in turn, produces a range of taphonomic variation among different prey taxa due to morphological differences and body size. For example, the range of mammalian prey body sizes typically consumed whole by the common barn owl (*Tyto alba*) extends up to roughly 80 g before the prey is dismembered and consumed in parts (Vanitha and Kanakasabai, 2009). Diurnal raptors, such as eagles, hawks, and harriers, engage in a similar feeding behavior when consuming prey too large to digest whole (Andrews, 1990). While this behavior is well documented, the resulting taphonomic profile of the skeletal element patterning and bone surface modifications is less well-defined.

The small mammal assemblage at Liang Bua (Flores, Indonesia) poses a unique taphonomic problem compared with other small mammal bone assemblages. First, the overwhelming majority of identified small mammal remains at Liang Bua belong to the Murinae subfamily (Old World rats and mice) of rodents, consisting of prey species that are lacking in comparative taphonomic studies. Second, the murine species recovered from Liang Bua range in body size from roughly 50 g up to 3.5 kg (Veatch et al., 2019). Prior to ~3 ka at Liang Bua, the possible accumulating agents responsible for the small mammal assemblage are limited to either raptors or hominins since the island lacks any endemic mammalian carnivores and the endemic reptilian carnivore (Komodo dragon) tends to dissolve bone completely once ingested (Sutikna et al., 2018; D'Amore and Blumenschine, 2009). It is also likely that prey remains deposited from avian and hominin activity become interspersed given the likelihood of overlapping activity between these two potential predators at the site. Thus, more actualistic experiments involving avian and human subjects consuming murines of diverse body sizes are needed to compare skeletal element profiles, fragmentation, and bone damage between these two predators, and thus, refine criteria to identify the accumulators of the small mammal remains at Liang Bua.

To this end, two experimental studies were conducted to test how prey body size

affects the taphonomic signature of each predator. The first involves an ethnoarchaeological study where individuals from neighboring hamlets surrounding Liang Bua volunteered to provide the bones of hunted wild animals for taphonomic analysis. The second involves an actualistic experiment where rats of various body sizes were fed to two Verreaux's Eagle Owls (*Bubo lacteus*), King vultures (*Sarcoramphus papa*), and Lappet-faced vultures (*Torgos tracheliotos*) at Zoo Atlanta in Atlanta, GA, USA. Thus, the aims of this chapter are to: (1) expand the range of taphonomic studies to consider prey of various body sizes of the same skeletal plan; (2) explore the taphonomic variation caused by avian and human damage; and (3) develop criteria that can be used to identify or exclude the accumulators of small mammal remains in archaeological bone assemblages.

4.2 Methods and Materials

Observational experiment: Hunting and cooking sample preparations

A total of 16 volunteers from the neighboring hamlets of Liang Bua (Teras, Bere, Golo Manuk, and Langke) agreed to participate in the form of either a "hunter" or "chef" (IRB00100901). Hunting often took place at night because this is when the animals are most active. Each hunting group was provided a handheld GPS device to track the location of their hunt while searching for and capturing local small animals (Figure 4.1). Participants traveled relatively short distances before successfully capturing an animal (longest hunt recorded was 10.85 km with an average distance of 4.31 km) upon which the animals were brought back to their homes and prepared the following day. It is important to note that participants in the study did not consume any animal that was not already part of their diet or hunt animals considered vulnerable or endangered under the IUCN Red List.

During the 2018 field season, a total of 10 hunting excursions produced 15 small

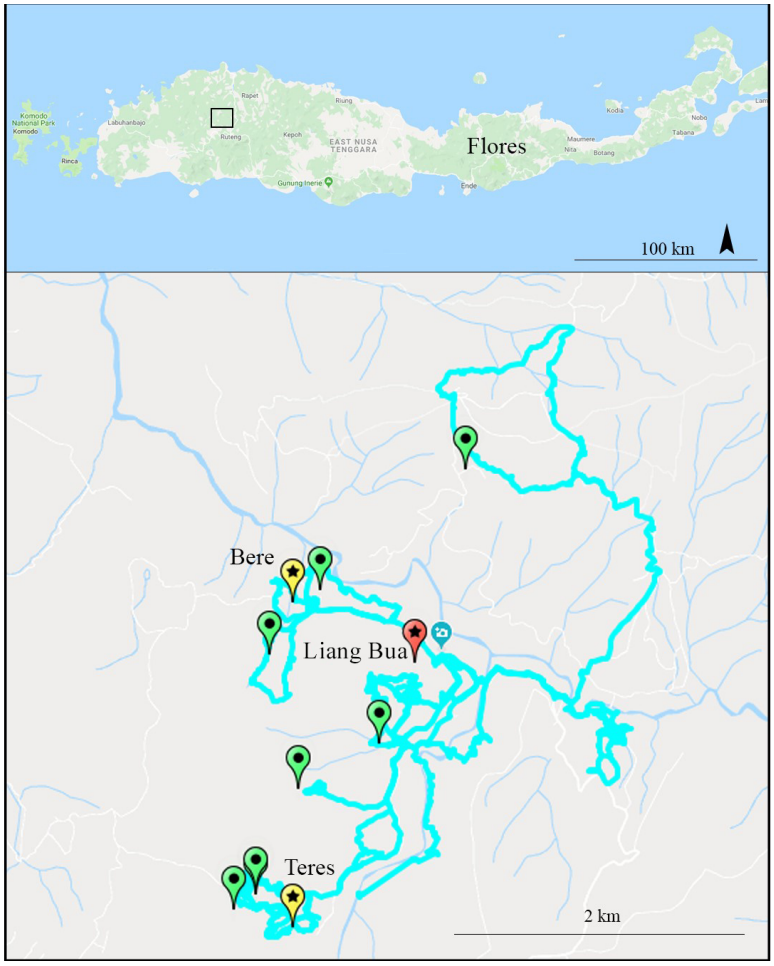

Figure 4.1: Foraging pathways recorded using GPS. Liang Bua is shown with a red pin, and Bere and Teras shown with a yellow pin. Locations where animals were captured are marked with a green pin. Rivers are shown in blue and roads are shown in white.

Figure 4.2: Parang and pisau used for the disarticulation of small animals.

animals (Table 4.1). All animals underwent a similar cooking process: first, animals were roasted over a fire pit to cook the meat while also singeing the fur from the body (if mammal) (Figure 4.3). Participants often used a bamboo stick to brush the burnt fur off the body as they disintegrated. Water was also frequently poured over the animal to help clean the body after being exposed to open flames. After the animal was cooked (often until the body was no longer "limp"), each specimen was placed on several banana leaves and eviscerated before being chopped, cut, and disarticulated using a parang (a long and slightly curved metal knife), a pisau (small metal knife), and/or hands (Figure 4.2). One animal (ID 10) was hung up vertically while being eviscerated and disarticulated instead of on a flat surface. In all cases, the main goal of the butcher was to reduce the animal into small portions that could easily fit in a small pot to boil with vegetables and spices creating a stew-like dish to be served over rice. After the meal was completed, all participants were instructed to carefully collect bones that were not consumed for taphonomic analysis.

The 2019 field season focused on hunting the giant rat, *Papagomys armandvillei*, and participants switched to using stone tools and bamboo knives in replacement of the metal knives. This change was to consider how non-modern (flaked chert) and biodegradable (bamboo knives) tools affect the frequency, location, and/or shape of cutmarks on the bone surfaces of smaller animals. Together with the 2018 data set, this provided a total sample of seven *P. armandvillei* butchered with parangs (n=3), stone tools (n=3), and bamboo (n=1). All animals underwent similar cooking and preparation processes as the 2018 sample. However, video recordings were not

Figure 4.3: Participant holding the tail of a giant rat *Papagomys armandvillei* while singeing the hairs off the animal by roasting it over a fire.

Table 4.1: Summary of animals collected around Liang Bua

Year	ID	Taxon	Number of individuals	Tools used	Age	Weight (g)	Manggarai	Indonesian	English
2017	13	*Papagomys armandvillei*	1	Parang	young adult	N/A	Betu	Tikus besar	Giant rat
2018	5	*Dobsonia peronii*	1	Parang	juvenile	600	Niki	Kalong	Western naked-backed fruit bat
2018	9	*Dobsonia peronii*	6	Parang	adult	3600	Niki	Kalong	Western naked-backed fruit bat
2018	8	*Macaca fascicularus*	1	Parang	juvenile	800	Kode	Monyet	Macaque
2018	6	*Papagomys armandvillei*	1	Parang	adult	2500	Betu	Tikus besar	Giant rat
2018	10	*Papagomys armandvillei*	1	Parang	adult	1300	Betu	Tikus besar	Giant rat
2018	2	*Paradoxurus hermaphroditus*	1	Parang	adult	4800	Kula	Musang	Civet
2018	1	*Pitta* sp.	1	Parang	unknown	80*	Caker	Burung	Blue-winged pitta
2018	3	*Rattus rattus*	1	Parang	adult	600	Lawo	Tikus	Black rat
2018	4	*Varanus* sp.	1	Parang	juvenile	700	Veti	Biawak	Varanid
2019	20	*Dobsonia peronii*	1	Stone Tools	adult	N/A	Niki	Kalong	Western naked-backed fruit bat
2019	16	*Hystrix javanica*	1	Stone Tools	juvenile	1800	Motang	Landak	Porcupine
2019	14	*Papagomys armandvillei*	1	Bamboo	adult	3900	Betu	Tikus besar	Giant rat
2019	17	*Papagomys armandvillei*	1	Stone Tools	young adult	1100	Betu	Tikus besar	Giant rat
2019	18	*Papagomys armandvillei*	1	Stone Tools	young adult	1400	Betu	Tikus besar	Giant rat
2019	19	*Papagomys armandvillei*	1	Stone Tools	juvenile	700	Betu	Tikus besar	Giant rat
2019	15	*Rattus rattus*	1	Bamboo	adult	N/A	Lawo	Tikus	Black rat

* Estimated body weight based on species average (74-90 g) (Erritzoe, 2020).

collected during this field season.

All of the 2018 and 2019 animal bones were cleaned using a combination of 2 parts water and 1 part hydrogen peroxide (3% solution) and are curated at Pusat Penelitan Archeologi Nasional (ARKENAS), the National Research Center for Archaeology, in Jakarta, Indonesia. The 2018 sample was analyzed prior to the start of the 2019 field season. Unfortunately the remaining 2019 sample was not analyzed due to travel restrictions caused by the COVID-19 outbreak. Therefore, the focus of this study will report on the taphonomic and videographic data collected from the 2018 field season.

Video recordings of each cooking session were analyzed using BORIS, an event coding software for behavioral data. A combination of state and point events were identified and recorded to measure the frequency and duration of butchery behavior, such as roasting, cutting, and chopping, for each animal (Table 4.2). A series of linear regression models were performed to determine whether animals body size affected how the animal was butchered as well as the resulting taphonomic affects left on the bone surfaces. Finally, informal interviews and conversations with participants on hunting were taken to better understand the decisions made while hunting for and

Table 4.2: Ethogram for recording the types of behaviors observed while preparing the animals.

Ethogram:		
Code	Type	Description
Roasting	State	When the animal is in contact with the flames over a fire
Picking	State	When a participant removes the fur/feathers from the animal, either by hand or by tool
Butchering	State	The act of dismembering, tearing, removing or disarticulating parts of the animal by tool and/or hand
Stewing	State	When the animal is contained in an iron pot roasting over the fire
Cleaning	State	The act of pouring water over the animal, rinsing, or scraping the animal to clean it
Chopping	Point	Single action event where a tool is used forcefully to separate or disconnect tissue
Slicing/cutting	Point	Single action event where a tool is used to carefully remove soft tissue from bone, usualy at a 45 degree angle in a single slice motion
Sawing	Point	A repeated forward and backward motion using a knife to cut tissue

cooking small game.

Actualistic experiment: Feeding sample preparation

A series of controlled feeding sessions took place at Zoo Atlanta to determine how prey body size affects raptor taphonomic signatures, specifically within owl and vulture species. Verreaux's Eagle Owl, also known as the Milky Eagle Owl (MEO), is a raptor with low to medium degrees of modification that overlap with damage caused by the common barn owl (*Tyto tyto*) and eagles (*Aquila* sp.) (Andrews, 1990), the two most likely raptors responsible for the small mammal assemblage at Liang Bua (Meijer et al., 2013). Two MEO individuals were fed a total of 13 rats of small (n=4), medium (n=2), and large (n=2) body sizes. Similarly, one King vulture was fed a total of 5 rats of medium (n=4) and large (n=1) body size and two Lappet-faced vultures were fed a total 37 rats of small (n=31), medium (n=4), and huge (n=2) body sizes. The average weight of the rats within the small, medium, large, and huge body size categories are defined in this study as 47 g, 175 g, 501 g, and 816 g, respectively. All rat specimens were procured through Zoo Atlanta and are within the dietary restrictions for each animal.

The rats were first weighed collectively to record the total "wet" weight, body size, and number of rats prior to feeding. The staff was instructed to feed the raptors only mice in between the scheduled feeding sessions in order to minimize unwanted remains in the resulting owl pellets and vulture casts (regurgitated mass). The raptors were

perceived to be done when either the animal swallowed the feed whole or when the birds cleaned their beaks by rubbing them against a flat surface. Duration of feeding varied from 12 minutes to an hour and a half depending on the size of the feed. All pellets and casts from the enclosure were collected upon notification from Zoo staff following the feeding session and/or before other scheduled meals. Surface finds (i.e., unwanted or unfinished rats) were not included in analysis because the study focused on skeletal elements contained within the pellets to reflect an assemblage of pellet-only accumulation. Also, any remaining flesh or rat carcasses were not re-introduced into the enclosures for a secondary feeding to more accurately reflect feeding behavior in the wild (i.e., owls tend to not return to a feeding site and continue feeding on a previous meal). A total of 3 pellets containing small, medium, and large sized rats were collected from the MEO enclosure while the King vulture produced 1 cast of a medium sized rat and 2 partially consumed surface remains from the extra-larger body size group. The Lappet-Faced vultures consumed all introduced rat samples but no casts were recovered following these sessions (i.e., samples were fully digested). Partially digested bone fragments were removed from the pellets and cast using tweezers, identified to skeletal element, measured, and photographed.

4.2.1 Zooarchaeological and Taphonomical Methods

Skeletal element representation and quantification

For both studies, the portion of preserved bone was identified along with the orientation of paired elements (left or right) regardless of size. Most specimens were identified to a specific skeletal element. Specimens lacking diagnostic or discernible features were labeled as either vertebrae fragment, cranial fragment, or long bone shaft fragment where possible, or unidentified fragment. The maximum length of all bone fragments were measured using digital hand calipers to the nearest 0.01 mm.

A series of zooarchaeological indices was calculated to document the skeletal com-

position of each sample. These included: number of specimens (n), number of identified skeletal specimens (NISP), minimum number of elements (MNE), minimum number of individuals (MNI), and minimum anatomical units (MAU) (Lyman, 1994). The fraction-summation method was used to calculate MNE following Klein and Cruz-Uribe (1984) and involves recording a portion of features identifiable on each specimen on a 10% scale between 0 and 1. This method is particularly effective for recording small mammal bones since these elements tend to preserve better than large mammal bones, and tend to fracture in consistent locations while retaining diagnostic features. MNI and MAU were calculated by taking the maximum MNE value of a sample and then dividing element (i) MNE value by the number of times i occurs in the skeleton, respectively (Lyman, 1994).

Measuring the frequency of observed skeletal elements against the expected is critical to understanding how different anatomical parts are affected by predators (i.e., butchering and digestion). In small mammal taphonomy, the most commonly used index to capture this value is the Relative Abundance Index (RA). Here, the relative abundance of each element was calculated using the following formula proposed by Dodson and Diane (1979) and Brain (1969):

$$\%RA = 100 \times \frac{MNE_{\mathrm{i}}}{MNI \times E_{\mathrm{i}}} \tag{4.1}$$

where %RA: relative abundance, $\mathrm{MNE_i}$: minimum number of skeletal elements i, MNI: minimum number of individuals, $\mathrm{E_i}$: the number of times element i occurs in the prey skeleton.

Principal components analyses (PCA) were performed using the relative abundance (%RA) of skeletal elements from each predator-prey group (e.g., MEO-small, Human-giantRats) to determine if skeletal-part profiles can be used to differentiate between predator type (avian and human). To facilitate the interpretations of the multivariate analysis, an ANOVA was run to determine if the intra- and inter-specific

differences observed within each predator-prey group were significant. Published data from Armstrong (2015), Armstrong and Avery (2014), and Andrews (1990) were included in the statistical comparisons to consider how other avian predators and prey types, as well as samples collected from wild owl pellets and eagle nests, compare with the results of this study.

Finally, in order to evaluate the relationship between recovered skeletal elements, four indices were calculated following Andrews (1990), including: postcranial to cranial elements ((femora + humeri) / (mandibles + maxillae)), lower limb versus upper limb elements ((tibia + ((radius + ulna)/2)) / (femur + humerus)), anterior to posterior limb elements ((scapula + humerus + ((radius + ulna)/2)) / (pelvis + femur + tibia)), and axial to appendicular elements ((atlas + axis + (cervical/5) + (thoracic/12) + (lumbar/7) + (sacra/4)) / ((humerus/2) + (radius/2) + (ulna/2) + (femur/2) + (patella/2) + (tibia/2))). Values greater than 1 indicate a greater representation of postcrania, lower limbs, anterior limbs, and appendicular limbs, relative to cranial, upper limb, posterior limb, and axial elements, respectively.

Long Bone Fragmentation and Breakage

Patterns of long bone fragmentation were summarized according to the frequency of complete, proximal, shaft, and distal fragments by each predator (Tables 4.13 and 4.6). Long bone breakage morphology (fracture angle, fracture outline, and fracture edge) was recorded following **?**, with the addition of recording a secondary entry for the fractured outline, and summarized according to body size (where possible) and predator (Tables 4.14 and 4.7). Recording a secondary outline entry was made because small mammal long bone shafts aren't as cylindrical as human bones (the sample for which these categories are based), and thus, they tend to break slightly differently when fresh or dry. A second entry therefore allows for more detailed assessment where there is more than one adequate descriptor for the outline of a break. Degrees

of fragmentation for all bones were estimated by considering the relationship between NISP and MNE values for each element (Tables 4.11 and 4.5).

Surface Modifications

Each element was analyzed for bone surface modifications (BSM) using a 20x-220x DinoLight digital microscope with an extended depth of field and a 20X handheld lens. Surface alterations due to digestion (e.g., acidic punctures and corrosive etching) of teeth and bones were observed and recorded following Andrews (1990) and summarized according to Lloveras et al. (2008a). The frequency and location of the following modification types were recorded:

- **Punctures**: The bone surface has collapsed under localized pressure creating a hole in the cancellous and cortical bone (Binford, 1981; Fernández-Jalvo and Andrews, 2016; Armstrong and Avery, 2014). Possible agents responsible include carnivores, plants, insects, birds, and humans (Fernández-Jalvo and Andrews, 2016).

- **Pits**: Circular indentations on the cortical bone surface that does not penetrate cancellous bone (Binford, 1981; Blumenschine, 1988; Blumenschine et al., 1996; Landt, 2007; Fernández-Jalvo and Andrews, 2016). Possible agents responsible include carnivores, insects, birds, and trampling (Fernández-Jalvo and Andrews, 2016). Human teeth also create "pits" but are distinct and are described separately below.

- **Scores**: Linear indentations on the exterior surface of bone that form straight, curved, or sinuous trajectories (Binford, 1981; Blumenschine et al., 1996; Landt, 2007; Shipman, 1981; Fernández-Jalvo and Andrews, 2016). Possible agents responsible include carnivores, plants, insects, birds, and humans (Fernández-Jalvo and Andrews, 2016). Possible agents responsible for creating linear marks

with U-shaped cross section include carnivore chewing, plant roots, insects, beak marks, herbivore and rodent gnawing whereas those with V-shaped cross section include human cut marks and carnivore teeth(Fernández-Jalvo and Andrews, 2016).

- **Notches**: Semi-circular indentations located along a broken bone margin or bone edge (Binford, 1981; Blumenschine et al., 1991; Brain, 1981; Capaldo and Blumenschine, 1994; Fernández-Jalvo and Andrews, 2016). Possible agents responsible include human percussion marks and carnivores (Fernández-Jalvo and Andrews, 2016). Human tooth marks can also cause double-arched notches when chewing bone (Fernández-Jalvo and Andrews, 2011).

Marks that met specific criteria associated with human modification were identified using the following definitions:

- **Cutmarks**: Criteria for defining cutmarks are highly variable due to morphological similarities with carnivore tooth marks and experimentally made trampled assemblages (Potts and Shipman, 1981; Shipman, 1983; Blumenschine et al., 1996; Domínguez-Rodrigo et al., 2009a, 2012; Fernández-Jalvo and Andrews, 2016). For the purposes of this experimental study, cutmarks were identified using features outlined by Domínguez-Rodrigo et al. (2009a). Cutmark morphology was further categorized using criteria outlined by Thompson et al. (2015): 1) slice: an angled incision to the bone surface; 2) cut: an incision perpendiicular to the bone surface; 3) shave: small curls of bone peeling away from a slice; 4) scrape: broad, shallow fields often with dimpling; 5) single chop: short, deep cuts; 6) repeated chops: deep, broad, non-parallel striations (Potts and Shipman, 1981); 7) and saw: multiple striae occurring in a patch.

- **Human tooth marks**: Like cutmarks, marks formed by human teeth are highly variable, and can include double-arched punctures and/or pits, crescent

shaped pit with internal striations, wide and shallow linear scores caused by dragging incisors on the bone surface, and triangular puncture marks made from premolars and canines (Landt, 2007, 2004; Fernández-Jalvo and Andrews, 2016, 2011).

4.3 Results

4.3.1 Observational experiment: rat butchery

Videographic data

A series of linear regression models were used to test whether animal body size affects the way that animals are butchered (Figure 4.4). All variables are positively correlated with body size, but total preparation time (Figure 4.4 A) was the only variable that showed a significant relationship with animal body size ($p = 0.049$, adj $R^2 = 0.48$). However, the individual amount of time spent stewing, cleaning, butchering, picking, or roasting did not show significant relationships with animal body size ($p > 0.05$). Interestingly, the amount of observed cutmarks for each individual animal was significantly correlated with the total amount of point events ($p = 0.03$, adj $R^2 = 0.54$) (i.e., the total number of times a participant cut, sawed, or chopped the animal using a tool). While the relationship between animal body size and total point events was not significant below the 0.05 level ($p = 0.06$), the strong correlation between the two suggest that greater processing intensity is somewhat related to animal body size, and can potentially be inferred from the frequency of cutmarks in a fossil assemblage.

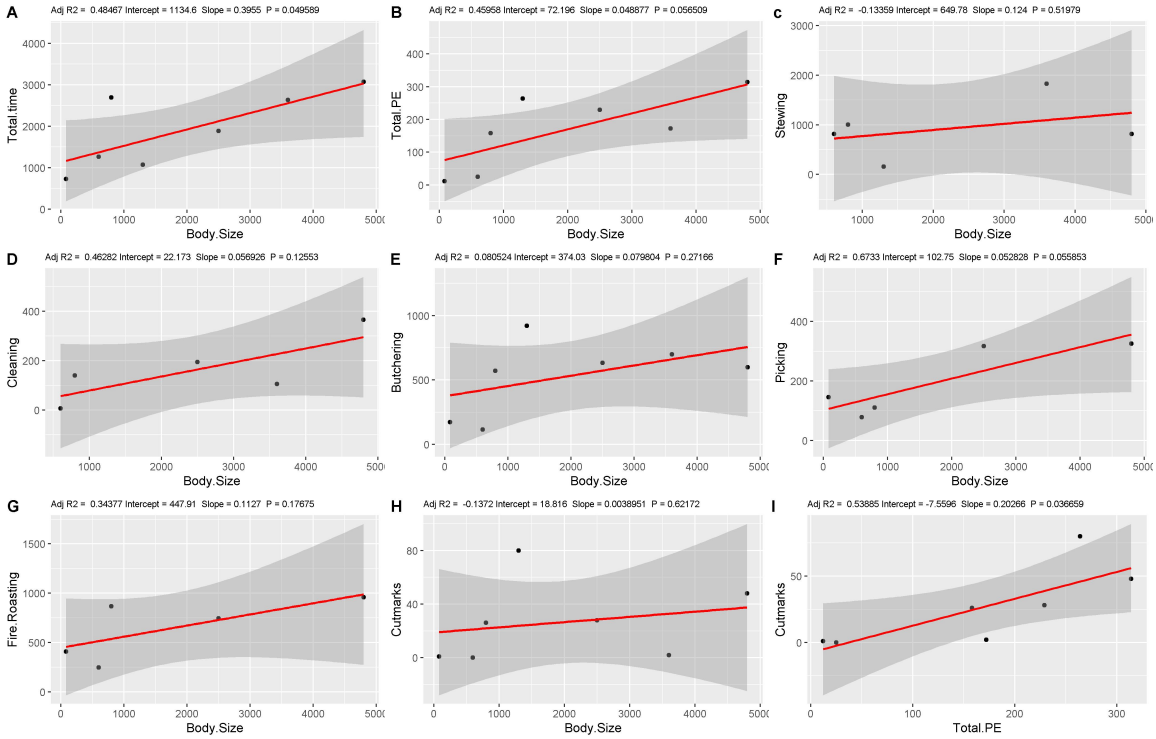

Figure 4.4: (A – G) Linear regression models showing the relationship between animal body size (g) and time (seconds) spent in each activity, as well as (H) animal body size (g) and the total point events. (I) Linear regression model of total point events against number of observed cutmarks.

Skeletal element representation

A total of 1,514 bones and bone fragments were recovered from butchering small animals and 1,134.4 (75%) of these make up the total minimum number of skeletal elements (MNE). A total of 1,319 elements (968.1 MNE) belonged to mammalian species (73%) while the remaining 27% of elements belonged to avian and varanids. Overall, the dentary and long bone elements were the most consistently well represented elements across all mammalian species, with the axial and distal appendage elements showing greater variation among individuals.

Table 4.3 shows the anatomical composition of the total bone sample. The average relative abundance for mammalian species was calculated at 52.2% indicating a considerable loss of bone. The results also demonstrate that the teeth, mandibles,

Table 4.3: Summary of zooarchaeological index values (NISP, MNE, MNI, MAU, %RA)

Papagomys armandvillei	MNI	3			*Rattus rattus*	MNI	1		*Macaca fascucularis*	MNI	1		*Dobsonia peronii*	MNI	7		*Paradoxurus hermaphroditus*	MNI	1	
Element	NISP	MNE	MAU	RA	NISP	MNE	MAU	RA	NISP	MNE	MAU	RA	NISP	MNE	MAU	RA	NISP	MNE	MAU	RA
Crania	10	4	0.2	6.7	15	15	0.8	75.0	17	15	0.8	75.0	66	58.8	2.9	42.0	16	16	0.8	80.0
Maxilla	6	3	1.5	50.0	2	2	1.0	100.0	2	2	1.0	100.0	10	10	5.0	71.4	2	2	1.0	100.0
Mandible	6	6	3.0	100.0	2	2	1.0	100.0	2	2	1.0	100.0	11	11	5.5	78.6	2	2	1.0	100.0
Teeth	48	48	3.0	100.0	16	16	1.0	100.0	19	19	0.8	79.2	102	102	3.6	52.0	28	28	0.9	87.5
Clavicle	4	4	2.0	66.7	0	0	0.0	0.0	1	1	0.5	50.0	0	0	0.0	0.0	0	0	0.0	0.0
Rib	71	55.6	1.5	51.5	4	3	0.1	8.3	18	17	0.5	47.2	77	59.8	1.7	23.7	38	13.5	0.4	37.5
Atlas	2	2	2.0	66.7	0	0	0.0	0.0	1	1	1.0	100.0	2	1	1.0	14.3	1	1	1.0	100.0
Axis	2	2	2.0	66.7	0	0	0.0	0.0	1	1	1.0	100.0	2	1	1.0	14.3	1	1	1.0	100.0
Cervical	10	7	1.0	33.3	5	5	0.7	71.4	5	4	0.6	57.1	12	10	1.4	20.4	3	3	0.4	42.9
Thoracic	34	6	0.5	15.4	9	9	0.7	69.2	12	11.5	0.9	88.5	46	43	3.3	47.3	15	6.3	0.5	48.5
Lumbar	15	1	0.2	5.6	3	2.5	0.4	41.7	6	6	1.0	100.0	24	23.5	3.9	56.0	8	5.7	1.0	95.0
Sacral	6	1	0.3	8.3	0	0	0.0	0.0	3	3	0.8	75.0	3	3	0.8	10.7	4	3	0.8	75.0
Caudal	39	36	1.0	33.3	0	0	0.0	0.0	16	15	0.4	41.7	2	2	0.1	0.8	20	14.2	0.4	39.4
Scapula	7	4	2.0	66.7	1	1	0.5	50.0	2	2	1.0	100.0	11	8.9	4.5	63.6	5	2	1.0	100.0
Innominate	7	4	2.0	66.7	2	2	1.0	100.0	1	1	0.5	50.0	6	6	3.0	42.9	5	2	1.0	100.0
Humerus	8	4	2.0	66.7	2	2	1.0	100.0	2	2	1.0	100.0	21	10.8	5.4	77.1	8	2	1.0	100.0
Radius	9	5	2.5	83.3	2	2	1.0	100.0	1	1	0.5	50.0	13	10	5.0	71.4	3	2	1.0	100.0
Ulna	5	5	2.5	83.3	2	2	1.0	100.0	1	1	0.5	50.0	0	0	0.0	0.0	4	2	1.0	100.0
Femur	11	6	3.0	100.0	2	2	1.0	100.0	1	1	0.5	50.0	10	9	4.5	64.3	5	2	1.0	100.0
Tibia/Fibula	12	6	3.0	100.0	2	2	1.0	100.0	1	1	0.5	50.0	8	8	4.0	57.1	5	2	1.0	100.0
Patella	0	0	0.0	0.0	0	0	0.0	0.0	0	0	0.0	0.0	0	0	0.0	0.0	0	0	0.0	0.0
Talus	5	5	2.5	83.3	1	1	0.5	50.0	2	2	1.0	100.0	0	0	0.0	0.0	0	0	0.0	0.0
Calcaneus	5	5	2.5	83.3	0	0	0.0	0.0	1	1	0.5	50.0	0	0	0.0	0.0	0	0	0.0	0.0
Phalanges	32	17	0.3	10.1	0	0	0.0	0.0	11	8	0.1	14.3	0	0	0.0	0.0	8	4	0.1	7.1
Metapodials	25	24	1.2	40.0	1	0	0.0	0.0	13	13	0.7	65.0	8	8	0.4	5.7	0	0	0.0	0.0
Compact	9	9	0.4	13.6	0	0	0.0	0.0	0	0	0.0	0.0	0	0	0.0	0.0	0	0	0.0	0.0
Non-ID Fragment	2				0				0				0				1			
Vert Indet.	3				0				0				0				3			
Long Bone Frags	0				0				0				0				6			
n:	393	269.6	AVG:	53.9	71	68.5		48.7	139	129.5		65.1	525	385.8		31.3	191	113.7		62.0
NISP:	388				71				139				525				181			

maxillae, scapulae, pelves, and long bones have the highest survival rate ($> 60\%$), while the crania, ribs, non-caudal vertebrae, and the talus are moderately represented ($> 30\%$). The clavicle, caudal vertebrae, calcaneus, and metapodials are minimal (between 20% and 30%), while the phalanges and compact bones were scarce.

Generally, larger animals, like the giant rats (*P. armandvillei*) and civet (*P. hermaphroditus*), preserved greater frequencies of bone elements compared to smaller animals, such as the black rat (*Rattus rattus*). The macaque preserved the most elements (MNE = 129.5) when controlling for MNI, but the civet also had a high element count (MNE = 113.7) along with the largest number of bones (n = 191; NISP = 181) than the other specimens. This is likely due to the greater processing intensity necessary to reduce a larger animal to fit within a small container for boiling (see Section 4.2). The giant rats (MNI = 3) contained slightly fewer bone fragments per individual (n = 131), while the black rat contained the fewest specimens (n & NISP = 71) and identified elements (MNE = 68.5). Similarly, the fruit bats, also smaller in body size, showed fewer skeletal element abundances (NISP = 75; MNE = 55.1) per individual. The relative abundance (Table 4.3) and skeletal element proportion

indices (Table 4.4) therefore suggest a number of important details.

Table 4.4: Relative values of skeletal elements comparing proportions of postcranial to cranial elements (PC/C)[a], lower limb to upper limb (ZE/ST)[b], anterior to posterior limb elements (AN/PO)[c], and axial to appendicular elements (AX/AP)[d] for each individual

Indices	*Papagomys armandvillei*	*Rattus rattus*	*Macaca fascicularis*	*Dobsonia peronii*	*Paradoxurus hermaphroditus*	*Varanus* sp.	*Pitta* sp.
MNI	3	1	1	7	1	1	1
PC/C	100.0	23.5	17.6	28.4	22.2	22.2	30.8
ZE/ST	110.0	100.0	66.7	65.7	100.0	100.0	87.5
AN/PO	81.3	83.3	166.7	107.4	100.0	100.0	137.5
AX/AP	48.4	42.1	178.8	61.9	93.8	-	-

[a] (femur + humerus) / (mandibles + maxillae) x 100
[b] (tibia + ((radius + ulna)/2)) / (femur + humerus) x 100
[c] (scapula + humerus + ((radius + ulna)/2))) / (pelvis + femur + tibia) x 100
[d] (atlas + axis + (cervical/5) + (thoracic/12) + (lumbar/7) + (sacra/4)) / ((humerus/2) + (radius/2) + (ulna/2) + (femur/2) + (patella/2) + (tibia/2)) x 100.

For the giant rat's (*P. armandvillei*) skeletal element profile, the proportion indices (Table 4.4) suggest the following: 1) postcranial fragments were equally preserved compared to cranial fragments (PC = C); 2) lower limb bones were slightly more frequently preserved than the upper limb bones (ZE > ST); 3) the anterior limb bones were slightly less represented compared to posterior limb bones (AN < PO); and 4) axial bones were underrepresented compared to appendicular bones (AX < AP).

Similarly, the black rat (*R. rattus*) proportion indices (Table 4.11) suggest that: 1) postcranial bones greatly outnumber cranial elements (PC < C); 2) Lower and upper limb bones were equally preserved (ZE = ST); 3) the anterior limb bones were preserved less frequently than the posterior limb bones (AN < PO); and 4) axial bones were underrepresented compared to appendicular bones (AX < AP).

Conversely, the proportion indices for the macaque (*Macaca fascicularis*) (Table 4.11) suggest that: 1) postcranial fragments are significantly underrepresented compared to cranial fragments (PC < C); 2) lower limb bones were less frequently

represented than the upper limb bones (ZE < ST); 3) the anterior limb bones were more frequently represented than the posterior limb bones (AN > PO); and 4) axial bones were more frequently represented than appendicular bones (AX > AP).

The proportion indices for the fruit bats (*Dobsonia peronii*)(Table 4.11) were similar to the macaque, and suggest that: 1) postcranial fragments are underrepresented compared to cranial fragments (PC < C); 2) lower limb bones were less frequently represented than the upper limb bones (ZE < ST); 3) the anterior limb bones were more frequently represented than the posterior limb bones (AN > PO); and 4) axial bones were less frequently represented than appendicular bones (AX < AP).

Lastly, the proportion indices for the civet (*Paradoxurus hermaphroditus*)(Table 4.11), suggest that: 1) postcranial fragments are significantly underrepresented compared to cranial fragments (PC < C); 2) lower limb bones were as equally represented as the upper limb bones (ZE = ST); 3) the anterior limb bones were as equally represented as the posterior limb bones (AN = PO); and 4) axial bones were slightly less frequently represented than appendicular bones (AX < AP).

Fragmentation and breakage patterns

Fragmentation indices (NISP/MNE) and long bone fragmentation patterns were calculated for each individual (Tables 4.5 and 4.6). The black rat (*R. rattus*) showed the least amount of fragmentation among all elements, but the pitta bird, fruit bats, and macaque also showed similar patterns of low degrees of fragmentation (< 1.1). This pattern was similarly observed when excluding podial and dental elements, except for the fruit bats which showed a slightly higher degree of fragmentation, which is likely driven by the greater frequency of long bone breakage (Table 4.6). It is interesting to note that when a single bat (MNI = 1) was butchered, there were relatively few broken long bones (25%), but when multiple individuals (MNI = 6) were butchered together, the frequency of long bone fragments substantially increased (84%). Over-

all, the fragmentation patterns show that larger body sized animals are subject to greater rates of bone breakage, such as the giant rats and civet. When excluding podial and dental elements, the degree of fragmentation increased again in larger animals reflecting the tendency of cranial, long bone, and axial elements to break during butchery.

Table 4.5: Bone fragmentation for individual body sizes: fragmentation [a] (NISP/MNE all bones), fragmentation [b] (NISP/MNE excluding compact bones and teeth), and animal body weight

Species	Fragmentation a	Fragmentation b	Average Animal Body Weight (g)
Rattus rattus	1.03	1.03	60
Pitta sp.	1.08	1.08	80
Dobsonia peronii	1.10	1.17	600
Varanus sp.	1.20	1.09	700
Macaca fascicularis	1.06	1.06	800
Papagomys armandvillei	1.38	1.63	1,900
Paradoxurus hermaphroditus	1.48	1.77	4,800

a NISP/MNE all bones
b NISP/MNE excluding podia and teeth

Table 4.6: Fragmentation of all long bones according to fragment type: NISP (number of identified long bone specimens), complete (unbroken), shaft (diaphysis only), Prox (proximal end of the bone), Dist (distal end of the bone), and Total Fragmentation (sum of shaft, proximal, and distal fragments). The specimens are ordered by net weight (g), smallest to largest body size.

Species	Animal ID	Net body weight (g)	NISP	Complete (%)	Shaft (%)	Prox (%)	Dist (%)	Total Fragments
Rattus rattus	3	60	10	6 (60)		4 (40)		4 (40)
Pitta sp.	1	80	12	4 (33)	1 (8)	5 (41)	2 (16)	8 (66)
Dobsonia peronii	5	600	8	6 (75)		1 (12)	1 (12)	2 (25)
Varanus sp.	4	700	12	12 (100)				0 (0)
Macaca fasicularus	8	800	7	6 (85)		1 (15)		1 (15)
Papagomys armandvillei	10	1300	10	10 (100)				0 (0)
Papagomys armandvillei	6	2500	17	3 (17)	3 (17)	6 (35)	5 (29)	14 (83)
Dobsonia peronii	9	3600	43	7 (16)	6 (14)	21 (48)	9 (21)	36 (84)
Paradoxurus hermaphroditus	2	4800	33		17 (51)	9 (27)	7 (21)	33 (100)
Papagomys armandvillei	13	N/A	5	5 (100)				0 (0)
Total			157	59 (37)	27 (17)	47 (30)	24 (15)	98 (62)

Table 4.7 shows the types of long bone breakage observed for each individual animal. The long bones recovered from the varanid (ID 4), the single bat specimen (ID 5), and two giant rat specimens (ID 10 and 13) did not show any fractured long bone ends. Among all individuals with broken long bones, the fractured ends

showed a greater amount of oblique (typically referring to fresh breaks) fracture angles compared to right angled fractures (typically referring to dry breaks). This is consistent with an overall pattern of fresh breaks characterized by smooth edges and V-shaped/oblique outlines.

Table 4.7: Summary of long bone breakage patterns. Secondary fracture "oblique" and "'curved" outlines are included.

				Fracture Angles				Fracture Outlines				Fracture Edge			
Species	Animal ID	Unbroken ends (n)	Fractured Ends (n)	Oblique	Oblique/Right	Right	Indet.	Oblique	Curved	Intermediate	Transverse	Jagged	Smooth	Intermediate	Indet.
Pitta sp.	1	15	9	9					9				9		
Paradoxurus hermaphroditus	2	16	38	32	4	2		20	24		3	4	32	2	
Rattus rattus	3	5	5	5				2	3			1	2	2	
Varanus hooijer	4	12	0												
Dobsonia peronii	5	9	0												
Papagomys armandvillei	6	18	14		12	1	1	11	9		1	4	7	2	1
Macaca fasicularus	8	6	1	1					1				1		
Dobsonia peronii	9	45	41	31	7	2	1	4	40	5	3	2	35	2	2
Papagomys armandvillei	10	14	0												
Papagomys armandvillei	13	5	0												
Total		145	108	78	23	5		37	86		7	11	86	8	

Bone surface modifications

A total of 244 bone surface modifications (BSM) reflecting butchery (cutmarks) or consumption (tooth marks) were identified (Table 4.8 and Figure 4.5). The most commonly identified anthropogenic marks were slices (39%) followed by classic cutmarks (27%) and deep cutmarks (11%), then by tooth marks (9%), and chopped marks (5%). Pits (2%), punctures (0.4%), and scrapes (3%) were also identified but in extremely low frequencies. The larger animals ($>$ 800 g) all showed a greater percentage of total marks compared to smaller animals ($<$ 800 g). For example, the civet (20%), all three giant rats that were butchered separately (33%, 19%, and 11%), and macaque (14%), have noticeably higher frequencies of anthropogenic marks compared to the varanid (*Varanus* sp.)(1%), fruit bats (*Dobsonia peronii*) (0.8%), black rat (*Rattus rattus*) (0%), and pitta bird (*Pitta* sp.) (0.4%).

The frequency and location of BSM on the three giant rat specimens are summarized in Figure 4.6 and Table 4.9. The ribs showed the greatest frequency of cutmarks, but when accounting for the anatomical unit (i.e., adjusting for the number of times an element occurs in a rat skeleton), the pelvis shows a greater percentage of cut-

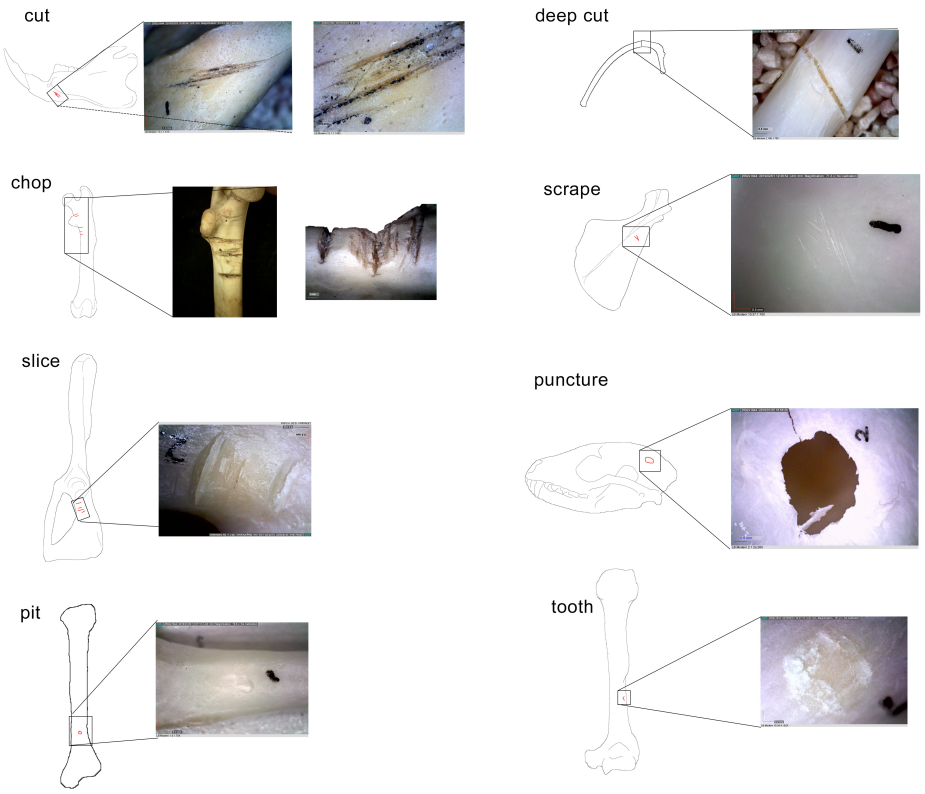

Figure 4.5: Examples of the types of trace marks identified from human butchering and consumption of small animals.

Table 4.8: Count of anthropogenic traces according to individual animal or group of animals butchered together

BSM total summary		BSM Type									
Taxon	Animal ID	Chop	Cut	Deep Cut	Pit	Puncture	Scrape	Slice	Tooth	Indet.	Grand Total
Pitta sp.	1				1						1
Paradoxurus hermaphroditus	2		7	17		1	1	22			48
Rattus rattus	3										0
Varanus sp.	4		1		1			1			3
Dobsonia peronii	5										0
Papagomys armandvillei	6	1	13	1				13			28
Macaca fasicularus	8		13	3			1	17			34
Dobsonia peronii	9				2						2
Papagomys armandvillei	10	3	21	6			3	40	4	4	81
Papagomys armandvillei	13	9	12	1			3	1	17	4	47
Grand Total		13	67	28	4	1	8	94	21	8	244

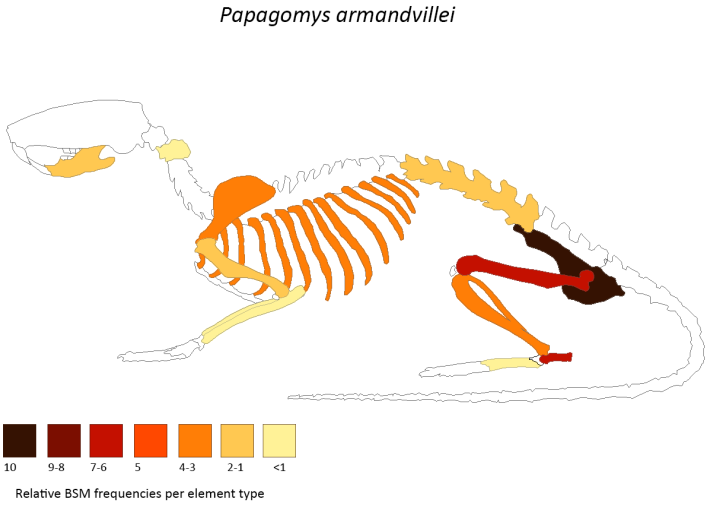

Figure 4.6: Frequency of cutmarks identified on skeletal elements for *Papagomys armandvillei* (n=3) relative to the frequency of element type in one skeleton.

marks, followed by the femur, calcaneus, scapula, tibia, and ribs. The distribution of cutmarks are consistent with disarticulation and defleshing (fire was used to remove mammalian fur so the bones were not skinned, see Section 4.2). Thus, the majority of marks are concentrated near the proximal ends of rib fragments, as well as the proximal and distal ends of long bones. Conversely, tooth marks were more commonly identified along the shaft or midshaft of long bones.

Burning damage was identified on the pitta bird (ID: 1), bats (ID: 9 5), macaque (ID: 8), giant rats (ID: 10), medium rat (ID: 3), and the varanid (ID: 2). The degree of burning damage caused by exposure to fire is summarized in Figure 4.7. Elements

Table 4.9: Location and frequency of bone surface modifications by type recorded from three *P. armandvillei* specimens.

		BSM Type							
Element	**Location**	**Chop**	**Cut**	**Deep Cut**	**Scrape**	**Slice**	**Tooth**	**Indet.**	**Grand Total**
Axis	Body					1			1
Calcaneus	Inferior surface		6			9			15
Clavicle	Shaft	1	2			4			9
	Distal				1	1			
Femur	Proximal epiphysis		1						15
	Proximal shaft	4	6	2				1	
	Midshaft					1			
Humerus	Proximal Shaft					1			5
	Distal Shaft		1				3		
Innominate	Distal Ilium					2			21
	Proximal Ischium					5			
	Ischium Shaft		3			4			
	Pubis		3			4			
Lumbar	Body		2				1		8
	Process			2		1			
	Wing		2						
Mandible	Inferior surface		2					3	5
Metatarsal	Midshaft		2						2
Radius	Distal epiphysis				1				1
Rib	Proximal shaft	6	9	3	1	18	7	2	56
	Midshaft		1				9		
Scapula	Proximal		2	1					8
	Body		1		2	1			
	Border	1							
Tibia	Proximal end		1			1			8
	Proximal Shaft	1							
	Midshaft		1						
	Distal Shaft				2			2	
Ulna	Proximal Shaft					1			3
	Midshaft		1				1		
Grand Total		13 (8%)	46 (29%)	8 (5%)	6 (4%)	54 (35%)	21 (13%)	8 (5%)	156

showing the highest degree of burning are more anteriorly positioned teeth (incisors, canines) and distal appendages (phalanges, distal ends of long bones). This pattern is consistent with other observations of burning in small mammals where the skin and soft tissue protect other elements during direct exposure to fire (Medina et al., 2012). Archaeological specimens reflecting this pattern of carbonized damage along the distal ends of incisors, phalanges, and lower limb bones would therefore reflect intentional and direct burning/roasting.

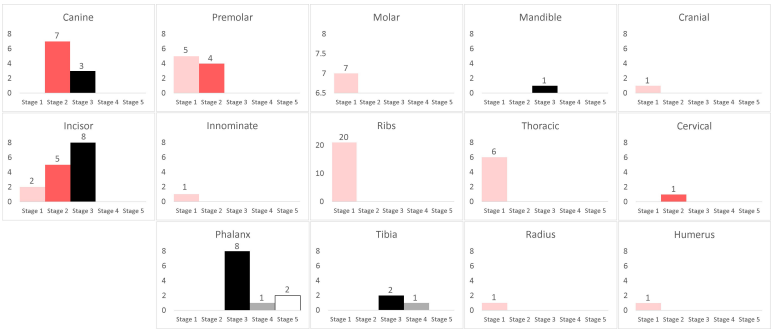

Figure 4.7: Degrees of burning damage according to element. Values represent NISP by burning stage following Stiner et al. (1995).

4.3.2 Actualistic experiment: owl pellets

Skeletal element representation

A total of 1,202 specimens were analyzed from three Milky Eagle Owl (MEO) pellets representing small, medium, and large prey body sizes and one King Vulture cast representing medium prey body size (Table 4.10). The King Vulture consumed all skeletal parts of the large prey size so this sample was not available for analysis. Similarly, the Lappet-faced vultures consumed all prey items from the small, medium, and huge prey body size samples so no casts were recovered from this raptor for analysis. Skeletal element abundances indices from the recovered samples include the total number of identified specimens (NISP), minimum number of elements (MNE), the minimum number of individuals (MNI), and the relative abundance are also shown (Table 4.10). While only four rats were fed to the MEO within the small body size category, the pellets contained a minimum number of eight individuals. Thus, the birds consumed animals as part of their regular diet in addition to those provided as part of this study.

The pellet containing small bodied prey produced the most elements, including in absolute (n = 492) and MNE (211.1) values. The pellet containing medium bodied prey contained fewer bone fragments (n = 198) compared to the large-bodied prey sample (n = 222), but has a greater MNE value (77 MNE) in comparison (34.1 MNE).

Table 4.10: Tabulation of zooarchaeological quantitative units (NISP, MNE, MNI, MAU, %RA) for each MEO pellet and vulture cast collected

MEO-Small	MNI	8			MEO-Medium	MNI	3		MEO-Large	MNI	2		Vulture Medium	MNI	1	
Element	NISP	MNE	MAU	RA	NISP	MNE	MAU	RA	NISP	MNE	MAU	RA	NISP	MNE	MAU	RA
Crania	19	2.6	0.2	1.63	15	2.3	0.2	3.83	13	1.0	0.1	2.50	0	0.0	0.0	0.00
Maxilla	6	2.9	1.8	18.13	2	1.0	0.5	16.67	1	0.7	0.4	17.50	1	1.0	0.5	50.00
Mandible	16	6.9	5.5	43.13	7	2.0	2.0	33.33	2	2.0	1.0	50.00	0	0.0	0.0	0.00
M1	5	3.0	2.5	18.75	1	1.0	0.5	16.67	1	1.0	0.5	25.00	2	1.0	0.5	50.00
M2	5	4.0	2.5	25.00	3	2.0	1.5	33.33	0	0.0	0.0	0.00	2	1.0	0.5	50.00
M3	2	1.0	1.0	6.25	1	1.0	0.5	16.67	0	0.0	0.0	0.00	1	1.0	0.5	50.00
I	9	6.0	4.5	37.50	0	0.0	0.0	0.00	2	1.0	1.0	25.00	2	0.0	0.0	0.00
m1	6	3.0	3.0	18.75	3	2.0	1.5	33.33	0	0.0	0.0	0.00	0	0.0	0.0	0.00
m2	7	5.0	3.5	31.25	2	1.0	1.0	16.67	0	0.0	0.0	0.00	0	0.0	0.0	0.00
m3	1	1.0	0.5	6.25	4	2.0	2.0	33.33	0	0.0	0.0	0.00	0	0.0	0.0	0.00
i	11	8.0	5.5	50.00	5	3.0	2.5	50.00	0	0.0	0.0	0.00	0	0.0	0.0	0.00
Clavicle	5	3.0	2.5	18.75	2	1.0	1.0	16.67	0	0.0	0.0	0.00	0	0.0	0.0	0.00
Rib	38	10.0	0.5	3.47	28	10.0	0.5	9.26	34	3.6	0.2	5.00	0	0.0	0.0	0.00
Atlas	2	0.8	0.8	10.00	2	0.8	0.8	26.67	0	0.0	0.0	0.00	0	0.0	0.0	0.00
Axis	1	1.0	1.0	12.50	1	1.0	1.0	33.33	0	0.0	0.0	0.00	0	0.0	0.0	0.00
Cervical	14	9.6	1.4	17.14	10	3.6	0.5	17.14	2	1.1	0.2	7.86	0	0.0	0.0	0.00
Thoracic	14	11.2	0.9	10.77	3	2.3	0.2	5.90	2	1.0	0.1	3.85	0	0.0	0.0	0.00
Lumbar	18	15.6	2.6	32.50	5	3.4	0.6	18.89	6	3.1	0.5	25.83	0	0.0	0.0	0.00
Sacral	5	3.8	1.0	11.88	3	1.7	0.4	14.17	2	0.7	0.2	8.75	0	0.0	0.0	0.00
Caudal	30	29.3	0.8	10.17	10	9.4	0.3	8.70	2	1.3	0.0	1.81	0	0.0	0.0	0.00
Scapula	10	4.5	4.3	28.13	2	1.0	0.9	16.67	1	0.7	0.4	17.50	0	0.0	0.0	0.00
Innominate	13	4.0	3.9	25.00	5	2.0	1.5	33.33	1	0.2	0.1	5.00	0	0.0	0.0	0.00
Humerus	8	2.0	2.0	12.50	4	2.0	1.5	33.33	3	2.0	1.5	50.00	0	0.0	0.0	0.00
Radius	5	2.0	1.5	12.50	3	2.0	1.0	33.33	4	1.0	1.0	25.00	1	1.0	0.5	50.00
Ulna	6	3.5	2.3	21.88	2	1.0	1.0	16.67	3	2.0	1.5	50.00	0	0.0	0.0	0.00
Femur	16	5.0	3.5	31.25	2	1.0	1.0	16.67	1	0.0	0.5	0.00	0	0.0	0.0	0.00
Tibia/Fibula	14	4.5	4.0	28.13	2	1.0	0.5	16.67	1	0.7	0.4	17.50	0	0.0	0.0	0.00
Patella	0	0.0	0.0	0.00	0	0.0	0.0	0.00	0	0.0	0.0	0.00	0	0.0	0.0	0.00
Talus	7	4.0	3.5	25.00	1	1.0	0.5	16.67	0	0.0	0.0	0.00	0	0.0	0.0	0.00
Calcaneus	7	4.0	3.5	25.00	1	1.0	0.5	3.00	0	0.0	0.0	0.00	0	0.0	0.0	0.00
Phalanges	45	41.0	0.7	9.15	13	12.5	0.2	7.44	8	8.0	0.1	7.14	0	0.0	0.0	0.00
Metapodials	10	9.0	0.6	5.63	5	2.0	0.2	3.33	6	3.0	0.2	7.50	0	0.0	0.0	0.00
Non-ID Fragment	51				29				67				0			
Vert Indet.	29				3				21				0			
Long Bone Frags	13				2				16				0			
Compact Indet.	21				1				3				0			
Cranial Frag.	23				16				20				0			
n:	492	211.2	AVG:	19.00	198	77		18.80	222	34.1		11.02	9	5		7.81
NISP:	355				147				95				9			

The relative abundance (Table 4.10) and skeletal element proportion indices (Table 4.11) therefore suggest the following:

The MEO pellet containing **small-bodied prey** is dominated by the dental and mandibular elements, with a relatively even representation of lumbar, hindlimb, and pelvic elements. Ribs and crania were less frequently represented. The proportion indices (Table 4.11) suggest that: 1) postcranial fragments were slightly less frequently ingested compared to cranial fragments (PC < C); 2) lower limb bones were more frequently ingested than the upper limb bones (ZE > ST); 3) the anterior limb bones greatly outnumber ingested posterior limb bones (AN > PO); and 4) axial bones greatly outnumber ingested appendicular bones (AX > AP).

Similarly, the MEO pellet containing **medium-bodied prey** is dominated by dental and mandibular elements, with a relatively even representation of pelvic and forelimb elements. Ribs, crania, and distal limb elements were represented less frequently. The proportion indices (Table 4.11) suggest that: 1) postcranial and cranial fragments were equally ingested (PC = C); 2) lower limb bones were more frequently ingested than the upper limb bones (ZE > ST); 3) the anterior limb bones were more frequently ingested than the posterior limb bones (AN > PO); and 4) axial bones were more frequently ingested than appendicular bones (AX > AP).

Comparatively, the MEO pellet containing **large-bodied prey** is dominated by mandibular and forelimb elements, with fewer dental, hindlimb, and carpal elements. The proportion indices (Table 4.11) suggest that: 1) postcranial fragments were more frequently ingested compared to cranial fragments (PC > C); 2) lower limb bones were more frequently ingested than the upper limb bones (ZE > ST); 3) the anterior limb bones were more frequently ingested than the posterior limb bones (AN > PO); and 4) axial bones were more frequently ingested than appendicular bones (AX > AP).

Table 4.11: Relative numbers of digested and deleted skeletal elements comparing proportions of postcranial to cranial elements (PC/C)[a], lower limb to upper limb (ZE/ST)[b], anterior to posterior limb elements (AN/PO)[c], and axial to appendicular elements (AX/AP)[d] for each body size.

Indices	Small	Medium	Large
Digested			
PC/C	75.9	100.0	148.1
ZE/ST	834.1	140.0	132.5
AN/PO	1266.5	513.3	501.6
AX/AP	1980.7	818.1	421.3

[a] (femur + humerus) / (mandibles + maxillae) x 100
[b] (tibia + (radius + ulna)/2) / (femur + humerus) x 100
[c] (scapula + humerus + (radius + ulna)/2) / (pelvis + femur + tibia) x 100
[d] (atlas + axis + (cervical/5) + (thoracic/12) + (lumbar/7) + (sacra/4)) / ((humerus/2) + (radius/2) + (ulna/2) + (femur/2) + (patella/2) + (tibia/2)) x 100

Fragmentation and breakage patterns

Fragmentation indices (NISP/MNE) and long bone fragmentation patterns were calculated for each sample (Tables 4.12 and 4.13). The pellet sample containing small body sized rats showed the least amount of fragmentation among all elements compared to the medium and large body sized samples. This is similarly observed in the long bones, where the small body sized pellet contained a relatively greater amount of complete bones compared to the others. Specifically, the pellet containing large body sized rats showed a significantly greater degree of fragmentation, overall and among the long bone elements, compared to the medium and small rat body sized samples. Degrees of fragmentation were also calculated without the compact bones

and teeth as these elements were typically intact. In these cases, the degree of fragmentation increased substantially reflecting the tendency of cranial, long bone, and axial elements to break during digestion in MEO.

Table 4.12: Bone fragmentation and specimen size for prey body sizes: fragmentation[a] (NISP/MNE all bones), fragmentation[b] (NISP/MNE excluding compact bones and teeth), minimum length, maximum length, standard deviation, mean size of specimens, and percent of specimens measuring <2 mm and <5 mm in length.

Prey Body Size Category	Fragmentation [a]	Fragmentation [b]	Min length	max length	mean length	SD length	<2	<5
Small	1.34	1.52	0.7	18.39	4.79	5.77	13.3	66.1
Medium	1.40	1.58	0.95	22.76	6.17	5.76	10.7	47.3
Large	2.22	2.71	1.23	37.64	6.25	5.76	4.1	46.8

a NISP/MNE all bones
b NISP/MNE excluding compact bones and teeth

Specimen lengths also varied between samples with medium-bodied prey retaining the longest specimens (Table 4.12). The mean length between all samples ranged between 4.7 and 6.2 mm. Almost half of each pellet contained specimens under 5 mm in length whereas 4% to 13% of specimens were less than 2 mm in length.

Table 4.13: Long bone fragmentation summary from MEO pellets according to prey body size

Prey body size	Element	NISP	complete (%)	shaft (%)	prox (%)	dist (%)	**Total Frag**
Small	Femur	7	6 (86)	0	0	1 (14)	**1 (14)**
	Tibia	9	1 (11)	2 (22)	5 (56)	1 (11)	**8 (89)**
	Humerus	5	1 (20)	1 (20)	1 (20)	2 (40)	**4 (80)**
	Radius	5	3 (60)	1 (20)	1 (20)	0	**2 (40)**
	Ulna	6	2 (33)	2 (33)	2 (33)	0	**4 (66)**
	Total	**32**	**13 (40)**	**6 (19)**	**9 (28)**	**4 (12)**	**19 (59)**
Medium	Femur	2	0	0	2 (100)	0	**2 (100)**
	Tibia	1	0	0	0	1 (100)	**1 (100)**
	Humerus	4	1 (25)	0	1 (25)	2 (50)	**3 (75)**
	Radius	2	1 (50)	0	0	1 (50)	**1 (50)**
	Ulna	2	1 (50)	0	0	1 (50)	**1 (50)**
	Total	**11**	**3 (27)**	**0**	**3 (27)**	**5 (45)**	**8 (72)**
Large	Femur	1	0	0	0	1 (100)	**1 (100)**
	Tibia	0	0	0	0	0	**0**
	Humerus	3	0	0	0	3 (100)	**3 (100)**
	Radius	2	0	0	2 (100)	0	**2 (100)**
	Ulna	3	0	1 (33)	2 (66)	0	**3 (100)**
	Total	**9**	**0 (0)**	**1 (11)**	**4 (44)**	**4 (44)**	**9 (100)**

Table 4.14 shows the types of breakage observed between the pellet samples. All samples showed an almost equal amount of right angled (typically referring to dry breaks) and oblique angled (typically referring to fresh breaks) fractures. However, the majority of the bones suggest an overall pattern of fresh breaks, characterized by smooth edges and V-shaped/oblique outlines. The relatively greater frequency of right angled fractures is likely due to the more irregular long bone structure observed in small mammals compared to the more cylindrical bone shafts of humans - the sample for which these categories are based (Villa and Mahieu, 1991). Additional comparisons between long bone elements with varying degrees of cylindrical shapes is needed to confirm.

Table 4.14: Occurrence of fracture angles, outlines, and edges for ingested long bones according to prey body size.

	Fracture angle				Fracture Outline (2 options)				Fracture Edge		
	oblique	right	oblique/right	Indet.	V-shaped	oblique	transverse	transverse/curved	Smooth	Jagged	Indet
MEO-Small	8 (30)	9 (34)	0 (0)	9 (34)	3 (7)	14 (35)	5 (12)	18 (45)	14 (53)	6 (23)	6 (23)
MEO-Medium	4 (40)	2 (20)	3 (30)	1 (10)	5 (45)	2 (18)	1 (9)	3 (27)	9 (90)	1 (10)	0 (0)
MEO-Large	12 (37)	14 (43)	3 (9)	3 (9)	19 (57)	6 (18)	3 (9)	5 (15)	31 (96)	1 (3)	0 (0)

Digestion

Table 4.15 shows the degree of digestive damage caused by MEO on the rat long bones, molars, and incisors recovered from the pellets. As expected, the majority of elements showed a light or medium degree of digestive damage consistent with previously described levels of digestion by the MEO (Andrews, 1990). However, there were a few elements, long bones and teeth, that showed a slightly heavier degree of damage within the small body sized pellet. Lastly, the few bones that were recovered from the vulture casts showed an extreme degree of digestion (Figure 4.8).

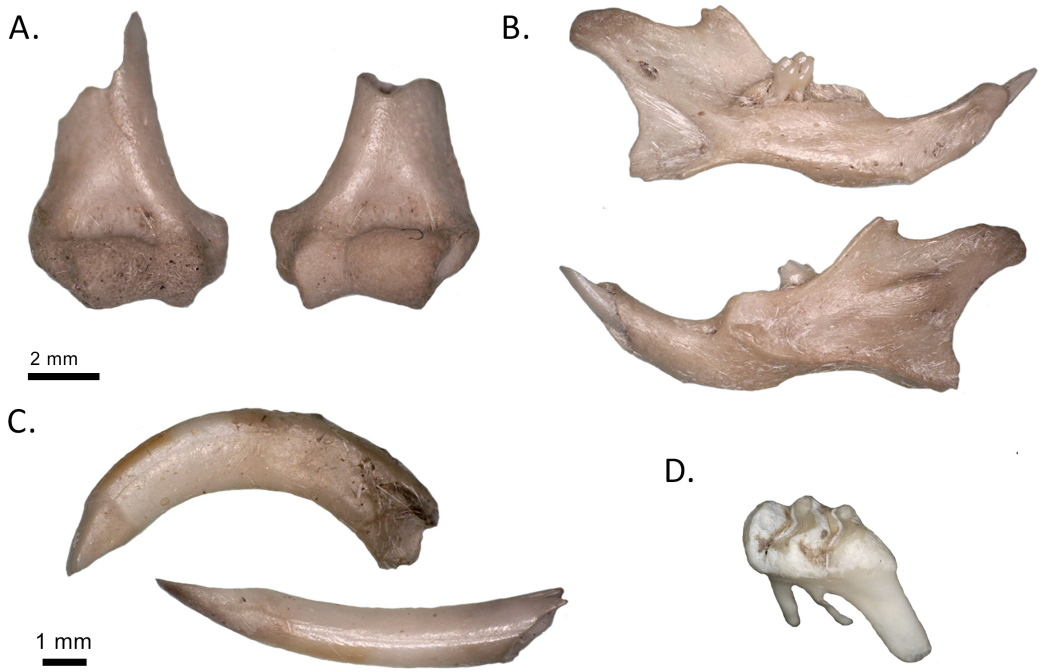

Figure 4.8: Examples of damage caused by digestion from MEO-small (A - C) and King Vultures (D). A. Distal humeri with medium (left) and light (right) degrees of digestive damage. B. A left mandibular fragment showing light digestion on the medial (upper) and lateral (lower) sides with a secondary molar and incisor preserved in the alveolus. Note the slight rounding and shine to the bone surface C. A maxillary (upper) and mandibular (lower) incisors showing light and very light degrees of digestion concentrated at the distal end of the tooth. D. Extremely digested maxillary first molar recovered from the vulture cast.

Table 4.15: Totals and frequencies of damage caused by owl digestion for prey body sizes

		Digestion							All Elements	
Predator	Prey Body Size	Null	Very Light	Light	Medium	Heavy	Extreme	Indet.	Digested	Undigested
					Identified Long Bone Elements					
Owl	Small	2 (4)	-	25 (50)	19 (38)	3 (6)	1 (2)	0 (0)	513	0
	Medium	2 (12)	-	7 (38)	9 (56)	0 (0)	0 (0)	0 (0)	232	0
	Large	1 (7)	-	7 (50)	6 (42)	0 (0)	0 (0)	0 (0)	231	0
Vulture	Medium	0 (0)	-	0 (0)	0 (0)	0 (0)	1 (0)	0 (0)	6	0
	Large	0 (0)	-	0 (0)	0 (0)	0 (0)	0 (0)	0 (0)	0	98
	Extra Large	0 (0)	-	0 (0)	0 (0)	0 (0)	0 (0)	0 (0)	0	123
					Incisors (all)					
Owl	Small	0 (0)	5 (25)	10 (50)	2 (10)	0 (0)	2 (10)	1 (5)		
	Medium	0 (0)	3 (60)	2 (40)	0 (0)	0 (0)	0 (0)	0 (0)		
	Large	0 (0)	0 (0)	1 (50)	1 (50)	0 (0)	0 (0)	0 (0)		
					Molars (all)					
Owl	Small	0 (0)	0 (0)	21 (81)	4 (15)	1 (4)	0 (0)	0 (0)		
	Medium	0 (0)	0 (0)	15 (100)	0 (0)	0 (0)	0 (0)	0 (0)		
	Large	0 (0)	0 (0)	0 (0)	1 (100)	0 (0)	0 (0)	0 (0)		
Vulture	Medium	0 (0)	0 (0)	0 (0)	0 (0)	0 (0)	3 (100)	0 (0)		

4.3.3 Owls, Vultures, and Humans as Small Prey Accumulators

To determine if the observed differences between prey skeletal element-part profiles are sufficient to distinguish between predators, a series of principal components analyses (PCA) were performed using the relative abundance (%RA) values from avian and human modified prey items (Figure 4.9 and Table 4.17). Three comparative datasets from Armstrong (2015), Armstrong and Avery (2014), and Andrews (1990) were included to determine if other controlled feeding experiments involving different avian predator-prey species combinations and wild samples of eagle and owl small prey accumulations support the results from this study (Figure 4.10). Lastly, Tables 4.16 and 4.18 presents the results of an analysis of variance (ANOVA) conducted to determine if the observed differences in the PCAs among the predator-prey combinations presented in this study and from the literature were significant at the 0.05 level.

Figure 4.9 shows distinct clusters between the human and avian modified samples.

Table 4.16: Raw p-values uncorrected significance (in bold) matrix comparing predator and prey combinations as shown in Figure 4.9.

Predator	MEO			Vulture	Human				
ANOVA	Small	Medium	Large	Medium	GiantRats	Small*Rattus*	Bats	Macaque	Civet
Owl-Small		0.97	**0.03**	**0.00**	**0.00**	0.16	0.26	**0.00**	**0.00**
Owl-Medium			0.06	**0.00**	**0.00**	0.14	0.24	**0.00**	**0.00**
Owl-Large				**0.00**	**0.00**	**0.04**	**0.04**	**0.00**	**0.00**
Vulture-Medium					**0.00**	**0.00**	**0.00**	**0.00**	**0.00**
Human-GiantRats						0.71	**0.02**	0.33	0.25
Human-SmallRattus							0.27	0.27	0.29
Human-Bats								**0.00**	**0.01**
Human-Macaque									0.95
Human-Civet									

The vulture-medium sample plots farther along the negative end of the first component than the MEO cluster and is significantly different from each MEO-prey and human-prey samples (Table 4.16). Within the MEO cluster, the samples containing small and medium body-sized rats overlap with one another whereas the large-rat sample loads slightly more negatively along the second component axis. This suggests that there is greater similarity between the MEO-small and MEO-medium rat samples compared with the MEO-large rat sample. This is somewhat supported by the ANOVA results as the MEO-large rat sample is significantly different from the MEO-small rat sample ($p = 0.03$) but not from the MEO-medium rat sample ($p = 0.06$) (but see Nuzzo (2014)), and there is also no significant difference between the MEO-small and MEO-medium rat samples ($p > 0.05$).

For PC1 and PC2, the human-modified cluster including mammalian prey species shows more variation, but all group combinations load positively along the first component. The smaller animals weighing less than 800 g (i.e., the human-bats and the human-small*Rattus* samples), however, plot close together and more centrally. There is no significant difference between these two groups (human-bats and the human-small*Rattus* ($p = 0.27$) samples) while there are significant differences between the fruit bats and giant rats ($p = 0.02$), macaque ($p < 0.00$), and civet ($p = 0.01$)

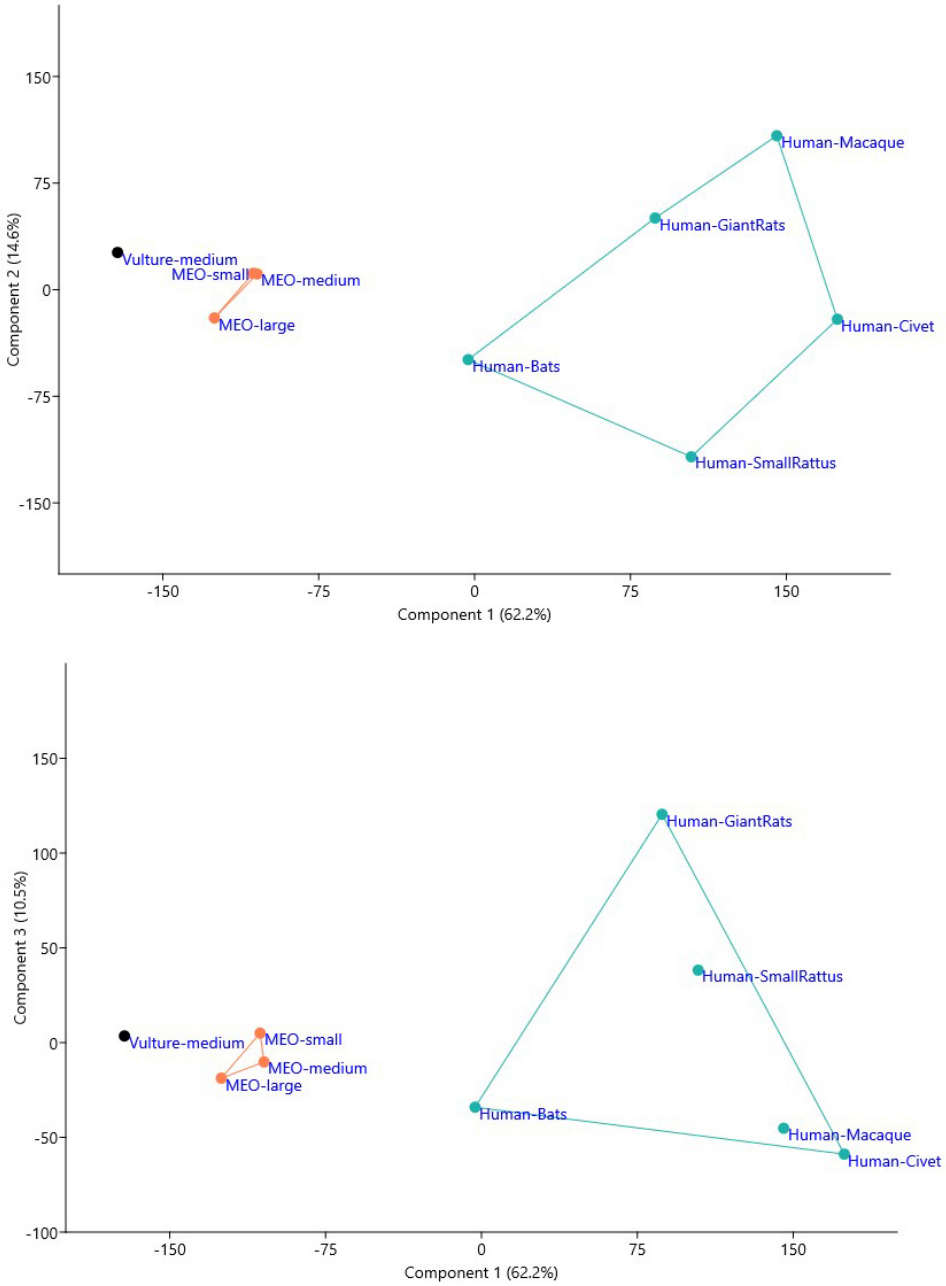

Figure 4.9: Comparison of skeletal element relative abundance (%RA) profiles (principal components analysis using a variance-covariance matrix performed on 25 variables) among vulture (black) and MEO (orange) digested samples, and human (green) butchered sample groups. Shown is the projection of predator-prey group scores of the first, second, and third principal components with variance explained by each component.

(Table 4.16). Otherwise, all other combinations of prey species butchered by human subjects are not significantly different from one another. The human-bats and human-small*Rattus* samples are also not significantly different from the MEO-small or MEO-medium samples suggesting that the skeletal element-part profiles of these smaller animals are more challenging to differentiate compared with those of relatively larger-bodied prey species.

Since there is considerable taphonomic overlap and variability among avian predators, comparisons with another controlled feeding experiment (Armstrong, 2015) and small prey assemblages collected from wild owl pellets and eagle nests (Armstrong and Avery, 2014; Andrews, 1990) were included to increase sample size and evaluate if the results from this study are supported by other sources (Figure 4.10 and Table 4.18). Three discernible but overlapping clusters of eagle (red), owl (orange), and human (green) accumulators form along the first principal component, which explains 56.2% of the total variance. This gradient indicates that vultures and eagles cause the most amount of skeletal element loss whereas humans cause the least. This agrees with the literature where eagles and other diurnal raptors are known to cause more damage from digestion resulting in greater amounts of element loss compared to owls and other nocturnal species (Andrews, 1990; Armstrong, 2016). The results also indicate that in relation to eagles and owls, humans cause the least amount of damage resulting in minimal element loss. While humans can completely consume smaller-bodied prey, like mice (< 50 g) (Meyer-Rochow et al., 2015), this comparative analysis shows that when humans butcher small mammals larger than roughly 600 g, the skeletal-part profile of these animals may provide additional criteria for discerning avian from human accumulators.

Based on this comparative analysis, the human-bats sample shows greater similarity to owls while the other human-prey samples plot outside the range of all avian prey patterns. Since none of the avian species included bats as prey items, the skele-

tal part profile of the human-bat predator-prey combination could be due to the way these animals were processed given their unique skeletal morphology. Otherwise, all human-prey combinations fall outside the range of skeletal abundances from avian predation suggesting that humans cause the least amount of skeletal element loss among small-bodied mammalian prey items.

The positive loadings along the first component are explained by the greater relative abundance of long bone elements, pelves, scapula, and mandibles, while the negative loadings are driven primarily by a greater abundance of distal appendages (Table 4.17). There is also greater variation between predators of the same species consuming prey items of different body plans (e.g., Eagle-Rabbit vs Eagle-GuineaPig, $p < 0.05$) than between prey with similar body plans but different body sizes (e.g., MEO-medium rats vs MEO-large rats, $p > 0.05$). This suggests that raptors consuming similar prey species with similar skeletal anatomy but of different body sizes does not affect the relative abundance profile of bone elements as much as when raptors are consuming prey species with diverse morphological skeletal structures.

Interestingly, the wild samples (represented by open circles) plot more towards the positive and negative end of the first and second component, respectively, and overlap with the human-prey cluster while the experimental samples (represented by closed circles) plot more towards the negative and positive end of the first and second component, respectively. This separation between wild -collected and experimentally-produced small prey assemblages suggests that the methodologies and/or predatory behavior involved with experimental studies may affect how prey skeletal-part patterns are produced.

Overall, the relative abundance of skeletal elements and the relative proportions of element parts are promising criteria for differentiating between human and avian accumulators at fossil sites where post-depositional attrition is low (i.e., minimal selective element removal by carnivores (Yellen, 1991b) or density-mediated element

loss (Pavao and Stahl, 1999)).

Table 4.17: Principal components eigenvalue and percent variance summaries for PCA analyses performed on data from this study (Figure 4.9) and using comparative datasets (Figures 4.10) from Armstrong (2015) and Armstrong and Avery (2014).

Figure 4.9	Number of variables	25	Figure 4.10	Number of variables	16
PC	Eigenvalue	% variance	PC	Eigenvalue	% variance
1	17188.4	62.2	1	7122.73	56.1
2	4035.09	14.6	2	1731.1	13.6
3	2891.85	10.4	3	1050.24	8.2
4	1430.45	5.1	4	746.894	5.8
5	1039.88	3.7	5	545.517	4.3
6	607.198	2.1	6	452.497	3.5
7	275.612	0.9	7	306.041	2.4
8	154.46	0.5	8	255.196	2.01
			9	139.208	1.1
			10	114.95	0.9
			11	102.466	0.8
			12	42.7912	0.3
			13	28.6617	0.2
			14	25.5324	0.2
			15	8.75115	0.1
			16	5.91316	0.04

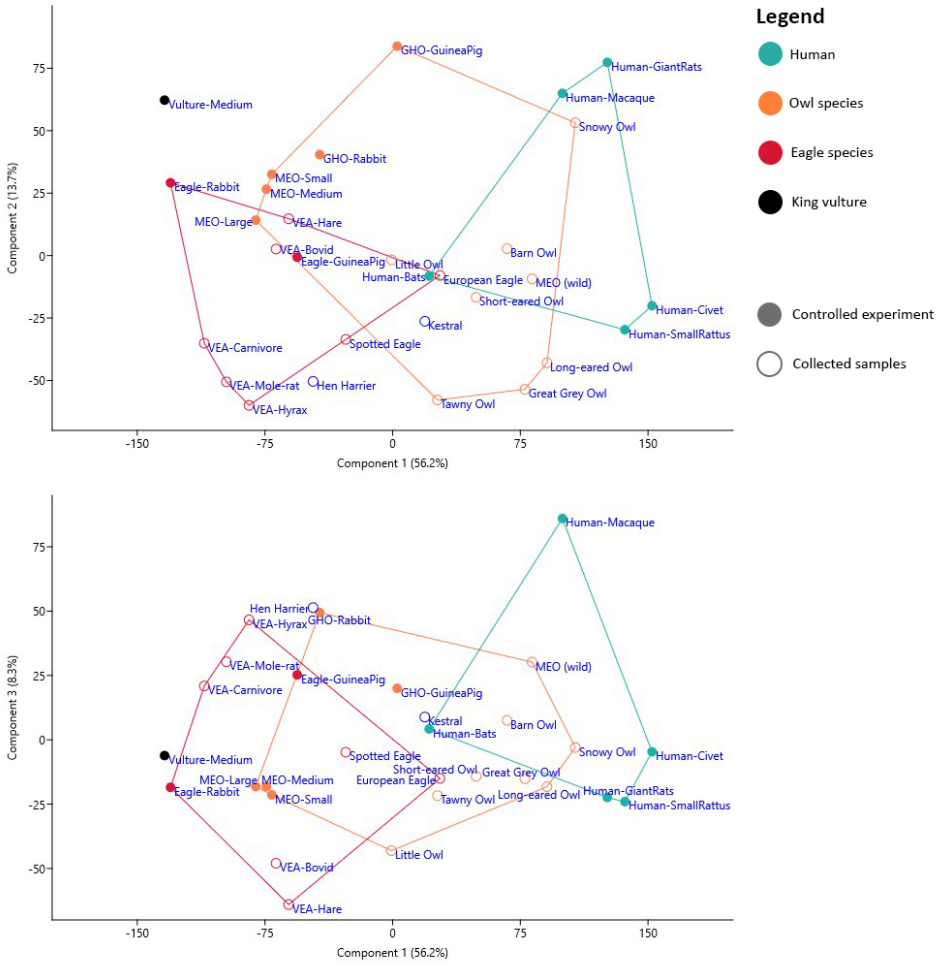

Figure 4.10: Comparison of skeletal element relative abundance (%RA) profiles (principal components analysis using a variance-covariance matrix performed on 16 variables) among vulture (black), owl species (orange), eagles (red), and other raptor (blue) digested samples, and human (green) butchered sample groups. Data from Armstrong (2015) are included as a comparison with another controlled feeding experiment involving other predator (Great Horned Owl (GHO) and Bald Eagle (Eagle)) and prey (guinea pig and rabbit) combinations. Relative abundance estimates published in Armstrong and Avery (2014) of bone samples collected from wild Verreaux's Eagle (VEA) nesting sites in South Africa are also included for additional comparisons. Also included are relative abundance estimates from wild pellet samples of various owl species published in Andrews (1990). Open symbols indicate wild-sourced samples while closed symbols indicate experimentally-produced samples. Shown is the projection of predator-prey group scores of the first, second, and third principal components with variance explained by each component.

Table 4.18: Raw p-values uncorrected significance (in bold) matrix comparing predator and prey combinations as shown in Figure 4.10 with comparative datasets from Armstrong (2015); Armstrong and Avery (2014) and Andrews (1990).

Reference	This Study									Armstrong (2015)				Armstrong and Avery (2014)					Andrews (1990)											
Predator	MEO			Vulture	Human					GHO		Eagle		Verreaux's Eagle					Barn Owl	Snowy Owl	Long-eared Owl	Short-eared Owl	Verreaux Eagle Owl	Spotted eagle	European Eagle	Great Grey Owl	Tawny Owl	Little Owl	Kestral	Hen Harrier
ANOVA	Small	Medium	Large	Medium	GiantRats	SmallRattus	Bats	Macaque	Civet	Rabbit	GuineaPig	ERabbit	GuineaPig	Hyrax	Mole-rat	Hare	Bovid	Carnivore												
MEO-Small		0.88	0.15	**0.00**	**0.00**	**0.02**	0.22	**0.00**	**0.01**	**0.03**	**0.00**	**0.00**	0.38	**0.02**	**0.01**	0.34	0.19	**0.00**	**0.00**	**0.00**	**0.01**	**0.02**	**0.00**	0.58	**0.01**	0.09	0.36	0.43	**0.03**	0.49
MEO-Medium			0.27	**0.00**	**0.00**	**0.02**	0.13	**0.00**	**0.01**	**0.01**	**0.00**	**0.00**	0.34	**0.02**	**0.01**	0.36	0.30	**0.01**	**0.00**	**0.00**	**0.00**	**0.00**	**0.00**	0.64	**0.00**	**0.04**	0.18	0.12	**0.03**	0.98
MEO-Large				**0.01**	**0.00**	**0.01**	0.08	**0.00**	**0.01**	**0.01**	**0.00**	**0.05**	**0.03**	**0.44**	0.40	0.51	0.73	0.18	**0.00**	**0.00**	**0.00**	**0.00**	**0.00**	0.12	**0.00**	**0.00**	**0.03**	**0.02**	**0.00**	0.31
Vulture-Medium					**0.00**	**0.00**	**0.00**	**0.00**	**0.00**	**0.00**	**0.00**	0.14	**0.00**	**0.00**	**0.01**	**0.00**	**0.00**	0.11	**0.00**	**0.00**	**0.00**	**0.00**	**0.00**	**0.00**	**0.00**	**0.00**	**0.00**	**0.00**	**0.00**	**0.00**
Human-GiantRats						0.92	**0.01**	**0.63**	0.55	**0.00**	**0.01**	**0.00**	**0.00**	**0.00**	**0.00**	**0.00**	**0.00**	**0.00**	0.15	0.69	0.37	**0.05**	0.21	**0.00**	**0.01**	0.17	**0.01**	**0.01**	**0.02**	**0.00**
Human-SmallRattus							0.06	0.88	0.90	0.05	0.11	**0.00**	**0.04**	**0.01**	**0.01**	**0.02**	**0.02**	**0.00**	0.22	0.48	0.26	0.17	0.25	**0.05**	0.10	0.20	0.09	**0.05**	0.11	**0.03**
Human-Bats								**0.02**	**0.02**	0.64	0.89	**0.01**	0.30	0.17	0.07	0.23	0.18	**0.03**	0.15	**0.01**	0.11	0.46	0.08	0.44	0.72	0.15	0.72	0.87	0.87	0.42
Human-Macaque									0.52	**0.00**	**0.00**	**0.00**	**0.00**	**0.00**	**0.00**	**0.00**	**0.00**	**0.00**	0.15	0.98	0.35	0.08	0.15	**0.00**	**0.01**	0.26	**0.04**	**0.00**	**0.01**	**0.00**
Human-Civet										**0.02**	**0.05**	**0.00**	**0.02**	**0.01**	**0.01**	**0.01**	**0.01**	**0.00**	0.06	0.20	0.14	0.07	0.12	**0.04**	**0.05**	0.12	**0.05**	**0.03**	**0.04**	**0.02**
GHO-Rabbit											0.07	**0.00**	0.24	**0.00**	**0.00**	**0.02**	**0.01**	**0.00**	**0.01**	**0.00**	0.09	0.25	**0.01**	0.32	0.46	0.25	0.85	0.60	0.42	0.06
GHO-GuineaPig												**0.00**	**0.01**	**0.00**	**0.00**	**0.00**	**0.00**	**0.00**	0.11	**0.00**	0.42	0.89	0.10	**0.03**	0.64	0.56	0.66	0.11	0.72	**0.01**
Eagle-Rabbit													**0.00**	0.29	0.32	**0.01**	**0.02**	0.77	**0.00**	**0.00**	**0.00**	**0.00**	**0.00**	**0.00**	**0.00**	**0.00**	**0.00**	**0.00**	**0.00**	**0.00**
Eagle-GuineaPig														**0.00**	**0.01**	0.19	**0.05**	**0.00**	**0.00**	**0.00**	**0.03**	**0.02**	**0.00**	0.90	0.06	0.13	0.64	0.66	0.13	0.30
MEO-Hyrax															0.73	0.12	0.31	0.36	**0.00**	**0.00**	**0.00**	**0.00**	**0.00**	**0.01**	**0.00**	**0.00**	**0.03**	**0.01**	**0.00**	**0.05**
MEO-Mole-rat																0.08	0.23	0.35	**0.00**	**0.00**	**0.00**	**0.00**	**0.00**	**0.01**	**0.00**	**0.00**	**0.01**	**0.00**	**0.00**	**0.03**
MEO-Hare																	0.56	**0.01**	**0.00**	**0.00**	**0.00**	**0.00**	**0.00**	0.40	**0.01**	**0.03**	0.19	0.11	**0.03**	0.64
MEO-Bovid																		0.07	**0.00**	**0.00**	**0.00**	**0.00**	**0.00**	0.08	**0.01**	**0.01**	**0.08**	**0.04**	**0.01**	0.40
MEO-Carnivore																			**0.00**	**0.00**	**0.00**	**0.00**	**0.00**	**0.00**	**0.00**	**0.00**	**0.00**	**0.00**	**0.00**	**0.02**
Barn Owl																				0.09	0.64	0.42	0.49	**0.01**	0.17	0.99	0.19	**0.03**	0.09	**0.01**
Snowy Owl																					0.46	0.06	0.36	**0.00**	**0.01**	0.31	**0.02**	**0.00**	**0.01**	**0.00**
Long-eared Owl																						0.56	1.00	**0.05**	0.32	0.64	0.11	0.06	0.28	**0.03**
Short-eared Owl																							0.32	**0.03**	0.90	0.99	0.27	0.09	0.42	**0.01**
Verreaux Eagle Owl																								**0.00**	0.08	0.69	0.17	**0.02**	0.07	**0.01**
Spotted eagle																									0.12	0.14	0.53	0.61	0.13	0.53
European Eagle																										0.69	0.58	0.25	0.84	**0.03**
Great Grey Owl																											0.21	0.28	0.51	0.08
Tawny Owl																												0.90	0.66	0.42
Little Owl																													0.44	0.31
Kestral																														0.06
Hen Harrier																														

4.4 Discussion

4.4.1 Human modifications

The ethnoarchaeological study involved burning and disarticulating a taxonomically diverse sample of small animals ranging in body sizes (80 g – 4.8 kg). Taphonomic analyses were conducted according to animal body size to determine if body size, regardless of taxonomic status, significantly affected how humans butcher each animal, and thereby, result in identifiable butchery patterns relevant for archaeological analysis. The results from this study suggest that animal body size is significantly related to cutmark frequency, bone breakage, and fragmentation. These results are discussed in detail below.

Bone surface modification

The observed cutmark frequencies and the location of marks on giant rat bone elements indicate that the pelvis and femur most commonly exhibit cutmarks (Table 4.9). These results are mostly in agreement with other experimental studies involving small mammal butchery where the hindlimb contained most cutmarks in controlled leproid samples (Lloveras et al., 2009). This study also observed a greater frequency of cutmarks on the calcaneus from giant rats during disarticulation compared to other similar studies (Table 4.9). When considering all mark types, there is a positive correlation with animal body size and the frequency of marks associated with disarticulation (Figure 4.8) per individual, but no statistically significant difference was detected, perhaps due to the small sample sizes. When incorporating published data sets to increase sample size, there is a significant relationship between the frequency of marks related to distarticulation and animal body size ($r^2 = 0.33$, $p = 0.007$, Figure 4.11). Moreover, the number of point events (i.e., number of times a knife was used to cut flesh) is also directly related to the frequency of cutmarks left on

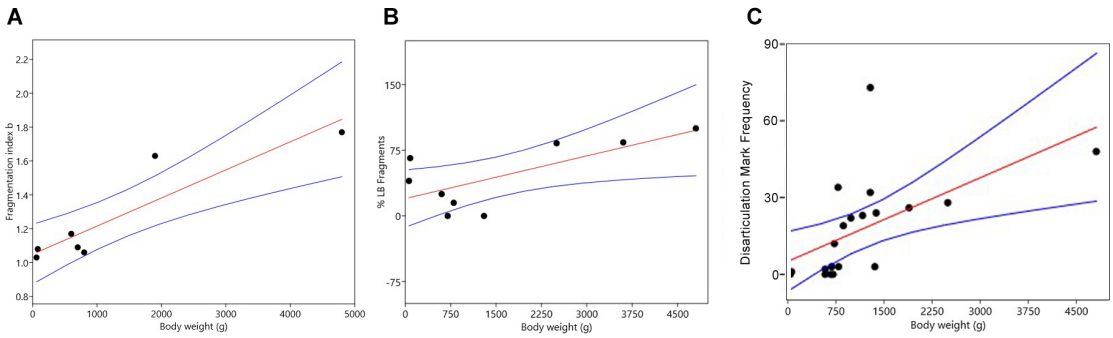

Figure 4.11: Linear regression models showing the relationship between animal body size (g) and (A) fragmentation (NISP/MNE) of all elements excluding compact bones and teeth; (B) long bone fragmentation (percent of broken long bones); and (C) frequencies of disarticulation marks identified on individual animals including data from Lloveras et al. (2009) and this study.

the bones surface (Figure 4.4) suggesting that cutmark frequencies in small mammal faunal assemblages are related to butchery intensity.

The observed frequency of tooth marks (8% of all mark types) were also in agreement with previous studies wherein consumption of rabbits left roughly 6% of tooth marks (Lloveras et al., 2009). The majority of tooth marks from this study were identified on two giant rat specimens (representing 13% of all mark types) (*P. armandvillei*), a result that is comparable to observed tooth mark frequencies for other murids (18% on giant pouched rats and 6% on mice and other murids according to Landt (2007)).

Previous experimental studies involving fire to cook small animals suggest that high degrees of localized burning damage on small mammal bones reflects intentional burning practices (Lloveras et al., 2009; Rhodes et al., 2016; Hockett and Ferreira Bicho, 2000; Henshilwood, 1997). Results from this study are consistent with this interpretation, as intensive burning damage was concentrated on the terminal ends of skeletal elements where there was minimal flesh cover, including anterior teeth (i.e., incisors and canines), phalanges, and tibia (Figure 4.7). Depending on the level of processing before the animal was burned, exposure to high temperature may also

affect additional elements reflecting additional processing patterns.

Bone fragmentation and breakage

Differential fragmentation among larger body size classes is frequently used to infer human transportation costs, processing decisions, and/or discard patterns (Blumenschine, 1991; Marean and Cleghorn, 2003; Marean and Spencer, 1991; Marean, 1991; Cannon, 2013). For small mammals, degrees of fragmentation are typically associated with the later stages of the butchery and consumptive process as small mammals do not need to be disarticulated before transporting back to camp sites, as is the case with large animals (Yellen, 1991a). Humans also modify smaller animals in a variety of ways that do not always result in fragmentation (i.e., they consume the animal whole or pull them apart without the use of knives). This creates a variety of fragmentation patterns in an archaeological assemblage that makes accurate interpretations challenging. Moreover, discard patterning does not always reflect the observed butchery process (Yellen, 1991b).

By butchering small animals with a variety of animal body sizes and body plans under the same premise (i.e., reduce the overall size of the animal to put into a small pot for boiling), this study was able to test whether animal body size affects pre-depositional fragmentation. Our results show that animal body size significantly affects the degree of element fragmentation (NISP/MNE) (p=0.004, r^2=0.82) prior to post-depositional destruction (Figure 4.11 and Table 4.5). Similarly, long bone fragmentation is significantly correlated with animal body size (p=0.03, r^2=0.49) suggesting that, like degrees of fragmentation, larger small mammals experience higher rates of long bone breakage compared to smaller mammals. However, this result is likely reflecting the intent of the butcher to boil the animal within a small pot (see Methods). Since post-depositional rates vary across archaeological sites, this fragmentation pattern may be visible under optimal circumstances (i.e., low post-depositional

destruction) but is likely to be overwritten by additional fragmentation due to other factors (e.g., sediment weight, natural bone attrition, etc). However, these results indicate that animal body size can affect the rates of element fragmentation, and thereby, be linked back to human processing intensity.

Observations on hunting rats at Liang Bua

Members from neighboring hamlets around Liang Bua live an agricultural lifestyle and rely mainly on domesticated foods, like chicken, pig, and goat, for the animal protein components of their diet. Still, many individuals choose to hunt local endemic animals because they either enjoy the taste of the animal and/or the thrill and social activity of hunting wild animals.

"... setiap minggu saya pergi ke hutan untuk berburu tikus bersama tetangga saya"

"... every week I go to the forest to hunt rats with my neighbor"

The most commonly captured and most desirable prey to hunt is the endemic Flores giant rat, *Papagomys armandvillei*. Average adult weights range from roughly 1 kg up to 3.5 kg with female rats weighing slightly less on average (Musser, 1981; Veatch et al., 2019) . These animals are widely distributed across the island but current population levels or distribution patterns are unknown. As burrowing rodents, the giant rat is mainly terrestrial but will spend some time in the trees to forage for leaves, buds, and fruits at night (Musser, 1981) and/or escape predators (participants, personal communication). Other mammals that are frequently hunted include fruit bats (*Dobsonia peronii*, *Pteropus lombocensis heudei*), macaques (*Macaca fascicularis*), porcupines (*Hystrix javanica*), and civets (*Paradoxurus hermaphroditus*). Varanids (*Varanus* sp.) and song birds are also captured if encountered.

"Landak lebih sulit diburu dibandingkan dengan tikus raksasa - mereka cenderung menggali liang dan jarang keluar. Betu akan bersembunyi di

pohon dan liang hanya jika ketakutan"

"Porcupine are harder to hunt compared to giant rats - they (porcupines) tend to burrow and rarely come out. Giant rats will hide in trees and burrow only when scared"

Because of their nocturnal and burrowing habits, catching giant rats is considered difficult without the help of dogs or other tools such as snares or nets. Many of these animals are caught using opportunistic strategies where clubs or large sticks are used to stun the animal by striking it on the head or back when encountered in rice fields or gardens. More strategic approaches include waiting next to trails left by local murines (Figure 4.12) and, again, stun them using a large stick as they run by. Some also place snares along the trails to capture rats as they try to run through the trap (Figure 4.13). Others choose to hunt the rats at night when the rats are more active as they forage for food in the trees. Individuals will ambush and stun them using a club or use dogs to collect the animal once encountered.

The perceived level of difficulty involved with hunting giant rats may be a generational affect where expert knowledge is diminishing over time. Older individuals described times when hunting giant rats was much more common compared to today. This change was described as the result of fewer animals, potentially due to over hunting, and a general loss of interest over time due to the presence of other protein sources (i.e., domesticated animals). Traditional snares used by locals are also less common now, but small netting traps are still used to collect other animals such as porcupines (Figure 4.13). It is also worth noting that participants displayed remarkable reflexes when encountering a giant rat or small murine. On several occasions, we observed participants capture smaller rats opportunistically through quick and precise movements without the aid of complex nets or technologies.

When cooking, individuals would approach the butchering and preparation process in several ways. After eviscerating the gut and organ contents, most participants

Figure 4.12: Examples of trails made by murines along the forest floor. Photographs were taken and provided by Peter Kjærgaard.

Figure 4.13: Traditional rat hunting snare (above) placed along rat trails disguised with foliage (bottom left) and [a demonstration of] a small netting tool used to corral porcupines (bottom right)

would carefully disarticulate the animals according to skeletal region, removing the limbs first followed by the pelvis and vertebrae using forceful chopping motions. One participant used string to tie the animal to a wooded post and hang at eye level to eviscerate and disarticulate the body while suspended (animal ID 10). Using this approach, the participant was noticeably more careful when cutting flesh and used more slicing actions compared to when participants chose to chop the animal with a large knife on a hard surface. This approach resulted in fewer broken bones (0 broken long bones) but also left the most amount of cutmarks identified in this study (73 marks, 34% of all marks in sample).

During this study, all animals were boiled with spices, but participants mentioned that they will also grill (or roast) the animals over fire to cook them. Boiling animals in a small pot (sometimes referred to as a cauldron or "kuali") cooks the animals faster than grilling, but this method is also a tradition in the community. When asked about whether boiling the animals was intended to also release bone marrow, and whether this was an important resource to collect, one participant mentioned the following (full transcript can be found in Appendix A):

> "Kita isap-isap tulangnya itu kita patahin kita isap-isap sumsumnya di-dalamnya lagi ... begini kalau pakai panci masaknya itu enak. Karena panci itu kan tutupnya rapat disamping dia cepat matang ya cepat matang toh sehingga cepat disajikan. Kalau pake kuali kan, kalau orang tidak tapi pake kuali karena pake kuali kan karena pake kuali kan lambat dia matang ... Lebih pilih pakai panci dan merupakan kebiasaan kami orang sini ... dipatah atau tulangnya kalau sebesar jari kelingking ini kan bisa digigit sama giginya kita kalau gigi kita masih bagus, taaak (bunyi tulang yang digigit) begitu dia kan patah. Atau kalau tulang babi hutan itu, habis kita isap tulang bagian luarnya itu, kita bisa pakai apa parang itu parang yang bukan tajam itu kah sebelah yang agak tebal sedikit itu, kita patahin

> pakai itu baru kita hisap, karena dia besar toh (tulangnya). Atau waktu potongnya itu kah missal potong bagian paha potong bagi dua kan sum-sumnya kan masih lengket di dalam tulang itu ketika masak nanti kan baru nanti kita isap nanti enak dia keluar toh, tinggal kita ambil sendok yang kecil korek atau kita hisaplah."
>
> "We suck the bones, we break them, we suck the marrow [out] again ... like this when using a cooking pot it's delicious. Because the pot has a tight lid on the side, it cooks quickly, so it cooks quickly so it's served quickly. If you use a cauldron, people don't use a cauldron because it cooks more slowly ... We prefer to use a pot and it's a habit for us people here ... to break [a] bone if it's as big as our little finger we can bite our teeth if our teeth are still good, "taaak" (sound of bone being bitten) that's how it's broken. Or if [a] boar bone, after we suck on the outer bone, we can use the machete, the non-sharp machete, the one that is a little thick, we break it and then we suck it, because it's big anyway (the bone). Or when you cut it, for example, cut the thigh, cut it in half, the marrow is still sticky in the bone when it cooks, then we'll suck it, it's delicious, it comes out anyway, we just have to take a small spoon or suck it."

Observations on butchering and cooking preparations for smaller animals reveal important considerations for interpreting faunal assemblages. First, individuals will apply different amounts of force to slice and disarticulate the animals as a matter of preference. This can result in varying degrees of superficial marks as well as overall mark frequency creating a highly variable assemblage. Second, the approach for extracting marrow that was observed—sucking on the ends of already broken bones—did not leave any discernable marks or features on the bone that reflected this process, unlike bite and percussion marks resulting from chewing and breaking long bones, respectively (Fernández-Jalvo and Andrews, 2011; Galán et al., 2009). This

result suggests that humans can access marrow from small mammal bones in ways that could be invisible taphonomically. Recovering high frequencies of cylindrical long bone shafts has also been an indication of marrow processing in rabbits (Rosado-Méndez et al., 2019), but more work is needed to explore the taphonomic signature of various marrow extraction methods in small mammals given the importance of marrow in a forager's diet (Speth and Spielmann, 1983; O'Brien and Liebert, 2014).

Avian Modification

The taphonomic effects of prey body size from avian predation is variable and reveals important considerations for zooarchaeological contexts. Comparisons of long bone fragmentation and breakage patterns among different prey body sizes, for example, reveal a noticeable pattern (Tables 4.13 and 4.14) where the long bones of larger-bodied prey fracture at higher rates compared to smaller-bodied prey (small = 50%, medium = 72%, large = 100%). This is consistent with other controlled feeding experiments where prey of larger body sizes (but different skeletal plans) fragmented at higher rates (Armstrong, 2015; Lopez, 2020).

Results from comparative analyses using relative abundance profiles showed that there is no discernible difference in the way that owls digest prey of the same skeletal plan but different body sizes. The only noticeable difference involving the relative proportion of elements is the ratio of cranial to postcranial elements (Table 4.11). The MEO pellet containing small-bodied prey preserved a relatively greater frequency of cranial fragments whereas the pellet containing medium-bodied prey contained an equal proportion of cranial to postcranial elements, and the pellet containing larger-bodied prey contained relatively fewer cranial compared to postcranial bones. This pattern suggests that owls consuming larger prey items will avoid consuming the head and focus more on consuming parts of the body (all other element proportion indices were consistent across pellets). This is an important behavioral feature to consider

when attempting to identify specific avian predators as contributors to an assemblage.

Finally, a comparison of skeletal element profiles including pellets generated from experimental studies and samples collected from the wild revealed a noticeable difference between these two methodological approaches. Pellets created in an experimental context retained relatively greater frequencies of smaller elements, such as tali, phalanges, calcanei, and vertebrae compared to samples collected in the wild, which retained a greater frequency of crania and mandibles (Figure 4.10). While there is a general trend where humans preserve relatively greater and more even element-part frequencies compared to owls, and eagles inflict the greatest amount of damage, the proportion of elements between experimentally produced samples from pellets collected from the wild have very different element-part profiles. This pattern should bring caution to relying on one kind of comparative dataset over the other when controlling for avian damage against zooarchaeological datasets (Andrews, 1990; Armstrong and Avery, 2014; López and Chiavazza, 2020; Romero et al., 2015; Kusmer, 1990; Dodson and Diane, 1979; Fernandez et al., 2016).

4.5 Conclusion

This study provides a taphonomic assessment of rats and other small animals of various body sizes (under 5 kg) modified by the milky eagle owl, vultures, and people from Flores, Indonesia to test the taphonomic effects of prey body size on avian and human predation. Data sets from the literature were included in comparative analyses to explore the taphonomic signatures of humans versus those of predatory birds in the absence of diagnostic trace identifications. The results reveal taphonomic differences between these accumulators beyond what is available in the taphonomic literature, as well as variation between prey of different body sizes of small animals.

The results of this study reveal that the relative abundance profile of skeletal

elements is a promising means of differentiating human from avian accumulators when there are no cutmarks nor evidence of digestion in a mixed assemblage. Generally, humans tend to preserve a greater percentage of elements per individual prey item resulting in higher element survival rates (31.3 – 65.1%) whereas the MEO tends to delete relatively more elements (7.81 – 19%) (Tables 4.10 and 4.3). The element survival rate within the human butchered sample also tends to follow prey body size where the bones of larger prey items have a greater chance of surviving the butchery and consumption process over smaller prey items. In the MEO samples, this intra-species difference is only observed in relation to the cranial versus postcranial remains, with smaller prey items preserving a relatively greater proportion of cranial bones compared with larger prey items. The implication for faunal analysis is that variability is introduced by both the predator and the prey depending on the prey body size. Results from this study will help to further differentiate between human and avian predators at archaeological assemblages where humans and avian predators have contributed to the accumulation of small mammal remains.

Chapter 5

Reconstructing the Paleoecology of Liang Bua using $\delta^{13}C$ and $\delta^{18}O$ Stable Isotopes from Murine Rodents

5.1 Introduction

Island Southeast Asia plays a critical role in hominin dispersals and speciation as multiple archaic hominins are now known to have occupied the region (Dubois, 1896; Brown et al., 2004; Morwood et al., 2004; Détroit et al., 2019) with at least one species present as early as 1.49 Ma (Morwood et al., 2003; Matsu'ura et al., 2020). Discoveries in Indonesia, including *Homo erectus* on Java (Dubois, 1896), *Homo floresiensis* on Flores (Brown et al., 2004; Morwood et al., 2004, 2005), and in the Philippines with *Homo luzonensis* on Luzon (Détroit et al., 2019), as well as yet unknown populations of archaic hominins on Sulawesi (van den Bergh et al., 2016b) and possibly more broadly within Southeast Asia (Teixeira et al., 2021) reveal a complex system of ho-

minin dispersals and diversification during the Pleistocene (Dennell and Roebroeks, 2005; Hublin, 2021). In a region with extensive volcanism and fluctuating sea levels (Voris and Museum, 2000), hominins would have experienced a number of environmental challenges during both glacial and inter-glacial periods, including changes in habitat availability and water accessibility (Dennell and Roebroeks, 2005).

During periods of glacial activity, receding coastlines exposed dry savanna-like grasslands coupled with nutrient rich montane and woodland forests connecting landmasses over the Sunda shelf (Dennell, 2010; Bird et al., 2005b). Debates surround how these environmental changes affected hominin biogeography, such as whether an expanding dry savanna corridor facilitated megafaunal and hominin dispersals (Bird et al., 2005b; Harrison et al., 2006). Moreover, patches of montane forests rich in plant and animal taxa as well as reliable water sources may have also been a valuable and sustainable habitat for hominins to exploit (Bird et al., 2005b). To reach Flores and other islands located east of the Wallace Line, migrating hominins would have had to cross open ocean, and ultimately, survive on the resources provided by these islands.

The earliest hominins on Flores arrived by at least ~1 Ma based on evidence of Oldowan-like artifacts recovered from central Flores (Brumm et al., 2010). Fluvial deposits dating to ~700 ka containing *H. floresiensis*-like dentognathic remains at Mata Menge also contain faunal remains associated with more-open habitats, such as *Stegodon florensis* and *Hooijeromys nusatenggara*, both of which show a C_4-dominated diet based on stable isotope evidence (Brumm et al., 2016). The recovery of other rare avian remains, including ducks, swans, and eagle owls, further suggests the presence of wetlands and/or patches of forested habitats in addition to the more dominate dry grasslands as supported by pollen and phytolith records (Brumm et al., 2016). These early contexts suggest that hominins on Flores likely inhabited a savanna-like grassland habitat accompanied by *Stegodon* and large murines, but these contexts

also highlight the potential importance for proximity to wetlands or more nutrient-rich habitats.

In western Flores at Liang Bua, excavations have revealed a rich and complex record of stone artifacts, faunal remains, and skeletal elements attributed to *H. floresiensis* and *H. sapiens* (Brown et al., 2004; Morwood et al., 2004, 2005; Sutikna et al., 2018; Morwood and Jungers, 2009; Moore and Brumm, 2007; Sutikna, 2016; Sutikna et al., 2016). Evidence of *H. floresiensis* occurs at Liang Bua ~190 – 50 ka based on skeletal and artifact distributions while the earliest cultural and possibly skeletal evidence of *H. sapiens* at the site occurs ~46 ka (Sutikna et al., 2016; Sutikna, 2016). A recent study based on the relative abundances of murine fauna suggests that Liang Bua was exposed to more-open and dry conditions ~190 – 60 ka before shifting to more-closed conditions between ~60 – 50 ka due to a shift in murine relative abundances (Veatch et al., 2019). This change coincides with the disappearance of skeletal remains attributed to *H. floresiensis* and other large bodied fauna (e.g., *Stegodon*, Marabou storks, and vultures), suggesting that *H. floresiensis* used the cave less often or stopped using it altogether when environmental conditions around Liang Bua were no longer optimal (Veatch et al., 2019).

Paleoenvironmental records sourced from speleothems from Liang Luar (Scroxton, 2014; Westaway et al., 2017; Griffiths et al., 2013) and Liang Neki (Westaway et al., 2007b)—cave systems within a 2 km radius of Liang Bua—as well as from eastern Java together detail local environmental responses to changes in regional climatic conditions spanning the past ~92 ka (Scroxton, 2014; Westaway et al., 2009c,b). From ~92 to 55 ka, δ^{13}C profiles suggest a more-open but fluctuating environment before changing abruptly to more-closed conditions (Scroxton, 2014; Westaway et al., 2009c,b). Between 49 and 39 ka, fast speleothem growth rates coupled with depleted δ^{18}O values and enriched δ^{13}C values suggests a wet and organically-rich environment with closed woodland conditions before transitioning to more dry and organically poor conditions

beginning ~36 until 18 ka (Westaway et al., 2007b, 2009c,b). A return of Australasian monsoons is observed beginning ~18 ka causing an increase in regional sea levels and expanding closed-canopy conditions until ~11 ka when a wet and organically-rich environment with lush humid forests, increased humidity, and rising sea levels became more stable during the early Holocene (Westaway et al., 2009c,b; Ayliffe et al., 2013; Denniston et al., 2017).

This study aims to further explore the local ecological conditions surrounding Liang Bua using the abundant murine faunal record throughout the ~190 ka stratigraphic sequence. Previous studies shows that murine body size estimates using postcrania track reasonably well with species and habitat types, suggesting that the relative abundance of murine body sizes broadly corresponds to habitat availability (Veatch, 2014; Veatch et al., 2019). Thus, known or estimated habitat preferences for each of the Flores murines suggest that a range of habitats were available near Liang Bua (Table 5.1). Specifically, these data suggest that *H. floresiensis* was exposed to more-open (~190 – 60 ka) and more-closed conditions (~60 – 50 ka) while *H. sapiens* were exposed to more-closed conditions (~49 – 3 ka) before anthropogenic landscape modification for agricultural practices and prompted the return of more-open habitat adapted murines (Veatch et al., 2019). However, habitat preferences or diets for many of these murines are unknown or have only been estimated using ecomorphology (see Table 5.1).

Flores is home to at least eight endemic murine species (*Papagomys armandvillei, Papagomys theodorverhoeveni, Spelaeomys florensis, Hooijeromys nusatenggara, Komodomys rintjanus, Paulamys naso, Rattus hainaldi, Rattus exulans*, and an undescribed giant shrew-rat) that range in body size, ecological preference, and behavior (Table 5.1). Of these eight, only four are extant species (*Papagomys armandvillei, Paulamys naso, Rattus exulans*, and *Rattus hainaldi*) known to currently inhabit Flores while another (*Komodomys rintjanus*) survives on the nearby satellite islands of

Rinca and Padar (Musser and Boeadi, 1980). *Rattus exulans* is also now widespread across Southeast Asia but is hypothesized to have originated on the island of Flores (Thomson et al., 2014). Finally, an undescribed extinct giant shrew-rat was identified based on dentognathic remains recovered from Liang Bua (Veatch et al., 2019).

Little is known regarding the habitat preferences and diets for the Flores murines as they are largely inferred from dentary ecomorphological features (Table 5.1) (Musser, 1981). Therefore, this study uses $\delta^{13}C$ and $\delta^{18}O$ values from bone and enamel carbonate attributed to various murine species and body size categories recovered from Liang Bua to (1) examine their dietary preferences and how these preferences change through time, and (2) explore the local paleoecological context for *H. floresiensis* (~190 – 50 ka) and *H. sapiens* (~47 – 46 ka and ~18 to present).

Table 5.1: The extinct and extant Flores murines.

Taxon	Body Size Category	Body Mass Range (g)	Flores Endemic[1]	Extant	Known or Presumed Diet[2]	Known or Presumed Behaviors[2]	Known or Presumed Habitat Preferences[2]	Original Descriptions
Papagomys armandvillei	Size 5	1,200–2,500[3]	yes	yes	leaves, fruits, and insects	terrestrial, burrowing	closed, semi-closed	Jentink (1892); Sody (1941)
Papagomys theodorverhoeveni	Size 4	600–1,600[4]	yes	uncertain	fruits and insects	terrestrial	closed, semi-closed	Hoojier (1957b); Musser (1981)
Spelaeomys florensis	Size 4	600–1,600[4]	yes	uncertain	leaves, flowers, buds	arboreal	closed	Hoojier (1957b)
Shrew-rat	Size 4	600–1,600[5]	yes	uncertain	earthworms, insects, fruits	terrestrial	closed	Veatch et al. (*in prep*)
Hooijeromys nusatenggara	Size 3	300–600[4]	yes	uncertain	unknown	terrestrial	open, semi-open	Musser (1981)
Paulamys naso	Size 2	100–200[6]	yes	yes	fungi, insects, snails, earthworms	terrestrial, burrowing	closed, semi-closed	Musser (1981); Musser et al. (1986)
Komodomys rintjanus	Size 2	100–200[7]	yes	yes	unknown	terrestrial	open, semi-open	Sody (1941); Musser and Boeadi (1980)
Rattus norvegicus	Size 2	150–300[8]	no	yes	omnivore	terrestrial	commensal	Berkenhout (1769)
Rattus rattus/tanezumi	Size 2	100–230[8]	no	yes	omnivore	terrestrial	commensal	Temminck (1844)
Rattus argentiventer	Size 2	100–220[4]	no	yes	omnivore	terrestrial	commensal	Robinson and Kloss (1916)
Rattus hainaldi	Size 1	40–100[9]	yes	yes	unknown	terrestrial, nesting	closed, semi-closed	Kitchener et al. (1991)
Rattus exulans	Size 1	40–100[9]	no[10]	yes	omnivore	terrestrial	commensal	Peale (1848)

[1] known only from Flores and/or satelite islands of Komodo, Rinca, and Padar
[2] based on information in Musser (1981), Musser and Boeadi (1980), Kitchener et al. (1991), and Suyanto (1998)
[3] based on data in Musser (1981) and three extant specimens with known body masses (1,495–2,285 g) in the collections of the Zoological Museum in Bogor, Indonesia
[4] based on molar sizes and other information in Musser (1981)
[5] based on morphological comparisons in Veatch et al. (*in prep*)
[6] based on molar sizes and other information in Musser (1981) and Musser et al. (1986) and one extant specimen with a known body mass of 120 g (Kitchener et al., 1991)
[7] based on molar sizes and other information in Musser and Boeadi (1980) and Musser (1981)
[8] based on recorded body weights of specimens in the collections of the National Museum of Natural History (USNM) in Washington, D.C.
[9] based on body weights and other information of Rattus exulans in Tamarin and Malecha (1972), but applies to small Rattus sp. generally
[10] although currently widespread, this taxon may have originally been endemic to Flores (Thomson et al., 2014)

5.2 Materials and Methods

A total of 514 bone (humeri, femora, mandibles, maxilla, calcanei) and enamel (molars, incisors) samples were selected for carbon and oxygen stable isotope analysis across units 1A (~190 – 120 ka), 1B (~120 – 60 ka), 2 (~60 – 50 ka), 4 (~47 – 46 ka), 6 (~18 – 13 ka), 8A (~11 – 5 ka), 8B (~5 – 3 ka), and 8C (~3 ka to present). Dental, mandibular, and maxillary fragments were identified to the species level while postcranial fragments were measured and assigned to a body size category (Veatch, 2014; Veatch et al., 2019). One dental and two bone fragments (molar, mandible, and femur) from *Stegodon floresiensis insularis*, two *Varanus komodoensis* bone fragments, and one *Hystrix* sp. femur were also analyzed for stable carbon and oxygen isotopes and are reported here.

Previous studies involving stable isotope analyses at Liang Bua show a strong correlation with depth (time) and collagen degradation (Anderson, 2011; Munizzi, 2013). Environmental factors, such as high moisture content in the surrounding sediment as well as diagenetic processes, can increase the rate of collagen loss and limit analyses at locations with high temperatures, humidity, and soil moisture, like Liang Bua (Munizzi, 2013). Conversely, $\delta^{18}O$ values from enamel carbonate samples from Liang Bua were shown to be reasonably intact due to the highly dense interwoven hydroxyapatite crystals in enamel (Munizzi, 2013). Thus, in order to reliably track changes in $\delta^{18}O$ and $\delta^{13}C$ ratios within older deposits, carbon and oxygen isotopes were measured from carbonate extracted from both enamel and bone samples. Additional precautions were taken for testing the validity of the bone samples to control for exogenous carbon and oxygen uptake during diagenesis (Koch et al., 1997). For example, specimens returning higher CO_2 values than expected during analysis were flagged and subjected to a Fourier transform infrared spectroscopy (FTIR) analysis to evaluate the chemical composition and validate whether contamination had occurred.

Samples were sent to the Laboratory for Bioarchaeological Sciences at the Univer-

sity of Central Florida and prepared for $\delta^{18}O$ and $\delta^{13}C$ analysis by Dr. Tosha Dupras using established procedures for enamel and bone carbonate (Garvie-Lok et al., 2004; Koch et al., 1997; Lee-Thorp and van der Merwe, 1987, 1989; Yoder and Bartelink, 2010). Procedures for removing organic materials and secondary carbonate from bone and enamel are summarized as follows: 1) samples were cleaned with excess trabecular bone or dentine removed before being ground into a fine powder (< 180 microns) and weighed. 2) A solution containing 0.04 ml of 2% reagent-grade bleach was added to breakdown trace organics, such as collagen. Solutions for enamel were set for 24 hours while bone was left for 72 hours. 3) Samples were rinsed and treated with acetic acid to remove absorbed diagenetic carbonates for four hours before being rinsed and frozen until dried. 4) Dried samples were weighed and stored in a cool dry place before being sent to the University of Florida's Light Stable Isotope Mass Spec Lab in the Department of Geological Sciences for $\delta^{18}O$ and $\delta^{13}C$ enamel and bone carbonate analysis.

5.2.1 $\delta^{18}O$ and $\delta^{13}C$ Analysis

Carbon stable isotope analysis was used to reconstruct the paleodiets of murine fauna from Liang Bua based on the photosynthetic pathways of plants commonly ingested in herbivorous mammals. Plants with relatively more enriched ^{13}C compared to ^{12}C, for example, are considered C_4 plants (e.g., tropical grasses, sedges, maize, etc.) while ones with a depleted ^{13}C intake relative to atmospheric CO_2 tend to have a lower ratio of ^{13}C to ^{12}C and are considered C_3 plants (e.g., leaves and most other plants except succulents) (Lee-Thorp and Sponheimer, 2006; Deniro, 1987). When ingested by animals, the plants' carbon isotopic composition is reflected in bone and enamel carbonate. In tropical ecosystems, organisms with enriched $\delta^{13}C$ values (~ +1 to –3 ‰) reflect a primarily grass-based (or C_4) diet while depleted $\delta^{13}C$ values (~ –13 ‰ or lower) indicate a leaf-based (or C_3) diet (Lee-Thorp and Sponheimer, 2006;

Roberts et al., 2015b; Jim et al., 2004). Organisms that reflect $\delta^{13}C$ values between these boundaries are considered mixed feeders who consume a combination of C_4 and C_3 plants. Thus, any changes in $\delta^{13}C$ values within murine species/body size category can be used to evaluate changes in the availability of different ecosystems, such as more-open grasslands (C_4) or intermediate forests (C_3), while differences between species/body sizes should indicate habitat and dietary preferences.

Oxygen stable isotope analysis can provide additional proxies for paleoecological conditions, such as temperature, rainfall, altitude, and primary sources of water (Kohn et al., 1996; Delgado Huertas et al., 1995). Most studies have focused on larger mammalian fauna and their ecologies for interpreting oxygen isotopes, but sampling smaller mammals to reflect more local ecological signatures is becoming more frequent and refined for interpreting paleoenvironments (Gehler et al., 2012; Hopley et al., 2006; Jeffrey et al., 2015; Yeakel et al., 2007). Jeffrey et al. (2015), for example, demonstrates that $\delta^{18}O$ values from small mammals are a reliable proxy for paleo-aridity and track reasonably well with meteoric water intake (but see Delgado Huertas et al. (1995)). Thus, any changes in murine $\delta^{18}O$ values at Liang Bua will likely reflect a combination of temperature change and/or aridity.

Other considerations include differences in $\delta^{13}C$ and $\delta^{18}O$ values between molars and incisors sampled from the same individual. Since murine incisors grow continuously throughout life and molars form while *in utero* until weeks after birth, isotope values from incisors have the potential to reflect a context at death compared to molars that form during development and nursing. However, since murines have both a relatively narrow home range and a r-selected evolutionary strategy, any observed differences between incisor and molar isotope values are likely negligible given the temporal resolution of the overall sample.

The international Vienne Pee Dee Belemnite (VPDB) standard for isotopes (Deniro, 1987) was used to report both carbon and oxygen isotope ratios from carbonates in

standard delta notation:

$$\delta = [\frac{R_{sample}}{R_{standard}} - 1] * 1000 \quad (5.1)$$

where R represents $^{13}C/^{12}C$ and $^{18}O/^{16}O$ ratios. δ values are reported as permil (‰) relative to the standard VPDB values for carbonates. Results are reported and compared using the mean, standard deviation, range, and coefficient of variation between murine body sizes, species, and stratigraphic units for both $\delta^{18}O$ and $\delta^{13}C$. To test for significance between groups, a non-parametric pairwise Mann-Whitney U test was performed using RStudio (version 1.4.1103) to evaluate differences between and within murine body sizes and stratigraphic units at the 0.05 level.

5.3 Results

A total of 370 samples were successful in producing reliable $\delta^{13}C$ and $\delta^{18}O$ ratios (Table 5.2). Of these, 93 were dental specimens (incisors, molars) (Table 5.3) and 277 were bone (femurs, humeri, calcanei, mandibles, and maxillas) (Table 5.4). 144 samples were either too small for analysis or were deemed unreliable due to unusually high levels of CO_2 captured during analysis. The chemical composition of these samples are currently being tested using FTIR analysis to evaluate contamination. A pairwise comparison between enamel and bone samples within units show a significant difference in $\delta^{13}C$ and $\delta^{18}O$ values in Units 1B and 8C ($p < 0.0001$) but not in Unit 8B ($p = 0.27$ and $p = 0.35$) (Other units did not have an appropriate sample size for comparison).

Murine samples from Liang Bua show a full range of C_3 and C_4 feeding ecology, with some species showing a preference for C_4 resources (e.g., *Komodomys rintjanus*) and others showing a greater preference for C_3 resources (e.g., *Papagomys armandvillei*) (Table 5.3). Overall, $\delta^{13}C$ values range from –13.77 to –2.68‰ with an average of –6.7‰ +/- 2.58σ and $\delta^{18}O$ values range from –6.19 to –1.89‰ with an

Table 5.2: Summary of $\delta^{13}C$ and $\delta^{18}O$ values from combined enamel and bone apatite samples according to murine body size, stratigraphic unit, and hominin occupation.

Murine				$\delta^{13}C$								$\delta^{18}O$							
Body Size	Units	Occupation	*n*	AVG	SDV	CV%	Min	Max	Occ. AVG	Occ. SDV	Occ. CV%	AVG	SDV	CV%	Min	Max	Occ. AVG	Occ. SDV	Occ. CV%
Size 1	1A	*H. floresiensis*	2	-7.68	0.60	7.8	-8.1	-7.3				-3.47	1.21	35.0	-4.3	-2.6			
(<100 g)	1B	*H. floresiensis*	18	-6.94	1.79	25.8	-8.8	-3.7	-6.86	1.71	24.9	-4.64	0.79	17.0	-5.7	-2.7	-4.43	0.74	16.7
	2	*H. floresiensis*	14	-6.65	1.74	26.1	-8.6	-3.9				-4.29	0.49	11.4	-4.9	-3.3			
	4	*H. sapiens*	6	-4.55	1.44	31.8	-6.9	-3.2				-3.55	0.84	23.8	-4.5	-2.5			
	6	*H. sapiens*	2	-8.84	1.48	16.8	-9.9	-7.8				-4.34	0.08	1.7	-4.4	-4.3			
	8A	*H. sapiens*	3	-10.25	3.66	35.7	-12.7	-6.1	-8.55	2.26	26.4	-4.00	0.17	4.2	-4.2	-3.9	-4.40	0.82	24.9
	8B	*H. sapiens*	5	-10.14	1.34	13.2	-11.8	-8.2				-4.80	0.45	9.5	-5.5	-4.3			
	8C	*H. sapiens*	39	-8.81	1.70	19.2	-11.6	-5.3				-4.51	0.82	18.3	-6.2	-3.1			
Size 2	1A	*H. floresiensis*	38	-3.87	0.50	13.0	-5.0	-2.9				-4.20	0.42	10.0	-5.0	-3.4			
(~100 – 200 g)	1B	*H. floresiensis*	39	-4.03	0.89	22.2	-7.5	-2.9	-4.00	0.86	26.4	-4.28	0.93	21.7	-5.9	-3.1	-4.21	0.72	17.1
	2	*H. floresiensis*	5	-4.73	2.04	43.2	-6.8	-2.2				-3.81	0.69	18.1	-4.4	-2.9			
	4	*H. sapiens*	5	-4.36	1.05	24.1	-5.4	-3.2				-4.76	0.97	20.4	-6.0	-3.5			
	6	*H. sapiens*	3	-7.13	0.53	7.4	-7.7	-6.7				-4.31	0.40	9.4	-4.7	-3.9			
	8A	*H. sapiens*	4	-11.07	1.72	15.6	-13.0	-9.6	-7.76	2.44	31.4	-4.99	0.45	9.0	-5.5	-4.5	-4.74	0.78	24.9
	8B	*H. sapiens*	4	-9.03	1.11	12.3	-10.3	-8.0				-5.22	0.45	8.7	-5.8	-4.7			
	8C	*H. sapiens*	67	-7.76	2.34	30.1	-12.7	-2.7				-4.71	0.80	17.1	-7.9	-3.3			
Size 3	1A	*H. floresiensis*	5	-4.97	2.88	57.8	-10.1	-3.1				-4.48	0.83	18.4	-5.5	-3.4			
(~300 – 600 g)	1B	*H. floresiensis*	2	-4.43	0.61	13.8	-4.9	-4.0	-5.72	2.26	26.4	-4.76	1.78	37.4	-6.0	-3.5	-4.53	0.85	18.9
	2	*H. floresiensis*	4	-7.29	0.71	9.7	-8.2	-6.6				-4.48	0.65	14.6	-5.3	-3.8			
	4	*H. sapiens*		-	-	-	-	-				-	-	-	-	-			
	6	*H. sapiens*		-	-	-	-	-				-	-	-	-	-			
	8A	*H. sapiens*	22	-10.74	2.14	19.9	-15.7	-7.1	-10.08	2.14	21.2	-5.10	0.77	15.1	-6.8	-3.5	-4.97	0.74	24.9
	8B	*H. sapiens*	7	-10.50	0.94	8.9	-11.7	-9.4				-5.13	0.32	6.1	-5.5	-4.7			
	8C	*H. sapiens*	8	-7.91	1.45	18.3	-10.5	-6.0				-4.46	0.74	16.6	-5.3	-3.3			
Size 4	1A	*H. floresiensis*		-	-	-	-	-				-	-	-	-	-			
(~600 – 1,600 g)	1B	*H. floresiensis*	5	-6.64	2.29	34.5	-9.8	-3.4	-6.77	2.07	26.4	-4.43	0.98	22.1	-5.7	-3.3	-4.29	0.94	21.9
	2	*H. floresiensis*	1	-7.37	-	-	-7.4	-7.4				-3.60	-	-	-3.6	-3.6			
	4	*H. sapiens*	1	-2.39	-	-	-2.4	-2.4				-3.46	-	-	-3.5	-3.5			
	6	*H. sapiens*		-	-	-	-	-				-	-	-	-	-			
	8A	*H. sapiens*	7	-11.46	1.43	12.5	-12.5	-9.3	-9.16	2.93	32.0	-4.92	0.68	13.7	-6.2	-3.9	-4.55	0.74	24.9
	8B	*H. sapiens*	1	-6.64	-	-	-6.6	-6.6				-4.72	-	-	-4.7	-4.7			
	8C	*H. sapiens*	5	-7.81	0.53	6.8	-8.3	-7.1				-4.22	0.63	14.9	-5.1	-3.6			
Size 5	1A	*H. floresiensis*	5	-6.37	2.86	45.0	-9.4	-2.9				-3.76	0.45	12.0	-4.2	-3.1			
(~1,200 – 2,500 g)	1B	*H. floresiensis*	1	-3.74	-	-	-3.7	-3.7	-6.28	2.52	26.4	-5.47	-	-	-5.5	-5.5	-4.09	0.69	16.9
	2	*H. floresiensis*	2	-7.32	1.74	23.7	-8.5	-6.1				-4.22	0.21	5.0	-4.4	-4.1			
	4	*H. sapiens*	4	-6.14	2.85	46.3	-8.7	-2.1				-3.62	0.72	20.0	-4.2	-2.8			
	6	*H. sapiens*	8	-10.45	3.33	31.8	-13.8	-5.1				-3.25	1.14	35.2	-5.8	-1.9			
	8A	*H. sapiens*	5	-12.01	0.68	5.7	-12.5	-10.8	-9.86	2.64	26.7	-4.99	0.51	10.3	-5.5	-4.2	-4.28	1.03	24.9
	8B	*H. sapiens*	6	-10.36	1.37	13.2	-12.3	-8.4				-5.00	0.55	10.9	-5.6	-4.3			
	8C	*H. sapiens*	11	-9.53	1.81	18.9	-12.3	-7.2				-4.56	0.73	16.0	-5.6	-3.4			

Table 5.3: Summary of $\delta^{13}C$ and $\delta^{18}O$ values from enamel carbonate according to species, stratigraphic unit, and hominin occupation.

	Murine				δ13C		δ18O	
Species	Body size	Units	Occupation	*n*	AVG	SDV	AVG	SDV
Hooijeromys nusatenggara	Size 3	8A	*H. sapiens*	5	-9.47	0.77	-4.80	0.60
Hooijeromys nusatenggara	Size 3	8C	*H. sapiens*	4	-7.77	1.90	-3.97	0.67
Komodomys rintjanus	Size 2	1A	*H. floresiensis*	16	-3.93	0.56	-4.22	0.45
Komodomys rintjanus	Size 2	1B	*H. floresiensis*	12	-3.38	0.28	-3.38	0.16
Komodomys rintjanus	Size 2	8C	*H. sapiens*	22	-6.46	1.70	-4.32	0.52
Papagomys armandvillei	Size 5	1A	*H. floresiensis*	3	-4.67	2.32	-3.75	0.57
Papagomys armandvillei	Size 5	8B	*H. sapiens*	2	-9.03	0.94	-5.23	0.07
Papagomys armandvillei	Size 5	8C	*H. sapiens*	2	-8.63	2.09	-3.75	0.53
Papagomys theodorverhoeveni	Size 4	8C	*H. sapiens*	4	-7.90	0.56	-4.14	0.69
Paulamys naso	Size 2	6	*H. sapiens*	2	-7.20	0.73	-4.33	0.57
Small Rattus sp.	Size 1	1B	*H. floresiensis*	1	-5.10	-	-2.72	-
Small Rattus sp.	Size 1	8C	*H. sapiens*	14	-8.38	1.35	-4.03	0.73
Stegodon florensis insularis		1B	*H. floresiensis*	1	-3.22	-	-2.59	-

average of –4.25‰ +/- 0.75σ (Tables 5.2).

Differences in $\delta^{13}C$ and $\delta^{18}O$ ratios between incisors and molars from the same individuals were first evaluated to explore isotope ratios during different stages of enamel formation and development (Table 5.5) (Catón and Tucker, 2009). Figure 5.1 shows the difference in carbon and oxygen isotope values between mandibular incisors and molars belonging to the same individual, expressed as $d^{13}C_{incisor-molar}$ and $d^{18}O_{incisor-molar}$. Absolute differences in inter-tooth $\delta^{13}C$ values from size 2 mandibles (*K. rintjanus*) in Unit 1A (Average Δ0.39‰ +/- 0.33 σ) and Unit 1B (Average Δ0.27‰ +/- 0.17 σ) are both $<$ 1 ‰. A single specimen (*Paulamys naso*) from Unit 6 had a difference in $\delta^{13}C$ values of 1.03‰ and three large bodied individuals (*H. nusatenggara* and *P. armandvillei*) averaged Δ0.99‰ +/- 0.47 σ from Unit 8A. Individuals from Unit 8C showed the greatest $d^{13}C_{incisor-molar}$ values with an average of Δ1.7 ‰ +/- 1.36 σ from 21 individuals. $d^{18}O_{incisor-molar}$ showed a similar pattern where individuals in Units 1A (Average Δ0.32 ‰ +/- 0.5 σ) and 1B (Average Δ0.24 ‰ +/- 0.17 σ) showed small differences between teeth, while Units 6 (Δ0.81 ‰), 8A (Average Δ0.78 ‰ +/- 0.6 σ), and 8C (Average Δ0.54 ‰ +/- 0.42 σ) showed a

Table 5.4: Summary of $\delta^{13}C$ and $\delta^{18}O$ values from bone carbonate according to murine body size, stratigraphic unit, and hominin occupation.

Murine Body				δ13C		δ18O	
Size / Species	Units	Occupation	n	AVG	SD	AVG	SD
Size 1	1A	*H. floresiensis*	2	-7.68	0.60	-3.47	1.21
(<100 g)	1B	*H. floresiensis*	17	-7.04	1.78	-4.75	0.64
	2	*H. floresiensis*	14	-6.65	1.74	-4.29	0.49
	4	*H. sapiens*	6	-4.55	1.44	-3.55	0.84
	6	*H. sapiens*	2	-8.84	1.48	-4.34	0.08
	8A	*H. sapiens*	3	-10.25	3.66	-4.00	0.17
	8B	*H. sapiens*	5	-10.14	1.34	-4.80	0.45
	8C	*H. sapiens*	25	-9.06	1.84	-4.78	0.76
size 2	1A	*H. floresiensis*	22	-3.83	0.47	-4.18	0.40
(100 – 200 g)	1B	*H. floresiensis*	27	-4.32	0.93	-4.67	0.85
	2	*H. floresiensis*	5	-4.73	2.04	-3.81	0.69
	4	*H. sapiens*	5	-4.36	1.05	-4.76	0.97
	6	*H. sapiens*	1	-6.99	-	-4.29	-
	8A	*H. sapiens*	4	-11.07	1.72	-4.99	0.45
	8B	*H. sapiens*	4	-9.03	1.11	-5.22	0.45
	8C	*H. sapiens*	40	-8.51	2.43	-4.98	0.86
Size 3	1A	*H. floresiensis*	5	-4.97	2.88	-4.48	0.83
(300 – 600 g)	1B	*H. floresiensis*	2	-4.43	0.61	-4.76	1.78
	2	*H. floresiensis*	4	-7.29	0.71	-4.48	0.65
	4	*H. sapiens*	0	-	-	-	-
	6	*H. sapiens*	0	-	-	-	-
	8A	*H. sapiens*	17	-11.11	2.28	-5.20	0.80
	8B	*H. sapiens*	7	-10.50	0.94	-5.13	0.32
	8C	*H. sapiens*	4	-8.05	1.11	-4.94	0.46
Size 4	1A	*H. floresiensis*	0	-	-	-	-
(600 – 1,600 g)	1B	*H. floresiensis*	5	-6.64	2.29	-4.43	0.98
	2	*H. floresiensis*	1	-7.37	-	-3.60	-
	4	*H. sapiens*	1	-2.39	-	-3.46	-
	6	*H. sapiens*	0	-	-	-	-
	8A	*H. sapiens*	7	-11.46	1.43	-4.92	0.68
	8B	*H. sapiens*	1	-6.64	-	-4.72	-
	8C	*H. sapiens*	1	-7.44	-	-4.56	-
Size 5	1A	*H. floresiensis*	2	-8.91	0.72	-3.78	0.40
(1,200 – 2,500 g)	1B	*H. floresiensis*	1	-3.74	-	-5.47	-
	2	*H. floresiensis*	2	-7.32	1.74	-4.22	0.21
	4	*H. sapiens*	4	-6.14	2.85	-3.62	0.72
	6	*H. sapiens*	8	-10.45	3.33	-3.25	1.14
	8A	*H. sapiens*	5	-12.01	0.68	-4.99	0.51
	8B	*H. sapiens*	4	-11.02	1.03	-4.88	0.67
	8C	*H. sapiens*	9	-9.73	1.81	-4.74	0.66
Varanus komodoensis	1B	*H. floresiensis*	2	-3.41	0.03	-3.31	0.40
Hystrix sp.	8C	*H. sapiens*	1	-8.49	-	-4.54	-

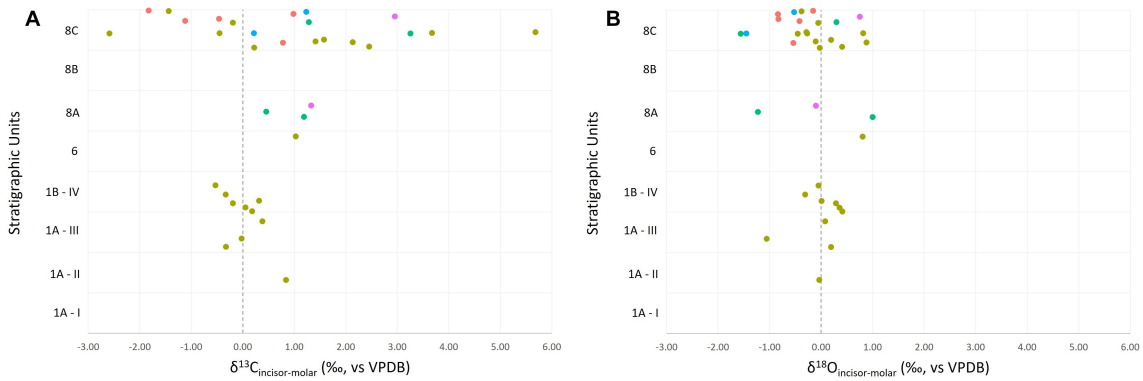

Figure 5.1: (A) $d^{13}C_{incisor-molar}$ and (B) $d^{18}O_{incisor-molar}$ from the same individuals according to unit. Stratigraphic units are displayed along the y axis with values jittered within each corresponding unit. Positive values indicate the incisor was more enriched in δ^{13}C or δ^{18}O while negative values indicate the molar is more enriched. Values are color coded according to murine body size (Size 1 = red; Size 2 = gold; Size 3 = green; Size 4 = blue; Size 5 = fuchsia).

greater range in inter-tooth δ^{18}O values. Overall, this shows that murines from Units 1A (~190 – 120 ka), 1B (~120 – 60 ka), 6 (~18 – 13 ka), and 8A (~11 – 5 ka) had a maximum $d^{13}C_{incisor-molar}$ difference of 1.33 ‰ and a maximum $d^{18}O_{incisor-molar}$ difference of 1.23 ‰, while murines from Unit 8C (~3 ka – present) had a maximum $d^{13}C_{incisor-molar}$ difference of 5.68 ‰ and a maximum $d^{18}O_{incisor-molar}$ difference of 1.56 ‰. In other words, murines dated to >~3 ka showed a relatively small difference in carbon isotopes (average 0.53 ‰) between the early stages of development (i.e., molars) and time of death (i.e., incisors) suggesting only a slight change in diet over the murines lifespan, while those dating to <~3 ka showed a relatively greater change in diet over their lifespans (average 1.71 ‰).

5.3.1 Units 1A – 2 (~190 – 50 ka): *Homo floresiensis*

Comparisons of δ^{13}C values between murine body size categories indicate that the dominant size 2 murine (*Komodomys rintjanus*) consumed C_4 grasses almost exclusively while murines from other body size categories (1, 3, 4, and 5) were more eclectic foragers showing a contribution of both C4 and C3 vegetation as part of their diets

Table 5.5: Inter-tooth comparison of individuals sampled for $\delta^{13}C$ and $\delta^{18}O$ according to species and stratigraphic unit shown in Figure 5.1).

					d13C (‰, vs VPDB)					d18O (‰, vs VPDB)				
Unit	Species	Size	Tooth	n	AVG	SDV	Min	Max	Avg ‰ difference	AVG	SDV	Min	Max	Avg ‰ difference
8C	Rattus sp.	1	incisor	5	-8.45	1.59	-10.88	-6.95	0.33	-4.31	0.69	-5.38	-3.57	0.56
			molar	5	-8.12	1.48	-10.41	-6.26		-3.75	0.70	-4.84	-3.09	
	Komodomys rintjanus	2	incisor	9	-5.73	1.94	-7.17	-2.68	1.23	-4.30	0.37	-4.90	-3.59	0.11
			molar	9	-6.47	1.23	-8.36	-4.77		-4.19	0.59	-5.31	-3.30	
	Rattus sp.	2	incisor	2	-6.28	0.60	-6.71	-5.86	2.90	-3.83	0.16	-3.95	-3.72	0.85
			molar	2	-9.18	0.49	-9.53	-8.84		-4.68	0.12	-4.76	-4.60	
	Hooijeromys nusatenggara	3	incisor	2	-6.64	0.84	-7.24	-6.04	2.27	-4.29	0.86	-4.89	-3.68	0.63
			molar	2	-8.91	2.24	-10.49	-7.32		-3.66	0.46	-3.98	-3.33	
	Papagomys theodorverhoeveni	4	incisor	2	-7.54	0.65	-7.99	-7.08	0.72	-4.63	0.68	-5.11	-4.16	0.99
			molar	2	-8.26	0.07	-8.31	-8.21		-3.65	0.02	-3.66	-3.63	
	Papagomys armandvillei	5	incisor	1	-7.16	-	-	-	2.95	-3.38	-	-	-	0.75
			molar	1	-10.11	-	-	-		-4.13	-	-	-	
8A	*Hooijeromys nusatenggara*	3	incisor	2	-9.08	0.63	-9.53	-8.63	0.82	-4.80	0.51	-5.16	-4.44	0.11
			molar	2	-9.90	1.15	-10.71	-9.08		-4.69	1.06	-5.44	-3.94	
	Papagomys armandvillei	5	incisor	1	-8.36	-	-	-	1.33	-5.28	-	-	-	0.10
			molar	1	-9.69	-	-	-		-5.18	-	-	-	
6	*Paulamys naso*	2	incisor	1	-6.69	-	-	-	1.03	-3.92	-	-	-	0.81
			molar	1	-7.72	-	-	-		-4.73	-	-	-	
1B	*Komodomys rintjanus*	2	incisor	6	-3.42	0.30	-3.80	-3.13	0.95	-3.33	0.19	-3.55	-3.05	0.12
			molar	6	-3.34	2.42	-3.70	-2.93		-3.44	0.12	-3.56	-3.23	
1A	*Komodomys rintjanus*	2	incisor	2	-3.68	0.21	-3.83	-3.53	0.18	-4.52	0.24	-4.69	-4.35	0.43
			molar	2	-3.50	0.01	-3.51	-3.50		-4.09	0.64	-4.54	-3.63	

(Figure 5.2). In Units 1A and 1B, size 2 murines (n = 77) also have a relatively narrow $\delta^{13}C$ range (–7.5 to –2.9‰; 17.6 average CV%) compared to other murine body sizes with a greater C_3 component (–10.1 to –2.9‰; 30.8 average CV%), which are also less represented (n = 38). Size 2 murines are also slightly more enriched in $\delta^{13}C$ on average in Unit 1A (– 3.87‰) compared to 1B (–4.03‰) and 2 (– 4.73‰) suggesting a slight increase in C_3 resources in Unit 1B, and subsequently, Unit 2 (Table 5.2). Moreover, all murine body size categories show an overlapping range of $\delta^{18}O$ values in Units 1A, 1B, and 2 between –6 and –2.6‰ and averaging –4.2‰ in Unit 1A and slightly shifting to –4.4‰ in Unit 1B before returning to –4.2‰ in Unit 2 (Table 5.2). In addition, two *Varanus komodoensis* and two *Stegodon florensis insularis* samples from Unit 1B all correspond to a C4 dominated diet, or consuming herbivores with a heavy C4 dietary component in the case of the Komodo dragon (Tables 5.3 and 5.4).

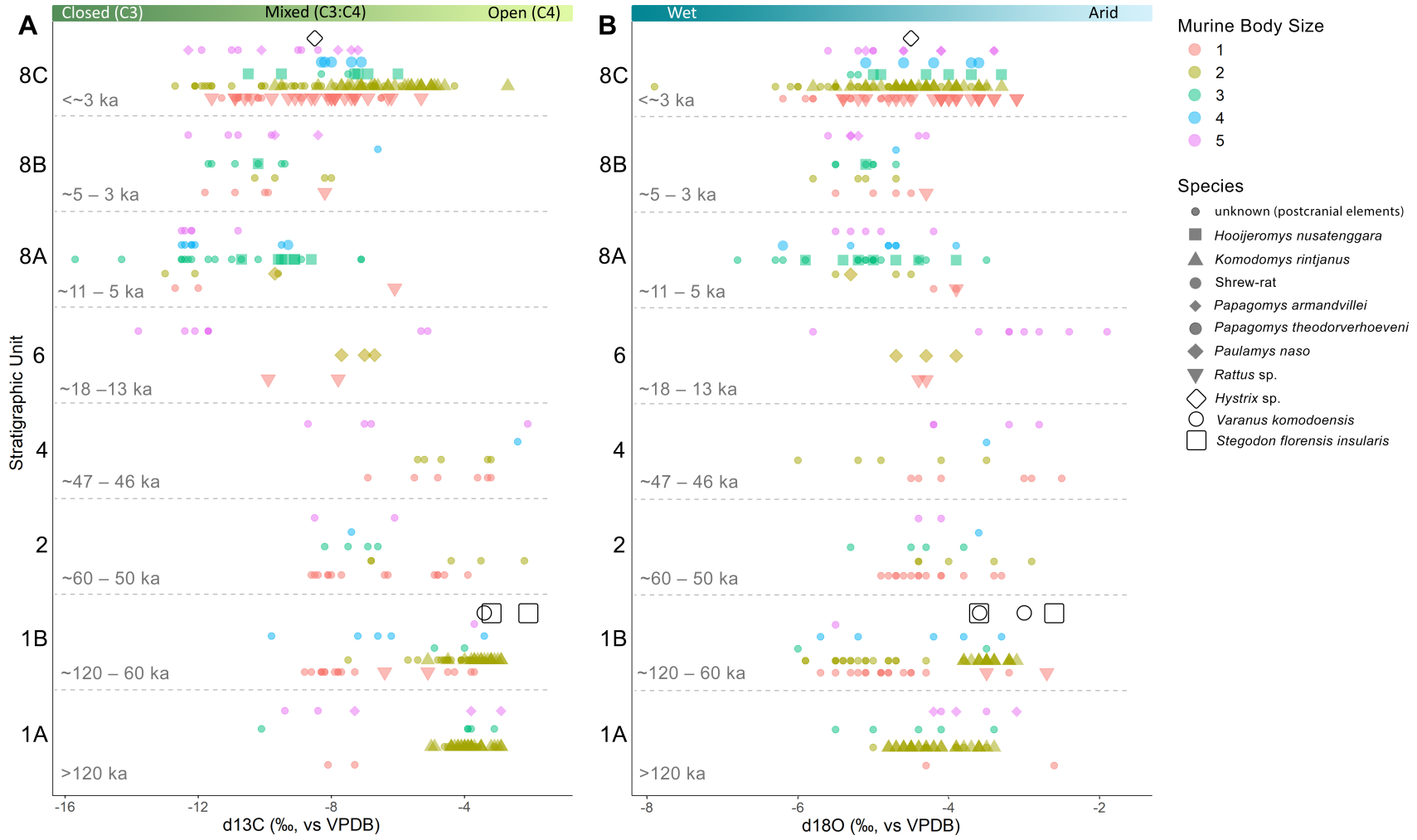

Figure 5.2: Plotted $\delta^{13}C$ (A) and $\delta^{18}O$ (B) values from enamel and bone carbonate samples according to body size (color), species (shapes), and stratigraphic units (y axis). Bone samples are represented by small circles while enamel samples are represented by species (shapes).

5.3.2 Units 4, 6 – 8C (~47 – 46 ka, and 18 ka present): *Homo sapiens*

Unit 4 (~47 – 46 ka) shows a slight shift in the distribution of $\delta^{13}C$ and $\delta^{18}O$ values compared to Unit 2 with a $\delta^{13}C$ range of –8.72 to –2.08‰ and a $\delta^{18}O$ range of – 6.02 to –2.53‰ to reflect a greater intake of C4 resources (Figure 5.2). Size 1 murines in particular show a shift in $\delta^{13}C$ values from averaging –6.65‰ in Unit 2 to –4.55‰ in Unit 4—the most enriched $\delta^{13}C$ average recorded for this murine body size category (Table 5.2).

Unit 6 (~18 – 11 ka) shows the largest range in both $\delta^{13}C$ (–13.77 to –5.08‰) and $\delta^{18}O$ (–5.76 to –1.89‰) values (Figures 5.2 and 5.3; Table 5.2). Compared to Unit 4, size 2 murines show a large shift towards a more mixed feeding ecology in Unit 6 (average of –7.13‰) as well as slightly more wet ecosystems (–4.31‰ $\delta^{18}O$). Size 1 murines also shift towards more mixed and wet feeding ecology (average of –8.84‰ $\delta^{13}C$; average of –4.34‰ $\delta^{18}O$) while six of the eight size 5 specimens show a true C3 diet (average –12.21‰) for the first time and two are more mixed (average –5.18‰).

All murine body size categories in Unit 8A (~11 – 5 ka) continue to shift towards a more C3-rich diet. Size 3 murines (*Hooijeromys nusatenggara*) show the largest range of $\delta^{13}C$ values from a more mixed diet (–7.10‰) to a true C3 diet (–15.65‰) that overlap with all other murine body sizes. A single mandibular specimen identified as the shrew-rat shows a highly depleted $\delta^{18}O$ value (–6.16‰) with a more mixed $\delta^{13}C$ value (–9.27‰) indicating that the shrew-rat, and some size 3 murines with a $\delta^{18}O$ value of <–6‰, inhabited a slightly different niche compared to other murines at this time. However, the $\delta^{13}C$ averages for all murine body sizes show a similar preference for C3 resources for the first time (ranging between –12.01 and –10.25‰) (Table 5.2; Figure 5.4).

Unit 8B (~5 – 3 ka) shows a similar shift in all murine body sizes to reflect a slightly more mixed diet compared to Unit 8A (Figure 5.4). A single size 4 sample

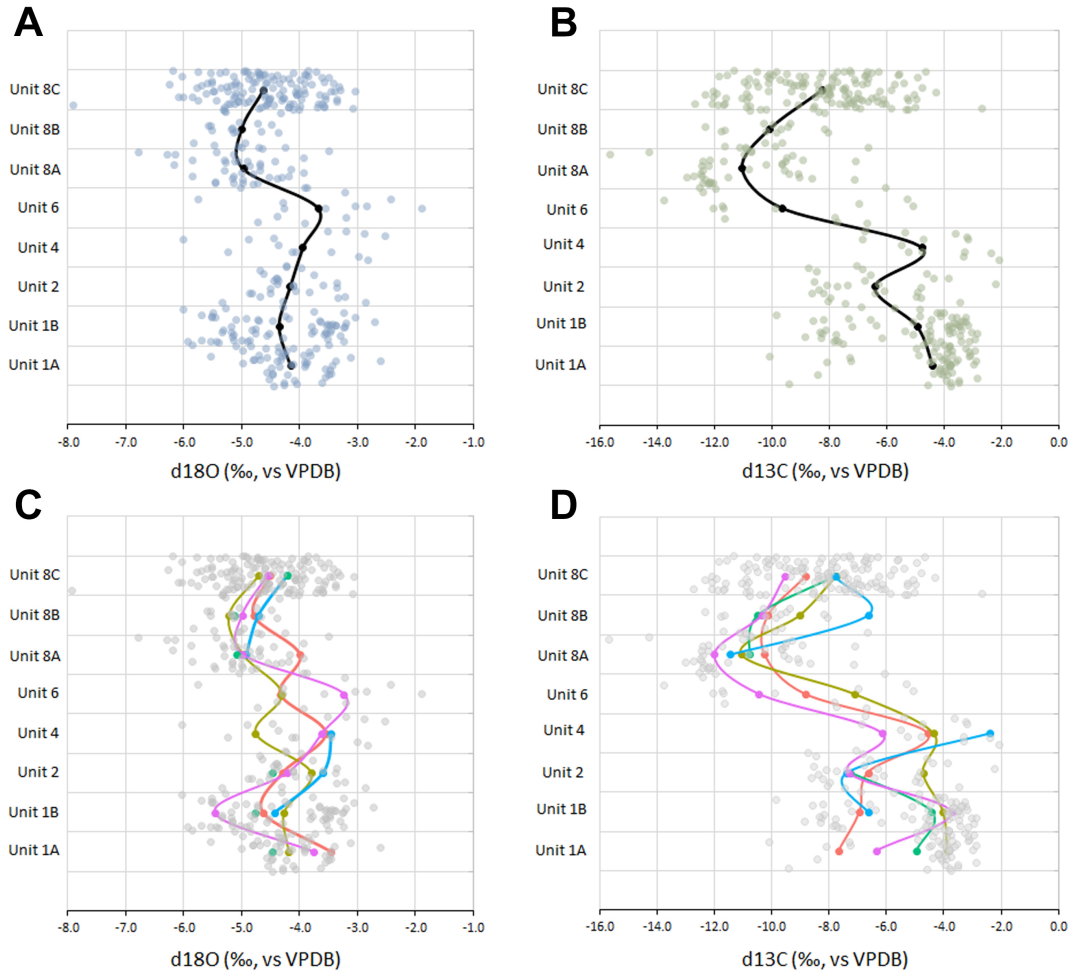

Figure 5.3: (A–B) Jittered $\delta^{13}C$ (green) and $\delta^{18}O$ (blue) values from enamel and bone carbonate samples with each units mean value plotted in black. (C–D) Jittered $\delta^{13}C$ and $\delta^{18}O$ values plotted in gray with the units mean values plotted according to body size (Size 1 = red; Size 2 = gold; Size 3 = green; Size 4 = blue; Size 5 = fuchsia).

shows that largest change in $\delta^{13}C$ values (–11.46‰ in 8A to –6.64‰ in 8B) while all other body sizes show an average $\delta^{13}C$ of <–9‰ (Table 5.2). Lastly, a shift in the average $\delta^{13}C$ and $\delta^{18}O$ values from Unit 8B to 8C is observed within all murine body sizes from a slightly greater C3 dietary preference to one encompassing a wide range of C4 and C3 resources (Figure 5.4). This trend indicates a change in resource availability that resulted in a variety of diets and habitats within all murines species and body sizes.

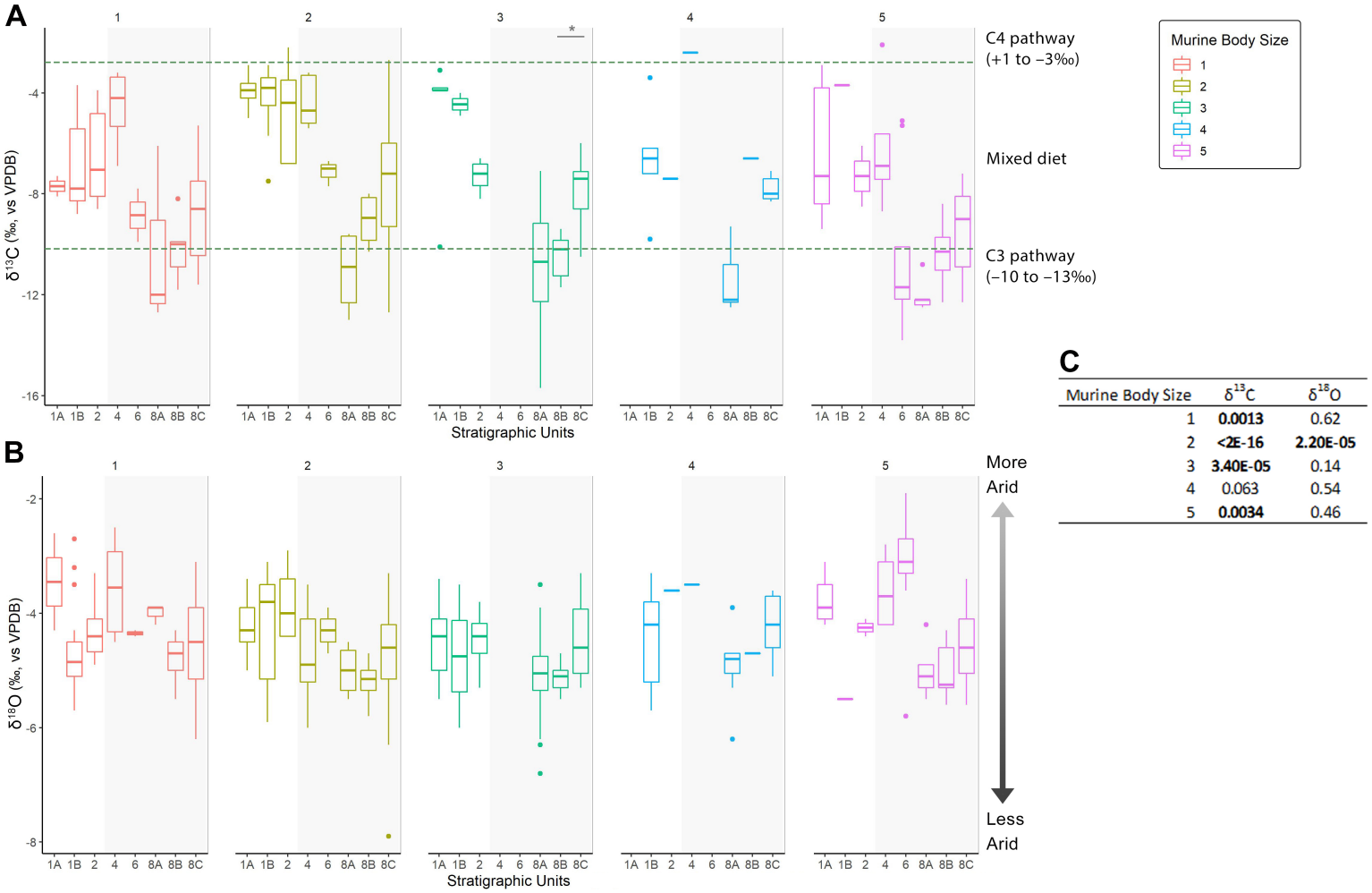

C

Murine Body Size	$\delta^{13}C$	$\delta^{18}O$
1	**0.0013**	0.62
2	**<2E-16**	**2.20E-05**
3	**3.40E-05**	0.14
4	0.063	0.54
5	**0.0034**	0.46

Figure 5.4: (A - B) Boxplots showing the mean (bar), 25th and 75th quartiles (box), 1.5∗ the inter-quartile range (whiskers), and outliers (points) of $\delta^{13}C$ and $\delta^{18}O$ values extracted from enamel and bone carbonate samples and graphed according to murine body size and stratigraphic units. Grey bars highlight units associated with *H. sapiens* while the white bars contains units associated with *H. floresiensis*. Asterisks indicate level of significance between successive groups using the Mann-Whitney U statistical test: * <= 0.05. Murine body sizes are grouped along the x axis and color coded: size 1 = red, size 2 = gold, size 3 = green, size 4 = blue, size 5 = purple. (C) BH corrected *P* values from a pairwise Mann-Whitney U statistical analysis comparing mean $\delta^{13}C$ and $\delta^{18}O$ values of murine body sizes between *H. floresiensis* units (1A – 2) and *H. sapiens* units (4, 6 – 8C).

5.4 Discussion

5.4.1 Diets of the Liang Bua Murines

The average $\delta^{13}C$ values for each murine body size is roughly in agreement with known or presumed dietary preferences (Table 5.1) (Musser, 1981). When preferred resources are available, *Komdomys rintjanus* consumes mostly C4 resources while *Rattus exulans*, *Rattus hainaldi*, *Paulamys naso*, *Hooijeromys nusatenggara*, *Papagomys theodorverhoeveni*, and *Papagomys armandvillei* are more opportunistic with individuals showing a preference for either C3 and/or mixed resources. Interestingly, all murines show a shift in $\delta^{13}C$ values depending on the availability of resources within different stratigraphic units. This suggests that, while the Liang Bua murines tend to prefer a specific kind of ecosystem, they can be more flexible foragers under different ecological circumstances consuming the most readily available resources. For example, previous $\delta^{13}C$ studies on *Hooijeromys nusatenggara* from the Middle Pleistocene deposits in the So'a Basin of central Flores showed a hyper C4 diet (ranging between ~–2 and +1‰ VPDB), which suggested that, like *Stegodon*, *H. nusatenggara* preferred more grassland ecosystems (Brumm et al., 2016). At Liang Bua, however, a majority of *H. nusatenggara* specimens showed a mixed feeding ecology from Units 8A – 8C while the majority of postcranial specimens with an estimated size category corresponding to *H. nusatenggara* from Unit 1A showed a hyper C4 diet (with 1 specimen showing a preference for C3 resources).

The observed $\delta^{13}C$ value for a mandibular fragment identified as a shrew-rat (–9.28‰) is consistent with hypothesized habitat preferences based on ecomorphology (Veatch et al., *in prep*). The minuscule molars and powerful, robust incisors, for example, suggested an adaptation for exploiting tropical montane-forested resources, such as extracting insects burrowed in logs or snags (Veatch et al., *in prep*). The incorporation of C4-consuming insects likely explains the slightly more mixed but

C3 dominate diet, but additional sampling of this species with other insectivorous mammals, like micro-bats, is needed to further explore the isotopic ranges of these animals at Liang Bua.

5.4.2 Inter-tooth $\delta^{13}C$ and $\delta^{18}O$ variation

Differences observed in $d^{13}C_{incisor-molar}$ and $d^{18}O_{incisor-molar}$ ratios have the potential to reveal variation in diet near time at birth compared to time at death (Jeffrey et al., 2015). Permanent molars, for example, tend to reflect a more restricted temporal period (i.e., breeding season) while continuously growing incisors are likely more variable as they are not seasonally restricted in their growth patterns. Results in $d^{13}C_{incisor-molar}$ ratios of size 2 murines show a <1‰ difference in Units 1A and 1B indicating that seasonal variation was extremely low. In contrast, individuals in Units 6, 8A, and especially 8C retained a large but variable distribution of $d^{13}C_{incisor-molar}$ ratios (<6‰ difference) indicating a greater difference in diet between developmental stages. Moreover, Units 6 and 8A were also the only units to have all positive $d^{13}C_{incisor-molar}$ ratios indicating that, based on this sample, murines were breeding in more forested or C3 dominated environments and exploiting more open ones during later stages of life.

For reconstructing paleoecology, these results suggest 1) a variety of vegetation types were available to murines during different life history stages; 2) size 2 murines within Units 1A and 1B were highly specialized throughout life; and 3) dietary strategies within murine species on Flores can change over time depending on food availability.

5.4.3 Paleoecology at Liang Bua

The $\delta^{13}C$ and $\delta^{18}O$ results from murine fauna at Liang Bua confirms previous paleoecological interpretations using the relative abundance of murine body sizes (Veatch

et al., 2019), broadly supports paleoenvironmental patterns from speleothem records from Flores (Westaway et al., 2007b, 2009c,b,a; Griffiths et al., 2009; Ayliffe et al., 2013), and reveals important paleoecological hominin-rodent interactions.

From ~190 – 60 ka (Units 1A and 1B), Liang Bua was likely exposed to a combination of grasslands, inhabited mostly by size 2 murines, with patches of nearby C3 vegetation that size 1, size 3, size 4, and size 5 murines also exploited in addition to the abundant grasslands (Figure 5.4). Unfortunately, current paleoenvironmental reconstructions are limited to the past 92,000 years making comparisons with the majority of this temporal period challenging (Scroxton, 2014; Westaway et al., 2009b), but the carbon stable isotope values are in agreement with a previous zooarchaeological study that suggested Units 1A and 1B represented a more-open habitat based on the relative abundance of size 2 murines (1A: 77%; 1B: 66%) (Veatch et al., 2019). *Stegodon* remains also make up a large portion of the non-murine faunal abundances in both Units 1A (1.56%) and 1B (6.77%) (Sutikna et al., 2018) with a now confirmed C4 diet (average $\delta^{13}C$ of –2.66‰). In addition, faunal associations between Komodo dragons, Marabou storks, vultures, *Stegodon*, and *H. floresiensis* in Unit 1B (and somewhat in Unit 1A) further indicates that grasslands supported a range of fauna at Liang Bua between ~190 – 60 ka, including large carnivorous animals, large herbivores, and murines of various body sizes (Veatch et al., 2019; Sutikna et al., 2018).

While there is no major shift in murine dietary preferences in Unit 2 compared to Unit 1B, the proportion of available resources may have changed after ~60 ka. For example, previous zooarchaeological studies at Liang Bua suggest that the relative abundance of murine body sizes shift to a greater representation of size 1 murines in Unit 2 (80%) compared to Unit 1B (32%) (Veatch et al., 2019). Carbon stable isotope ratios reported here indicate that size 1 murines had a more mixed diet with a mean difference between the more-open habitat adapted size 2 murines of ~ –2.88‰. Thus,

the loss of murines preferring more-open habitats (size 2) in favor of more mixed feeding strategies (size 1) may indicate that the environment in Unit 2 is somehow functionally different from Unit 1B, potentially due to changes in predatory behavior, a reduction of suitable micro-habitats for size 2 murines, or both.

The deposition of T3, a large volcaniclastic mass flow dated to ~50 ka, marks a significant change in both stone tool raw material selection and faunal assemblages that is likely due to the arrival of *H. sapiens* (Sutikna et al., 2016, 2018). The carbon stable isotope results indicates that murine diets of all body sizes shifted slightly towards more C4 within the successive Unit 4 (~47 – 46 ka). While Unit 4 has a relatively small sample size compared to other units, the $\delta^{13}C$ ratios for size 1 and size 2 murines overlap for the first time, suggesting a slight change in the availability of resources. Nonetheless, these results suggest that grasslands were still dominant when *H. sapiens* first arrived at Liang Bua (Sutikna, 2016).

Liang Bua experienced a transition from drier and more-open conditions beginning ~36 until ~19 ka based on speleothem isotope data from Flores (Westaway et al., 2009c,b, 2007a). At ~18 ka, a rapid shift towards wetter conditions causing an increase in water availability and forested resources was detected in speleothem records sourced from western Flores and eastern Java (Westaway et al., 2009c,b). This time period also coincides with Heinrich Stadial 1 (~18 – 15 ka) —a period of global environmental perturbation resulting from the collapse of the northern hemisphere ice shelves causing a rise in atmospheric CO2 driving deglaciation (Ayliffe et al., 2013; Denniston et al., 2013). On Flores, local conditions experienced an increase in rainfall during this climatic period but the return of the monsoons did not occur until after 15 ka (Westaway et al., 2009c,b). Depleted $\delta^{18}O$ values from speleothems also indicate that from ~15 – 5 ka, Flores experienced a closed-canopy and wet conditions that stabilized during the early Holocene (Westaway et al., 2009c,b; Griffiths et al., 2009).

Results from $\delta^{13}C$ and $\delta^{18}O$ analyses of the murine fauna in Units 6 (~18 – 13 ka), 8A (~11 – 5 ka), and 8B (~5 – 3 ka) are in agreement with the paleoenvironmental reconstruction discussed above. Murines from Unit 6 showed the largest range in both $\delta^{13}C$ and $\delta^{18}O$ suggesting a combination of available resources during a time when Flores was experiencing a shift from more-open and dry environments to an increase in rainfall. Murine $\delta^{18}O$ values also do not shift to reflect an increase in precipitation until after the return of the monsoons in Unit 8A (~11 – 5 ka) and the isotopic signatures for both $\delta^{13}C$ and $\delta^{18}O$ ratios is maintained in Unit 8B (~5 – 3 ka) during the early to middle Holocene.

Unit 8C (~3 ka – present) is the first unit at Liang Bua to show a noticeable change in murine ecology that were likely due to human impacts on the local environment. Beginning at ~3 ka, the first appearance of pottery, adzes, and production of C4 agricultural products created an environment where murines could exploit a wide range of resources (Sutikna et al., 2018). Indeed, murines of all body sizes and species retain the largest range of both $\delta^{13}C$ and $\delta^{18}O$ ratios compared to all other units suggesting that all murines adopted a more opportunistic food strategy in response to human modification to the local environment.

5.5 Conclusion

Carbon and oxygen stable isotope values from murine fauna provide a local paleoecological proxy for reconstructing the preferred diets of extinct murines while also revealing the availability of local resources for hominins through time. These results support previous hypotheses suggesting that Liang Bua was exposed to more-open conditions during the time of *H. floresiensis*, but also revealed important ecological changes in older deposits that may have facilitated migrations and/or changes in the use of the cave by *H. floresiensis* and other avian predators between ~60 and 50

ka. Changes in the relative abundance of murine fauna while maintaining enriched $\delta^{13}C$ and $\delta^{18}O$ ratios, for example, suggests a functional change in local grassland ecosystems from ~60 – 50 ka. In the context of foraging *H. sapiens* beginning around 47 ka, Liang Bua was also exposed to more-open and drier conditions before slowly transitioning towards an increase in both C3 vegetation availability and precipitation that allowed for more-forested adapted murines to become more locally abundant beginning ~18 ka (Veatch et al., 2019). At ~3 ka, agriculturalists functionally altered the landscape for food and animal domestication providing a mixture of C3 and C4 resources in an environment dominated by C3 vegetation (Sutikna et al., 2018, 2020; Julianto et al., 2020). Overall, these results reveal important paleoecological considerations and contextual information for interpreting faunal abundances and hominin activity in the past, as well as hominin occupation and the use of local resources at Liang Bua.

Chapter 6

Zooarchaeology and Taphonomy of Small Mammal Remains at Liang Bua, Flores

6.1 Introduction

Flores is an oceanic island located east of the biogeographic barrier known as the Wallace line and is well known for the discovery of *Homo floresiensis* at Liang Bua, a limestone archaeological cave site located in the Manggarai province of western Flores (Fig 6.1). Stone artifacts have long been documented in early Middle Pleistocene deposits in the So'a Basin region of central Flores (Morwood et al., 1998, 2004, 2009) as well as in more recent cave deposits associated with modern human remains in western Flores, indicating a long history of hominins on the island (Maringer and Verhoeven, 1977; Morwood et al., 2009). Until the arrival of *H. sapiens*, it was originally believed that *H. erectus* was responsible for manufacturing the earliest stone artifacts on Flores despite a lack of recovery of diagnostic skeletal remains (van den Bergh et al., 1996). Continued excavations on Flores now demonstrate that hominins

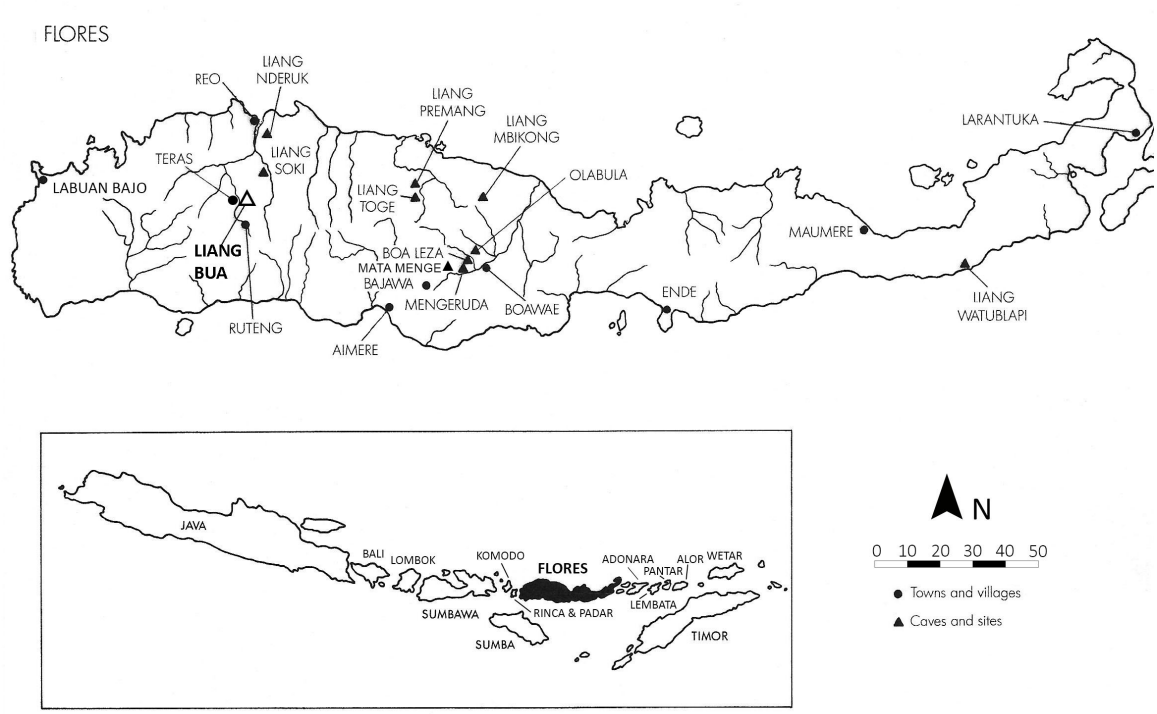

Figure 6.1: Location of Flores within the Indonesian archipelago and Liang Bua in relation to other towns and archaeological sites on Flores. Image modified from original provided by Guy Musser.

were present on Flores as early as ~1 million years ago (Brumm et al., 2010), with early Middle Pleistocene stone artifacts and *Homo floresiensis*-like dentognathic remains recovered from Mata Menge (Brumm et al., 2006, 2016; van den Bergh et al., 2016a), and Late Pleistocene skeletal and cultural remains attributed to *Homo floresiensis* recovered from Liang Bua (Brown et al., 2004; Morwood et al., 2004, 2005; Sutikna et al., 2018; Moore and Brumm, 2007).

Excavations at Liang Bua have revealed rich and complex stratified deposits of Middle to Late Pleistocene and Holocene material since the 1960s, including non-overlapping temporal boundaries of *H. floresiensis* and *H. sapiens*, as well as the transition from foraging to a farming subsistence strategy in the latter (Sutikna, 2016; Sutikna et al., 2016, 2018; Morwood et al., 2009; Oliveira et al., 2020). Skeletal evidence of *H. floresiensis* is currently bracketed between ~100 – 60 ka with behavioral evidence (i.e., stone artifacts reasonably attributable to *H. floresiensis*) occurring

until ~50 ka (Sutikna, 2016). In contrast, skeletal and cultural evidence of *H. sapiens* is found throughout the Holocene deposits at the site (Morwood et al., 2009; Moore et al., 2009; Sutikna, 2016; Sutikna et al., 2016) and recent research suggests that this evidence extends as far back as ~46 ka (Morley et al., 2017; Sutikna, 2016; Sutikna et al., 2018). The presence of polished stone adzes and Neolithic burials with grave goods marks the transition to a more sedentary lifestyle at ~3 ka (Sutikna et al., 2018; Julianto et al., 2020).

The faunal sequence at Liang Bua from ~190 to 50 ka ago is comprised of only five animals larger than ~3 kg — *Homo floresiensis*, a dwarf subspecies of proboscidean (*Stegodon florensis insularis*), giant marabou stork (*Leptoptilos robustus*), vulture (*Trigonoceps* sp.), and Komodo dragon (*Varanus komodoensis*) (Sutikna et al., 2018; Meijer et al., 2013; van den Bergh et al., 2009, 2008; Hocknull et al., 2009). The disappearance of all five of these larger animals, including *H. floresiensis*, at ~50 ka suggests a type of interdependency existed among these taxa (e.g., a sole large herbivore surrounded by a scavenging guild), and their mutual extinction (or local extirpation in the case of the Komodo dragon) is plausibly related to some major event, such as the arrival of *H. sapiens* and/or environmental change (Sutikna et al., 2016, 2018; Veatch et al., 2019). The earliest appearance of non-endemic fauna occurs at ~7 ka with the Sulawesi warty pig (*Sus celebensis*), followed by the Eurasian pig (*Sus scrofa*), Javanese porcupines (*Hystrix javanica*), long-tailed macaque (*Macaca fascicularis*), and masked palm civets (*Paradoxurus hermaphroditus*) at ~3 ka, and then deer (*Rusa* sp.), and dog (*Canis familiaris*) as soon as ~1 ka, and finally, bovid (*Bos* sp.) and horse (*Equus* sp.) within the last ~500 years (Sutikna et al., 2018; van den Bergh et al., 2009; Sutikna et al., 2020).

Small mammals make up an overwhelming majority of skeletal remains compared to all other faunal groups at Liang Bua, 92% of which belong to multiple species of murine rodents (i.e., rats). During the time of *H. floresiensis*, murines represent

~85 – 94% of the total faunal assemblage compared to ~55 – 79% when *H. sapiens* used the cave (Sutikna et al., 2018). Like other Wallacean islands (disconnected from continental mainlands), Flores is home to a variety of endemic murines ranging is diverse body sizes and habitats, including eight endemic (four extant and four extinct) and four commensal species (all extant) from ~50 g to 2.5 kg in body weight (Musser, 1981; Veatch et al., 2019).

Paleoenvironmental interpretations based on the relative abundances of murine rodents from Liang Bua suggest that *H. floresiensis* was exposed to a more-open and potentially dry environment from ~190 – 60 ka (Veatch et al., 2019). From about 60 - 50 ka, the environment shifted to a more-forested ecology, and may explain why the disappearance of the more-open habitat adapted fauna, such as *Stegodon*, Marabou storks, vultures, and Komodo dragons, either disappear or significantly reduce in numbers at this time (Sutikna et al., 2018; Veatch et al., 2019). Speleothem records from Java and Flores indicate that this more-closed, wet and organically-rich environment continued until ~39 ka when a decrease in rainfall led to a more dry but stable environment until ~17 ka (Westaway et al., 2009c,b,a). This regional signal is somewhat supported by the local murine abundances at Liang Bua, with a gradual increase in more-open habitat adapted murines from ~47 to 13 ka. However, given the greater abundance of more-closed habitat adapted murines at this time, Liang Bua was likely exposed to a more mixed or patchy environment (Veatch et al., 2019). Rainfall returned with the monsoons at ~15 – 11 ka and Liang Bua was again exposed to a more wet and stable environment that continues until modern human populations began clearing land for planting crops ~3 ka ago, enabling more open-habitat adapted murines to return (Westaway et al., 2009a; Veatch et al., 2019).

The combined faunal and environmental patterns emerging from Liang Bua suggests that *H. floresiensis* (~190 – 50 ka) and *H. sapiens* (~46 – present) were exposed to very different landscapes and ecosystems, with the former living in a dry

and primarily open terrain with a large herbivore and competing scavengers whereas the lived in a closed and wet but fluctuating environment (Westaway et al., 2009b; Veatch et al., 2019). Interestingly, there are no technological or typological differences between the stone artifacts associated with *H. floresiensis* and *H. sapiens* that may have otherwise provided some insight to their adaptive strategies (Moore et al., 2009). Both assemblages are generally Oldowan-like resembling the 1.2 – 1.9 Ma Oldowan and Developed Oldowan assemblages from Oldupai Gorge, Tanzania, with both characterized by choppers, bifaces, burins, perforators, blades, and bipolar cores (Moore and Brumm, 2008). However, the stone artifacts attributed to *H. floresiensis* are primarily made of silicified-tuff (Moore et al., 2009; Moore and Brumm, 2007, 2008; Sutikna et al., 2018) whereas *H. sapiens* show a greater preference for manufacturing artifacts made of chert (Moore et al., 2009; Sutikna et al., 2018). This difference in raw material selection may indicate that *H. floresiensis* was choosing to manufacture artifacts from more readily available resources (silicified-tuff is the most abundant resource around Liang Bua) while *H. sapiens* preferentially selected and transported a more valued resource from longer distances (Sutikna et al., 2018). Moreover, the presence of edge-gloss on artifacts with minimal edge-damage suggests that *H. sapiens* were cutting softer material, such as bamboo or grasses, possibly for basketry, mat weaving, or making traps or snares for catching smaller animals (Moore et al., 2009). Thus, *H. floresiensis* and *H. sapiens* were using similar tools in very different ways that may be related to either adaptations used to exploit specific environments, reflecting behavioral preferences, or both.

The stratigraphic and behavioral contexts associated with *H. floresiensis* were initially interpreted as revealing a surprisingly complex behavioral repertoire for a small-brained hominin, and was used to support the hypothesis that *H. floresiensis* was a relic lineage of a dwarfed population of *H. erectus* (Morwood et al., 2004). Hominin remains recovered from Sector IV were described as being surrounded with

juvenile *Stegodon* fragments and a dense concentration of chert-made complex stone artifacts, including blades, micro-blades, points, and perforators – all interpreted as "big game" hunting technology (Morwood et al., 2004). Now known to be the products of *H. sapiens*, the juxtaposition of these stone artifacts and (reworked) large animal remains initially suggested that *H. floresiensis* was selectively hunting juvenile *Stegodon* into the terminal Pleistocene using a surprisingly sophisticated skill set (Morwood et al., 2004, 2005). Moreover, preliminary cutmarks reported on two *Stegodon* fragments (van den Bergh et al., 2009) as well as advanced neurological adaptations based on virtual endocast reconstructions (Falk et al., 2009, 2005a,b) and evidence of fire-use seemed to support the idea of a small-brained yet behaviorally complex hominin.

Despite several studies on the abundant faunal remains at Liang Bua (Morwood et al., 2005; Hoek Ostende et al., 2006; van den Bergh et al., 2008, 2009; Locatelli, 2010; Meijer et al., 2010; Meijer and Due, 2010; Locatelli et al., 2012; Meijer et al., 2013; Ouwendijk et al., 2014; Veatch, 2014; Locatelli et al., 2015; Veatch et al., 2019; Sutikna et al., 2018, 2020), a taphonomic approach to understanding the nature of the bone assemblages is currently lacking. Any implications for complex behaviors, including subsistence and foraging strategies, for hominins at Liang Bua is attributable only through the association of stone artifacts and faunal remains. Here, the relationship between smaller animals and hominins is explored to determine how an archaic hominin incorporated smaller mammals of diverse body sizes and ecological preferences into their diets compared to modern human foragers and agriculturalists. To this end, this chapter seeks to reconstruct how past hominin foragers interacted with diverse ecologies and environmental changes and to reveal the systems of ecological knowledge used by *H. sapiens* and *H. floresiensis* at Liang Bua through their dietary and foraging behaviors.

The central aims of this study are to (1) establish the primary accumulating agents

responsible for the small mammal assemblages at Liang Bua and (2) compare hominin subsistence patterns on small mammal remains for *H. floresiensis*, foraging *H. sapiens*, and agricultural *H. sapiens*. As Flores is an oceanic island with a depauperate fauna, the list of potential accumulating agents is relatively small and includes: avian raptors (e.g., common barn owls, eagles, kites), varanids (Komodo dragons) and hominins (*H. floresiensis* and *H. sapiens*) (Meijer et al., 2013; Sutikna et al., 2018). Komodo dragons and some of the more carnivorous birds, like vultures, tend to have high levels of digestive acid that dissolves bone (D'Amore and Blumenschine, 2009) and thus small mammal remains accumulated by these taxa will most likely be minimal due to considerable digestive damage. The Flores fossil record notably lacks any endemic mammalian carnivores, but civets and domestic dogs were introduced to the island by *H. sapiens* beginning ~3 ka ago (van den Bergh et al., 2009; Sutikna et al., 2020) and may contribute to a portion of the small mammal assemblage after their arrival. Thus, for a majority of the stratigraphic sequence (~190 – 3 ka ago), the most likely predators responsible for the small mammal assemblage are either avian or hominin. In addition, any distinctions between avian predators will contribute to understanding the source of faunal specimens and potential temporal-spatial mixtures during the initial stages of site formation.

6.2 Materials and Methods

6.2.1 Stratigraphic Units

Faunal elements used in this study were sampled from Sector XI – a 2 x 2 m excavated square located along the eastern wall of the cave (Figure 6.2). The stratigraphic units of Sector XI are summarized in Figure 6.3 and are defined by a series of dated tephras (Sutikna, 2016; Sutikna et al., 2016, 2018). Elements reasonably attributed to stratigraphic Units 1, 6, and 8 were sampled from Sector XI. Additional subdivisions

of Units 1 and 8 into two (1A and 1B) and three (8A, 8B, and 8C) subunits were made based on a gravel-rich layer and the presence of a shell midden, respectively (Sutikna, 2016; Sutikna et al., 2016). Within Sector XI, Unit 1A (~190 – 120 ka) is defined as all deposits underlying a gravel-rich layer dated to ~120 ka. Unit 1B (~120 – 60 ka) includes the *H. floresiensis*-bearing sedimentary deposits that are capped by tephras T1 and T2. A series of additional tephras (T3 – T5) and interlaid flowstones continue to accumulate above Unit 1B along the southern wall while a series of erosional events in the northern part of the square created a sloping surface with younger sediments deposited unconformably on top of older deposits to the south (Figure 6.3). These younger deposits are delineated as Unit 6 (~18 – 13 ka) and is defined as all unconforming sedimentary layers resting above tephra T6 but beneath tephras T7 and T8. Unit 8A includes all sediments above T8 and is dated ~12 – 5 ka cal. BP. Unit 8B contains sediments dated ~5 – 3 ka cal. BP and includes a large accumulation of shell (Sutikna et al., 2018; Julianto et al., 2020). Lastly, Unit 8C is dated ~3 ka cal. BP – present and includes the first appearance of pottery and polished stone adzes (Sutikna et al., 2018; Julianto et al., 2020).

For the purposes of this study, Units 1A and 1B are further subdivided into three (1A-I, 1A-II, and 1A-III) and two (1B-IV and 1B-V) levels to distinguish between undated sediment changes and overlapping layers within these deposits (Figure 6.3). These divisions were originally made to help distinguish between older and younger deposits within Units 1A and 1B while efforts to re-date these units were underway. They are defined as follows: Unit 1A-I contains sediments that occur immediately beneath an undated gravel-rich layer, which is defined as Unit 1A-II, and Unit 1A-III contains sediments resting immediately above Unit 1A-II and extending until the dated gravel-rich layer (~120 ka). Unit 1B-IV contains a combination of hard, brownish clay with fragments of limestone that accumulate towards the southern part of the square while Unit 1B-V contains light brown clay sediments that lay on top

Figure 6.2: Excavation plan of Liang Bua showing the location of 37 excavated sectors (light pink) and Fr. Verhoeven's initial excavation from 1965. Each square of the red grid represents 2 sq meters. Murine skeletal remains included in this study were sampled from Sector XI indicated by dark peach color and a thick black outline. A selected specimen from Sector XXVI is included in this study as a supplement to systematically-sampled remains from Sector XI. Plan layout was created and provided by Thomas Sutikna.

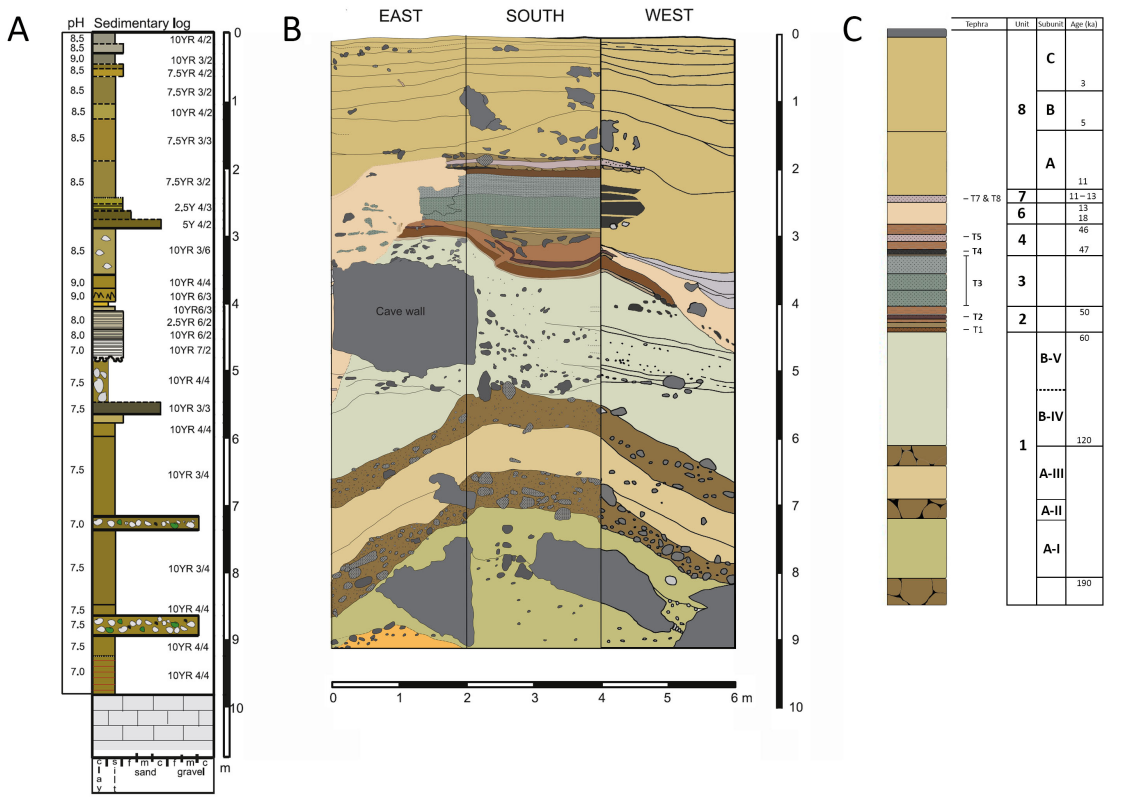

Figure 6.3: Stratigraphic drawings of Sector XI: (A) sedimentary log from Morwood et al. (2009). (B) stratigraphy of Sector XI. Images for the east and south walls are provided by Thomas Sutikna and the west wall modified from Morwood et al. (2009). (C) Simplified summary of the tephras, units, subunits, and age estimates for sector XI.

of Unit 1B-IV and slopes towards the northern section of the square. Unit 1B-IV is therefore likely younger than 1B-V. Both 1B-IV and 1B-V occur above the gravel-rich layer and are capped by tephras T1 and T2.

Excavations of Sector XI were conducted in 10 cm intervals (referred to as spits) following an initial 15 cm interval for roughly 3 meters and then excavators began following geological and sedimentary layers in addition to spits (Sutikna, 2016; Sutikna et al., 2016). Sediment descriptions and depths were recorded for each layer (where possible) before being manually dry sieved followed by wet sieving using a 2 mm mesh size to collect smaller remains. All elements were identified to a faunal group (if possible) and bagged by element type according to their respective spit level and

sedimentary layer. All faunal bags are cataloged and curated at the Pusat Penelitian Arkeologi Nasional in Jakarta, Indonesia. Lastly, tables reporting elements from wall cleanings are referred to separately as "R".

6.2.2 Zooarchaeological and taphonomic methods

A zooarchaeological and taphonomic analysis was conducted to identify small mammal accumulations from raptors and humans, the two most likely predators responsible for the accumulation of small mammal remains at Liang Bua. A combination of taphonomic methods proposed by Andrews (1990) and Fernandez-Jalvo and Andrews (1992), as well as recommendations by Armstrong (2015) and Williams (2001), were followed to determine the category of avian predator using three primary taphonomic and zooarchaeological variables: relative abundance of skeletal elements, breakage and fragmentation patterns, and digestion (Table 6.1). Signs of anthropogenic damage are based on another set of variables, including the relative abundance of skeletal elements, *in situ* burning patterns, and anthropogenic bone surface modifications (BSM) such as cutmarks and tooth marks.

Table 6.1: Predator digestion categories for murid teeth according to Andrews (1990).

Digestion Stages	Damage Extent	Predatory Category	Molar digestion	incisor digestion
Digestion absent or minimal	molars 0-3% incisors 8-13%	0a	Barn owl, long-eared owl, short-eared owl, Verreaux eagle owl	Barn owl, short-eared owl, snowy owl
Light/moderate digestion	molars 4-6% incisors 20-30% (tips only)	0b	Snowy owl, spotted eagle owl, great grey owl	Long-eared owl, Verreaux eagle owl, great grey owl
Moderate digestion	molars 18-22% incisors 50-70%	1	European eagle owl, tawny owl	European eagle owl spotted eagle owls, tawny owl, little owl
Heavy digestion	molars 50-70% incisors 60-80%	2	Little owl, kestrel, peregrine	Kestrel, peregrine
Extreme digestion	molars 50-100% incisors 100% (dentine corroded)	3	Hen harrier, buzzard, red kite	Hen harrier, buzzard

Taxonomic identification and murine body size categories

Previous studies at Liang Bua show that rats comprise ~78% of the total faunal assemblage (Sutikna et al., 2018) and are taxonomically diverse with 8 endemic species (4 extant, 4 extinct) and 1 of possibly 4 commensal species (all extant) have been previously identified at Liang Bua (Table 6.2) (Veatch, 2014; Veatch et al., 2019; Locatelli, 2010; Locatelli et al., 2012, 2015). Here, murine species were identified using dentognathic remains (maxillary and mandibular molars and incisors) and confirmed based on diagnostic features, morphology, and size (see Musser (1981)) (Tables 6.2 and 6.4). Previous faunal studies showed that *Komodomys* likely comprises a majority of the murines in Unit 1B with some small endemic *Rattus* sp., *Paulamys*, *Hooijeromys*, *Spelaeomys* and *Papagomys* also represented, while Unit 8C contains a more even distribution of murine species (Veatch et al., 2019). This study aims to confirm the temporal boundaries and relative abundances of all murine species, as well as possibly identify the presence of any previously undocumented murine rodents at Liang Bua (Table 6.5).

Table 6.2: The extinct and extant Flores murines.

Taxon	Body Size Category	Body Mass Range (g)	Flores Endemic[1]	Extant	Known or Presumed Diet[2]	Known or Presumed Behaviors[2]	Known or Presumed Habitat Preferences[2]	Original Descriptions
Papagomys armandvillei	Size 5	1,200–2,500[3]	yes	yes	leaves, fruits, and insects	terrestrial, burrowing	closed, semi-closed	Jentink (1892); Sody (1941)
Papagomys theodorverhoeveni	Size 4	600–1,600[4]	yes	uncertain	fruits and insects	terrestrial	closed, semi-closed	Hoojier (1957b); Musser (1981)
Spelaeomys florensis	Size 4	600–1,600[4]	yes	uncertain	leaves, flowers, buds	arboreal	closed	Hoojier (1957b)
Shrew-rat	Size 4	600–1,600[5]	yes	uncertain	earthworms, insects, fruits	terrestrial	closed	Veatch et al. (*in prep*)
Hooijeromys nusatenggara	Size 3	300–600[4]	yes	uncertain	unknown	terrestrial	open, semi-open	Musser (1981)
Paulamys naso	Size 2	100–200[6]	yes	yes	fungi, insects, snails, earthworms	terrestrial, burrowing	closed, semi-closed	Musser (1981); Musser et al. (1986)
Komodomys rintjanus	Size 2	100–200[7]	yes	yes	unknown	terrestrial	open, semi-open	Sody (1941); Musser and Boeadi (1980)
Rattus norvegicus	Size 2	150–300[8]	no	yes	omnivore	terrestrial	commensal	Berkenhout (1769)
Rattus rattus/tanezumi	Size 2	100–230[8]	no	yes	omnivore	terrestrial	commensal	Temminck (1844)
Rattus argentiventer	Size 2	100–220[4]	no	yes	omnivore	terrestrial	commensal	Robinson and Kloss (1916)
Rattus hainaldi	Size 1	40–100[9]	yes	yes	unknown	terrestrial, nesting	closed, semi-closed	Kitchener et al. (1991)
Rattus exulans	Size 1	40–100[9]	no[10]	yes	omnivore	terrestrial	commensal	Peale (1848)

[1] known only from Flores and/or satelite islands of Komodo, Rinca, and Padar
[2] based on information in Musser (1981), Musser and Boeadi (1980), Kitchener et al. (1991), and Suyanto (1998)
[3] based on data in Musser (1981) and three extant specimens with known body masses (1,495–2,285 g) in the collections of the Zoological Museum in Bogor, Indonesia
[4] based on molar sizes and other information in Musser (1981)
[5] based on morphological comparisons in Veatch et al. (*in prep*)
[6] based on molar sizes and other information in Musser (1981) and Musser et al. (1986) and one extant specimen with a known body mass of 120 g (Kitchener et al., 1991)
[7] based on molar sizes and other information in Musser and Boeadi (1980) and Musser (1981)
[8] based on recorded body weights of specimens in the collections of the National Museum of Natural History (USNM) in Washington, D.C.
[9] based on body weights and other information of Rattus exulans in Tamarin and Malecha (1972), but applies to small Rattus sp. generally
[10] although currently widespread, this taxon may have originally been endemic to Flores (Thomson et al., 2014)

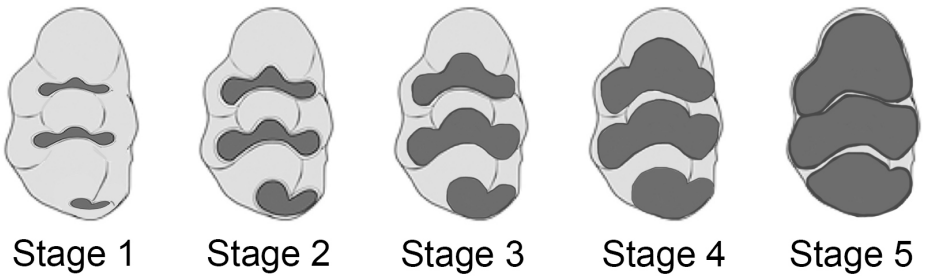

Figure 6.4: Approximate stages of molar wear using criteria established here. Molar illustration modified from Marin-Monfort et al. (2019)

Molar wear stages using criteria established here were recorded to estimate the age of individuals ranging from juveniles (stage 1) to old adults (stage 5) (Figure 6.4). These stages are qualitatively defined as: stage 1 = almost no to slight evidence of cusp reduction; stage 2 = ~25% of cusp reduction but maintaining separation of cusplets; stage 3 = ~50% of cusp reduction where cusps and cusplets begin to or have merged together; stage 4 = ~75% of cusp reduction where the majority of cusps have merged together but an enamel outline of cusp configuration is maintained; and stage 5 = little to no distinction of cusp patterns or enamel outlines.

Previous faunal studies using postcranial features to gauge murine body sizes suggest the presence of at least five body size categories at Liang Bua (Table 6.2) (Veatch, 2014; Veatch et al., 2019). For the purposes of this study, previous descriptors used to classify murine body sizes, such as "small", "medium", "large", "huge", and "giant" (Veatch, 2014; Veatch et al., 2019), will be referred to as size 1, size 2, size 3, size 4, and size 5 murine body size categories, respectively (Table 6.6). This change is to remove any ambiguity when describing the general size of a species and when referring to a specific murine body size category. Linear measurements were collected on the femur (AP head diameter), humerus (distal articular breadth), calcaneus (maximum length), tibia (distal breadth), and pelvis (acetabular breadth)

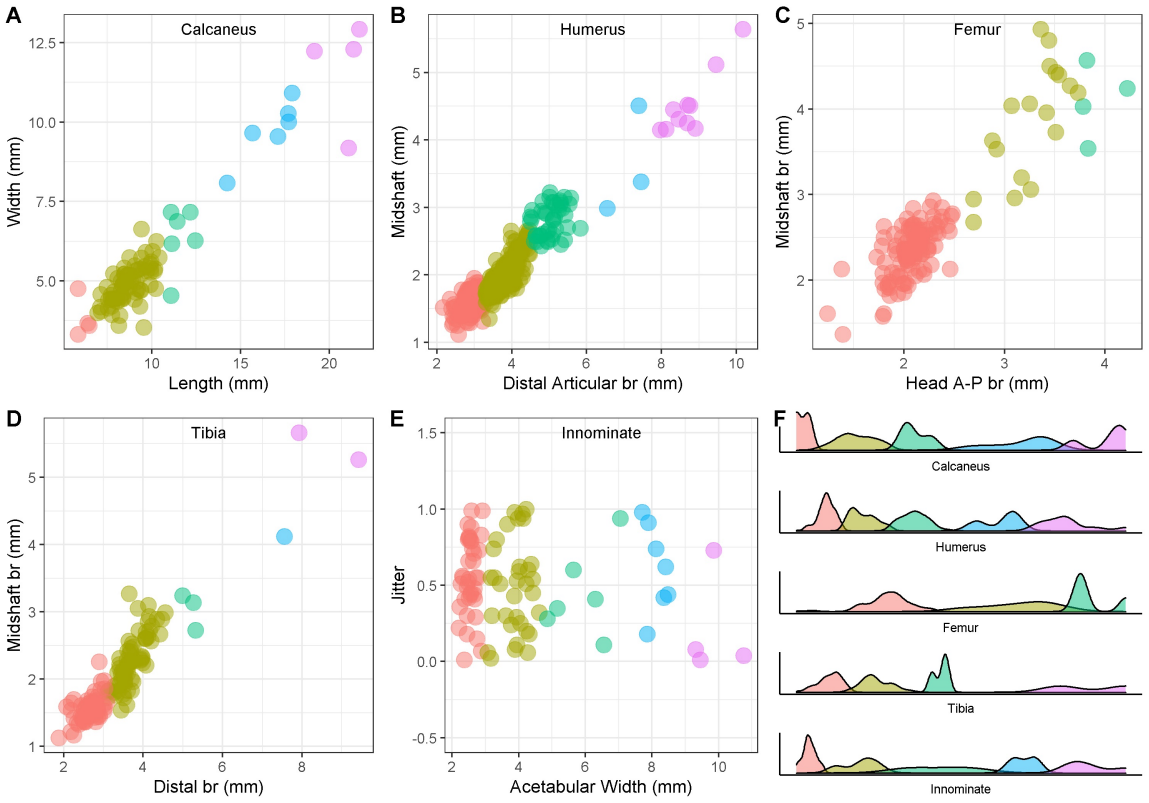

Figure 6.5: Classification of elements to murine body size categories based on a series of measurements that reliably reflect animal body size. Plots include: (A) calcaneus (B) humerus (C) femur (D) tibia (E) innominate (F) frequency distribution of assigned body size categories according to element. Murine body size categories are represented by Size 1 = red, Size 2 = gold, Size 3 = green, Size 4 = blue, and Size 5 = fuchsia.

to determine between five reasonably distinct body size categories: size 1 (<100 g), size 2 (~100 – 300 g), size 3 (~300 – 600 g), size 4 (~600 – 1100 g), and size 5 (>~1100 g) (Figure 6.5, Table 6.6) (Veatch et al., 2019). A mid-shaft breadth measurement was also recorded for all long bone elements as an additional proxy for body size. Once established, MNI and %RA values were calculated using these skeletal elements to evaluate differences in the relative abundance of murines of various body sizes (Tables 6.7).

Sampling and skeletal element representation

A total of 6,296 cranial and postcranial murine skeletal specimens were sampled across the six stratigraphic units present in Sector XI representing ~11% of the total murine elements recovered from this sector. The sampling strategy aimed to maximize samples from each temporal period representing *H. floresiensis* and *H. sapiens* (foraging and agricultural), while also taking into consideration the size of the unit. Units 1A-I, 1A-II and 6 were sampled across most excavated spits (94%), while every other spit was sampled for Units 8A, 8B, and 8C (63%) due to the relatively greater volume of bone recovered from these units. Similarly, only two spits were sampled from level 1A-III (28%) and one spit was sampled from level 1B-IV (2%) due to the high densities of bone within these layers. While Unit 1B-V is represented in this sector, bone fragments contained within this unit were not sampled. All faunal elements were sampled equally (e.g., postcranial, teeth, cranial, etc.) from Sector XI, with the exception of femora belonging to Units 1A, 1B, and 6. Bone accumulation rates were calculated for each stratigraphic unit based on the number of spits sampled (taking into account multiple sedimentary layers) and the total volume of sediment excavated from Sector XI (Table 6.3).

Table 6.3: Sediment and bone accumulation rates for specimens sampled from Sector XI

Stratigraphic Unit	1A			1B		6	8A	8B	8C
Level	I	II	III	IV	V				
Unit Estimated Age Range*	120,000 - 190,000			60,000 - 120,000		13,000 - 18,000	5000 - 11,000	3000 - 5000	0 - 3000
Years per Unit	70,000			60,000		5000	6000	2000	3000
Sediment volume (m^3) per 1 ka	0.11			0.2		0.4	1.1	1.0	1.4
Total Sediment volume (m^3)	3.4	1.1	3.4	3	9.4	2	6.4	2	4.2
Sampled sediment volume (m^3)	3.1	1.1	0.8	0.02	0	2	3.6	1.6	2
NISP	628	235	2147	570	-	312	953	896	564
Bone accumluation per m^3	203.9	217.6	2,684	28,500	-	156	264.7	560	282
MNI	37	13	157	42	-	30	59	64	32
MNI accumluation per m^3	12	12	197	2,100	-	15	17	40	16

*Estimated age ranges from Sutikna et al., 2016 and Roberts et al., 2009

All skeletal specimens were identified by element type, orientation (left or right), and location (mandibular or maxillary) where possible. Specimens lacking diagnostic

or discernible features were labeled as either a vertebrae fragment, cranial fragment, long bone shaft fragment, or unidentified fragment. A maximum length was recorded for all fragments using digital hand calipers taken to the nearest 0.01 mm.

A series of zooarchaeological indices were calculated to document the skeletal composition of each stratigraphic unit. These include: number of specimens (nsp), number of identified skeletal specimens (NISP), minimum number of elements (MNE), minimum number of individuals (MNI), and minimum anatomical units (MAU) (Lyman, 1994). The fraction-summation method was used to calculate MNE following Klein and Cruz-Uribe (1984) and involves recording a portion of features identifiable on each specimen on a 10% scale between 0 and 1. This method is particularly effective for recording small mammal bones since these elements tend to preserve better than large mammal bones, and tend to fracture in consistent locations while retaining diagnostic features. MNI and MAU were calculated by taking the maximum MNE value of a sample and dividing an element (i) MNE value by the number of times i occurs in the skeleton, respectively (Lyman, 1994).

The relative abundance of each element was calculated using the following formula proposed by Dodson and Diane (1979) and Brain (1969):

$$\%RA = 100 \times \frac{MNE_{\mathrm{i}}}{MNI \times E_{\mathrm{i}}} \tag{6.1}$$

where %RA: relative abundance, $\mathrm{MNE_i}$: minimum number of skeletal elements i, MNI: minimum number of individuals, $\mathrm{E_i}$: the number of times element i occurs in the prey skeleton.

In order to evaluate the relationship between skeletal elements, four indices were calculated following Andrews (1990), including: postcranial to cranial elements ((femora + humeri) / (mandibles + maxillae)), lower limb versus upper limb elements ((tibia + (radius + ulna)/2) / (femur + humerus)), anterior to posterior limb elements ((scapula + humerus + (radius + ulna)/2) / (pelvis + femur + tibia)), and axial to

appendicular elements ((atlas + axis + (cervical/5) + (thoracic/12) + (lumbar/7) + (sacra/4)) / ((humerus/2) + (radius/2) + (ulna/2) + (femur/2) + (patella/2) + (tibia/2))). Values greater than 1 indicates a greater representation of postcrania, lower limbs, anterior limbs, and appendicular limbs relative to cranial, upper limb, posterior limb, and axial elements, respectively.

Taphonomic methods

Patterns of long bone fragmentation are summarized according to the frequency of complete, proximal, shaft, and distal fragments by stratigraphic unit (Table C.3). Long bone breakage morphology (fracture angle, fracture outline, and fracture edge) was recorded following **?**, with the addition of recording a secondary entry for the fractured outline, and summarized according to body size (where possible) and stratigraphic unit (Figure 6.11). Recording a secondary outline entry was made because small mammal bones are not as cylindrical as human bones (the sample for which these categories are based), and thus, they tend to break slightly differently when fresh or dry. A second entry therefore allows for more accurate assessment where there is more than one adequate descriptor for the outline of a break. Differences in the fractured margin surface were also recorded to account for pre-, post-depositional, recent, or combination of (i.e., multiple fracture events) fractures, as well as rounding of breaks due to avian digestion (Figure 6.10).

Degrees of fragmentation for all bones were estimated by considering the relationship between NISP and MNE values for each element (Table 6.11). Mandibular and maxillary breakage is summarized according to Andrews (1990) with the addition of one mandibular breakage category (F) to reflect bone fragments without the alveolus (Figure 6.6).

All bone surface modifications (BSMs) were identified using a 20x-220x DinoLight digital microscope with an extended depth of field and a 20X handheld lens. Surface

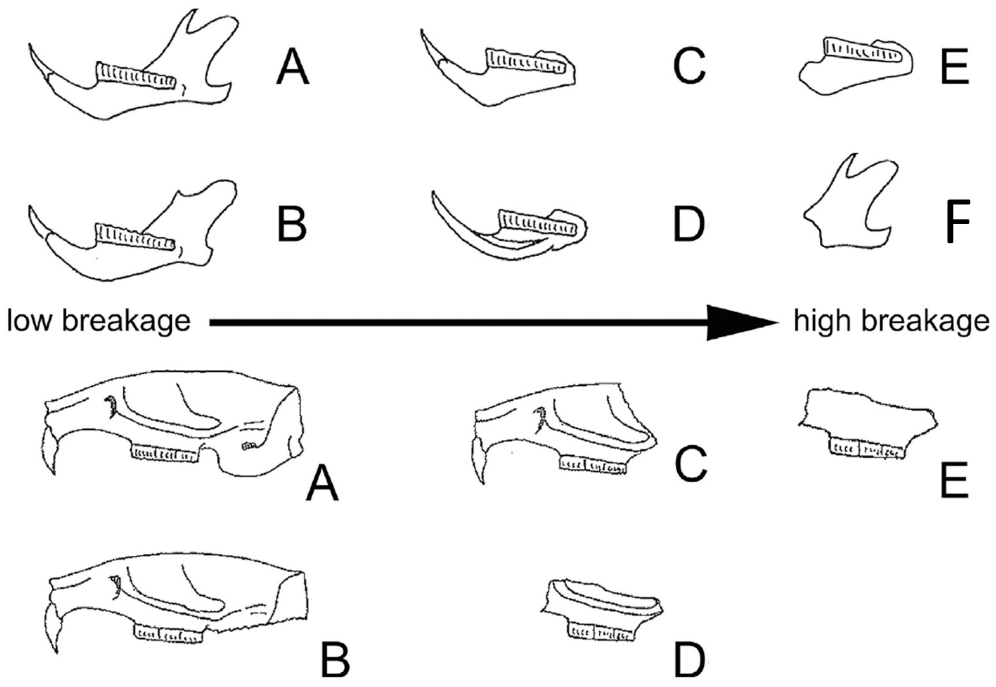

Figure 6.6: Mandibular and maxillary breakage categories following (Andrews, 1990) with an additional category (F) to represent mandibular fragments without the alveolus. Image modified from Fernández-Jalvo et al. (2016)

alteration due to avian digestion on teeth, distal humeri, and proximal femora were recorded following Andrews (1990) and Lloveras et al. (2008a) and summarized by each element type and murine body size according to stratigraphic unit (Figure 6.15). An additional digestive stage was defined and recorded for "very light" acidic damage identified on incisors where slight etching in the form of enamel flaking and a matte-like surface was visible—an independent observation also made by Williams (2001) (Table B.1, Appendix B). Two forms of digestion were recorded for long bones: (1) acidic damage where degrees of rounded perforations along the distal articular surfaces of the humeri and the proximal femoral head were identified following Andrews (1990), and (2) corrosive damage where increased smoothing, shine, and rounding occurs due to digestion but perforation of the distal and/or proximal ends does not occur. This form of damage is likely due to extremely light digestion affecting the distal and proximal diaphyseal ends but has not yet been recorded or used to define digestive

patterns in the taphonomic literature. Each bone specimen was also examined and scored for levels of weathering for small mammals (Andrews, 1990), burning (Stages 1 through 5) (Rhodes et al., 2016), iron and manganese staining (Fernandez-Jalvo and Avery, 2015; Rhodes et al., 2016), microbial and/or insect bioerosion damage (Domínguez-Rodrigo and Barba, 2006) and post-depositional damage (Thompson, 2005).

The frequency and location of frequent bone surface modifications were recorded using criteria adopted from the literature and summarized according to stratigraphic unit and element type:

- **Punctures**: The bone surface has collapsed under localized pressure creating a hole in the cancellous and cortical bone (Binford, 1981; Fernández-Jalvo and Andrews, 2016; Armstrong and Avery, 2014). Possible agents responsible include carnivores, plants, insects, birds, and humans (Fernández-Jalvo and Andrews, 2016).

- **Pits**: Circular indentations on the cortical bone surface that does not penetrate cancellous bone (Binford, 1981; Blumenschine, 1988; Blumenschine et al., 1996; Landt, 2007; Fernández-Jalvo and Andrews, 2016). Possible agents responsible include carnivores, insects, birds, and trampling (Fernández-Jalvo and Andrews, 2016). Human teeth also create "pits" but are distinct and are described separately below.

- **Scores**: Linear indentations on the exterior surface of bone that form straight, curved, or sinuous trajectories (Binford, 1981; Blumenschine et al., 1996; Landt, 2007; Shipman, 1981; Fernández-Jalvo and Andrews, 2016). Possible agents responsible include carnivores, plants, insects, birds, and humans (Fernández-Jalvo and Andrews, 2016). Possible agents responsible for creating linear marks with U-shaped cross section include carnivore chewing, plant roots, insects, beak

marks, herbivore and rodent gnawing whereas those with V-shaped cross section include human cut marks and carnivore teeth(Fernández-Jalvo and Andrews, 2016).

- **Notches**: Semi-circular indentations located along a broken bone margin or bone edge (Binford, 1981; Blumenschine et al., 1991; Brain, 1981; Capaldo and Blumenschine, 1994; Fernández-Jalvo and Andrews, 2016). Possible agents responsible include human percussion marks and carnivores (Fernández-Jalvo and Andrews, 2016). Human tooth marks can also cause double-arched notches when chewing bone (Fernández-Jalvo and Andrews, 2011).

Marks that met specific criteria associated with human modification were identified using the following definitions:

- **Cutmarks**: Criteria for defining cutmarks are highly variable due to morphological similarities with carnivore tooth marks and experimentally made trampled assemblages (Potts and Shipman, 1981; Shipman, 1983; Blumenschine et al., 1996; Domínguez-Rodrigo et al., 2009a, 2012; Fernández-Jalvo and Andrews, 2016). For the purposes of this experimental study, cutmarks were identified using features outlined by Domínguez-Rodrigo et al. (2009a). Cutmark morphology was further categorized using criteria outlined by Thompson et al. (2015): 1) slice: an angled incision to the bone surface; 2) cut: an incision perpendiicular to the bone surface; 3) shave: small curls of bone peeling away from a slice; 4) scrape: broad, shallow fields often with dimpling; 5) single chop: short, deep cuts; 6) repeated chops: deep, broad, non-parallel striations (Potts and Shipman, 1981); 7) and saw: multiple striae occurring in a patch.

- **Human tooth marks**: Like cutmarks, marks formed by human teeth are highly variable, and can include double-arched punctures and/or pits, crescent shaped pit with internal striations, wide and shallow linear scores caused by

dragging incisors on the bone surface, and triangular puncture marks made from premolars and canines (Landt, 2007, 2004; Fernández-Jalvo and Andrews, 2016, 2011).

Statistical analyses were conducted using R and RStudio version 1.3.1093 and PAST version 4.0. Taxonomic and body size evenness through the stratigraphic sequence was measured using the unbiased Simpson Diversity index (1 – D'), to test the probability that two randomly sampled specimens will belong to different species or body size categories. An unbiased Simpson index value close to 0 indicates that a given stratigraphic unit is dominated by a single murine species or body size category. For species, values ~0.88 (1–1/9, where 9 is the total number of identified taxa) indicate all species are equally abundant, whereas values ~0.8 (1–1/5, where 5 is the number of body size categories) indicate all murine body sizes are equally abundant.

Finally, the relationships between stratigraphic units based on a series of taphonomic variables were examined using linear regression models, squared chord distance analysis, and correspondence analysis to measure the contribution and effect of taphonomic processes across all units (Faith, 2013) (Figure 6.27). Four correspondence analyses were run to evaluate the contribution of (1) all taphonomic variables, (2) all except burning damage, (3) anthropogenic variables only, and (4) avian taphonomic variables only. To facilitate the interpretation of the multivariate results, differences in the abundances of taphonomic variables between each adjacent stratigraphic units were evaluated for statistical significance using adjusted residuals derived from contingency table analysis (e.g., Grayson and Delpech (2003); Lyman (2008)). The adjusted residuals are equal to standard normal deviates, in which absolute values greater than 1.96 are significant ($p<0.05$).

6.3 Results

The murine faunal remains at Liang Bua are very well preserved. An average of 83% of cortical bone surface visibility and 0.3% of the sample were unidentified elements across all stratigraphic units.

6.3.1 Taxonomic representation and murine body size

All murine taxa previously identified at Liang Bua were confirmed using mandibular and maxillary molars and incisors, including *Papagomys armandvillei, Papagomys theodorverhoeveni, Hooijeromys nusatenggara, Komodomys rintjanus*, the shrew-rat, and *Paulamys naso* (Table 6.5). While *Spelaeomys florensis* was not identified within the sample collected in this study, previous faunal studies suggest that this murine is relatively rare at Liang Bua compared to other murine species (Veatch et al., 2019; Locatelli et al., 2012; Locatelli, 2010). Its absence is therefore likely due to sampling bias in Sector XI. Fragments resembling *Rattus exulans* and *Rattus hainaldi* were also identified, but the condition of their remains made it difficult to confidently assign a species ID to these fragments. Instead, fragments reasonably belonging to either *Rattus hainaldi* or *Rattus exulans* based on size and morphology are tabulated together as size 1 *Rattus* sp.. Additional methods and comparisons with museum specimens are needed to confidently identify these fragments.

Changes in species diversity throughout the stratigraphic sequence reveals a noticeable difference between units associated with more open environments (Units 1A – 1B: ~190 – 60 ka) and more-closed ones (Units 6 – 8B: ~18 – 5 ka) (Figure 6.7). With some variation, Units 1A and 1B are dominated by *Komodomys rintjanus*, a size 2 murine that prefers more-open habitats, with a few species preferring more-closed environments, such as *Papagomys armandvillei* and size 1 *Rattus* sp. (Table 6.5). Conversely, Units 6 through 8C contain a more even distribution of murine taxa, but

Table 6.4: Dental metrics of identified murine taxa from Sector XI. Measurements include molar length (lg), breadth (br), and incisor depth (dpt) of the maxillary and mandibular molars, and lower incisors. Mean and range values are provided and recorded in mm.

Element	Measurement	*Papagomys armandvillei*	*Papagomys theodorverhoeveni*	*Hooijeromys nusatenggara*	Shrew-rat	*Komodomys rintjanus*	*Paulamys naso*	*Rattus* sp. (size 2)	*Rattus* sp. (size 1)
M1	lg	7.6 (6.68 - 8.12)	5.72	-	-	3.9 (3.05 - 4.62)	-		2.63
	br	4.9 (4.72 - 5.25)	3.64	-	-	2.8 (2.55 - 3.65)	-		1.64
M2	lg	5.18 (4.82 - 5.75)	4.77	-	-	2.7 (2.04 - 3.3)	-		1.7 (1.74 - 1.79)
	br	4.7 (4.57 - 4.74)	3.61	-	-	2.7 (1.99 - 2.97)	-		1.6 (1.49 - 1.65)
M3	lg	4.5 (4.37 - 4.66)	3.51	-	-	2.5 (2.19 - 2.84)	-		1.9 (1.5 - 2.29)
	br	3.9 (3.95 - 4)	3.01	-	-	2.2 (1.86 - 2.72)	-		1.5 (1.23 - 1.94)
m1	lg	6.0 (5.63 - 6.35)	5.6 (5.5 - 5.6)	5 (4.67 - 5.26)	-	3.5 (2.95 - 3.92)	3.4 (3.11 - 3.78)	3.3 (3.14 - 3.49)	2.4 (2.03 - 2.93)
	br	4.0 (3.82 - 4.34)	3.6 (3.44 - 3.71)	3.3 (3.1 - 3.5)	-	2.2 (1.96 - 2.61)	2.1 (1.93 - 2.31)	2 (1.91 - 2.07)	1.5 (1.3 - 1.63)
m2	lg	4.8 (4.35 - 5.11)	4 (3.94 - 4.07)	3.7 (3.46 - 3.95)	-	2.6 (2.06 - 3.24)	2.5 (2.13 - 2.69)	-	1.7 (1.4 - 1.9)
	br	4.4 (4.09 - 4.75)	3.7 (3.68 - 3.72)	3.4 (3.24 - 3.69)	-	2.5 (2.24 - 2.88)	2.3 (2.18 - 2.54)	-	1.5 (1.4 - 1.73)
m3	lg	4.8 (4.62 - 5.03)	3.1 (2.88 - 3.39)	3.3 (3.01 - 3.53)	-	2.3 (1.82 - 2.95)	2.2 (2.1 - 2.3)	1.71	1.4 (1.2 - 1.74)
	br	4.2 (4.02 - 4.63)	3.4 (3.35 - 3.51)	3.1 (3.03 - 3.15)	-	2.4 (1.97 - 2.6)	2 (1.84 - 2.22)	1.9	1.3 (1.22 - 1.41)
i	dpt	-	3.0 (2.93 - 3.16)	3 (2.12 - 3.67)	3.7 (3.61 - 3.77)	1.8 (1.37 - 2.15)	2.1 (1.97 - 2.18)	1.91	1.5 (1.1 - 1.79)
	br	2.55	2.1 (1.85 - 2.22)	1.6 (1.35 - 1.8)	2 (1.84 - 2.13)	1.2 (0.86 - 1.5)	1.3 (1.32 - 1.39)	1.42	0.9 (0.7 - 1.09)

Table 6.5: Murine species representation according to stratigraphic unit.

	Occupation	*H. floresiensis*								*H. sapiens*							
	Unit	1A-I		1A-II		1A-III		1B-IV		6		8A		8B		8C	
Species	Body Size Category	NISP	MNI	NISP	MNI	NISP	MNI	NISP	MNI	NISP	MNI	NISP	MNI	NISP	MNI	NISP	MNI
Papagomys armandvillei	5	2	2	2	1	4	1	0	0	0	0	5	1	11	2	20	4
Papagomys theodorverhoeveni	4	0	0	0	0	0	0	0	0	0	0	3	1	9	1	5	1
Spelaeomys florensis	4	0	0	0	0	0	0	0	0	0	0	0	0	0	0	0	0
Hooijeromys nusatenggara	3	0	0	0	0	0	0	2	1	0	0	22	3	6	1	0	0
Shrew-rat	3	0	0	0	0	0	0	0	0	0	0	2	1	2	1	3	2
Komodomys rintjanus	2	145	20	43	6	456	40	53	7	3	1	0	0	0	0	19	2
Paulamys naso	2	0	0	0	0	0	0	0	0	8	2	4	1	0	0	5	1
Rattus sp.	1 or 2	0	0	0	0	0	0	0	0	1	1	14	5	8	2	22	4
Rattus hainaldi / Rattus exulans	1	5	1	0	0	0	0	0	0	15	2	22	5	24	4	21	3
	Total	**162**	**23**	**45**	**7**	**460**	**41**	**55**	**8**	**27**	**6**	**72**	**17**	**60**	**11**	**95**	**17**

with a noticeable absence of *Komodomys rintjanus* until Unit 8C (Figure 6.7, Table 6.5).

Estimations of murine body sizes using postcrania confirms the presence of five body size categories and their relative abundance throughout the stratigraphic sequence (Tables 6.6 and 6.7). Stratigraphic Units 1A and 1B are dominated by size 2 murines with significantly fewer elements from other body size categories. Similar to the changes observed in murine species abundances, Units 6 – 8C contain a relatively greater amount of large and small murines with a notable absence of size 2 murines. Using the unbiased Simpson's diversity index, an analysis of evenness confirms a relatively uneven distribution of murine body sizes in Units 1A and 1B (~0.4 – 0.55) compare to Units 6 – 8C (~0.6 – 0.7) (Figure 6.8). While the patterns of taxonomic and body size evenness are similar, there is a greater difference in species evenness compared to body size, and is likely due to (1) natural preservation bias for postcra-

nial versus dental elements, and/or (2) the postcrania of younger or older individuals could cross over into adjacent body size categories and dilute the evenness values.

Table 6.6: Measurement values (mm) delineating murine body size categories according to element. Category estimates for the lower incisors were made using a combination of depth and breadth.

Element	Measurement	Size 1	Size 2	Size 3	Size 4	Size 5
Calcaneus	Max Length	<6.5	6.9 - 10.49	10.5 - 13	13.01 - 18	>18.01
Humerus	Distal Articular Breadth	<3.3	3.31 - 4.49	4.5- 5.6	5.61- 7.5	>7.51
Femur	Proximal Head Diameter (AP)	<2.5	2.51 - 3.75	3.76 - 5.5	5.51 - 7.7	>7.71
Tibia	Distal Breadth	<3.1	3.11- 4.7	4.71 - 7	7.01 - 8.9	>8.91
Innominate	Acetabular Width	<3	3.01 - 4.7	4.71 - 7.5	7.51 - 9	>9.01
Lower incisor	Breadth	<0.99	1 - 1.65	1.66 - 1.85	1.5 - 2.17	>1.8
Lower incisor	Depth	<1.9	1.46 - 2.55	2.11 - 2.65	2.9 - 3.2	>3.21

Table 6.7: Murine body size NISP and MNI values according to stratigraphic unit. Values are based on postcranial and dental elements that fall within the value range of each body size category (see Tables 6.6 and 6.4).

	H. floresiensis								*H. sapiens*							
Unit	1A-I		1A-II		1A-III		1B-IV		6		8A		8B		8C	
Murine Body Size	NISP	MNI	NISP	MNI	NISP	MNI	NISP	MNI	NISP	MNI	NISP	MNI	NISP	MNI	NISP	MNI
Size 5	7	2	2	1	5	1	1	1	1	1	46	9	33	5	33	4
Size 4	0	0	1	0.9	3	1.8	0	0	3	3	39	5	41	4	24	2
Size 3	11	3.4	5	1	36	13	11	1.5	14	5.9	82	18.9	49	17.1	17	2
Size 2	361	30	108	10.5	1366	125	312	36	77	16	115	15.3	49	6.1	123	11.1
Size 1	58	13	12	3	168	30	61	13	70	14	306	36.3	293	46.9	188	16
TOTAL	437	48.4	128	16.4	1578	170.8	385	51.5	165	39.9	588	84.5	465	79.1	385	35.1

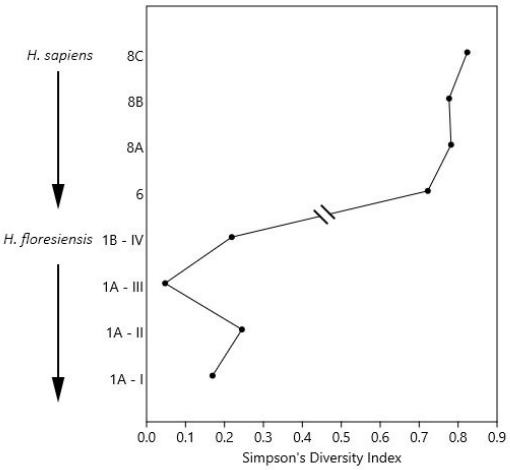

Figure 6.7: Simpson's diversity index of murine MNI counts according to stratigraphic unit (see Table 6.5).

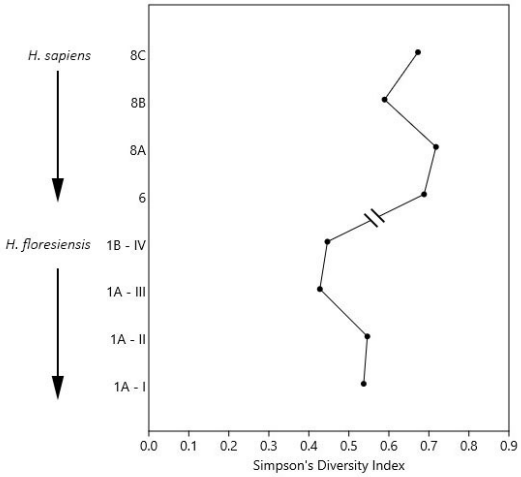

Figure 6.8: Simpson's diversity index for murine body sizes categories according to stratigraphic unit (See Table 6.7).

6.3.2 Skeletal element representation

Tables 6.8 and 6.9 summarize skeletal element representation for all units associated with *H. floresiensis* and *H. sapiens*, respectively. A total of 4,732.6 minimum number of elements (MNE) was calculated for the entire sample, of which 1,999.9 are cranial and dental elements, and 2,732.7 are postcranial elements. Femora were not sampled in Units 1A, 1B, or 6 because they were unavailable for study and should not reflect real abundances compared to other elements (some epiphyses were confirmed as femoral epiphyses that were previously misidentified – see Section 6.2). Incisors, humeri, and tibiae are the most well represented elements in both the total sample and across units. Units 1A and 1B showed a greater relative abundance of molars, incisors, and calcanei compared to Units 6 and 8A – 8C, while humeri and tibias were slightly more represented in the latter units. Ribs and vertebrae are the rarest elements across all units. While slight differences are observed in the relative abundance of skeletal elements across units, there are no significant differences between

Table 6.8: Tabulation of zooarchaeological index values (NISP, MNE, MNI, MAU, %MAU, and RA) for stratigraphic Units 1A – 1B (*H. floresiensis* layers). Note: femora for these units were unavailable for study.

	1A-I					1A-II					1A-III					1B-IV				
Element	NISP	MNE	MAU	%MAU	RA	NISP	MNE	MAU	%MAU	RA	NISP	MNE	MAU	%MAU	RA	NISP	MNE	MAU	%MAU	RA
Crania	25	2.7	1.4	3.9	0.4	10	1.5	0.8	7.1	0.6	78	13.3	6.7	5.5	0.4	48	15.5	7.8	20.4	1.8
Maxilla	19	6.0	3.0	8.6	8.2	8	2.7	1.4	12.8	10.4	66	30.5	15.3	12.6	9.7	7	4.5	2.3	5.9	5.4
Mandible	15	14.0	3.0	8.6	19.2	2	2.0	1.4	12.8	7.7	97	75.7	15.3	12.6	24.1	9	9.0	2.3	5.9	10.7
M1	33	33.0	16.5	47.5	45.2	10	10.0	5.0	47.4	38.5	63	63.0	31.5	26.1	20.1	13	13.0	6.5	17.1	15.5
M2	23	23.0	11.5	33.1	31.5	7	7.0	3.5	33.2	26.9	47	46.8	23.4	19.4	14.9	5	5.0	2.5	6.6	6.0
M3	10	10.0	5.0	14.4	13.7	5	5.0	2.5	23.7	19.2	30	30.0	15.0	12.4	9.6	3	3.0	1.5	3.9	3.6
I	50	49.0	24.5	70.5	67.1	17	17.0	8.5	80.6	65.4	173	173.0	86.5	71.6	55.1	82	82.0	41.0	107.9	97.6
m1	21	21.0	10.5	30.2	28.8	5	5.0	2.5	23.7	19.2	69	68.8	34.4	28.5	21.9	13	13.0	6.5	17.1	15.5
m2	14	14.0	7.0	20.1	19.2	3	3.0	1.5	14.2	11.5	65	65.0	32.5	26.9	20.7	6	6.0	3.0	7.9	7.1
m3	5	5.0	2.5	7.2	6.8	3	3.0	1.5	14.2	11.5	45	45.0	22.5	18.6	14.3	1	1.0	0.5	1.3	1.2
i	77	69.5	34.8	100.0	95.2	20	20.0	10.0	94.8	76.9	289	286.0	143.0	118.3	91.1	76	76.0	38.0	100.0	90.5
Clavicle	0	0.0	0.0	0.0	0.0	0	0.0	0.0	0.0	0.0	0	0.0	0.0	0.0	0.0	1	1.0	0.5	1.3	1.2
Rib	0	0.0	0.0	0.0	0.0	0	0.0	0.0	0.0	0.0	2	2.0	0.1	0.0	0.0	1	1.0	0.0	0.1	0.1
Atlas	0	0.0	0.0	0.0	0.0	0	0.0	0.0	0.0	0.0	2	2.0	2.0	1.7	1.3	0	0.0	0.0	0.0	0.0
Asix	1	1.0	1.0	2.9	2.7	0	0.0	0.0	0.0	0.0	3	3.0	3.0	2.5	1.9	2	2.0	2.0	5.3	4.8
Cervical	1	0.0	0.0	0.0	0.0	0	0.0	0.0	0.0	0.0	6	4.9	0.7	0.6	0.4	5	4.1	0.6	1.5	1.4
Thoracic	2	1.1	0.1	0.2	0.2	0	0.0	0.0	0.0	0.0	9	6.6	0.5	0.4	0.3	2	1.9	0.1	0.4	0.3
Lumbar	4	2.1	0.4	1.0	1.0	4	2.2	0.4	3.5	2.8	51	33.9	5.7	4.7	3.6	10	8.2	1.4	3.6	3.3
Sacral	3	0.2	0.1	0.1	0.1	2	0.7	0.2	1.7	1.3	9	5.6	1.4	1.2	0.9	4	2.4	0.6	1.6	1.4
Caudal	24	11.2	0.3	0.9	0.9	6	4.1	0.1	1.1	0.9	66	60.3	1.7	1.4	1.1	10	8.7	0.2	0.6	0.6
Scapula	9	7.8	3.9	11.2	10.7	3	3.0	1.5	14.2	11.5	23	19.9	10.0	8.2	6.3	3	2.0	1.0	2.6	2.4
Innominate	24	9.4	4.7	13.5	12.9	21	8.0	4.0	37.9	30.8	0	0.0	0.0	0.0	0.0	31	14.1	7.1	18.6	16.8
Humerus	72	50.3	25.2	72.4	68.9	15	10.8	5.4	51.2	41.5	277	241.7	120.9	100.0	77.0	51	41.4	20.7	54.5	49.3
Radius	16	4.9	2.5	7.1	6.7	2	0.0	0.0	0.0	0.0	51	24.5	12.3	10.1	7.8	8	7.2	3.6	9.5	8.6
Ulna	33	21.1	10.6	30.4	28.9	10	7.0	3.5	33.2	26.9	106	80.5	40.3	33.3	25.6	24	22.5	11.3	29.6	26.8
Femur	3	2.5	1.3	3.6	3.4	1	1.0	0.5	4.7	3.8	12	11.0	5.5	4.6	3.5	7	7.0	3.5	9.2	8.3
Tibia/Fibula	95	36.9	18.5	53.1	50.5	66	21.1	10.6	100.0	81.2	358	183.5	91.8	75.9	58.4	97	56.2	28.1	73.9	66.9
Patella	0	0.0	0.0	0.0	0.0	0	0.0	0.0	0.0	0.0	0	0.0	0.0	0.0	0.0	0	0.0	0.0	0.0	0.0
Talus	0	0.0	0.0	0.0	0.0	0	0.0	0.0	0.0	0.0	1	1.0	0.5	0.4	0.3	2	2.0	1.0	2.6	2.4
Calcaneus	19	19.0	9.5	27.3	26.0	3	3.0	1.5	14.2	11.5	42	42.0	21.0	17.4	13.4	12	12.0	6.0	15.8	14.3
Phalanges	1	1.0	0.0	0.1	0.0	2	1.0	0.0	0.2	0.1	0	0.0	0.0	0.0	0.0	0	0.0	0.0	0.0	0.0
Metapodials	24	21.0	2.1	6.0	2.9	7	5.0	0.5	4.7	1.9	96	89.0	8.9	7.4	2.8	23	22.0	2.2	5.8	2.6
Long-Bone Frag.	0					1					1					1				
Non-ID Fragment	2					0					0					0				
Non-ID Cranial	0					0					3					8				
Vert Indet.	3					2					5					2				
TOTAL	628	436.7				235	143.1				2145	1708.5				567	443.7			
MNI	37					13					157					42				

units and all the units are similar to the total sample ($p = 0.86$, $F = 0.528$).

The relationships between skeletal elements using standard indices for small mammal assemblages are shown in Table 6.10. All units show a greater abundance of postcrania and appendicular elements compared to cranial and axial elements, respectively. Since femora from Units 1A, 1B, and 6 were not incorporated in the sample, the ZE/ST and AN/PO indices representing the distal-to-proximal and anterior-to-posterior limb ratios should be interpreted with caution, respectively. Units where femora were included in data collection (Units 8A, 8B, and 8C) show a slightly greater representation of proximal and posterior limb elements.

	6					8A					8B					8C				
Element	NISP	MNE	MAU	%MAU	RA	NISP	MNE	MAU	%MAU	RA	NISP	MNE	MAU	%MAU	RA	NISP	MNE	MAU	%MAU	RA
Crania	0	0.0	0.0	0.0	0.0	8	4.5	2.3	4.1	0.4	5	1.8	0.9	1.5	0.1	4	2.0	1.0	3.3	0.3
Maxilla	2	0.5	0.3	0.9	0.8	0	0.0	0.0	0.0	0.0	6	4.4	2.2	3.6	3.4	5	4.3	2.2	7.1	6.9
Mandible	6	5.5	0.3	0.9	9.2	27	20.8	0.0	0.0	17.7	21	18.3	2.2	3.6	14.3	27	24.1	2.2	7.1	38.6
M1	1	1.0	0.5	1.9	1.7	0	0.0	0.0	0.0	0.0	5	5.0	2.5	4.1	3.9	2	2.0	1.0	3.3	3.2
M2	1	1.0	0.5	1.9	1.7	0	0.0	0.0	0.0	0.0	4	4.0	2.0	3.3	3.1	3	3.0	1.5	4.9	4.8
M3	0	0.0	0.0	0.0	0.0	0	0.0	0.0	0.0	0.0	4	3.5	1.8	2.9	2.7	2	2.0	1.0	3.3	3.2
I	6	6.0	3.0	11.3	10.0	23	23.0	11.5	20.9	19.6	17	17.0	8.5	13.9	13.3	20	20.0	10.0	32.9	32.1
m1	5	5.0	2.5	9.4	8.3	12	12.0	6.0	10.9	10.2	10	10.0	5.0	8.2	7.8	16	16.0	8.0	26.3	25.6
m2	6	6.0	3.0	11.3	10.0	15	14.7	7.4	13.3	12.5	8	8.0	4.0	6.5	6.3	17	17.0	8.5	28.0	27.2
m3	3	3.0	1.5	5.7	5.0	7	5.5	2.8	5.0	4.7	7	7.0	3.5	5.7	5.5	9	8.5	4.3	14.0	13.6
i	53	53.0	26.5	100.0	88.3	112	108.0	54.0	97.9	91.8	65	64.0	32.0	52.4	50.0	41	40.0	20.0	65.8	64.1
Clavicle	0	0.0	0.0	0.0	0.0	7	5.4	2.7	4.9	4.6	4	3.7	1.9	3.0	2.9	4	3.0	1.5	4.9	4.8
Rib	27	8.4	0.2	0.9	0.8	144	56.3	1.6	2.8	2.7	66	22.6	0.6	1.0	1.0	53	29.9	0.8	2.7	2.7
Atlas	0	0.0	0.0	0.0	0.0	0	0.0	0.0	0.0	0.0	0	0.0	0.0	0.0	0.0	0	0.0	0.0	0.0	0.0
Axis	0	0.0	0.0	0.0	0.0	0	0.0	0.0	0.0	0.0	0	0.0	0.0	0.0	0.0	1	1.0	1.0	3.3	3.2
Cervical	0	0.0	0.0	0.0	0.0	1	0.9	0.1	0.2	0.2	0	0.0	0.0	0.0	0.0	4	3.6	0.5	1.7	1.6
Thoracic	1	0.3	0.0	0.1	0.1	1	0.9	0.1	0.1	0.1	0	0.0	0.0	0.0	0.0	0	0.0	0.0	0.0	0.0
Lumbar	1	0.7	0.1	0.4	0.4	0	0.0	0.0	0.0	0.0	2	1.5	0.3	0.4	0.4	2	1.7	0.3	0.9	0.9
Sacral	0	0.0	0.0	0.0	0.0	0	0.0	0.0	0.0	0.0	1	0.7	0.2	0.3	0.3	0	0.0	0.0	0.0	0.0
Caudal	1	1.0	0.0	0.1	0.1	5	5.0	0.1	0.3	0.2	9	7.8	0.2	0.4	0.3	11	9.4	0.3	0.9	0.8
Scapula	2	2.0	1.0	3.8	3.3	5	5.0	2.5	4.5	4.3	3	3.0	1.5	2.5	2.3	7	6.0	3.0	9.9	9.6
Innominate	19	9.7	4.9	18.3	16.2	24	12.6	6.3	11.4	10.7	40	24.9	12.5	20.4	19.5	26	18.1	9.1	29.8	29.0
Humerus	43	40.1	20.1	75.7	66.8	127	110.3	55.2	100.0	93.8	143	122.2	61.1	100.0	95.5	61	53.7	26.9	88.3	86.1
Radius	18	17.0	8.5	32.1	28.3	43	26.0	13.0	23.6	22.1	38	23.0	11.5	18.8	18.0	13	12.0	6.0	19.7	19.2
Ulna	16	14.0	7.0	26.4	23.3	51	40.6	20.3	36.8	34.5	60	38.8	19.4	31.8	30.3	28	24.3	12.2	40.0	38.9
Femur	0	0.0	0.0	0.0	0.0	119	92.4	46.2	83.8	78.6	146	113.1	56.6	92.6	88.4	78	60.8	30.4	100.0	97.4
Tibia/Fibula	82	52.3	26.2	98.7	87.2	163	98.8	49.4	89.6	84.0	127	64.7	32.4	52.9	50.5	92	52.2	26.1	85.9	83.7
Patella	0	0.0	0.0	0.0	0.0	0	0.0	0.0	0.0	0.0	1	0.0	0.0	0.0	0.0	0	0.0	0.0	0.0	0.0
Talus	0	0.0	0.0	0.0	0.0	0	0.0	0.0	0.0	0.0	0	0.0	0.0	0.0	0.0	0	0.0	0.0	0.0	0.0
Calcaneus	1	1.0	0.5	1.9	1.7	4	4.0	2.0	3.6	3.4	5	5.0	2.5	4.1	3.9	5	5.0	2.5	8.2	8.0
Phalanges	1	0.0	0.0	0.0	0.0	5	0.0	0.0	0.0	0.0	20	3.0	0.1	0.1	0.1	9	2.0	0.0	0.1	0.1
Metapodials	18	14.8	1.5	5.6	2.5	35	33.0	3.3	6.0	2.8	71	61.0	6.1	10.0	4.8	21	19.0	1.8	5.9	3.0
Long-Bone Frag.	1					7					5					3				
Non-ID Fragment	1					0					0					0				
Non-ID Cranial	0					2					0					0				
Vert Indet.	1					0					1					0				
TOTAL	316	242.3				947	679.7				894	638.0				564	440.6			
MNI	30					59					64					32				

Table 6.9: Tabulation of zooarchaeological index values (NISP, MNE, MNI, MAU, %MAU, and RA) for stratigraphic Units 6 – 8C (*H. sapiens* layers). Note: femora for Unit 6 were unavailable for study.

Table 6.10: Relative numbers of skeletal elements comparing proportions of postcranial to cranial elements (PC/C)[a], lower limb to upper limb (ZE/ST)[b], anterior to posterior limb elements (AN/PO)[c], and axial to appendicular elements (AX/AP)[d] for each stratigraphic unit. (Note: data collection on femora were not finished for Units 1A, 1B, and 6)

	H. floresiensis				*H. sapiens*			
Indices	1A-I	1A-II	1A-III	1B-IV	6	8A	8B	8C
PC/C	2.64	2.51	2.37	3.58	6.68	9.74	10.36	4.03
ZE/ST	0.94	2.08	0.93	1.46	1.69	0.65	0.40	0.61
AN/PO	1.45	0.57	1.62	0.75	0.92	0.72	0.77	0.59
AX/AP	0.02	0.02	0.04	0.07	0.002	0.001	0.002	0.01

a (femur + humerus) / (mandibles + maxillae)
b (tibia + (radius + ulna)/2) / (femur + humerus)
c (scapula + humerus + (radius + ulna)/2) / (pelvis + femur + tibia)
d (atlas + axis + (cervical/5) + (thoracic/12) + (lumbar/7) + (sacra/4)) / ((humerus/2) + (radius/2) +(ulna/2) + (femur/2) + (patella/2) + (tibia/2))

6.3.3 Element fragmentation and breakage

Degrees of element fragmentation across all units are summarized in Table 6.11. Units 1A-I and 1A-II contain the highest degrees of fragmentation when including all elements and when excluding compact bones and teeth. All other units show a comparable degree of moderate fragmentation, with the most recent stratigraphic unit (8C) showing the lowest amount. Overall, there is a significant positive correlation between stratigraphic unit and fragmentation[b] ($r^2 = 0.59$, $p = 0.026$) where more recent layers contain a greater proportion of complete elements in comparison to older stratigraphic units. This is also supported by a significant positive correlation between mean fragment length and temporal depth ($r^2 = 0.82$, $p = 0.002$) where more recent stratigraphic units contain larger specimens compared to older deposits. However, this difference is also likely due to the relative abundance of smaller body-sized taxa within older units (1A and 1B) compared to larger-bodied taxa within more recent units (6 and 8A – 8C) (see Section 6.3.1). When considering the average percent of complete specimens according to skeletal element type, there is a weak and non-significant correlation through time for both non-long bone elements ($r^2 = 0.13$, $p = 0.39$) and long bone elements ($r^2 = 0.4$, $p = 0.09$) (Tables C.1 and C.2).

Table 6.11: Bone fragmentation according to stratigraphic unit: fragmentation[a] (NISP/MNE all bones), fragmentation[b] (NISP/MNE excluding compact bones and teeth), and fragment size summary statistics. Lengths are in mm.

Occupation	Unit	Fragmentation[a]	Fragmentation[b]	Min length	Max length	Mean length	SD length	%<2 mm	%<5 mm
H. sapiens	8C	1.28	1.36	1.35	51.06	15.14	7.87	0.08	0.18
	8B	1.40	1.49	1.2	48.89	15.64	8.06	0.07	0.12
	8A	1.39	1.51	1.11	78.77	16.29	7.69	0.08	0.14
	6	1.30	1.44	1.17	49.37	14.55	7.81	0.13	0.22
H. floresiensis	1B-IV	1.28	1.53	1.1	44.45	9.8	7.62	0.14	0.37
	1A-III	1.26	1.52	1.22	38.97	9.54	8.06	0.10	0.37
	1A-II	1.64	2.34	1.15	26.41	8.9	7.76	0.10	0.31
	1A-I	1.44	2.02	1.1	31.7	8.48	7.96	0.11	0.38

Long bone breakage morphology was analyzed to gauge the degree of post- and pre-depositional breakage (**?**). Fresh breaks, or green fractures, tend to preserve a more oblique fracture angle and smooth, V-shaped/curved fracture outlines while

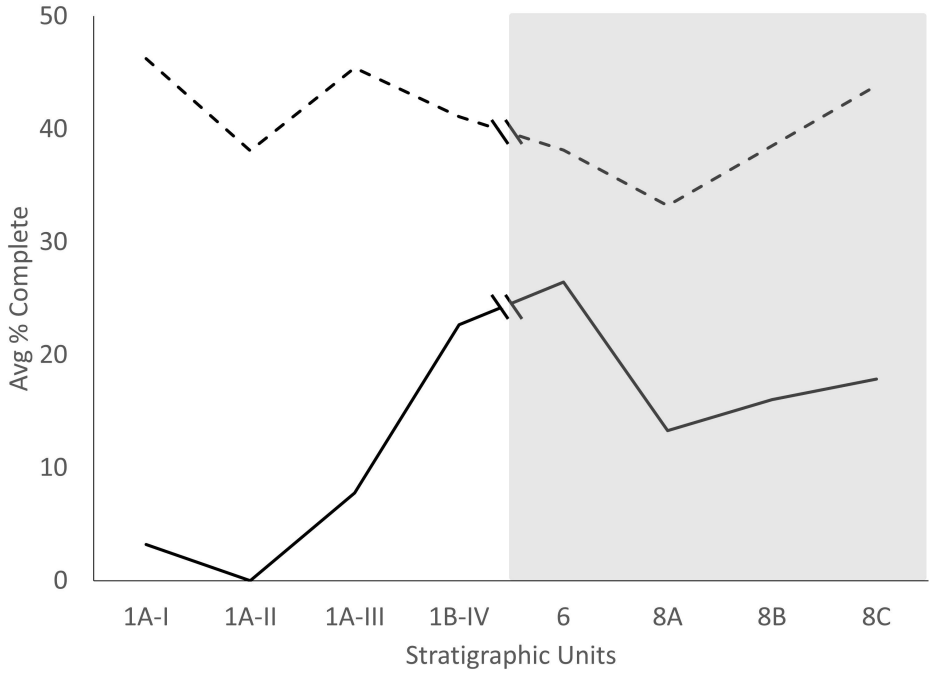

Figure 6.9: Average percent complete long bone (solid line) and non-long bone (broken line) according to stratigraphic unit. Units containing *H. sapiens* are shaded in grey. Data are summarized in tables presented in Appendix C.

long bones broken while dry will result in more rough, transverse fracture outlines and right-angled fractures. A total of 3,118 fractured long bone ends were analyzed and compared against assemblages with known breakage patterns from **?** (Figure C.1 in Appendix C). Figure 6.11 reports fracture morphology frequencies, percentages of break types, and the relationship between *H. floresiensis* and *H. sapiens* units according to murine body sizes.

There are no significant correlations between the relative frequencies of right-angled fractures or rough fractured edges when considering all aggregated murine body sizes and stratigraphic units, but a significant correlation was found in the relative frequencies of transverse fractured outlines ($r^2 = 0.54$, $p = 0.04$). In other words, there is no relationship between dry fractures compared to either the more recent or older deposits but there are significantly more broken long bones with transverse outlines in older deposits compared to more recent ones. Interestingly, long bones

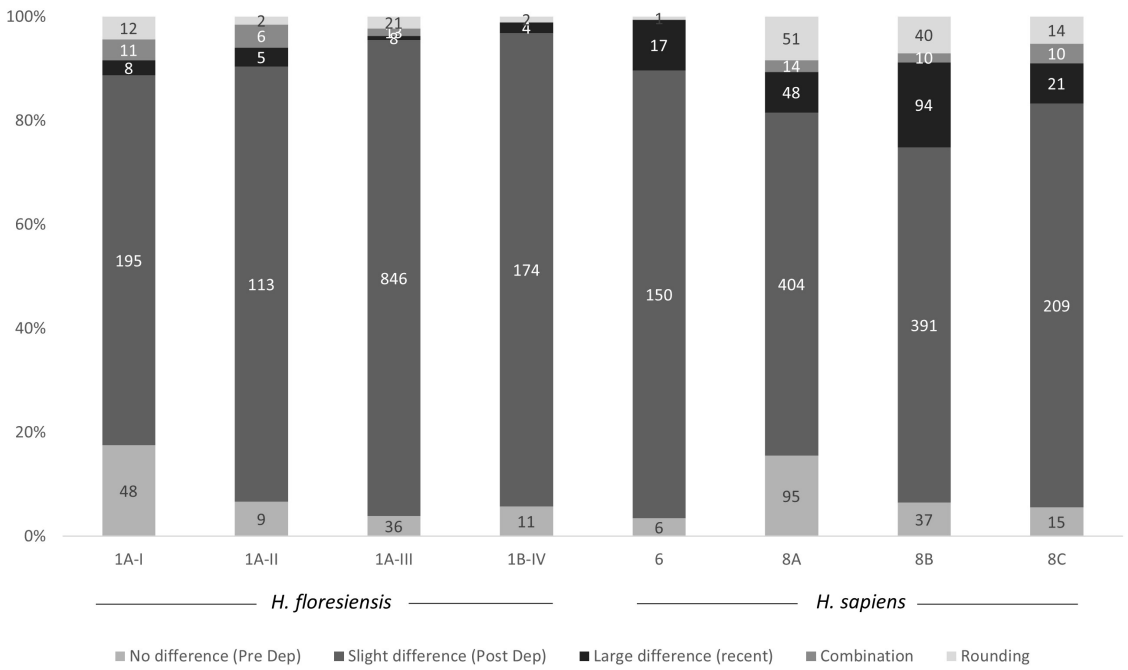

Figure 6.10: Differences in the fracture margin surface appearance compared to external cortical bone surface appearance. Values are represented as percentage for each stratigraphic unit with the total value for each type included.

assigned to murine body sizes 1 and 3 – 5 do show a strong correlation between right-angled fractures ($p = <0.05$) and successive stratigraphic units indicating that post-depositional breakage is driving long bone fracture morphology for these murine body size categories. This is also supported by the majority of post-depositional breaks identified along fractured margins (Figure 6.10). A discriminant analysis involving a comparison between murine body size categories, stratigraphic units, and known fresh and dry break assemblages shows only three unit-to-body size combinations that resemble fresh breaks (1A-I size 5; 1A-I all body sizes; 1A-I indeterminate body size). Otherwise, all other unit-to-body size combinations resemble a dry and/or mixed assemblage comprised of both fresh and dry breaks (Table C.4, Figure C.1). Overall, small mammal long bones from all levels and stratigraphic units are heavily affected by post-depositional damage with the exception of giant murines from Unit 1A-I (*H. floresiensis*, <120 ka).

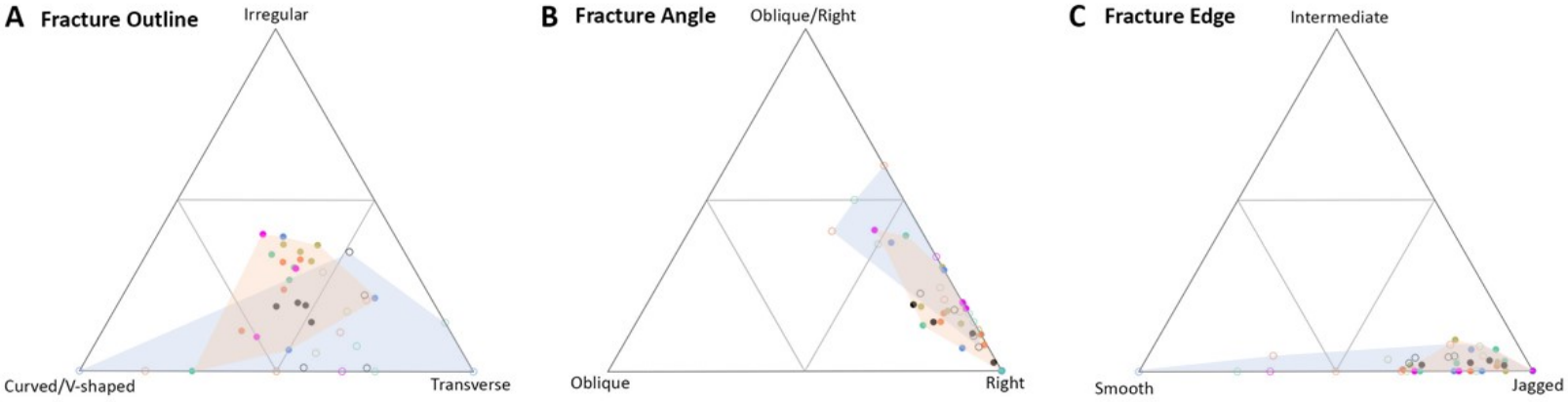

Legend

Size 1 =
Size 2 =
Size 3 =
Size 4 =
Size 5 =

H. sapiens =
H. floresiensis =

D

	Fracture Outlines			Fracture Angle			Fracture Edge		
Unit	Curved/V-shaped	Transverse	Irregular	Right	Oblique	Oblique/Right	Rough	Smooth	Intermediate
8C	72 (27)	115 (43)	81 (30)	204 (77)	18 (7)	42 (16)	214 (86)	29 (12)	6 (2)
8B	173 (34)	237 (47)	93 (18)	478 (86)	7 (1)	69 (12)	465 (87)	52 (10)	16 (3)
8A	175 (31)	218 (29)	165 (30)	410 (69)	59 (10)	121 (21)	414 (71)	165 (28)	7 (1)
6	67 (41)	62 (38)	33 (20)	168 (94)	2 (1)	9 (5)	162 (91)	15 (8)	2 (1)
1B-IV	37 (20)	97 (52)	54 (29)	146 (77)	6 (3)	37 (20)	149 (79)	34 (18)	6 (3)
1A-III	190 (22)	533 (60)	159 (18)	757 (81)	19 2)	154 (17)	748 (80)	128 (14)	57 (6)
1A-II	58 (46)	68 (54)	1 (1)	116 (86)	2 (1)	17 (13)	101 (74)	31 (23)	4 (3)
1A-I	62 (32)	124 (65)	5 (3)	158 (57)	33 (12)	86 (31)	170 (61)	99 (35)	10 (4)

Figure 6.11: Ternary plots showing degrees of long bone breakage damage according to **?**. Closed circles represent units associated with *H. sapiens* (Units 6 and 8A– C) while open circles represent units associated with *H. floresiensis* (Units 1A-I – 1A-III and 1B-IV). (A) Fracture outline (B) Fracture angles (C) Fracture edges (D) Table summarizing total degrees of damage with percentages in parentheses.

Mandibular and maxillary breakage shows varying degrees of fragmentation from light to extreme, with neither breakage category being statistically significant across stratigraphic units (p >0.05) (Table 6.12). In other words, there is no relationship with mandibular or maxillary breakage patterns through time. All breaks were of post-depositional origin as there were no fractured margins exhibiting rounding, polishing, or smoothing that may indicate breaks from owl digestion. Any breaks caused by avian digestion were likely re-fractured after deposition rendering them taphonomically invisible.

Table 6.12: Mandibular and maxillary bone breakage according to Andrews (1990) summarized by stratigraphic unit. NISP and percentages (%) are given.

	Occupation	*H. floresiensis*								*H. sapiens*							
	Unit	1A-I		1A-II		1A-III		1B-IV		6		8A		8B		8C	
Element	Category	NISP	%	NISP	%	NISP	%	NISP	%	NISP	%	NISP	%	NISP	%	NISP	%
Mandible	A	0	0.00	0	0.00	1	1.03	0	0.00	2	33.33	4	14.81	0	0.00	3	11.11
	B	0	0.00	0	0.00	6	6.19	0	0.00	0	0.00	2	7.41	1	4.76	3	11.11
	C	11	73.33	2	100.00	58	59.79	8	88.89	3	50.00	16	59.26	17	80.95	18	66.67
	D	0	0.00	0	0.00	0	0.00	0	0.00	0	0.00	0	0.00	0	0.00	0	0.00
	E	3	20.00	0	0.00	25	25.77	0	0.00	1	16.67	2	7.41	2	9.52	1	3.70
	F	1	6.67	0	0.00	7	7.22	1	11.11	0	0.00	3	11.11	1	4.76	2	7.41
Maxilla	D	2	10.53	0	0.00	9	13.64	1	14.29	0	0.00	0	0.00	3	50.00	3	60.00
	E	17	89.47	8	100.00	57	86.36	6	85.71	2	100.00	0	0.00	3	50.00	2	40.00

6.3.4 Bone surface modifications

Post- and pre-depositional patterns

Alteration of bone surfaces due to post- and pre-depositional processes, including weathering damage, exfoliation, manganese staining, and burning is summarized by pre-defined stages according to stratigraphic unit (Figures 6.12 and 6.13). Collectively, these data reveal interesting and distinct taphonomic patterns within each stratigraphic unit. Units 1A-I and 1A-II contain a greater degree of damage due to weathering, exfoliation, and manganese staining compared to Unit 1A-III, and to a lesser extant, 1B-IV. Unit 6 closely resembles Unit 1B-IV with similar patterns of manganese staining and weather damage. The first appearance of burning also occurs in Unit 6 but is not extensive until Unit 8A. The most extreme stages of burning

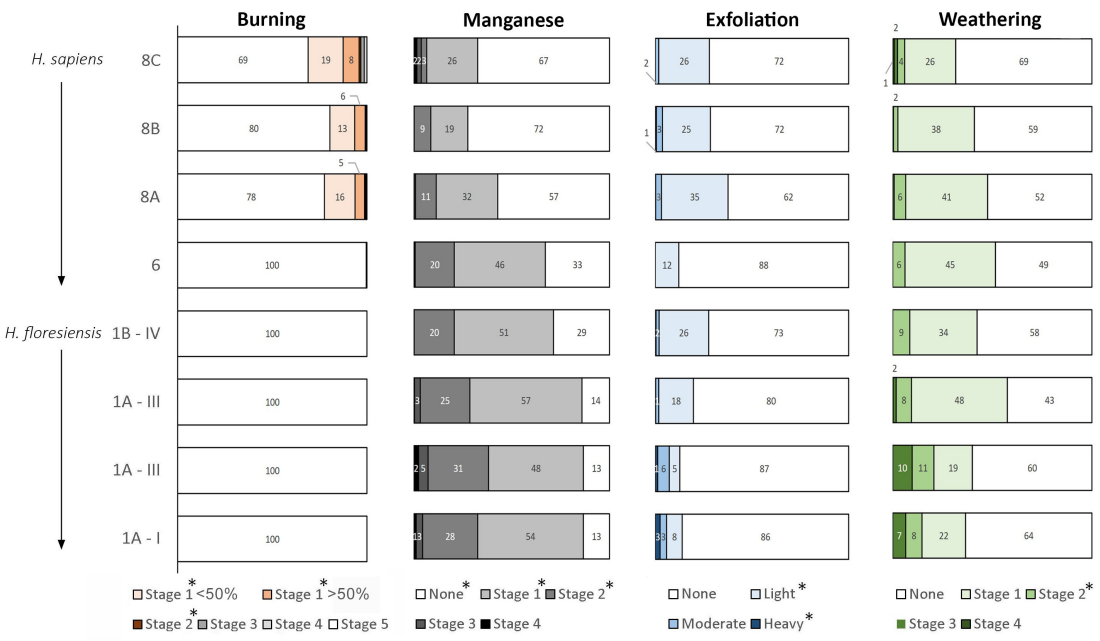

Figure 6.12: Percentages of damage caused by burning (red), manganese-oxide staining (gray), exfoliation (blue), and weathering (green) by pre-defined stages according to stratigraphic units. Asterisks indicate stage values that are significantly correlated with depth.

(calcined bone) are observed in Unit 8B but a greater relative abundance of intensive burning is observed in Unit 8C. Both manganese staining and weathering damage are reduced in Units 8A and 8B until Unit 8C when greater degrees of damage are observed.

The greatest difference between adjacent units is observed between Units 6 and Unit 8A with a chord distance (CD) value of 0.33, as well as between Units 1A-II and 1A-III (CD = 0.24) (Figure 6.13). These differences are largely driven by a reduction in stage 2 weathering damage ($r^2 = 0.74$, $p = 0.005$) and an increase in light degrees of exfoliation ($r^2 = 0.55$, $p = 0.03$). Units 1A-I and 1A-II are also the most similar to one another (CD = 0.06) compared to all other successive units.

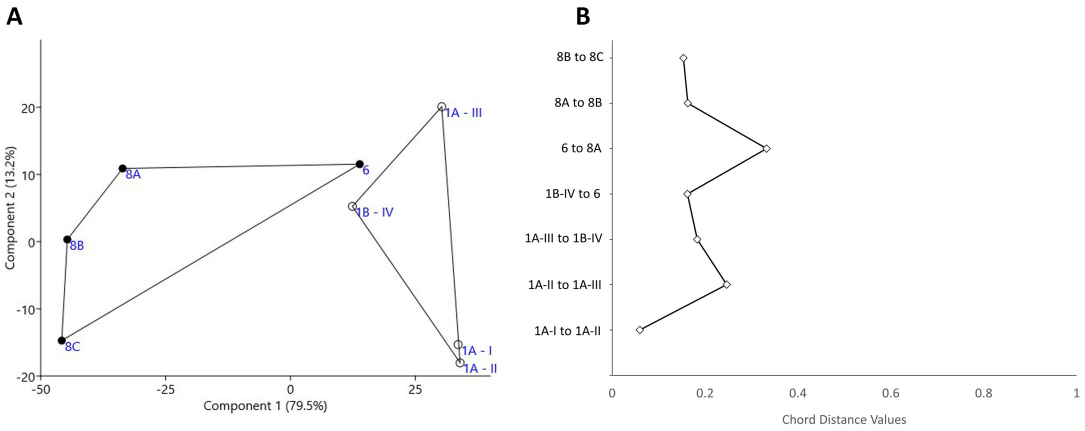

Figure 6.13: Analyses exploring the relationship between post- and pre-depositional damage caused by weathering, manganese staining, exfoliation, and burning to stratigraphic units. A) Principal components analysis: units associated with *H. sapiens* and more-closed environments are represented by filled circles while units associated with *H. floresiensis* and more-open environments are represented by open circles. Variable loadings are shown in Figure D.1. B) Squared chord distance analysis showing the observed difference between adjacent units. Values nearing 1 indicate extreme change while values nearing 0 indicate no change between units.

The first appearance of burning is observed in Unit 6 where a single rib fragment exhibited stage 3 damage (carbonized bone). Unit 8A - 8C contained mostly superficial burning (Stage 1) caused by exposure to a lower heat source reaching an estimated maximum temperature of 300°C (Shipman et al., 1984). Calcined (stage 5) and carbonized (stages 3 and 4) bones were also identified but in extremely low frequencies relative to more lightly burned bone. Only one specimen, a size 5 mandibular incisor from Unit 8A, contained evidence of highly localized stage 3 damage indicative of direct burning (Figure 6.14).

Figure 6.14: Mandibular incisor with carbonized burning damage located on the tip from Unit 8A. Note the color differences between the dentine and the outer enamel.

Avian digestion patterns

Avian digestive damage was recorded on all incisors, molars, distal humeri, and proximal femora (Figure 6.15). Since not all femora were sampled across units, results are reported for the teeth and distal humeri until the femora can be incorporated. Damage to the distal humeri due to avian digestion was rare, with mostly light degrees

of digestion and no obvious patterning of digestive categories through time (Figure 6.15–C). In all but Units 6 and 1B-IV the majority of size 2 molars fall within the light digestive category while size 3 molars show very light digestion damage (Figure 6.15–B). Size 1 molars also vary within units with the majority showing light or very light degrees of damage. Conversely, the incisors showed a more reliable pattern for comparison across all units due to their greater relative abundance. Thus, Units 1A and 1B are characterized by "very light" or an absence of damage with a maximum of <11% of other digestive categories ("light", "moderate", or "heavy") represented. Conversely, stratigraphic Units 6 through 8C contain relatively greater amounts of "light" and "moderate" digestive damage on the incisors.

Murine Age profiles

Age profiles of murine body sizes based on toothwear are summarized in Figure 6.16. The majority of molars belonging to murine body sizes 1, 2, and 4 show minor occlusal wear indicating young individuals (toothwear stages 1 and 2) while murine body size 3 is 100% represented by young individuals. Murine body size 5 is composed of specimens primarily of adult and old adult age range based on more extensive wear damage (toothwear stage 3 – 5). Molars that show evidence of avian digestion (body sizes 1 though 3) also show an increasing proportion of younger individuals as body size increases (Figure 6.16 – A). Conversely, body sizes that do not show evidence of avian digestion (sizes 4 and 5) show a decreasing trend of younger individuals. This suggests that avian predators were likely selecting murines as prey based on an optimal body size for consumption while hominins were targeting larger bodied murines represented by older individuals. Moreover, Units 1A, 1B, and 6 are comprised of a majority of young murines (>64%), while young murines make up <60% in Units 8A – 8C (Figure 6.16 – B).

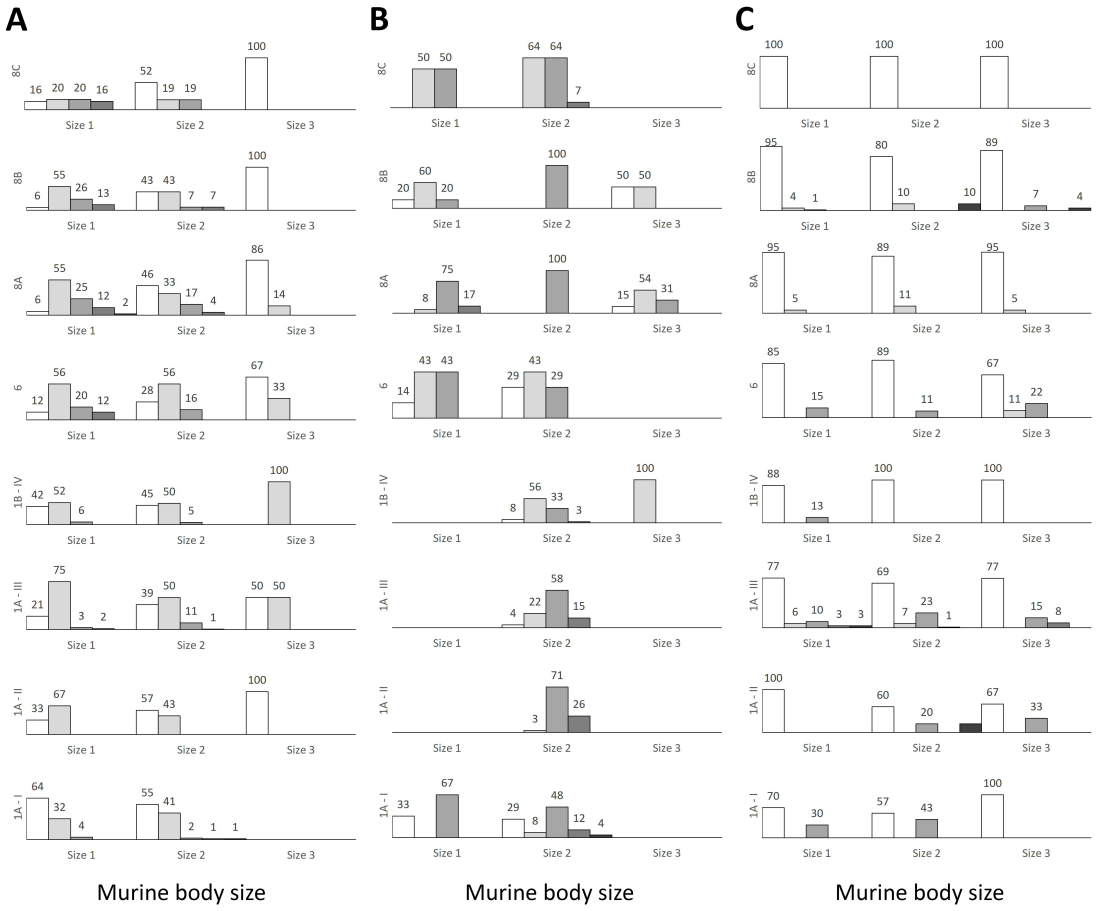

Figure 6.15: Stages of avian digestive damage for A) incisors, B) molars, and C) humeri according to stratigraphic unit and murine body size categories. Stages are defined by Andrews (1990) and (Lloveras et al., 2008a) with an additional "Very Light" category (see table B.1), and are represented by white (none), light grey (very light), medium grey (light), grey (moderate), dark grey (heavy), and black (extreme).

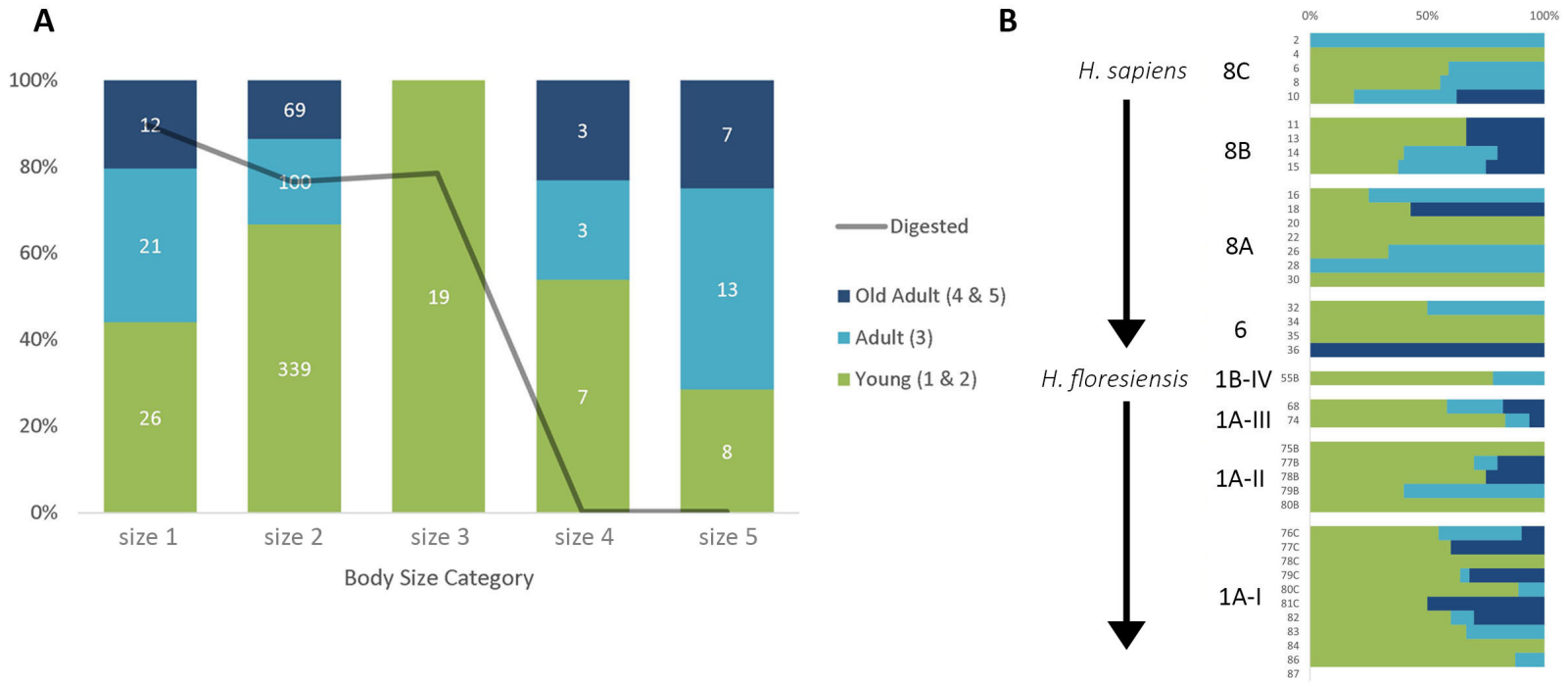

Figure 6.16: Toothwear stages of mandibular and maxillary molars by (A) murine body size and presence of avian digestive damage, and (B) stratigraphic unit and excavated spit.

Non-anthropogenic bone surface modifications

All bone surface modifications are summarized in Tables 6.14 and 6.13. A total of 704 marks were recorded with 479 of them identified to a source of origin (Table 6.14). The majority of identified marks were pits (51.7%) with superficial cracks emanating away from the center of the marks and were found in a variety of shapes and sizes (Figure 6.17 – D-F). Some of these marks broke through the cortical bone surface creating a puncture, but most were shallow, round pits with some crushing along the edge of the pit and characterized by star-like cracking. The marks are found on all element types and in all locations indicating a random non-preferential occurrence. These marks mostly resemble insect activity and could be the result of termites, but no sinuous grooves were found along the pit and puncture edges that are typically found on marks created by termite jaws (Fernández-Jalvo and Andrews, 2016). Additional higher resolution microscopy and local comparative experiments are needed to confirm the type of insect, but the mark morphology and the randomness of these marks indicate high levels of insect activity within Units 1A-III and 1B-IV. Other non-anthropogenic marks identified to an agent and/or source include rodent gnawing (0.4%), root damage (1.5%), bacteria (0.4%), and punctures from avian beaks and/or talons (2.3%) but all in extremely low frequencies (Table 6.14).

The majority of non-identified marks were pits (45%) and scores (27%) with notches (7%), punctures (7%), pit and scoring (0.9%), scrapes (5%), shave (0.9%), as well as indeterminate amorphous (3%) and linear (2%) marks also represented (Table 6.13). Most of these marks were found on elements where body size was indeterminate (54%) and from stratigraphic Units 8A – 8C and 1A-III.

Anthropogenic bone surface modifications

Evidence of anthropogenic damage includes cutmarks (25%) and tooth marks (18.5%), with one unidentified perforation mark (Table 6.14). The majority of cutmarks were

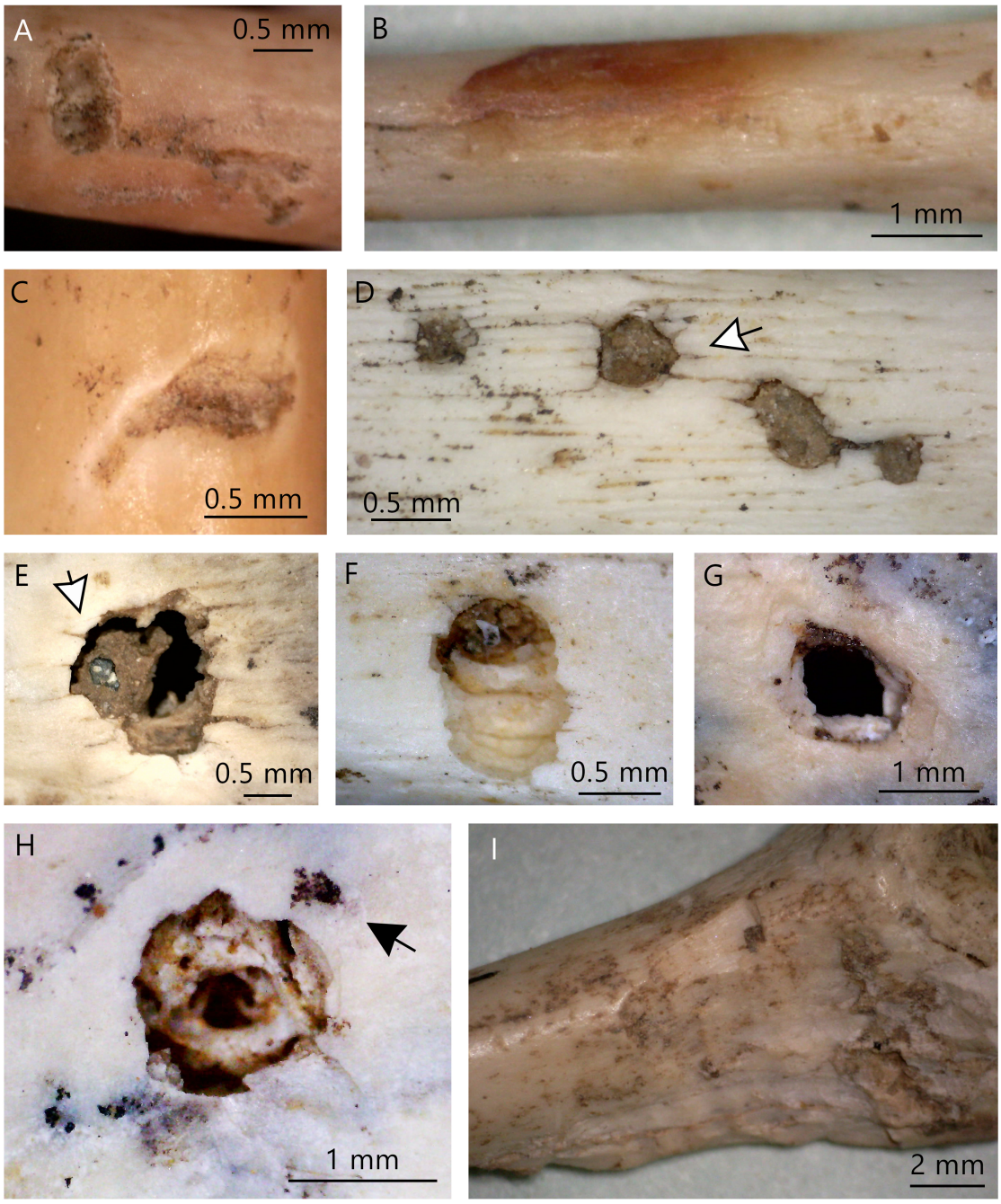

Figure 6.17: A selection of other pre- and post-depositional types of modification identified on murine elements at Liang Bua. (A) A dendritic root pit and pathway (B) Oxidized iron staining (C) Irregular pit likely caused by root damage (D - F) Irregular pits and punctures with slight crushing around the interior margin and star-like cracking emanating around the exterior margin (white arrows) (G - H) Punctures with internal crushing along the interior margin indicative of avian talon damage. Also highlighted are dendritic-shaped stains from manganese (black arrow) in the surrounding sediment (I) Rodent gnawing marks.

Table 6.13: Frequency of unidentified amorphous and linear marks according to stratigraphic unit and murine body size.

		Non-Identified Amorphous					Non-Identified Linear				
Occupation	Units	Notch	Pit	Puncture	Pit&Score	Amorphous Indet.	Score	Scrape	Shave	Linear Indet,	**Total**
H. Sapiens	8C		16	5		1	6	1	1		**30**
	8B	2	29	3	1	2	22	5		1	**65**
	8A	4	22	5			15	1			**47**
	6	1	11	1			3				**16**
	R					1					**1**
H. floresiensis	1B-IV	1									**1**
	1A-III	5	16	2		3	12	4		2	**44**
	1A-II	2	6	1			1		1		**11**
	1A-I	2	2		1		2	1		2	**10**
	Total	**17**	**102**	**17**	**2**	**7**	**61**	**12**	**2**	**5**	**225**
Murine Body Size											
	Size 1	2	7	5			1				**15**
	Size 2	3	20	2	2	3	17	5	1		**53**
	Size 3	1	9				3			4	**17**
	Size 4	2	2	1		1	1				**7**
	Size 5	2	4			2	2	1			**11**
	Indet.	7	60	9		1	37	6	1	1	**122**
	Total	**17**	**102**	**17**	**2**	**7**	**61**	**12**	**2**	**5**	**225**

identified in Units 1A-III (31%) and 8B (40%) while the majority of tooth marks were found in Units 1A-III (23.5%) and 8C (31.5%) (Figures 6.19 and 6.20). When accounting for the relative abundance of skeletal elements, both the frequency of high confidence cutmarks and the frequency of cutmarked bone relative to NISP indicate high levels of butchery activity in Unit 8B followed by Units 1A (all levels), 8C, and to a lesser extent in Units 8A, 6, and 1B-IV (Figure 6.18). A full description of each bone containing evidence of hominin activity in the form of high confidence cutmarks and tooth marks are described in Appendix E.

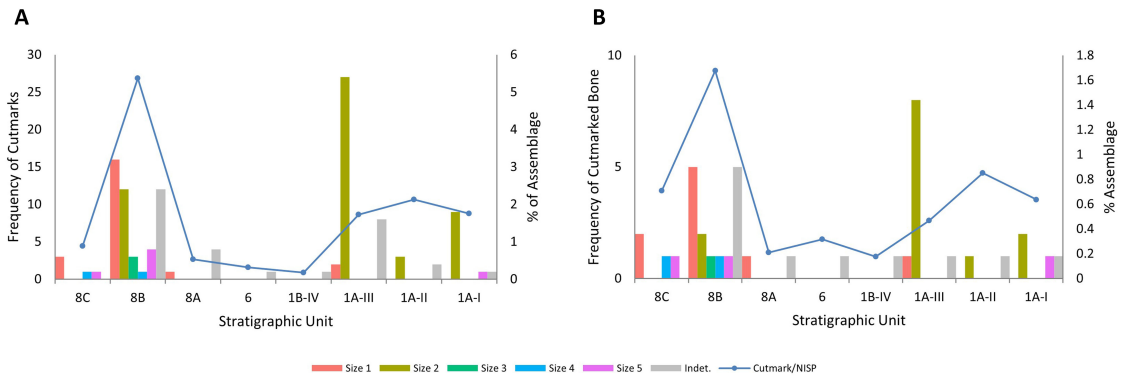

Figure 6.18: A) Frequency of high confidence cutmarks according to murine body size and stratigraphic unit. Percentage of total cutmarks per NISP for each stratigraphic unit is also included. B) Frequency of cutmarked bone according to murine body size and stratigraphic unit. Percentage of cutmarked bone per NISP for each stratigraphic unit is also included.

Table 6.14: Frequency of identified marks according to stratigraphic unit and murine body size.

		Identified BSM origin								
Occupation	Unit	Beak/Talon	Cut-Mark	Hominin Tooth Mark	Perforated Mark	Insect	Rodent gnaw marks	Root	Bacteria	**Total**
H. Sapiens	8C	0	5	28	0	3	1	2	0	**25**
	8B	6	48	16	0	1	0	2	2	**9**
	8A	2	5	8	0	3	1	3	0	**259**
	6	0	1	1	0	8	0	0	0	**33**
	R	0	6	0	0	1	0	0	0	**7**
H. floresiensis	1B-IV	2	1	0	0	30	0	0	0	**10**
	1A-III	0	37	21	0	201	0	0	0	**22**
	1A-II	0	5	4	0	0	0	0	0	**75**
	1A-I	1	11	11	1	1	0	0	0	**39**
	Total	**11**	**119**	**89**	**1**	**248**	**2**	**7**	**2**	479
Murine Body Size										
	Size 1	7	22			20		3	1	**53**
	Size 2	0	51	38	0	133	0	2	0	**224**
	Size 3	0	3	10	0	10	1	0	0	**24**
	Size 4	0	2	10	0	0	0	0	0	**12**
	Size 5	0	12	7	1	1	0	0	0	**21**
	Indet.	4	29	24	0	84	1	2	1	**145**
	Total	**11**	**119**	**89**	**1**	**248**	**2**	**7**	**2**	479

Table 6.15: Frequency of cutmarked bone according to element, stratigraphic unit, and murine body size.

Occupation	Unit	Element	Size 1	Size 2	Size 3	Size 4	Size 5	Indeterminate	Total
H. sapiens	8C	Femur	0	0	0	1	0	0	1
		Humerus	1	0	0	0	1	0	2
	8B	Cranial	0	0	0	0	0	1	1
		Femur	3	2	0	0	0	1	6
		Humerus	2	0	1	0	1	0	4
		Innominate	0	0	0	1	0	1	2
		Radius	0	0	0	0	0	1	1
		Tibia	0	0	0	0	0	1	1
	8A	Femur	1	0	0	0	0	0	1
		Innominate	0	0	0	0	0	1	1
		Tibia	0	0	0	0	0	1	1
		Calcaneus	0	0	0	0	1	0	1
		Humerus	0	0	0	0	1	0	1
	6	Tibia	0	0	0	0	0	1	1
	R	Humerus	0	0	0	0	1	0	1
H. floresiensis	1B-IV	Innominate	0	0	0	0	0	1	1
	1A-III	Calcaneus	0	1	0	0	0	0	1
		Caudal	0	0	0	0	0	1	1
		Humerus	0	1	0	0	0	0	1
		Mandible	0	2	0	0	0	0	2
		Maxilla	0	1	0	0	0	0	1
		Tibia	0	3	0	0	0	1	4
	1A-II	Humerus	0	0	0	0	0	1	1
		Tibia	0	1	0	0	0	0	1
	1A-I	Humerus	0	1	0	0	1	0	2
		Long bone Fragment	0	0	0	0	0	1	1
		Tibia	0	1	0	0	0	0	1
		Total	8	13	1	2	6	13	42

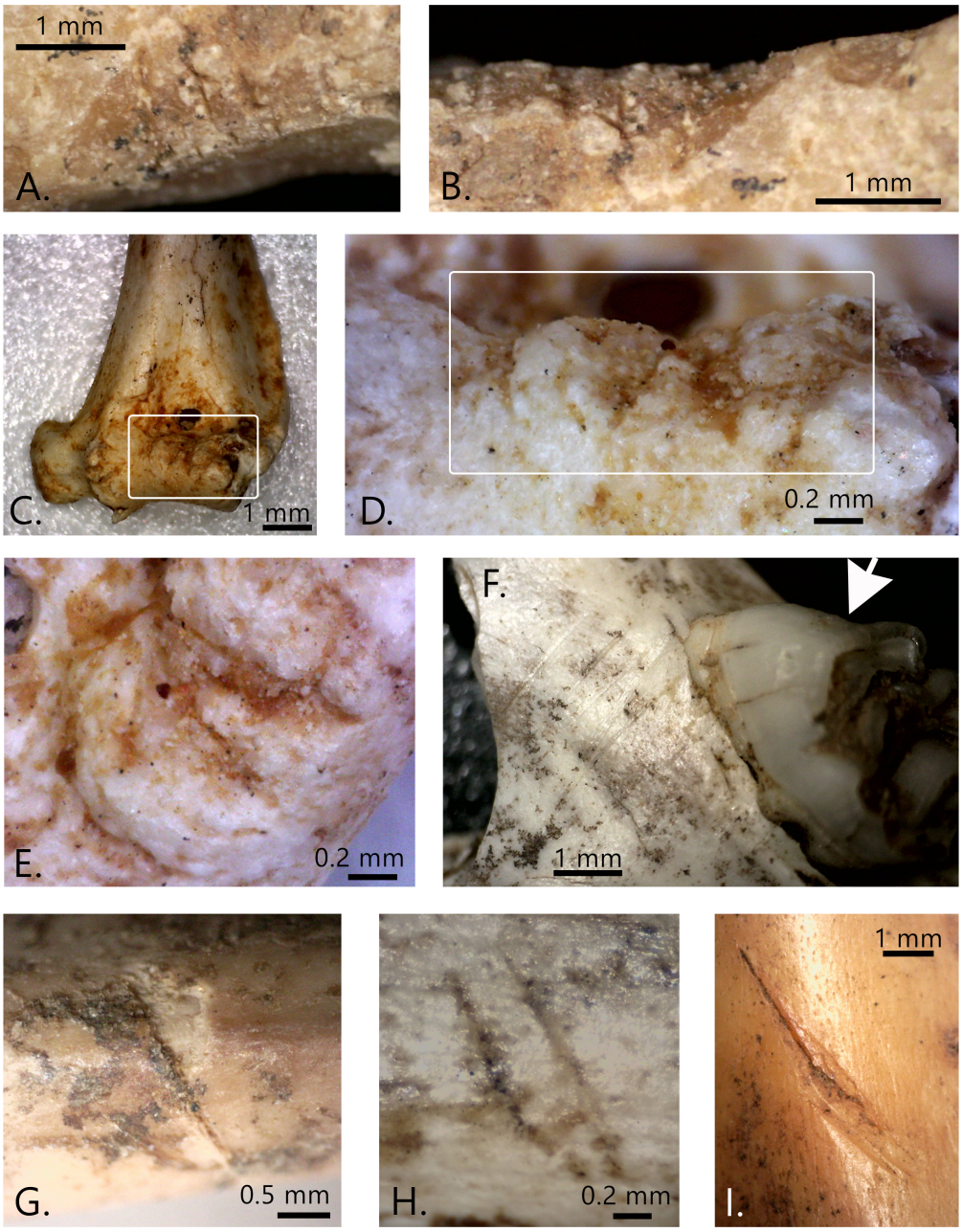

Figure 6.19: A selection of anthropogenic scores identified as cutmarks on murine elements. (A – B) Three v-shaped parallel scores with a slice "lip" identified on a caudal vertebrae from Unit 1A-III (ID: 7722.1-3). (C – E) Three scores with intense corrosive damage on the capitulum's bone surface obscuring morphological details of the marks. The marks were identified on a medium-sized humerus from Unit 1A-I (ID: 480.1-3). White boxes highlight the location of subsequent images. (F) Six shallow parallel scores identified on a maxilla belonging to *Komodomys rintjanus* with digestive damage on the maxillary first molar (white arrow) from Unit 1A-III (ID: 4275.1-6). (G) Narrow V-shaped mark with shoulder flaking identified on the distal shaft of a large-sized tibia from Unit 8A (ID: 5751.1). (H) Two parallel narrow V-shaped marks identified on a large-sized ilium from Unit 8B (ID: 3318.1-2). (I) Deep and narrow mark identified on the distal end of a giant-sized humerus from Unit 8C (ID: 5494.1).

Table 6.16: Frequency of elements with hominin tooth marks according to stratigraphic unit and murine body size.

Occupation	Unit	Element	Size 2	Size 3	Size 5	Indeterminate	**Total**
H. sapiens	8C	Humerus	0	0	1	0	**1**
		Tibia	1	0	0	0	**1**
	8B	Humerus	0	1	0	0	**1**
		Cranial	0	0	0	1	**1**
	8A	Femur	1	0	0	0	**1**
	6	Tibia	1	0	0	0	**1**
H. floresiensis	1A-III	Humerus	2	1	0	0	**3**
		Tibia	0	0	0	1	**1**
	1A-II	Tibia	1	0	0	1	**2**
	1A-I	Humerus	0	0	1	0	**1**
		Innominate	0	1	0	0	**1**
		Tibia	1	0	0	0	**1**
		Total	**7**	**3**	**2**	**3**	**15**

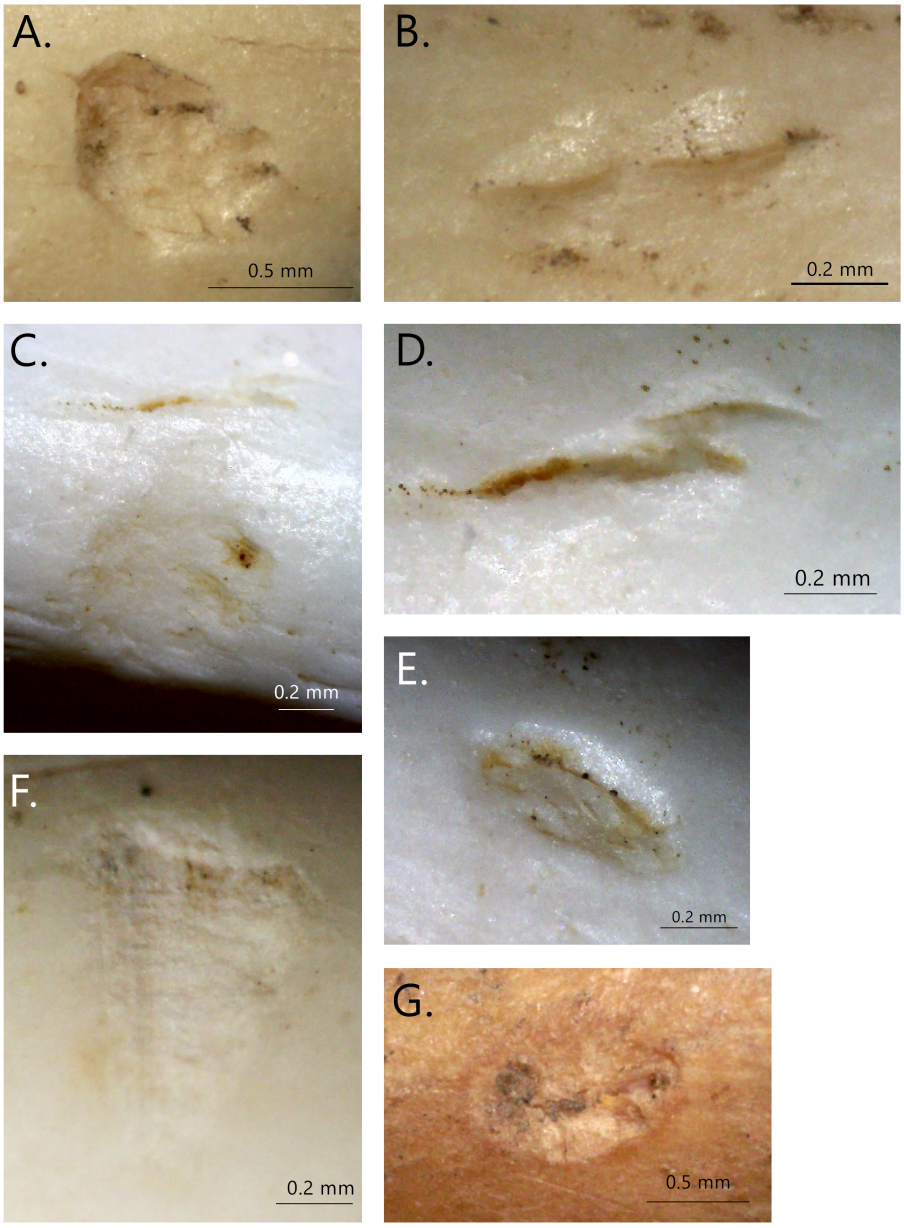

Figure 6.20: A selection of anthropogenic pits and scrapes identified as human toothmarks on murine elements. (A) Tooth pit with internal grooves identified on a medium-sized murine femur recovered from Unit 8A (ID: 5866.1) (B) Two shallow and continuous bisected tooth pits with crescent morphology identified on a medium-sized murine femur recovered from Unit 8A (ID: 5866.2) (C) Tooth scrape with similar shape and morphology seen in subfigure A identified on a medium-sized murine tibia recovered from Unit 1A-I (ID: 752.1) (D) Two continuous bisected tooth pits with crescent morphology identified on a medium-sized murine tibia recovered from Unit 1A-I (ID: 752.2) (E) Crescent shaped pit with internal crushing identified on a medium-sized murine tibia recovered from Unit 1A-I (ID: 752.3) (F) Crescent shaped indentation with scoring emanating away identified on a medium-sized murine tibia recovered from Unit 8C (ID: 5363.7) (G) Bisected pit with internal crushing identified on a giant-sized murine humerus recovered from Unit 8C (ID: 5494.3).

6.4 Discussion

6.4.1 Murine body size and taxonomy at Liang Bua

This study confirms the presence of previously identified murines at Liang Bua, including ones belong to size 1 (*Rattus exulans* and/or *Rattus hainaldi*), size 2 (*Komodomys* cf. *rintjanus*, *Paulamys naso*, and *Rattus* sp.), size 3 (*Hooijeromys* cf. *nusatenggara*), size 4 (*Papagomys theodorverhoeveni* and the shrew-rat), and size 5 (*Papagomys armandvillei*) murine body size categories (Musser, 1981; Musser et al., 1986; van den Bergh et al., 2009; Locatelli, 2010; Locatelli et al., 2012, 2015; Veatch, 2014; Veatch et al., 2019). The relative abundance of both murine species and body size categories show an uneven distribution of primarily size 2 taxa preferring more-open habitats (*Komodomys*) in Units 1A and 1B (~190 – 60 ka), and a more even distribution of size 1 and size 3 – 5 murine body sizes preferring more-closed/mixed habitats (*Rattus* sp., *Paulamys*, *Hooijeromys*, shrew-rat, *Papagmys* sp.) in Units 8A - 8C (~11 – 3 ka) (Veatch et al., 2019). Unit 6 only contained dentognathic remains attributed to *Komodomys*, *Paulamys*, and *Rattus* sp. indicating a slightly different environment and/or predatory activity compared to either Units 1A and 1B or 8A – 8C.

This is the first study to analyze the relative abundance of the currently unnamed shrew-rat dentognathic remains in comparison with other murine species in multiple units (Veatch et al., 2019), and found that the shrew-rat co-occurs in units with other insectivorous murines (*Paulamys*) as well as those preferring more-closed and wet environments (*Papagomys* sp.). Its temporal distribution ranges from Unit 8C (~3 ka – present) to Unit 8A (~11 – 5 ka). Intentional fire damage identified on a mandibular incisor provisionally assigned to the shrew-rat suggests that their accumulation may be human-mediated. An absence of the shrew-rat in Units 1A and 1B is likely a reflection of the dominant environment at the time and not necessarily a real absence. Like *P. theodorverhoeveni* and *S. florensis*, the first appearance of the shrew-rat likely

extends further back in time, possibly to the Middle and Early Pleistocene (Musser, 1981).

A smaller endemic murine (*R. hainaldi*) and a more widespread murine that potentially originated on Flores (*R. exulans*), were both identified in Sector XI, but the morphological similarity between these species makes it difficult to confidently assign these specimens to a species level. Additional comparisons with museum collections are needed to confirm fragments provisionally assigned to both *R. hainaldi* and *R. exulans*.

Spelaeomys florensis, an endemic size 4 murine, was not identified from Sector XI but has been previously documented at Liang Bua in deposits dating back to at least 120 – 60 ka (Unit 1B) (Veatch et al., 2019) as well as in Late Pleistocene and Holocene deposits until ~6 ka (van den Bergh et al., 2009). An abundance of *S. florensis* at Liang Toge, a Holocene archaeological cave site located ~40 km east of Liang Bua, suggests either 1) the micro-habitats specific to *S. florensis* during the Holocene were more conducive in more central Flores, 2) these micro-habitats allowed *H. sapiens* to hunt *S. florensis* near Liang Toge more frequently compared to Liang Bua, or 3) there is a spatial distribution bias of murine taxa at Liang Bua where Sector XI is too small of a sample to adequately capture the full range and relative abundance of murine species through time. Additional zooarchaeological and paleoenvironmental research at Liang Toge is needed to further explore the sites environmental and archaeological contexts in relation to Liang Bua, while a larger comprehensive sample of dentognathic remains from multiple sectors at Liang Bua is needed to more adequately explore the spatio-temporal distribution of all murine taxa.

6.4.2 Relative contributions of murine fauna by avian and hominin agents

The murine faunal assemblage at Liang Bua is the result of a combination of hominin and avian predation based on the relative abundances of cutmarked bone and digested incisors, respectively. Mandibular incisors are arguably the most reliable element to evaluate avian digestion across all stratigraphic units because 1) they are often the most frequently identified element within each stratigraphic unit; 2) murine body size can easily be estimated; and 3) criteria for estimating digestive damage is most reliable compared to molars and postcrania (Comay and Dayan, 2018). Thus, using mandibular incisor digestion and cutmarked bone frequencies as proxies for avian and human agents should provide reasonable assessments of the relative contribution of each agent to each stratigraphic unit, respectively.

Avian digestion

A cluster analysis was run using digestive categories for murine incisors (Figure 6.15) to determine the similarity of digestive damage across murine body sizes and stratigraphic units. Results show that murine body sizes largely cluster together in three groups independent of stratigraphic units (Figure 6.21 – A). Group 1 represents incisors with a majority of "very light" damage with some "light" and "moderate" damage also represented. This group is largely comprised of size 1 incisors with the addition of size 2 incisors from Unit 6. Group 2 represents incisors with a majority of "none" and "very light" digestive damage with some "light" and "moderate" damage as well. This group is largely comprised of incisors belonging to murine body size 2 with the addition of two units with size 1 (1B-IV and 1A-I) and size 3 (1A-III and 6) incisors. Lastly, group 3 contains incisors solely from murine body size 3 that do not show any or very slight evidence of digestion. These distinct clusters suggest that either (1) a different predator or combination of predators are consuming murines

based on their body sizes and/or environments (size 1 = more-closed and size 2 = more-open ecologies), or (2) a taphonomic bias is affecting the degree to which incisors are damaged by body size.

To better evaluate the results from the cluster analysis, a comparison was made between the percentage of digestive damage per stratigraphic unit and murine body size (size 1 and size 2) (Figure 6.21 – B). An analysis of variance (ANOVA) was also performed between body size groups to determine the level of significance. Results show that size 1 incisors consistently have a greater mean for all digestive categories with few showing no evidence of digestion. Conversely, size 2 incisors consistently have a lower mean for all digestive categories with significantly more showing no evidence of digestion (p <0.05). In other words, the difference driving the observed clustering patterns may be explained by smaller incisors showing greater degrees of digestive damage compared to more medium sized incisors. One explanation could be because small incisors have relatively thinner enamel, and thus, may be more susceptible to digestion compared to larger incisors. Alternatively, this could reflect differences in predator behavior where raptors that cause greater digestive damage targeted size 1 murines and raptors that cause relatively lighter digestive damage targeted size 2 murines.

Differences between units show a large change in digestive patterns between Units 1A-I and 1A-II, and between Units 1B-IV and 6 (Figure 6.21 – C). The first change is driven primarily by a dominance of undigested incisors and a reduction in modest amounts of damage ("light" and "moderate"), while the latter is driven by a relative increase in "very light", "light", and "moderate" digestion (Figure 6.15). There is also very little to no evidence of "heavy" or "extreme" levels of digestion on incisors suggesting that diurnal raptors like eagles and kits probably did not contribute to the the small mammal assemblage at large. Instead, a combination of owl predators (category 0 or 1) more reasonably fits the digestive damage results. Unfortunately, a lack

of actualistic studies on Southeast Asian raptor pellets precludes the identification of owl species specific to the region.

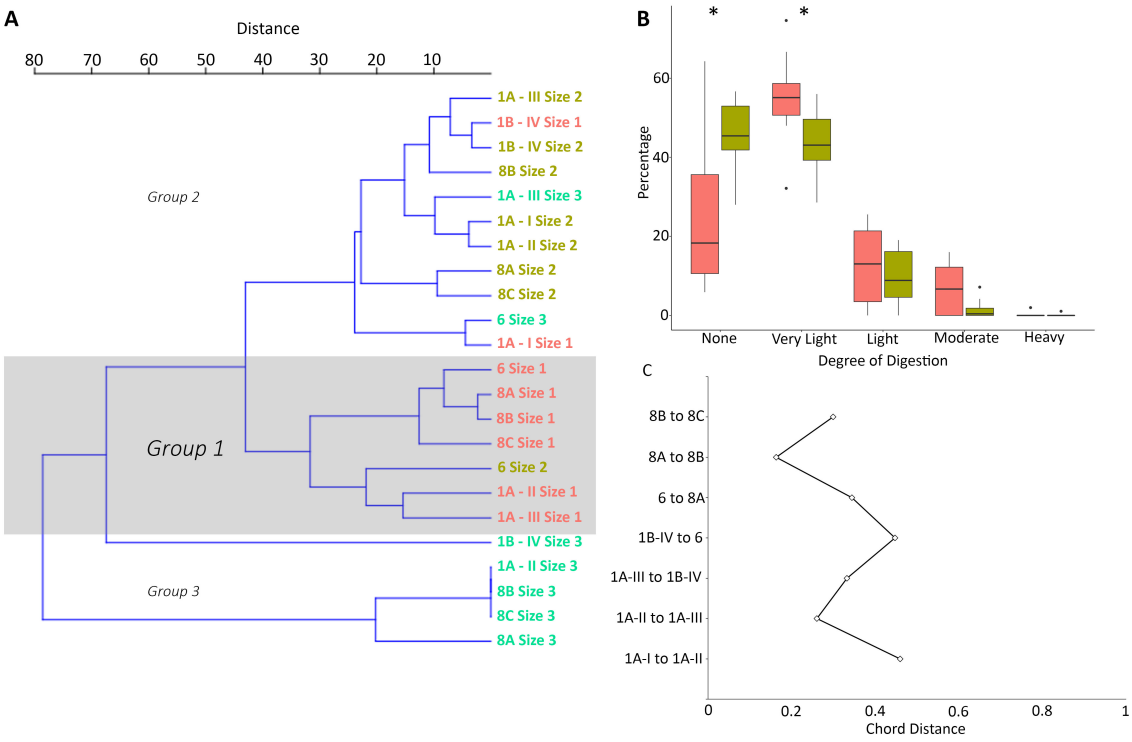

Figure 6.21: A series of analyses comparing the relative frequency of digestive categories for murine incisors. (A) Cluster analysis of murine body sizes and stratigraphic units. Colors delineate body size with units labeled within the figure. (B) box plots showing degrees of digestive damage for murine incisors from all units according to body size (size 1 = coral, size 2 = mustard). Asterisks indicates significance at the 0.05 level between body sizes. (C) Squared chord distance analysis of digestive categories for all murine body sizes to determine differences in adjacent units.

Hominin cutmark damage

Units 1A and 1B: *H. floresiensis*

Within stratigraphic units associated with *H. floresiensis* (Units 1A and 1B), the majority of cutmarked and tooth marked bones were identified as size 2 elements — the most abundant murine body size at this time — as well as size 5 (Table 6.15). Most elements with evidence of butchery were identified as long bones, with the addi-

tion of an innominate, calcaneus, caudal vertebra, mandible, and maxilla. According to Lloveras et al. (2009), cutmarks identified on maxillae, mandibles, and caudal vertebrae indicate skinning and tend to produce superficial cutmarks. The calcaneus is more demonstrative of disarticulation while the innominate and long bones reflect both disarticulation and defleshing. Given the low frequency of cutmarked bone relative to total NISP/unit and the fact that butchering small mammals is highly variable and can leave relatively few to no traces on bone (Lloveras et al., 2009), it is difficult to interpret the degree to which *H. floresiensis* was engaging in these activities. However, their presence on these bones does indicate the *H. floresiensis* likely skinned, disarticulated, and/or defleshed murines to some extent before consumption. This is consistent with the fact that currently there is no evidence indicating that *H. floresiensis* used fire to process their food (if they did, this behavior is currently taphonomically invisible), and thus, hominins would likely skin the animal before consuming the muscle tissue.

One humerus identified as a size 5 murine recovered from Unit 1A-I contains several anthropogenic marks that may reveal important insight into the dietary behaviors of *H. floresiensis*. These include one notch along the proximal metaphysis near the epiphyseal region, a series of overlapping linear marks on the proximal diaphysis, and a large pit also located on the proximal diaphysis (Figure 6.22). The bone is broken at the midshaft exhibiting post-depositional breakage morphology, while the proximal end is broken at the epiphyseal region with a semi-crenulated edge - possibly due to hominin chewing (Fernández-Jalvo and Andrews, 2011). The series of localized elongated grooves on the posterior surface of the diaphysis are indicative of chopping marks (Potts and Shipman, 1981), where the agent used a sharp edge to repeatedly chop and cut soft tissue causing wide indentations to the bones surface. At least eight multi-directional grooves form the main mark while five small striations were identified surrounding the main mark, indicating that the bone and/or tool was positioned

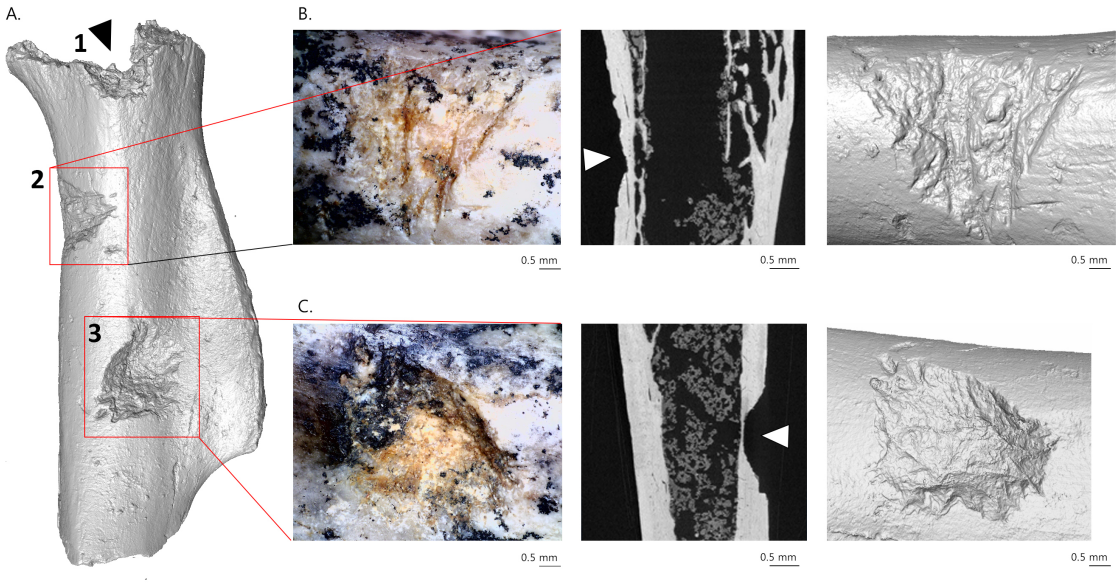

Figure 6.22: Microscopic computed tomography (micro-CT) images and photographs of a giant murine humerus (854.1-2) recovered from stratigraphic Unit 1A. (A) Micro-CT model showing the location of two marks on the proximal shaft. A notch near the humeral head is indicated by a black arrow. (B) A series of images showing a photograph (left), cross-section (middle), and 3D model (right) of localized multi-directional striations. (C) A series of images showing a photograph (left), cross-section (middle), and 3D model (right) of a deep pit.

in multiple orientations while being butchered. Figure 6.22 - B shows a cross-section of the mark (white arrow) indicating a wide but relatively deep indentation measuring a maximum width at 4.34 mm and depth at 0.7 mm. Sediment and black dendritic manganese staining are also present within the grooves indicating pre-depositional damage with extensive corrosion to the surface.

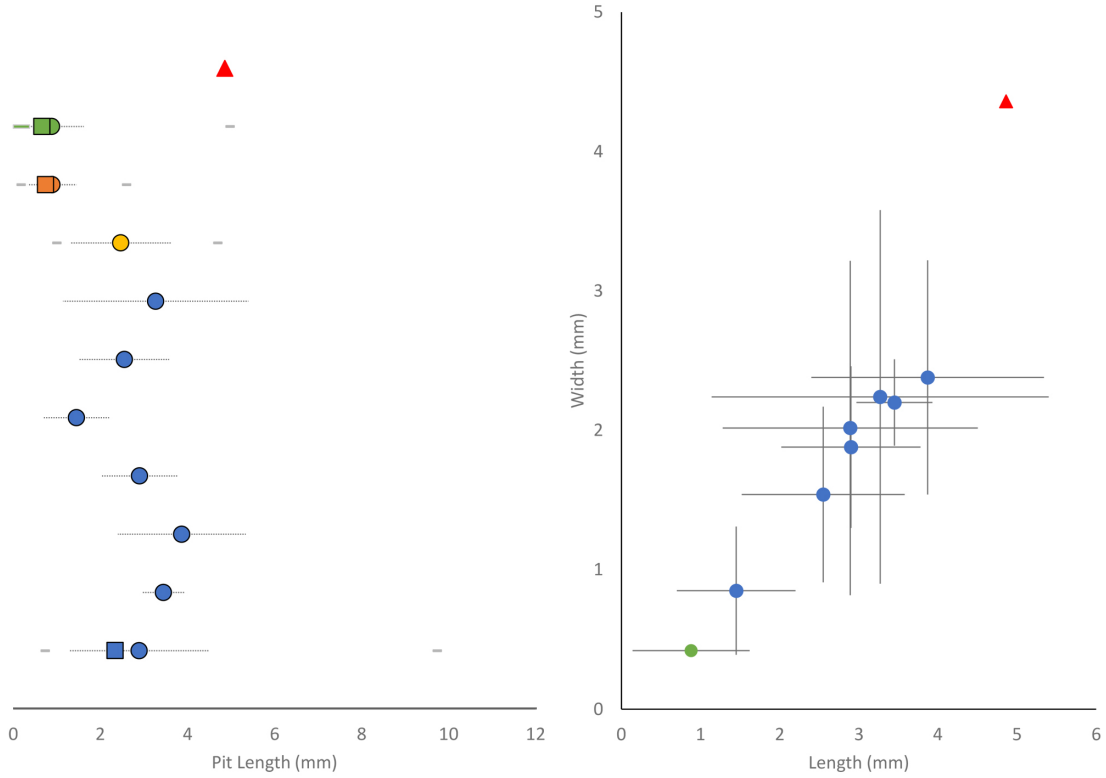

Figure 6.23: Comparison of available length and width dimensions of extant and fossil mammalian carnivore tooth pits (blue) (Domínguez-Rodrigo and Barba, 2006; Domínguez-Rodrigo and Piqueras, 2003), experimental percussive pits (yellow) (Galán et al., 2009), human Bofi forager tooth pits (orange) (Landt, 2007), and Komodo dragon tooth pits (green) (D'Amore and Blumenschine, 2009) against LB 854.2 pit (red triangle) (Figure 6.22). Squares = mean, circle = median, bars = stdv, and dash = outliers.

The second mark on bone 854 is a large pit located on the lateral side of the deltoid tuberosity near the mid-shalf (Figure 6.22 - C). The mark is irregular and oval in shape with multiple striations emanating away from the center of the mark. Heavy manganese staining towards the left side of the mark is also visible with slight bacterial damage to the surface. The cross-sectional shape is bowl-like (white arrow) measuring a maximum depth of 0.89 mm from the surface, and a maximum length and width of 4.86 mm and 4.36 mm, respectively. The mark nearly penetrates the cortical bone surface leaving a minimum width of 0.1 mm between the base of the pit and the internal cavity surface.

In comparison with other pits of known origin (Figure 6.23), the absolute length and width of the mark is outside the known range for tooth pits caused by mammalian carnivores and Komodo dragons (Domínguez-Rodrigo and Barba, 2006; Domínguez-Rodrigo and Piqueras, 2003; D'Amore and Blumenschine, 2009). The maximum length is also outside the range of human tooth pits, of which a width value was not available for comparison (Landt, 2007). The mark does fall within the maximum length of experimental percussive pits, although the pit does not morphologically resemble damage caused by hard- or soft-hammer percussion (Galán et al., 2009). Instead, the morphology suggests that a sharp edged tool was used forcefully, penetrating the cortical surface causing a deep, almost perforated, mark. Overall, the depth of the mark and the topography indicates that the mark was likely caused by a sharp tool used to open the medullary cavity.

Units 6 and 8A-8C: *H. sapiens*

Cutmarked bone from units associated with *H. sapiens* (Units 6 and 8A-C) included elements from all murine body size categories (Table 6.15). The majority of elements with cutmarks were identified as long bones, with the addition of two innominates, a calcaneus, and a cranial fragment. These butchery patterns align more with disarticulating and defleshing (Lloveras et al., 2009), although several marks on the talar facet of the calcaneus does indicate skinning of a size 5 murine (Appendix E).

One element (bone ID 562) shows evidence of human butchery on a size 5 murine humerus recovered from a wall cleaning along the southwest (barat daya) wall between 525 and 635 cm depth from Sector XXVI that includes the top portion of T6 (~18 kya). This humerus therefore derives from Unit 6, which is associated with foraging *H. sapiens*. Five perpendicular scores were identified extending from near the midshaft to the proximal end of the diaphysis (Figure 6.24). The marks are relatively wide, deep,

and do not retain the symmetrical V-shaped cross-section typical of a cutmark made from a stone artifact (Domínguez-Rodrigo et al., 2009a). Instead, the marks appear more U-shaped and asymmetrical with a more vertical edge along and displaced bone coupled with an opposite more shallow edge, each with extensive flaking along the margins (Figure 6.24 - D). Surface flaking and sediment collected within the scores make it difficult to identify internal morphology and requires additional higher resolution imaging. These general morphological features are consistent with the use of bamboo, but additional comparisons are needed to confirm this (West and Louys, 2007).

Other possible agents responsible for creating these marks include Komodo dragons, crocodiles, and large raptors. Komodo dragons are known to latch onto a large carcass with their jaws and rotate their head in an arcing motion to loosen muscle tissue from the bones before pulling back with significant force, leaving arched scores with irregular orientations on the bones surface (D'Amore and Blumenschine, 2009). Smaller animals, like a size 5 murine, are typically consumed whole before being dissolved by highly acidic stomach acids. Similarly, crocodiles can cause wide, parallel U-shaped scores on large animal carcasses while smaller animals are typically consumed whole. It is unlikely that these scores identified on bone 562 were from Komodo dragons or crocodiles, but similarities between known tooth scores from these predators and cutmarks warrants additional comparisons to confirm.

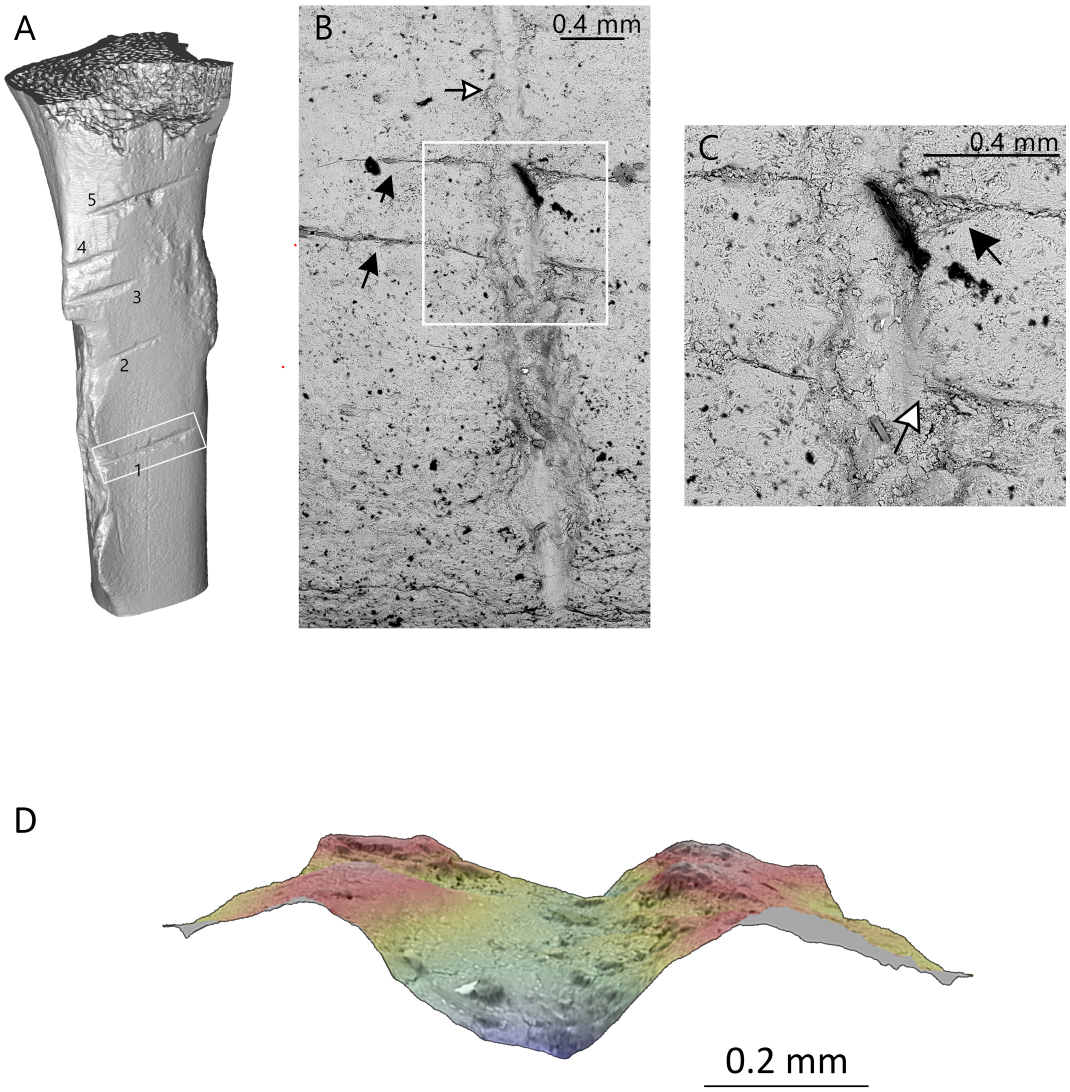

Figure 6.24: Microscopic computed tomography (micro-CT) and scanning electron microscopy (SEM) images of a giant murine humerus associated with *H. sapiens* foragers at Liang Bua (562.1-5). (A) Micro-CT image of the proximal end of a complete murine humerus showing the location of five elongated parallel scores running perpendicular to the bone. (B) Magnified SEM image of score 1 (white-filled arrow) showing disruption from two perpendicular cracks (black-filled arrows) likely due to weathering. (C) Magnified image of the white box in subfigure B showing displacement of bone over the lower crack (white-filled arrow) with flaking (black-filled arrow) near the upper crack. (D) Topography of mark 1 showing asymmetry and displaced bone on the right side.

Conversely, beaks and talons from raptors are known to cause U-shaped scoring, but these scores tend to be superficial and irregular (Fernández-Jalvo and Andrews,

2016). Scores identified from a modern eagle nest (*Aquila verreauxii*), for example, were described as being shallow, U-shaped, straight, but irregularly oriented (Armstrong and Avery, 2014). A comparison between the angle of scores relative to the long bone axis observed on bone 562 and scores made from eagle talons (Armstrong and Avery, 2014) indicate that score angles produced from eagle talons are highly variable compared to the more precise angles observed on bone 562 (Figure 6.25). Additional imaging and comparative analyses are needed to confirm possible agents responsible for these scores.

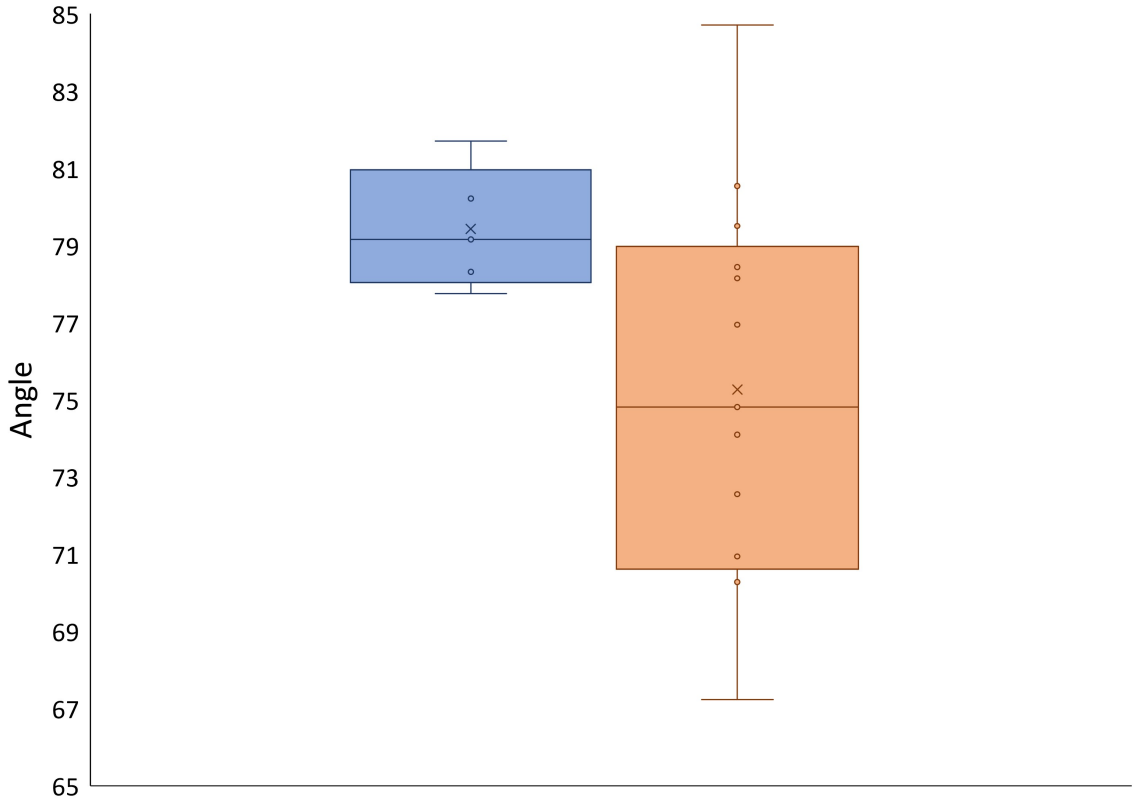

Figure 6.25: Angle of scores relative to long bone axis. Blue = scores on bone 562 from Sector XXVI. Orange = scores caused by eagle beaks and/or talons on a single radius sourced from Armstrong and Avery (2014).

Hominin and avian accumulating agents

Estimating the relative contribution of each agent, however, is difficult given that both avian and human agents were targeting similar sized murines and because both agents can accumulate small prey without causing bone surface damage (see Chapter 4). For example, *H. floresiensis* clearly consumed size 2 and size 5 murines in Units 1A and 1B while *H. sapiens* consumed murines of all body sizes based on cutmark frequencies (Table 6.15 and Figure 6.26). While there are many approaches to cooking and consuming small mammals, foragers do not typically consume the heads of animals much larger than mice (Andrade and Fernández, 2017). Assuming that *H. sapiens* did not consume the head and/or incisors of their small-bodied prey, humans are more likely to accumulate murines with an incisor digestive category of "none". Similarly, barn owls (*Tyto* sp.) inflict little to no damage during digestion (~87-92% of incisors show no evidence of digestion) and only consume animals whole if they weigh less than ~100 – 200 g. Otherwise, owls tend to tear and consume the body of their prey in parts first before being "done" or swallowing the remaining carcass depending on the preys body size (See Chapter 4). Thus, owls are likely to prey upon murines restricted to less than ~400 – 600 g while hominins could accumulate murines of all body sizes. This scenario is supported by the taphonomic results of this study where digestion was only observed on murines weighing <600 g (Murine body size 1 – 3, Figure 6.26) while cutmarks are observed on elements belonging to all body sizes. Thus, both owls and hominins accumulated murine body size categories 1 – 3 with each contributing a portion of prey items with an absence of digestive damage (100% for humans and an estimated 87 – 92% for *Tyto* sp.) (Andrews, 1990).

A comparison of digested incisors and cutmarked bone frequencies between all stratigraphic units reveals important considerations when drawing interpretations for accumulating agents of small mammal assemblages (Figure 6.26) (Andrews, 1990). Units 1A and 1B, for example, show an overlapping distribution of mandibular in-

cisors with evidence of digestion ("Very Light", "Light", "Moderate", "Heavy", and "Extreme" categories) and without digestion (category "none"). Unit 6 shows a slight separation between these two groups along murine body size, while Units 8A – 8C show digested incisors concentrated and non-digested incisors and murine body size. When combined with hominin behavioral data, there a correlation with cutmarked bone frequencies and non-digested distribution suggesting a relationship between non-digested abundances and hominin predation on murine fauna (Figure 6.26).

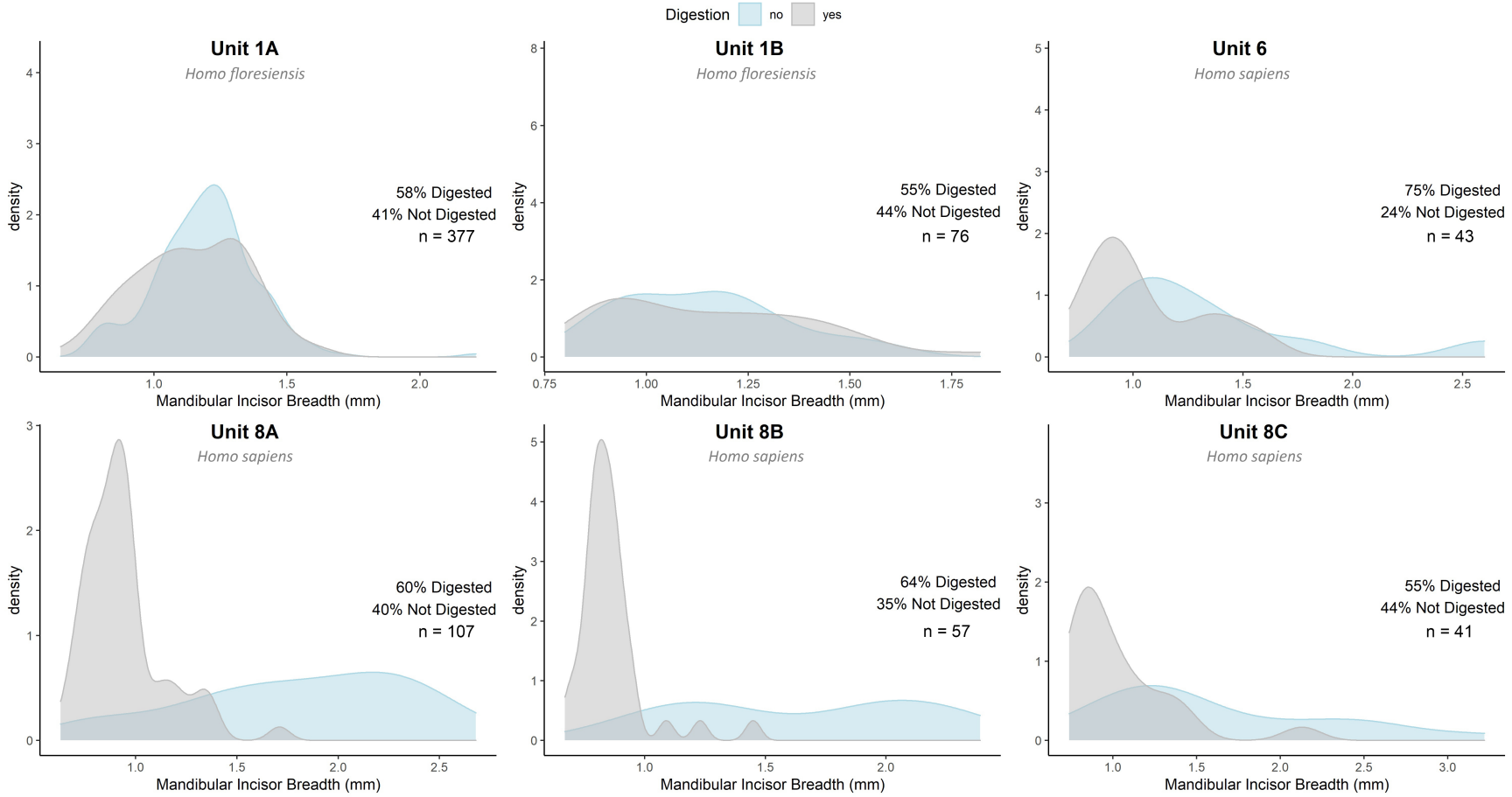

Figure 6.26: Summed density plots showing the presence (grey) and absence (blue) of digestion identified on murine mandibular incisors according to stratigraphic unit and element size (incisor breadth). The total number of incisors as well as the percentages of digested and none-digested incisors for each stratigraphic unit are also displayed.

6.4.3 A taphotype comparison between stratigraphic units

The taphonomy of small mammals at Liang Bua provides important insights into both raptors and hominins as accumulating agents of murine remains at the site through time. A correspondence analysis used a combination of taphonomic variables related to avian and hominin predation between all stratigraphic units to explore how these differences in predatory activity affect the spatial relationship between and within units simultaneously (Figure 6.27). When considering all variables, units associated with *H. floresiensis* (1A and 1B) cluster on the most negative end of axis 1, which explains 93.4% of the observed variance (Figure 6.27 – A). These deposits contain a relatively greater amount of size 2 murines, digested bone, and specimen abundance compared to units associated with *H. sapiens* (6 and 8A – 8C). Unit 6 plots between the *H. floresiensis* and *H. sapiens* cluster along axis 1, while Units 8A – 8C plot towards the positive end. These changes are largely driven by burning activity observe in Units 8A – 8C, as well as a greater representation of size 1 and size 3+ murines, cutmark frequency, and bones with no digestion. Since burning is restricted to units associated with *H. sapiens*, another correspondence analysis was run without it to remove this bias (Figure 6.27 – B). When removed, *H. floresiensis* and *H. sapiens* units retain similar clusters, suggesting that other taphonomic variables contribute to and explain group separation independent of burning.

A third correspondence analysis using variables related to human activity, such as cutmark frequency, bones with no digestion, and burning patterns, was run to determine how signals of human activity contribute to unit separation (Figure 6.27 – C). Units 8A – 8C cluster towards the positive end of axis 1 (85.1%) with Unit 8B plotting along the negative end of axis 2 (10.8%) due to higher frequency of cutmarks. Unit 6, a unit associated with *H. sapiens*, plots more in line with units associated with *H. floresiensis* (1A and 1B) due to a reduced frequency of cutmarks and burning damage. Behaviorally, Unit 6 appears more like Units 1A and 1B, suggesting either

1) that *H. sapiens* foragers utilized the cave and consumed local murine fauna in a similar pattern as *H. floresiensis*, or 2) sediments and materials within Unit 6 include reworked sediments and materials from Unit 1B (see discussion below).

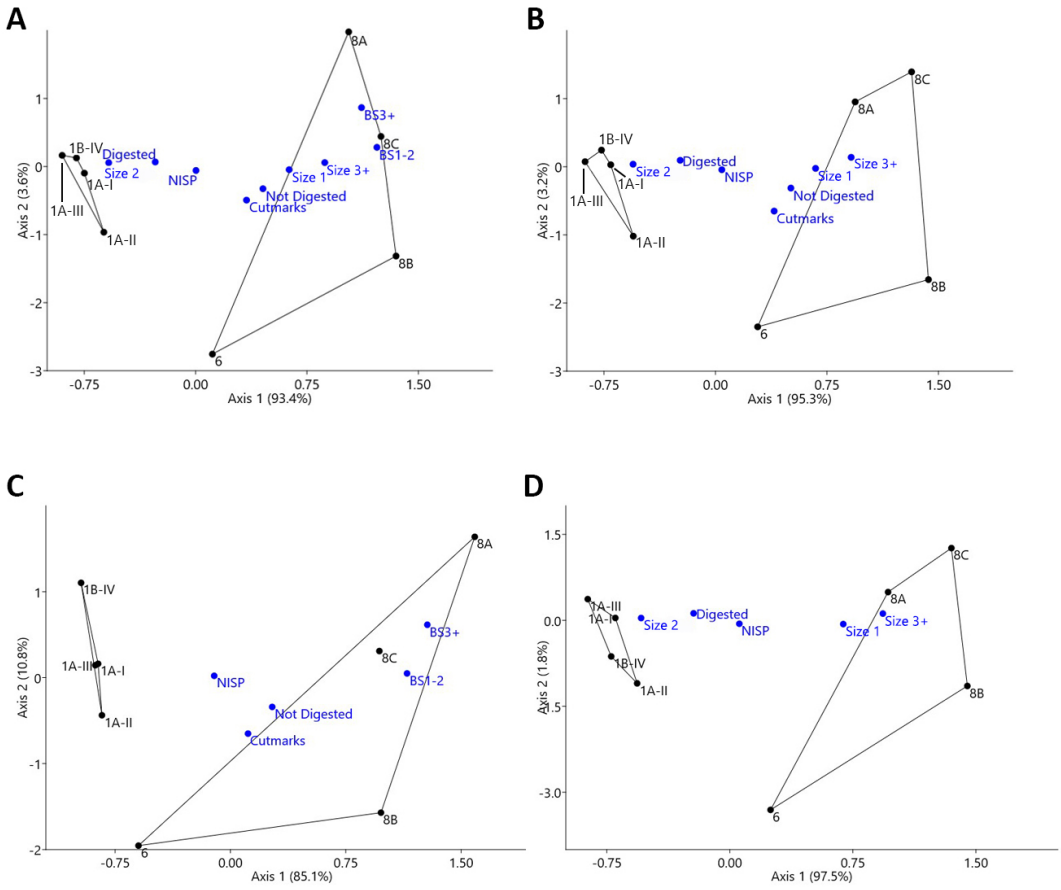

Figure 6.27: Correspondence analysis showing clusters of stratigraphic units associated with *H. floresiensis* (Units 1A – 1B) and *H. sapiens* (Units 6 – 8) using taphonomic and zooarchaeological variables, including NISP ("NISP'), digestion on humeri ("Not digested" and "Digested"), body size element frequency ("Size 1", "Size 2", and "Size 3+" to represent elements identified as size 3, size 4, and size 5), cutmark frequency ("Cutmarks"), and burning stages ("BS1-2" = burning stages 1 and 2, and "BS3+" = burning stages 3, 4, and 5). Analyses were run using a combination of variables, including: (A) All variables; (B) All variables minus burning stages; (C) NISP and variables indicating human modification only (i.e., cutmarks, burning stages, and undigested bone); (D) NISP and variables indicating avian modification only (i.e., digested bone and body size categories). Variance explained by the first and second axes are shown along with variable weighted variance included in the plotted space in blue.

A fourth correspondence analysis using variables related to avian activity, such as murine body size and digestion, was run to determine how signals of avian activity contribute to unit separation (Figure 6.27 – D). Results from this analysis are similar to previous results with Units 1A and 1B clustering negatively along axis 1 (97.5%) while Units 8A – 8C cluster towards the positive end, and Unit 6 plots between these two groups but more negatively along axis 2 (1.8%). Units 1A and 1B are dominated by both size 2 murines and a greater abundance of digested bone relative to Units 8A – 8C causing the separation between these two groups.

6.4.4 Taphonomy of small mammals through time

A synopsis of taphonomic and zooarchaeological results is provided below to broadly summarize the depositional context, taphonomic results, and avian and hominin predatory activity for each stratigraphic unit. A table summarizing the taphonomic and zooarchaeological results is shown in Table 6.17. Data from Chapter 5 are also included where appropriate to provide an ecological context using the most recent stable isotope datasets.

Occupation | Environment	*H. sapiens* | More-closed / Mixed / Wet				*H. floresiensis* | More-open / Dry			
Units	8C	8B	8A	6	1B-IV	1A-III	1A-II	1A-I
Accumulations Rates								
MNI per m^3	16	40	7	15	2100	197	12	12
Taxonomic represention								
Simpson's Diveristy Index	0.84	0.83	0.82	0.78	0.22	0.05	0.24	0.23
Murine Body Size								
MNI size 1|2|3|4|5								
Fragmentation								
NISP/MNE excluding compact bones and teeth	1.36	1.49	1.51	1.44	1.53	1.52	2.34	2.02
Long bone breakage patterns								
Pre-dep|post-dep|recent								
Weathering								
%Stage 1	25.5%	38.3%	41%	45.2%	33.7%	47.9%	19.4%	21.7%
%>Stage 1	5.9%	2.6%	6.5%	6.2%	8.6%	9.5%	20.6%	14.7%
Manganese Staining								
%Stage 1	26%	18.8%	31.5%	46.5%	50.7%	57.1%	48.5%	53.9%
%>Stage 1	6.6%	8.8%	11.5%	20.7%	20.8%	28.7%	38.2%	32.6%
Burning								
%Stage 1	18.5%	13.2%	16.2%	0%	0%	0%	0%	0%
%>Stage 1	12.6%	6.5%	6.3%	0.4%	0%	0%	0%	0%
Murine Age Profiles								
%Young|%Adult|%Old Adult								
Avian Digestion								
% Incisor digestion	66%	82.5%	74.7%	77.4%	56.2%	63.7%	45.9%	37.6%
Predator category	category 1	category 1-2	category 1	category 1-2	category 0b-1	category 1	category 0b	category 0b
Anthropogenic BSM								
Murine body sizes w/ cutmarks	Size 1, 4, 5 0.7%	Size 1 - 5, Indet. 1.7%	Size 1, Indet. 0.2%	Size 5, Indet. 0.3%	Size Indet. 0.2%	Size 2, 5, Indet. 0.5%	Size 2, Indet. 0.9%	Size 2, 5, Indet. 0.6%
Non-anthropogenic BSM								
% Insect	8%	1%	14%	80%	91%	78%	0%	4%

Table 6.17: Summary of zooarchaeological and taphonomic results according to hominin occupation, environment, and stratigraphic unit.

***H. floresiensis* units:**

Units 1A-I and 1A-II (>120 ka): The lower levels of stratigraphic Unit 1A – defined by an as yet undated gravel-rich layer and underlying layers of mixed clay and grey tuff fragments – contain the oldest deposits excavated from Sector XI (Sutikna, 2016; Sutikna et al., 2016; Morwood et al., 2005). The taphonomic and zooarchaeological signature of these two units are comparable suggesting that these sedimentary layers represent similar contexts (Table 6.17). Among these similarities include relatively low accumulation rates, uneven taxonomic representation, high degrees of fragmentation, greater weathering damage and manganese staining, and extremely low amounts of insect damage compared to other units associated with *H. floresiensis*. These results are broadly in agreement with previous studies where Unit 1A was hypothesized to be more-open and dry based on the relative abundance of murine body sizes (Veatch et al., 2019). Stable isotope values now also confirm that the local environment at the time was a combination of a more-open and dry environment with patches of nearby tree cover (see Chapter 5).

A previous spatio-temporal distribution analysis on all faunal abundances in Unit 1A estimated that 93.6% of identified skeletal elements were murine (Sutikna et al., 2018). If we assume that the digestive profiles of Units 1A-I and 1A-II represent avian assemblages, then the majority of these remains were likely deposited by a category 0a raptor based on extremely light digestive damage, such as the common barn owl (*Tyto* sp.) (Andrews, 1990). According to Meijer et al. (2013), barn owls were present in the Middle and Late Pleistocene deposits in Sector XI and may have been slightly larger in body size compared to extant species. Their generalist diet also tends to reflect the most naturally abundant prey items (ranging up to ~300 g) and are well known to forage in more-open landscapes that facilitate a specific hunting style involving low and long glides over open terrain (Andrews, 1990). Due to their high-metabolic rates, barn owls also tend to hunt more frequently, and consume

more rodents compared to other owls of similar body sizes (Marti, 1973). Eagles (*Aquila* sp.), kites (*Haliastur* cf. *indus*), and diurnal raptors (*Accipiter* sp.) were also identified in the Late Pleistocene deposits at Liang Bua (Meijer et al., 2013), but these raptors would have caused heavy digestive damage to the skeletons of their prey and only a few fragments contained heavy levels of digestive damage from these units (Figure 6.15). It is therefore likely that *Tyto* sp. and/or a combination of other unidentified owls were the main contributor(s) of size 1, size 2, and some size 3 murines in Unit 1A-I and 1A-II, with a much smaller contribution by eagles and/or diurnal raptors.

Cutmarks and human tooth marks on size 2 and size 5 murine fragments provide evidence that raptors were not the sole contributor of small mammals at Liang Bua (Figures 6.19 and 6.22). Unfortunately, surface corrosion, likely from the surrounding sediment, caused extensive surface flaking and chipping that made identification of marks difficult (Appendix E). However, a size 5 murine humerus with clear evidence of cutmarks and an attempt to extract bone marrow is thus far the oldest evidence of *H. floresiensis* consuming giant rats (*Papagomys* sp.) at Liang Bua. Given the enriched d13C values of size 2 murines during this time (see Chapter 5), it is likely that *H. floresiensis* foraged for medium sized murines (size 2) within more-open environments. Size 5 murines showed a range of d13C values extending from a true C4 diet to a mixed diet – a result that contradicts what is currently known about *Papagomys* sp. behavior. It is likely that while *Papagomys* sp. were consuming more grasses they probably lived within the patches of tree cover as is observed today. Thus, whether *H. floresiensis* foraged for the giant rats in the open grasslands or in the nearby shrublands is inconclusive.

Unit 1A-III (>120 ka): Sediment accumulated above the Unit 1A-II gravel-rich layer and under the Unit 1B-IV gravel-rich layer dated to ~120 ka represents the upper level of Unit 1A (Sutikna, 2016; Sutikna et al., 2016). Murine accumulation

rates relative to sediment accumulation substantially increased compared to Units 1A-I and 1A-II (Table 6.17). While only two out of twelve spits were sampled from this unit (spits 74 and 68), differences in the relative abundance between these two spits suggests that the increased accumulation of murine elements was gradual with a low degree of fragmentation relative to underlying units. Alternatively, increased accumulation near the top of Unit 1A-III could also be the result of reworked bone from the highly dense Unit 1B-IV immediately above (Table 6.17). Insect activity also significantly increases suggesting a local ecological change around Liang Bua, potentially from a change in humidity or micro-faunal habitats. However, d13C and d18O values from Units 1A-III, 1A-II, and 1A-I suggest similar environmental conditions (See Chapter 5) that otherwise may have explained the change in insect activity.

Digestive damage on murine incisors suggest a category 0b predator and/or a combination of raptors that caused slightly greater digestive damage compared to Units 1A-II and 1A-I. This slightly greater damage is likely the product of multiple avian species, including mostly owls (none to light damage) and occasional diurnal raptors (medium to extreme damage), that were likely the main accumulating agents in Unit 1A-III. Evidence of human butchery in the form of cutmarks were identified on primarily size 2 and size 5 murine elements indicating that *H. floresiensis* continued to forage for and consume murines from more-open habitats and possibly from nearby forested patches as well (Table 6.17).

Unit 1B-IV (~120 – 60 ka): Unit 1B-IV includes the lower of two levels identified within Unit 1B, which and is capped by both T1 and T2 (Sutikna, 2016; Sutikna et al., 2016). Murine accumulation rates peak at an estimated 2,100 MNI per m^3—{~11 times the rate from Unit 1A-III—and is consistent with previous faunal accumulation patterns (Sutikna et al., 2016, 2018; Veatch et al., 2019). This increase is first observed in the upper portions of Unit 1A-III but increases substantially in Unit 1B-IV creating a thick and dense layer of bone. Low degrees of weathering

damage, manganese staining, fragmentation rates, and a high amount of insect activity are very similar to those observed in Unit 1A-III, but 1B-IV contains a greater diversity of murine taxa suggesting a change in predator activity and/or environment relative to other taphonomic processes affecting these units. Overall, the taphonomy of Units 1A-III and 1B-IV are more similar to each other than to Units 1A-II and 1A-I independent of human and/or avian activity. Since only one of thirteen spits was sampled to represent Unit 1B-IV, additional sampling of the remaining spits is needed to further explore the taphonomic differences observed between this unit and the underlying units.

Unit 1B contains a clear association of *Stegodon*, Marabou stork, vulture, Komodo dragon, and *H. floresiensis* remains suggesting a type of interdependency existed between a sole large herbivore and a scavenging guild of avian, reptilian, and hominin predators at this time (Sutikna, 2016; Sutikna et al., 2016, 2018; van den Bergh et al., 2009). Unit 1B also contains the only skeletal elements identified to *H. floresiensis* while stone artifacts attributed to *H. floresiensis* are present within Unit 1A (and Unit 2) but accumulated at a much lower rate (80 NISP) compared to Unit 1B (4,308 NISP) (Sutikna et al., 2018). This could reflect either population densities, mobility patterns, or foraging preferences during different temporal intervals. For example, the relatively greater abundance of cutmarked murine elements in Unit 1A (0.5 - 0.9 all levels) compared to Unit 1B (0.2), in combination with the relative abundance of other larger-bodied faunal remains in Unit 1B, could reflect a difference in hominin foraging patterns between these two units. However, it is difficult to ascertain the degree of hominin predation on small mammals in Unit 1B compared to Unit 1A since only one out of thirteen spits were sampled from Unit 1B-IV in this study. Additional spit samples within this unit are needed to further explore hominin foraging patterns between these two units.

***H. sapiens* units:**

Unit 6 (~18 – 13 ka): Sediments accumulating unconformably above T1 and T2, as well as the eroded upper surface of Unit 1B but beneath T7, represent Unit 6 in Sector XI. Murine accumulation rates are low but with a noticeable increase in species richness compared to Units 1A and 1B, but still heavily represented by size 2 and size 1 murine body size categories. Fragmentation rates are moderate with similar degrees of low weathering damage and manganese staining, as well as a high degree of insect activity compared to Units 1B-IV and 1A-III (Table 6.17).

In Unit 6, avian digestive patterns reveal an increase in heavier degrees of damage in comparison to Units 1A and 1B (Figure 6.15). In these preceding units, the majority of damage was either "none" or "very light" while Unit 6 contains a large quantity of size 1 incisors with damage from the "light" and "moderate" categories. As a whole, this pattern of relatively more intense digestive damage could suggest a possible turnover in the avian population within Unit 6 (~18 – 13 ka) compared to Unit 1B (~120 – 60 ka) where eagles and/or other raptors are more active at Liang Bua from ~18 – 13 ka (but see Section 6.4.2).

H. sapiens foraging patterns within Unit 6 is ambiguous. One tibia with an unknown body size category shows evidence of butchery while a size 5 murine collected from Sector XXVI suggests that *H. sapiens* also consumed giant rats during this time. However, the small amount of sediment representing Unit 6 in sector XI sampled here in comparison to what is available from other sectors at Liang Bua may not accurately represent the full range of human activity within this unit, and this is further complicated by the possibility that some material has been reworked from Unit 2 in the southernmost portions of this sector. For example, evidence of intentional fire-use first appears at Liang Bua at ~46 ka (Unit 4) suggesting that fire-use was part of *H. sapiens* foraging repertoire at Liang Bua well before ~18 ka (Morley et al., 2017). Within Sector XI, the first occurrence of burnt bone appears in Unit 6 (Units

4 and 5 are not represented in sector XI) in extremely low frequencies (n = 1). The lack of burnt bone in Unit 6 could be the result of forager mobility, but the volume of material representing Unit 6 in Sector XI was likely too small of a sample to capture this behavior in more detail.

An alternative explanation could be that the environment around Liang Bua did not support populations of foragers, who instead frequented other locations around Flores. Paleoenvironmental data indicate that Unit 6 had an increase in rainfall and transitioned from more-open landscapes to a wetter climate with expanding montane and lowland forest fauna (Westaway et al., 2009c,b,a). Murine body size frequencies are also consistent with previous body sizes estimates for Unit 6, where size 1 and size 2 murines are most abundant with ~25% consisting of size 3 and larger-bodied murines (Veatch et al., 2019). Thus, during a time of environmental change, foraging *H. sapiens* may have preferred other locations until the return of the monsoons and more-forested adapted larger-bodied murines as observed in Unit 8A (Veatch et al., 2019; Sutikna et al., 2018; Westaway et al., 2009c,b,a). Moreover, Unit 6 in Sector XI was formed along a sloping surface while the surface in Unit 8A was more flat making it more ideal of a location for building and maintaining fires. This, along with the environmental changes, may explain the taphonomic differences observed between these two units.

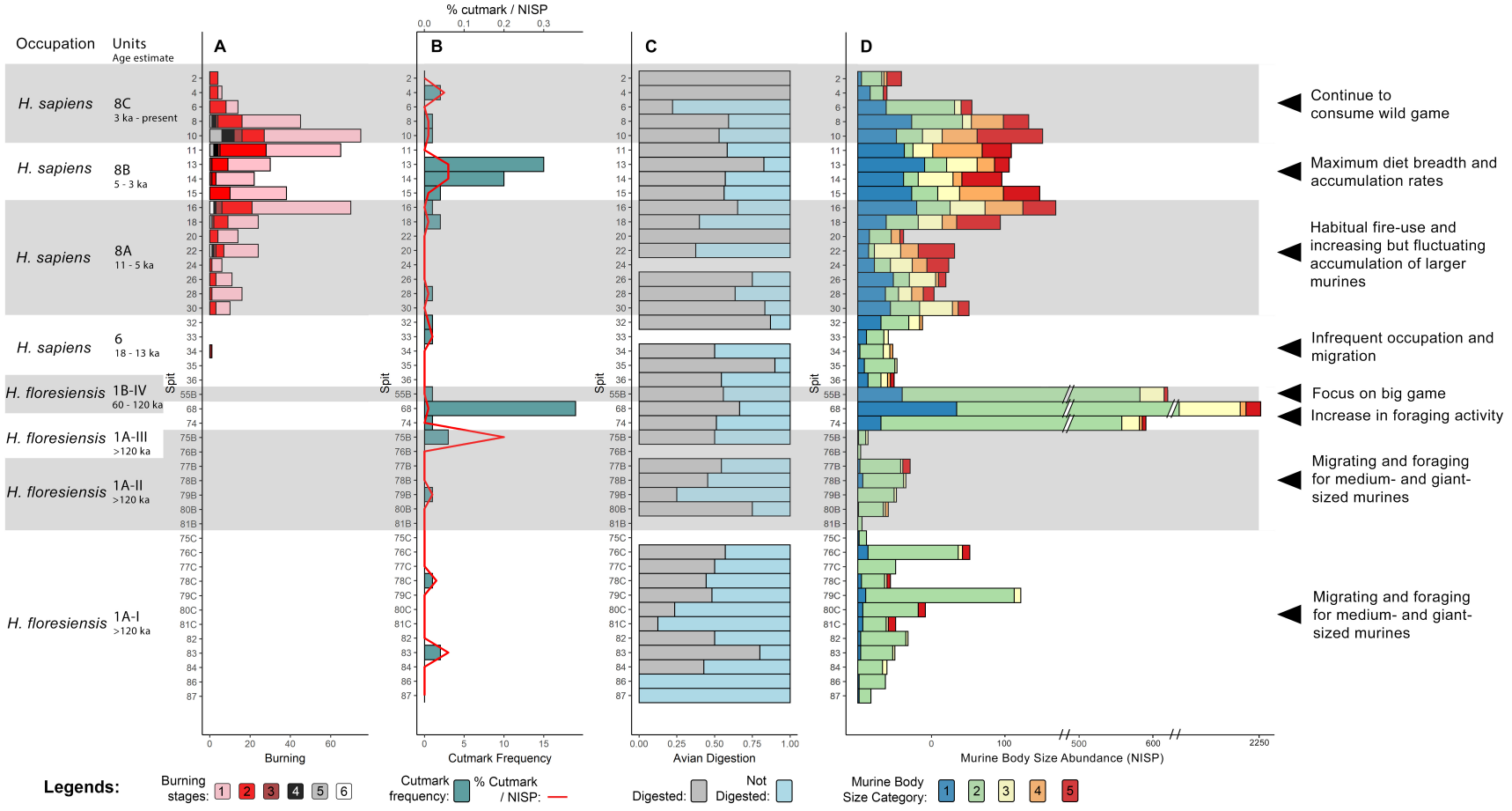

Figure 6.28: Interpretation of hominin activity according to unit with (A) burning patterns, (B) cutmark frequencies, (C) digestive damage, and (D) relative abundance of murine body size categories according to units (grey and white horizontal bars) and spits (y axis) sampled from Sector XI.

Unit 8A (~11 – 5 ka): Sediment accumulating above T8 with a date range between ~11 – 5 ka cal. BP represent Unit 8A (Sutikna, 2016; Sutikna et al., 2016, 2018). This unit contains the lowest murine accumulation rates compared to all other units but with a slightly more even representation of murine species. Fragmentation rates are moderate with very low degrees of weathering damage and manganese staining. Insect activity also decreases substantially from 80% in Unit 6 to 14% in Unit 8A. Like Unit 6, greater degrees of digestion suggest raptors with slightly more digestive damage to murine incisors were selecting primarily size 1 murines (with a small amount of size 2) from a mixed environment. An increase in diurnal raptor activity is also supported by an increase in raptor punctures from the beak and/or talons – features frequently observed in diurnal raptor pellets (Armstrong, 2015).

Unlike Unit 6, fire-use is ubiquitous throughout all layers of Unit 8A with fluctuations of burning intensities (Figure 6.28). All but one element reflected patterning indicative of tangential burning with non-localized intensities (i.e., elements located below (~80% category 1) or within (categories 3 – 5) a fire feature) (Rhodes et al., 2016). The one element that did show signs of processing through burning (i.e., for consumption) was a size 5 incisor (likely the shrew-rat based on size and morphology) (Figure 6.14). Experimental studies involved with roasting small mammals indicate that intentional or direct exposure to fire results in highly localized areas with little to no muscle tissue (Henshilwood, 1997), such as the incisor from Unit 8A illustrated in Figure 6.14.

Along with the increase in relative abundance of size 3 – 5 murines and cut-marks identified on both size 5 and size 1 murine elements, foraging *H. sapiens* were likely targeting more locally abundant murines as the climate shifted to a wet and organically-rich environment resulting in an increase in humid forests (Westaway et al., 2009c,b,a). Previous faunal abundances also show a slight increase in aquatic and terrestrial invertebrates (0.6% and 1.1%) and fish (0.6%) possibly indicating that

foraging *H. sapiens* began to diversify their diet in other ways compared to previous units (Sutikna et al., 2018). Together with the increase in murine species and body size diversity, cutmark frequency, and the first appearance of pigs (*Sus celebensis*) at ~7 ka towards the upper part of Unit 8A suggest that humans began to diversity their diet during the mid-Holocene (Sutikna et al., 2018).

Unit 8B (~5 – 3 ka): Unit 8B is defined by a noticeable change in faunal abundances between 5 and 3 ka, including a significant increase in fish (1.2%), frogs (22.4%), varanids (1.4%), and largely freshwater mollusks (19.9%) relative to other faunal groups (Sutikna, 2016; Sutikna et al., 2016, 2018). An introduction of other non-endemic animals also appears starting ~3 ka (Sutikna et al., 2018, 2020). Murine accumulation rates increased substantially compared to the preceding units while maintaining a moderate fragmentation rate and high species diversity, potentially indicating an increase in human population size, activity and/or sedentism. Frequencies of weathering damage, manganese staining, and insect activity are also reduced compared to preceding units.

Prior to adopting a sedentary lifestyle, humans began to expand their diet by incorporating a diverse range of murine species and body sizes compared to previous units (Figure 6.28). Unit 8B has the highest rates of cutmarks and the frequency of cutmarked bone relative to total murine NISP compared to all other units, indicating that *H. sapiens* incorporated a diverse range of murines of all body sizes while also increasing murine accumulation rates starting in the upper end of Unit 8A through Unit 8B. This expansion of diet breath, as well as intense harvest of freshwater shellfish, is consistent with other regions of the world prior to the adaptation of agriculture (Munro, 2004).

Unit 8C (~3 ka – present): This unit is defined by the earliest occurrences of pottery and includes multiple intentional burials with grave goods (Sutikna et al., 2018; Julianto et al., 2020). Beginning ~3 ka, humans adopted a sedentary lifestyle

and relied on agricultural and domesticated resources introduced to Flores, probably part of an Austronesian expansion into Southeast Asia (Sutikna, 2016; Sutikna et al., 2016, 2018; Morwood et al., 2009). In Unit 8C, the relative abundance of murines and fire-use decreased within this unit reflecting a transition in land-use due to agricultural activities. Cutmark frequencies also decreased in comparison to Unit 8B but maintained a relatively high rate of cutmarked bone (0.7 %) indicating that agriculturalists continued to consume murines of various body sizes (elements of size 1, 4, and 5 identified with cutmarks) after the uptake of food production. An increase in size 2 murines is also consistent with previous faunal studies indicating an expansion of C4 and C3 agricultural resources, such as millet and rice, respectively (Veatch et al., 2019; Sutikna et al., 2018).

6.5 Conclusion

The taphonomy of murine skeletal elements provides important insights into the foraging behaviors of *H. floresiensis* and *H. sapiens* (foraging and agriculturalists) at Liang Bua. These results highlight how Liang Bua was co-utilized by raptors and hominins through time, and how the availability of local small mammals affected land-use and mobility patterns. Moreover, these results reveal evidence of small mammal exploitation by *H. floresiensis* without the aide of complex technologies, and that *H. floresiensis* was exploiting murines from more-open environments. An absence of evidence of fire-use during temporal units associated with *H. floresiensis* suggests that fire was restricted to *H. sapiens*. Foraging *H. sapiens* also engaged in and preferred exploiting more-forested resources similar to that observed in other Late Pleistocene human foraging communities in Southeast Asia, such as at Lida Ajer in Sumatra (Louys and Meijaard, 2010), Niah Cave in Borneo (Piper et al., 2008), and Yuku from Papua New Guinea (Gaffney et al., 2021). Lastly, acquisition of smaller animals

continued after *H. sapiens* populations in the area adopted a sedentary lifestyle, and this continues today as a cultural tradition among the Manggarai in western Flores (see Chapter 4).

Chapter 7

Dissertation Conclusions

This dissertation aimed to understand the role of small mammals as a dietary resource for *Homo floresiensis* and *Homo sapiens* at Liang Bua, Flores, Indonesia. To accomplish this, murine rodent skeletal remains were sampled from non-overlapping stratigraphic units representing *H. floresiensis* (Units 1A and 1B) and *H. sapiens* (foragers: Units 6, 8A, and 8B; farmers: Unit 8C) and subjected to taphonomic analysis. Carbon and oxygen stable isotope analysis was also conducted using carbonate samples from murine bones and teeth sampled from units representing *H. floresiensis* (Units 1A, 1B, and 2) and *H. sapiens* (foragers: Units 4, 6, 8A, and 8B; farmers: Unit 8C) to establish the paleoecological context for each unit. To better assess the murine faunal assemblage at Liang Bua, taphonomic and zooarchaeological considerations for human and raptor accumulators were examined using ethnoarchaeological and experimental studies. Theoretical approaches to interpreting hominin behavior were also explored. To this end, I addressed these questions:

1. How can theoretical frameworks like niche construction theory contribute to our understanding of hominin foraging behaviors?

2. What are the defining features that distinguish between human and avian agents within a small mammal faunal assemblage?

3. Are the murine rodent skeletal remains from the Middle to Late Pleistocene and Holocene deposits at Liang Bua the result of human or avian agents, or a mixture of both?

4. How do the foraging strategies employed by *H. floresiensis* (~190 – 60 ka) and *H. sapiens* (~18 ka – present) compare with one another and how do any similarities or differences in behavior relate to the specific environmental and ecological contexts of these temporal intervals?

Each of these questions have been addressed, yielding important theoretical and methodological considerations for interpreting hominin subsistence on small mammals in the past. Moreover, this dissertation provided new insights into the dietary behavior for *H. floresiensis* and *H. sapiens* at Liang Bua that have important insight into the behavioral differences between these two hominins (Table 7.1). The remainder of this chapter summarizes and discusses the broader implications of this research and how this can inform future research directions at Liang Bua.

7.1 Hominin foraging behavior at Liang Bua

7.1.1 *H. floresiensis* (~190 – 60 ka):

Hominin and avian agents co-accumulated the murine faunal assemblage in Units 1A and 1B at Liang Bua, thereby, rejecting the null and first alternative hypotheses. Zooarchaeological and taphonomic results indicate that *H. floresiensis* consumed primarily size 2 (*Komodomys* cf. *rintjanus*; ~300 g) and size 5 (*Papagomys armandvillei*; ~2.5 kg) murines while raptors selected primarily size 2 murines—an optimal prey body size for owls. Since carbon stable isotope ratios for size 2 murines show a narrow and more specialized C4 diet—and are known to inhabit more-open environments today—it is likely that *H. floresiensis* and owls acquired size 2 murines within these more-open ecosystems (Musser, 1981). Conversely, carbon stable isotope ratios for

size 5 murines show a more eclectic foraging behavior where some individuals showed a preference for more C3 versus C4 resources but likely inhabited more-closed environments if possible—much like they do today—indicating that *H. floresiensis* exploited murines from both of these habitats. Thus, this data somewhat supports the second alternative hypothesis—which stated that *H. floresiensis* incorporated high ranking small mammals (i.e., size 5 murines) into their diets using simple technology in order to reduce niche overlap with other scavenging predators—and suggests that *H. floresiensis* was not selecting murines based on individual prey body size, but potentially based on availability and proximity to Liang Bua.

Zooarchaeological differences between Units 1A and 1B also suggest a functional change in the local ecology surrounding Liang Bua with important implications for hominin foraging behavior. While no dietary shifts were detected using carbon stable isotopes among murine species in Units 1A and 1B, changes in species richness between these two units (Simpson's Diversity Index for Unit 1A: 0.12 for all faunal groups, and 0.13 for murine species; Unit 1B: 0.25 for all faunal groups, and 0.22 for murine species) suggests a change in habitat heterogeneity at ~120 ka (Sutikna et al., 2018; Barr and Biernat, 2020). In other words, Liang Bua was likely exposed to a more homogeneous open landscape in Unit 1A where *H. floresiensis* relied on the resources provided by grasslands, such as size 2 murines, while a slight increase of habitat patches in Unit 1B resulted in a potential change in hominin foraging decisions where hominins chose to consume other prey items in lieu of murines. However, the small sample size in Unit 1B warrants additional sampling to determine the relative frequencies of anthropogenic and avian damage compared to Unit 1A. Moreover, additional taphonomic analyses of other faunal groups, such as *Stegodon*, from these units is needed to determine if *H. floresiensis* sought after other mammals in addition to or in replace of murines.

A large anthropogenic pit identified on a size 5 murine humerus suggests that *H.*

floresiensis may have attempted to extract marrow from a giant rat bone. While this behavior is observed in the Upper Paleolithic in Eurasia, extracting marrow from smaller animals in the hominin fossil record is less well documented, possibly due to the range of approaches for consuming marrow from small mammals (Rosado-Méndez et al., 2019; Yellen, 1991a). This is not surprising given that the techniques used by modern foraging groups to extract marrow from smaller animals can leave little to no trace of this behavior on the bones themselves (Yellen, 1991a). Also, given the importance of marrow in the hominin diet, it may not be surprising that *H. floresiensis* sought this resource from animals that were readily available.

Overall, it is clear that *H. floresiensis* selected murines in proportion to the dominant environment. There is so far no evidence that *H. floresiensis* transported murines from other locations on Flores, as they were likely captured locally as a reliable and potentially daily food source surrounding Liang Bua. It is also unlikely that *H. floresiensis* used traps or other complex technologies to capture murines. Based on ethnographic data, murines do not require specialized or complex technologies to successfully capture them if the hunter understands the animals behavior and habits —although individuals living around Liang Bua today choose to capture murines using traps and dogs, a tool as simple as a stick is just as efficient. With no evidence of fire-use, *H. floresiensis* also likely used stone tools to skin and disarticulate their prey based on the location of cutmarks on murine skeletal elements to aide in food processing. Together, this suggests that smaller animals were likely captured and consumed by *H. floresiensis* with ease using knowledge about murine behavior and habits.

7.1.2 *H. sapiens* (~18 ka to present):

Similar to the preceding units, hominin and avian agents co-accumulated the murine faunal assemblage in Units 6 through 8C at Liang Bua. Zooarchaeological and tapho-

nomic results indicate that the foraging and subsistence behaviors of *H. sapiens* are noticeably different compared to *H. floresiensis*. For example, fire-use and human activity inferred through burning and cutmark frequencies from Unit 6 in Sector XI are extremely low suggesting low population densities and/or frequent migrations by *H. sapiens*. However, charcoal samples and stone artifacts recovered within Unit 6 from other sectors suggest that Sector XI may not represent Unit 6 as well as other sectors (e.g., evidence of fire-use first appears in the stratigraphic sequence at ~41 ka) and requires additional sampling to estimate the degree to which humans utilized the cave within this unit (Sutikna et al., 2018; Morley et al., 2017).

Evidence of habitual fire-use is more noticeable in Unit 8A from Sector XI as well as the relative abundance of larger-sized murines suggesting a gradual increase of human activity in the cave with a noticeable peak at ~3 ka corresponding to the introduction of pottery (Sutikna et al., 2018). A large percentage of cutmarked bone associated with more-closed adapted murines suggest that foraging *H. sapiens* were utilizing forested, or more-closed, resources. This foraging strategy is similarly observed in Sri Lanka (Roberts et al., 2015a, 2017), Papua New Guinea (Gaffney et al., 2021; Gaffney, 2021), Sumatra (Louys and Meijaard, 2010), and Borneo (Barker et al., 2009) suggesting that foraging *H. sapiens* dispersing through Southern Asia into Southeast Asia likely relied on forested resources—a habitat previously thought to have been under exploited by Paleolithic foragers (Roberts and Petraglia, 2015). Moreover, foraging *H. sapiens* consumed murines in proportion to the dominant environment during the time of occupation, similar to *H. floresiensis*. In other words, there is no evidence that foraging *H. sapiens* collected murines from other locations, and were instead consuming more local and giant body-sized murines living around Liang Bua. Thus, this data somewhat supports the third alternative hypothesis—which stated that modern human foragers incorporated rats of various body sizes into their diets using technologies unavailable to *H. floresiensis*—and suggests that foraging *H. sapi-*

ens were targeting murines based on individual prey body size as well as availability and proximity to Liang Bua.

Between ~5 and 3 ka, humans began to consume murines of all other body sizes. This expansion of diet breadth—coupled with intensified shellfish harvesting—may indicate that other biodegradable technologies (i.e., nets, snares, traps) were used to collect these additional resources. Moreover, the concomitant increase in cutmark frequency, cutmarked murine body sizes, and other resources, such as shellfish, is consistent with an expanding diet prior to adopting agriculture and transitioning to a sedentary lifestyle. This time period more adequately supports the third alternative hypothesis, and shows a change of foraging goals for *H. sapiens* that likely are the result of population increases and/or reduction in mobility. Finally, the presence of cutmarks on large to giant-bodied size murines soon after ~3 ka suggest that humans continued to forage for endemic murines after the transition to farming—much as they do today. This supports the fourth alternative hypothesis—which stated that as agricultural practices emerged, agriculturalists continued to incorporate higher ranking giant murines into their diet but at a lower frequency compared to foragers—and suggests that agriculturalists were targeting murines based on individual prey body size as well as availability and proximity to Liang Bua. However, the disappearance of some of the larger-bodied murines, such as *Hooijeromys nusatenggara, Spelaeomys florensis*, and *Papagomys theodorverhoeveni*, may be due to over hunting by *H. sapiens* while transitioning to farming practices, and thus, were no longer available as a food resource.

7.1.3 Broader Implications

Hominin consumption of small mammals at Liang Bua provides important insight into human behavior in the past, as well as the role of smaller animals within hominin diets (Table 7.1). For example, both *H. floresiensis* and *H. sapiens* consumed

Table 7.1: Summary of behavioral differences between *H. floresiensis* and *H. sapiens*.

Homo floresiensis	*Homo sapiens*
– No evidence of fire-use	– Evidence of fire-use
– Direct evidence for consuming medium (300 g) and giant (2.5 kg) sized rats	– Direct evidence for consuming mostly larger bodied (>600 g) rats and some small (50 g) sized rats
– Processing included skinning and disarticulation of animals with stone tools	– Processing included disarticulation of animals with stone tools
– Evidence they exploited more open habitats	– Evidence they exploited more forested habitats
– Selected murines in their proportion to the environment	– Selected a wider range of murines prior to adopting agriculture
– Possible marrow extraction	– Marrow consumption inconclusive

murines that were more readily available during different temporal periods and environmental contexts. This suggests that murines were probably a reliable source of animal nutrients for both hominins given their relative ecological setting, even when larger animals, like *Stegodon*, were available in the case of *H. floresiensis*. Moreover, this similarity suggests that the relationship between hominin brain size and/or neurological complexity and the ability to capture small mammals is more complicated than had previously been assumed (Wynn and Coolidge, 2008; Conard et al., 2013). Although, while it is clear that both *H. sapiens* and *H. floresiensis* consumed small mammals, variation in the techniques used to capture and process them provides additional insight into their behavioral repertoire.

There are also notable differences in hominin foraging of small mammals at Liang Bua that highlight important behavioral distinctions in how *H. sapiens* and *H. floresiensis* interacted with their environment. Specifically, *H. sapiens* engaged in multiple forms of niche construction, including inceptive, perturbational, and counteractive forms of modification in order to forage for and process small game (Laland and O'Brien, 2010; Odling-Smee et al., 2003). For example, the use of fire to cook small-bodied prey and dismember them using stone artifacts made primarily from a

non-local raw material (e.g., chert) are prime examples of *H. sapiens* using inceptive and perturbation to initiate change to their current environment (Sutikna et al., 2018). Moreover, exploiting numerous murines from diverse ecologies, in addition to more local environments, is also demonstrative of the generalist-specialist ecological niche where, unlike other hominins, *H. sapiens* specialized in adaptations for living and foraging in a wide range of ecological zones (Roberts and Stewart, 2018). Additional taphonomic and zooarchaeological studies using other faunal groups will shed further light on how humans adapted to environments surrounding Liang Bua in addition to the murine assemblage. For example, isotopic data from Unit 4 suggests that the environment was still primarily open around Liang Bua, but a noticeable increase in megabat and micobat in this small unit may further indicate that *H. sapiens* were sourcing a wide array of resources from non-local environments (Sutikna et al., 2018).

Conversely, *H. floresiensis* seems to have engaged more in counteractive relocational forms of niche construction where individuals responded to environmental change by relocating to other areas that were more suitable (e.g., functional changes to the environment between Units 1A and 1B, and Units 1B and 2). For example, *H. floresiensis* preferred to manufacture stone artifacts from local raw materials, such as silicified tuff (Sutikna et al., 2018), and consumed local murine resources reflecting the most dominant environment at the time. When the environments heterogeneity changed at ~120 ka and again at ~60 ka, *H. floresiensis* seems to have responded by following the most suitable environment. Although, sample sizes used here for Unit 1B were low and requires additional taphonomic and zooarchaeological analyses from within Units 1A, 1B, and 2 to confirm how *H. floresiensis* responded to environmental changes and exploited resources within different ecologies. Still, the murine faunal assemblage between units associated with *H. sapiens* and *H. floresiensis* captures this important distinction between how *H. sapiens* adapt to environmental challenges (i.e., inceptive perturbation) versus *H. floresiensis* (i.e., counteractive relocation).

This dissertation also revealed important methodological considerations for conducting taphonomic and zooarchaeological studies at Liang Bua. For instance, sampling all elements from a single sector showed which elements are ideal for collecting different taphonomic variables. Mandibular incisors, for example, were the most reliable element for capturing murine body size, relative abundance, and avian digestion while also estimating the relative contribution of various body sized murines by avian and hominin agents within each unit. Additional taphonomic analyses using mandibular incisors across multiple sectors could provide a quick and thorough analysis where Sector XI did not adequately reflect specific units (e.g., Unit 6). Similarly, the humerus, another highly abundant element, was the most cutmarked bone across the entire assemblage studied here and could be used as a proxy for cutmark frequencies across a larger sample spanning other sectors and units in the cave. Moving forward, additional taphonomic analyses using this sampling technique will also reveal spatial accumulation patterns throughout different temporal areas of the cave to potentially reveal how *H. sapiens* and *H. floresiensis* utilized parts of the cave and why.

Appendix A

Chapter 4: Transcript on small mammal consumption at Liang Bua

Interview transcript with a participant from Teras, Flores, Indonesia

Transcript provided by Sekar Rizqi Amalia R. Location: Teras, Manggarai province, Flores, Indonesia.

[Bahasa Indonesia]

Narasumber: Stanis, 47 Tahun

Q: apakah mengonsumsi sumsumnya juga saat mengonsumsi hewan-hewan?

A: sumsum itu yang didalam tulang itu koh?

Q: Iya pak

A: oh, iya iya, lebih-lebih kalau sum-sum babi, kalau babi, babi hutan. Karena babi itu kan tulangnya besar, sumsumnya jadi enak.

Q: Kalau betu atau hewan-hewan kecil lainnya itu dimakan sumsumnya?

A: Iya,iya karena kita waktu makan itu kan saking nikmatnya itu tulangnya kita patahin toh. Kita patahin lalu kita isap-isap sumsumnya kan ada lubang sumsumnya entah betu, kelelawar. Jadi waktu kita makan sangking enaknya makanan itu kan disamping kita rasa

isinya (dagingnya), tulangnya kita isap, sangking enaknya kita patahin kita isap-isap lagi di dalam tulang itu.

Q: Hewan apa saja yang biasa dimakan dengan sumsumnya pak?

A: Betu, terus kalau kelelawar rasanya tidak ada sumsumnya e. kebanyakan betu dengan apa saja betu dengan babi hutan.

Q: Kalau landak pak?

A: ha landak ada, lebih-lebih di bagian tulang pahanya itu. Sama tulang, tulang paha sama sumsum yang di apa namanya itu tulang apa tulang punggung, tulang belakang.

Q: Sepengetahuan bapak semua orang disana makan dengan sumsumnya juga?

A: iya, rata-rata. Kayanya itu juga orang tua kami menyarankan justru itu yang paling penting daripada daging karena disitu dia kan banyak ini nilai gizinya.

[English]

Informant: Stanis, 47 Years Q: do you consume the marrow when you eat animals?

A: The marrow is inside the bone, right?

Q: Yes sir

A: oh, yes yes, the more so if pork marrow, if pork, wild boar. Because pork has large bones, the marrow is delicious.

Q: Is the marrow eaten by the betu or other small animals?

A: Yes, yes, because when we ate it was so delicious that we broke our bones anyway. We break it and then we suck on the marrow, right? There is a hole in the marrow, whether it's a bat. So when we eat, we taste the deliciousness of the food beside we taste the contents (the meat), we suck the bones, we break the delicious taste again in the bones.

Q: What animals do you eat with marrow, sir?

A: Betu, then the bats don't taste any marrow. Mostly betu with anything betu with wild boar.

Q: What about hedgehogs [porcupines], sir?

A: ha there is a hedgehog, the more so in the thighbone. The same bones, the femur and the marrow, in what is called the spine, the spine.

Q: To your knowledge, everyone there

ate the marrow too?

A: yes, on average. We think that our parents also suggested that it was the most important thing than meat because there it has a lot of nutritional value.

[Bahasa Indonesia]

Q: hewan-hewan tadi biar bisa diambil sumsumnya, bagaimana cara memasaknya?

A: ya kalau direbus, terus kadang juga kita bakar atau panggang. Terus kan kalau jaman sekarang kan orang taruh bumbu oseng ya dioseng juga bisa.

Q: Jadi walaupun tidak dengan direbus sumsum tetap bisa didapat ya?

A: iya, tetap. Biar dia dioseng juga kan didalam tetap saja. Malah kalau dioseng kan lebih enak ada bumbunya kan kita isap-isap tulangnya itu kita patahin kita isap-isap sumsumnya didalamnya lagi.

Q: Berarti tidak harus direbus ya biar bisa dapat sumsum?

A: tidak harus, karena dia kan ada didalam tulang toh atau di persendian itu misalnya

Q: wadah untuk masak biasanya menggunakan apa?

A: Kalau dulu sih kalau dulu rata-rata di panci ya. Tapi kalau sekarang ini kan bisa pakai kuali juga

Q: Kenapa pakai itu pak? Ada alasan tertentu?

A: begini kalau pakai panci masaknya itu enak. Karena panci itu kan tutupnya rapat disamping dia cepat matang ya cepat matang toh sehingga cepat disajikan. Kalau pake kuali kan, kalau orang tidak tapi pake kuali karena pake kuali kan karena pake kuali kan lambat dia matang. Kecuali kalau digoreng atau dioseng

Q: berarti lebih pilih pakai panci karena lebih cepat matang ya?

A: Lebih pilih pakai panci dan merupakan kebiasaan kami orang sini.

[English]

Q: So you can take the marrow from the animals, how do you cook it?

A: yes, if it is boiled, then sometimes we burn it or roast it. Then, nowadays, people put stir-fried spices, so they can also be cooked.

Q: So even if you don't boil the mar-

row you can still get it, right?

A: yes, still. Let him also be rubbed inside anyway. In fact, if it is fried, it is better with the spices, right? We suck the bones, we break the marrow, we suck the marrow in it again.

Q: So you don't have to boil it so you can get marrow?

A: You don't have to, because it's inside the bone anyway or in the joint, for example

Q: What containers for cooking are usually used?

A: In the past, the average was in the pan, right? But now you can use the cauldron too

Q: Why use that, sir? Any particular reason?

A: like this if you use a cooking pot it's delicious. Because the pot has a tight lid on the side, it cooks quickly, so it cooks quickly so it's served quickly. If you use a cauldron, people don't use a cauldron because they use a cauldron, because using a cauldron, it ripens slowly. Unless it's fried or fried

Q: means you prefer to use a pan because it cooks faster, huh?

A: We prefer to use a pot and it is our habit here.

[Bahasa Indonesia]

Q: Cara agar bisa dapat sumsumnya berarti yang dipatahin tadi ya pak?

A: Iya dipatah atau tulangnya kalau sebesar jari kelingking ini kan bisa digigit sama giginya kita kalau gigi kita masih bagus, taaak (bunyi tulang yang digigit) begitu dia kan patah. Atau kalau tulang babi hutan itu, habis kita isap tulang bagian luarnya itu, kita bisa pakai apa parang itu parang yang bukan tajam itu kah sebelah yang agak tebal sedikit itu, kita patahin pakai itu baru kita hisap, karena dia besar toh (tulangnya). Atau waktu potongnya itu kah missal potong bagian paha potong bagi dua kan sumsumnya kan masih lengket di dalam tulang itu ketika masak nanti kan baru nanti kita isap nanti enak dia keluar toh, tinggal kita ambil sendok yang kecil korek atau kita hisaplah.

Q: Paling enak sumsum apa pak?

A: kalau enak paling sumsum tuh kayanya sih babi hutan enak kan karena

sumsum babi hutan lebih besar lebih terasa ada di mulut kayanya dia lebih enak

Q: apa ada efek pada sumsumnya pak kalau dimasak dalam panci?

A: kalau dia direbus terlalu matang bisa keluar sumsumnya sendiri dari tulangnya waktu kita rebus toh tapi kalau masaknya pas-pas saja maka sumsunya tetap lengket dalam tulang. Yang paling bagus yang sedang-sedang saja jangan terlalu matang jangan juga yang terlalu tidak matang.

[English]

Q: How to get the marrow means what was done, right sir?

A: Yes, if the bone is broken or the size of the little finger can be bitten by our teeth if our teeth are still good, "taaak" (the sound of a bone being bitten) when it breaks. Or if the boar bone, after we suck on the outer bone, we can use the machete, the non-sharp machete, the one that is a little thick, we break it and then we suck it, because it's big anyway (the bone). Or when you cut it, for example, cut the thigh, cut it in half, the marrow is still sticky in the bone when it cooks, then we'll suck it, it's delicious, it comes out anyway, we just have to take a small matched spoon or suck it.

Q: What's the best marrow, sir?

A: The best marrow is delicious, the boar is delicious, because the marrow of the wild boar is bigger, it tastes better in the mouth, the taste is better.

Q: Is there any effect on the marrow sir if it's cooked in a pan?

A: If it is boiled too ripe, the marrow will come out of the bone itself when we boil it anyway but if it is cooked just right, the marrow remains sticky to the bone. The best ones are that are not too ripe, not too ripe.

Appendix B

Chapter 6: Digestive Damage

Table B.1: Definitions of avian digestive stages for murid molars and incisors summarized according to Fernández-Jalvo et al. (2016).

Molars	**Definitions of digestion stages**
Light	Rounded cusps with slightly smoother surface than non-worn teeth. Lateral surface appears more matt (=loss of shine).
Moderate	Pitted enamal surface all over the tooth enamel with incipient enamel reduction at the crown-root junction
Heavy	Enamel removed from the cusps and heavily pitted. Dentine is exposed but not affected or rounded. The lateral side shows enamel removed towards the height of the tooth and at the crown-root junction. Dentine/roots are not affected or rounded.
Extreme	Enamel formaing small islands or completely removed with or without dentine hollowed out and etched.
Incisors	
Very Light*	The tip of the incisor is matted with superficial flacking/shaving of enamel, but enamel is not removed. Slight rounding may be observed.
Light	Enamel shows pitting and a matt surface with a retraction of enamel on the tip leaving the dentine exposed and rounded. Somethings, enamel is totally removed from the tip and dentine is retracted, producing an uneven outline.
Moderate	Dentine becomes wavy. Enamel removed from almost half of the tooth.
Heavy	Enamel forms islands and is removed from almost half of the tooth.
Extreme	Enamel is completely removed or forming small islands. Dentine collapses in along the incisor.

* new category following (Williams, 2001).

Table B.2: Degrees of digestive damage according to isolated and *in situ* incisors and molars, as well as the proximal femur and distal humerus. Digestive stages labeled "Acidic" follows Andrews (1990) and "Corrosive" indicates level of corrosion from digestive enzymes along the distal or proximal shafts without the classic pitting on the distal or proximal articular surfaces of the humerus and femur, respectively. Degrees of damage are summarized by NISP and percentages according to stratigraphic unit and level.

		Digestion																Digestion														
	Unit	None		Very Light		Light		Medium		Heavy		Extreme		**Total**			Unit	None		Very Light		Light		Medium		Heavy		Extreme		**Total**		
Teeth		NISP	%	NISP	%	NISP	%	NISP	%	NISP	%	NISP	%			Teeth		NISP	%	NISP	%	NISP	%	NISP	%	NISP	%	NISP	%			
Incisors *in situ*	1A-I	1	0.33	1	0.33	0	0.00	0	0.00	1	0.33	0	0.00	**3**		Incisors *in situ*	6	0	0.00	1	0.33	2	0.67	0	0.00	0	0.00	0	0.00	**3**		
Isolated incisors	1A-I	77	0.63	43	0.35	1	0.01	1	0.01	0	0.00	0	0.00	**122**		Isolated incisors	6	12	0.24	28	0.56	7	0.14	3	0.06	0	0.00	0	0.00	**50**		
Incisors total	*1A-I*	*78*	*0.62*	*44*	*0.35*	*1*	*0.01*	*1*	*0.01*	*1*	*0.01*	*0*	*0.00*	***125***		*Incisors total*	*6*	*12*	*0.23*	*29*	*0.55*	*9*	*0.17*	*3*	*0.06*	*0*	*0.00*	*0*	*0.00*	***53***		
Molars *in situ*	1A-I	15	0.22	4	0.06	35	0.52	10	0.15	3	0.04	0	0.00	**67**		Molars *in situ*	6	3	0.21	6	0.43	5	0.36	0	0.00	0	0.00	0	0.00	**14**		
Isolated molars	1A-I	19	0.51	0	0.00	15	0.41	2	0.05	1	0.03	0	0.00	**37**		Isolated molars	6	0	0.00	0	0.00	0	0.00	0	0.00	0	0.00	0	0.00	**0**		
Molars total	*1A-I*	*34*	*0.33*	*4*	*0.04*	*50*	*0.48*	*12*	*0.12*	*4*	*0.04*	*0*	*0.00*	***104***		*Molars total*	*6*	*3*	*0.21*	*6*	*0.43*	*5*	*0.36*	*0*	*0.00*	*0*	*0.00*	*0*	*0.00*	***14***		
Postcrania																Postcrania																
Corrosive Femur	1A-I	NA		NA		NA		NA		NA		NA				Corrosive Femur	6	NA		NA		NA		NA		NA		NA				
Acidic Femur	1A-I	NA		NA		NA		NA		NA		NA				Acidic Femur	6	NA		NA		NA		NA		NA		NA				
Corrosive Humerus	1A-I	33	0.54	0	0.00	26	0.43	2	0.03	0	0.00	0	0.00	**61**		Corrosive Humerus	6	39	0.95	0	0.00	2	0.05	0	0.00	0	0.00	0	0.00	**41**		
Acidic Humerus	1A-I	43	0.70	17	0.28	0	0.00	0	0.00	0	0.00	1	0.02	**61**		Acidic Humerus	6	34	0.83	1	0.02	6	0.15	0	0.00	0	0.00	0	0.00	**41**		
Teeth																Teeth																
Incisors *in situ*	1A-II	2	1.00	0	0.00	0	0.00	0	0.00	0	0.00	0	0.00	**2**		Incisors *in situ*	8A	0	0.00	6	0.67	3	0.33	0	0.00	0	0.00	0	0.00	**9**		
Isolated incisors	1A-II	18	0.51	17	0.49	0	0.00	0	0.00	0	0.00	0	0.00	**35**		Isolated incisors	8A	22	0.28	33	0.42	16	0.21	7	0.09	0	0.00	0	0.00	**78**		
Incisors total	*1A-II*	*20*	*0.54*	*17*	*0.46*	*0*	*0.00*	*0*	*0.00*	*0*	*0.00*	*0*	*0.00*	***37***		*Incisors total*	*8A*	*22*	*0.25*	*39*	*0.45*	*19*	*0.22*	*7*	*0.08*	*0*	*0.00*	*0*	*0.00*	***87***		
Molars *in situ*	1A-II	0	0.00	0	0.00	15	0.71	6	0.29	0	0.00	0	0.00	**21**		Molars *in situ*	8A	2	0.08	7	0.27	15	0.58	2	0.08	0	0.00	0	0.00	**26**		
Isolated molars	1A-II	0	0.00	1	0.10	7	0.70	2	0.20	0	0.00	0	0.00	**10**		Isolated molars	8A	0	0.00	1	0.50	1	0.50	0	0.00	0	0.00	0	0.00	**2**		
Molars total	*1A-II*	*0*	*0.00*	*1*	*0.03*	*22*	*0.71*	*8*	*0.26*	*0*	*0.00*	*0*	*0.00*	***31***		*Molars total*	*8A*	*2*	*0.07*	*8*	*0.29*	*16*	*0.57*	*2*	*0.07*	*0*	*0.00*	*0*	*0.00*	***28***		
Postcrania																Postcrania																
Corrosive Femur	1A-II	NA		NA		NA		NA		NA		NA				Corrosive Femur	8A	25	0.27	0	0.00	53	0.57	13	0.14	2	0.02	0	0.00	**93**		
Acidic Femur	1A-II	NA		NA		NA		NA		NA		NA				Acidic Femur	8A	92	0.99	0	0.00	1	0.01	0	0.00	0	0.00	0	0.00	**93**		
Corrosive Humerus	1A-II	11	0.92	0	0.00	1	0.08	0	0.00	0	0.00	0	0.00	**12**		Corrosive Humerus	8A	67	0.59	0	0.00	46	0.41	0	0.00	0	0.00	0	0.00	**113**		
Acidic Humerus	1A-II	9	0.75	0	0.00	2	0.17	0	0.00	1	0.08	0	0.00	**12**		Acidic Humerus	8A	106	0.95	6	0.05	0	0.00	0	0.00	0	0.00	0	0.00	**112**		
Teeth																Teeth																
Incisors *in situ*	1A-III	5	0.23	10	0.45	7	0.32	0	0.00	0	0.00	0	0.00	**22**		Incisors *in situ*	8B	1	0.09	5	0.45	2	0.18	3	0.27	0	0.00	0	0.00	**11**		
Isolated incisors	1A-III	156	0.37	227	0.54	35	0.08	4	0.01	0	0.00	0	0.00	**422**		Isolated incisors	8B	10	0.19	27	0.52	11	0.21	4	0.08	0	0.00	0	0.00	**52**		
Incisors total	*1A-III*	*161*	*0.36*	*237*	*0.53*	*42*	*0.09*	*4*	*0.01*	*0*	*0.00*	*0*	*0.00*	***444***		*Incisors total*	*8B*	*11*	*0.17*	*32*	*0.51*	*13*	*0.21*	*7*	*0.11*	*0*	*0.00*	*0*	*0.00*	***63***		
Molars *in situ*	1A-III	9	0.03	55	0.21	160	0.60	43	0.16	0	0.00	0	0.00	**267**		Molars *in situ*	8B	4	0.22	11	0.61	3	0.17	0	0.00	0	0.00	0	0.00	**18**		
Isolated molars	1A-III	5	0.10	15	0.31	24	0.49	5	0.10	0	0.00	0	0.00	**49**		Isolated molars	8B	1	0.50	1	0.50	0	0.00	0	0.00	0	0.00	0	0.00	**2**		
Molars total	*1A-III*	*14*	*0.04*	*70*	*0.22*	*184*	*0.58*	*48*	*0.15*	*0*	*0.00*	*0*	*0.00*	***316***		*Molars total*	*8B*	*5*	*0.25*	*12*	*0.60*	*3*	*0.15*	*0*	*0.00*	*0*	*0.00*	*0*	*0.00*	***20***		
Postcrania																Postcrania																
Corrosive Femur	1A-III	NA		NA		NA		NA		NA		NA				Corrosive Femur	8B	65	0.55	0	0.00	38	0.32	11	0.09	4	0.03	0	0.00	**118**		
Acidic Femur	1A-III	NA		NA		NA		NA		NA		NA				Acidic Femur	8B	87	0.74	9	0.08	17	0.14	3	0.03	2	0.02	0	0.00	**118**		
Corrosive Humerus	1A-III	144	0.54		0.00	116	0.43	9	0.03	0	0.00	0	0.00	**269**		Corrosive Humerus	8B	96	0.79	0	0.00	21	0.17	3	0.02	1	0.01	0	0.00	**121**		
Acidic Humerus	1A-III	191	0.71	16	0.06	56	0.21	5	0.02	1	0.00	0	0.00	**269**		Acidic Humerus	8B	110	0.92	4	0.03	3	0.03	0	0.00	2	0.02	1	0.01	**120**		
Teeth																Teeth																
Incisors *in situ*	1B-IV	2	0.50	2	0.50	0	0.00	0	0.00	0	0.00	0	0.00	**4**		Incisors *in situ*	8C	5	0.36	5	0.36	3	0.21	1	0.07	0	0.00	0	0.00	**14**		
Isolated incisors	1B-IV	62	0.44	72	0.51	8	0.06	0	0.00	0	0.00	0	0.00	**142**		Isolated incisors	8C	11	0.33	13	0.39	6	0.18	3	0.09	0	0.00	0	0.00	**33**		
Incisors total	*1B-IV*	*64*	*0.44*	*74*	*0.51*	*8*	*0.05*	*0*	*0.00*	*0*	*0.00*	*0*	*0.00*	***146***		*Incisors total*	*8C*	*16*	*0.34*	*18*	*0.38*	*9*	*0.19*	*4*	*0.09*	*0*	*0.00*	*0*	*0.00*	***47***		
Molars *in situ*	1B-IV	2	0.09	15	0.65	6	0.26	0	0.00	0	0.00	0	0.00	**23**		Molars *in situ*	8C	0	0.00	11	0.39	16	0.57	1	0.04	0	0.00	0	0.00	**28**		
Isolated molars	1B-IV	1	0.06	9	0.50	7	0.39	1	0.06	0	0.00	0	0.00	**18**		Isolated molars	8C	0	0.00	0	0.00	0	0.00	0	0.00	0	0.00	0	0.00	**0**		
Molars total	*1B-IV*	*3*	*0.07*	*24*	*0.59*	*13*	*0.32*	*1*	*0.02*	*0*	*0.00*	*0*	*0.00*	***41***		*Molars total*	*8C*	*0*	*0.00*	*11*	*0.39*	*16*	*0.57*	*1*	*0.04*	*0*	*0.00*	*0*	*0.00*	***28***		
Postcrania																Postcrania																
Corrosive Femur	1B-IV	NA		NA		NA		NA		NA		NA				Corrosive Femur	8C	35	0.56	0	0.00	21	0.33	7	0.11	0	0.00	0	0.00	**63**		
Acidic Femur	1B-IV	NA		NA		NA		NA		NA		NA				Acidic Femur	8C	62	0.98	0	0.00	1	0.02	0	0.00	0	0.00	0	0.00	**63**		
Corrosive Humerus	1B-IV	10	0.20	0	0.00	40	0.78	1	0.02	0	0.00	0	0.00	**51**		Corrosive Humerus	8C	33	0.59	20	0.36	3	0.05	0	0.00	0	0.00	0	0.00	**56**		
Acidic Humerus	1B-IV	50	0.98	0	0.00	1	0.02	0	0.00	0	0.00	0	0.00	**51**		Acidic Humerus	8C	56	1.00	0	0.00	0	0.00	0	0.00	0	0.00	0	0.00	**56**		

Appendix C

Chapter 6: Element Fragmentation

Table C.1: Totals and percentages of non-long bone elements included in each breakage category within stratigraphic units 1A - 1B.

		Com.		Frag.			Com.		Prox		Shaft		Distal	
Unit	Element	N	%	N	%	Element	N	%	N	%	N	%	N	%
1A-I	Talus	0	0.0	0	0.0	Ribs	0	0.0	0	0.0	0	0.0	0	0.0
	Calcaneus	13	68.4	6	31.6	Metapodials	18	75	4	16.7	1	4.2	1	4.2
	Phalanges	1	100.0	0	0.0	Scapula	0	0	9	100.0	0	0.0	0	0.0
	Vertebrae	35	92.1	3	7.9	Pelvis*	0	0	20	83.3	2	8.3	2	8.3
	Incisors	112	88.2	15	11.8	Cranium**	17	39	2	4.5	-	-	25	56.8
1A-II	Talus	0	0.0	0	0.0	Ribs	0	0.0	0	0.0	0	0.0	0	0.0
	Calcaneus	3	100.0	0	0.0	Metapodials	3	42.9	2	28.6	1	14.3	1	14.3
	Phalanges	2	100.0	0	0.0	Scapula	0	0.0	3	100.0	0	0.0	0	0.0
	Vertebrae	1	7.1	13	92.9	Pelvis*	0	0.0	10	52.6	8	42.1	1	5.3
	Incisors	32	86.5	5	13.5	Cranium**	8	44.4	0	0.0	-	-	10	55.6
1A-III	Talus	1	100.0	0	0.0	Ribs	0	0.0	1	50.0	0	0.0	1	50.0
	Calcaneus	32	76.2	10	23.8	Metapodials	72	75.8	17	17.9	0	0.0	6	6.3
	Phalanges	0	0.0	0	0.0	Scapula	0	0.0	23	100.0	0	0.0	0	0.0
	Vertebrae	46	30.9	103	69.1	Pelvis*	-	-	-	-	-	-	-	-
	Incisors	438	94.8	24	5.2	Cranium**	45	31.3	21	14.6	-	-	78	54.2
1B-IV	Talus	2	100.0	0	0.0	Ribs	0	0.0	1	100.0	0	0.0	0	0.0
	Calcaneus	9	75.0	3	25.0	Metapodials	22	95.7	1	4.3	0	0.0	0	0.0
	Phalanges	0	0.0	0	0.0	Scapula	0	0.0	3	100.0	0	0.0	0	0.0
	Vertebrae	12	34.3	23	65.7	Pelvis*	0	0.0	19	61.3	3	9.7	9	29.0
	Incisors	155	98.1	3	1.9	Cranium**	5	7.9	2	3.2	-	-	56	88.9

* Pelvis: Com. = complete, Prox = Ilium + acetabula, Shaft = Ilium shaft, Dist. = Iscium
** Cranium: Com. = Maxilla, Prox = Maxilla with zygomatic, Dist = braincase

Table C.2: Totals and percentages of non-long bone elements included in each breakage category within stratigraphic units 6 – 8A-C.

		Com.		Frag.			Com.		Prox		Shaft		Distal	
Unit	Element	N	%	N	%	Element	N	%	N	%	N	%	N	%
6	Talus	0	0.0	0	0.0	Ribs	0	0.0	0	0.0	0	0.0	0	0.0
	Calcaneus	0	0.0	1	100.0	Metapodials	18	75	4	16.7	1	4.2	1	4.2
	Phalanges	1	100.0	0	0.0	Scapula	0	0.0	2	100.0	0	0.0	0	0.0
	Vertebrae	1	25.0	3	75.0	Pelvis*	0	0	13	68.4	4	21.1	2	10.5
	Incisors	48	81.4	11	18.6	Cranium**	2	100	0	0.0	-	-	0	0.0
8A	Talus	0	0.0	0	0.0	Ribs	0	0.0	0	0.0	0	0.0	0	0.0
	Calcaneus	2	50.0	2	50.0	Metapodials	3	42.9	2	28.6	1	14.3	1	14.3
	Phalanges	4	80.0	1	20.0	Scapula	0	0.0	5	100.0	0	0.0	0	0.0
	Vertebrae	6	75.0	2	25.0	Pelvis*	0	0.0	13	54.2	8	33.3	3	12.5
	Incisors	114	84.4	21	15.6	Cranium**	0	0.0	0	0.0	-	-	10	100.0
8B	Talus	0	0.0	0	0.0	Ribs	0	0.0	1	50.0	0	0.0	1	50.0
	Calcaneus	2	40.0	3	60.0	Metapodials	72	75.8	17	17.9	0	0.0	6	6.3
	Phalanges	20	100.0	0	0.0	Scapula	0	0.0	3	100.0	0	0.0	0	0.0
	Vertebrae	5	38.5	8	61.5	Pelvis*	0	0.0	28	70.0	8	20.0	4	10.0
	Incisors	71	85.5	12	14.5	Cranium**	5	45.5	1	9.1	-	-	5	45.5
8C	Talus	0	0.0	0	0.0	Ribs	0	0.0	1	100.0	0	0.0	0	0.0
	Calcaneus	2	40.0	3	60.0	Metapodials	22	95.7	1	4.3	0	0.0	0	0.0
	Phalanges	9	100.0	0	0.0	Scapula	0	0.0	6	85.7	0	0.0	1	14.3
	Vertebrae	10	55.6	8	44.4	Pelvis*	0	0.0	19	73.1	4	15.4	3	11.5
	Incisors	56	91.8	5	8.2	Cranium**	5	55.6	0	0.0	-	-	4	44.4

* Pelvis: Com. = complete, Prox = Ilium + acetabula, Shaft = Ilium shaft, Dist. = Iscium

** Cranium: Com. = Maxilla, Prox = Maxilla with zygomatic, Dist = braincase

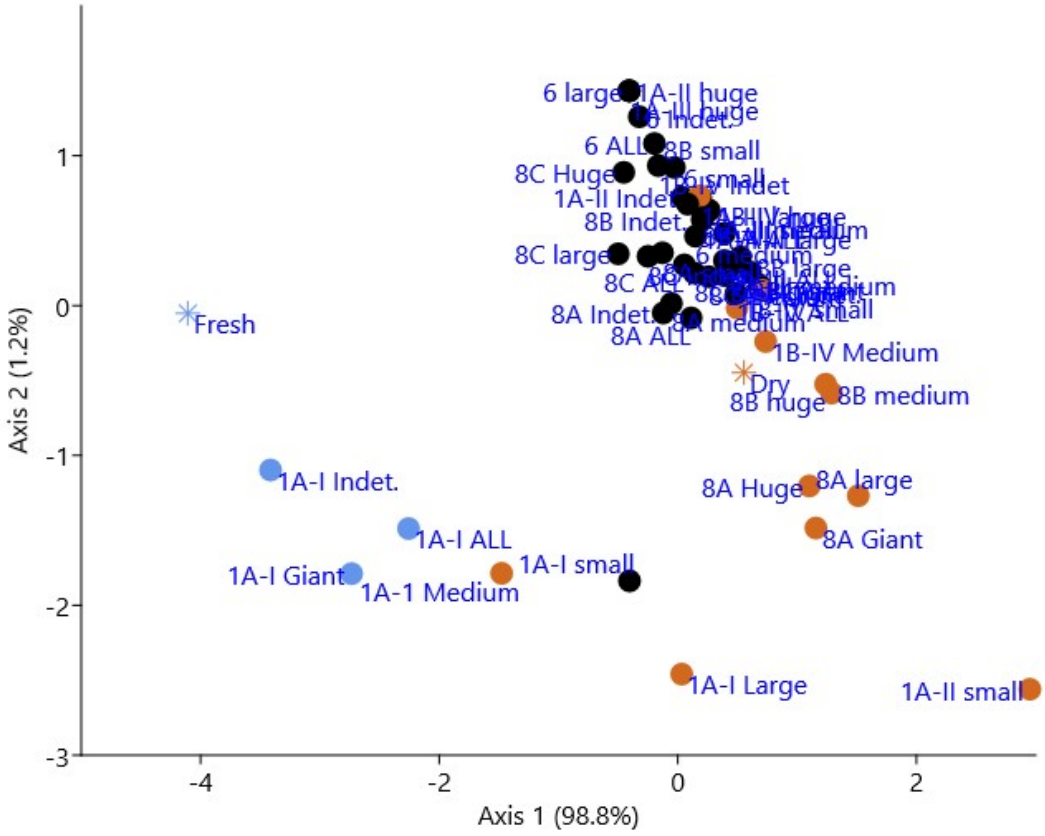

Figure C.1: Projection of scores from a linear discriminant function analysis on fracture angles from known fresh and dry long bone assemblages (**?**) against a combination of murine body sizes and stratigraphic units. Jacknifed classifications are color coded: Fresh = blue; Dry = brown; Unknown = black.

Table C.3: Totals and percentages of long bone elements included in each breakage category within stratigraphic units 1A - 1B and 6 - 8A-C.

		Com.		Prox		Shaft		Distal				Com.		Prox		Shaft		Distal	
Unit	Element	N	%	N	%	N	%	N	%	Unit	Element	N	%	N	%	N	%	N	%
	Humerus	9	13	6	8.6	22	31.4	33	47.1		Humerus	18	54.5	6	18.2	9	27.3	10	23.3
	Femur	-	-	-	-	-	-	-	-		Femur	-	-	-	-	-	-	-	-
1A-I	Tibia	0	0	8	8.4	59	62.1	28	29.5	6	Tibia	4	5.5	13	17.8	46	63.0	19	23.2
	Radius	0	0	5	31.3	9	56.3	2	12.5		Radius	6	33.3	11	61.1	0	0.0	1	5.6
	Ulna	0	0.0	19	57.6	14	42.4	0	0.0		Ulna	2	12.5	7	43.8	6	37.5	1	6.3
	Humerus	0	0.0	1	6.7	7	46.7	7	46.7		Humerus	48	37.8	11	8.7	30	23.6	38	29.9
	Femur	-	-	-	-	-	-	-	-		Femur	19	16.0	48	40.3	48	40.3	4	3.4
1A-II	Tibia	0	0.0	6	9.2	38	58.5	21	32.3	8A	Tibia	4	2.5	22	13.5	102	62.6	35	21.5
	Radius	0	0.0	0	0.0	1	50.0	1	50.0		Radius	3	7.0	20	46.5	13	30.2	7	16.3
	Ulna	0	0.0	2	20.0	8	80.0	0	0.0		Ulna	2	3.3	17	27.9	42	68.9	0	0.0
	Humerus	77	27.9	34	12.3	50	18.1	115	41.7		Humerus	50	35.0	16	11.2	29	20.3	48	33.6
	Femur	-	-	-	-	-	-	-	-		Femur	24	16.4	70	47.9	45	30.8	7	4.8
1A-III	Tibia	1	0.3	68	19.1	167	46.9	120	33.7	8B	Tibia	2	1.6	12	9.4	94	74.0	19	15.0
	Radius	1	2.0	19	37.3	22	43.1	9	17.6		Radius	4	10.5	19	50.0	14	36.8	1	2.6
	Ulna	1	0.9	57	53.8	47	44.3	1	0.9		Ulna	10	16.7	20	33.3	28	46.7	2	3.3
	Humerus	19	37.3	7	13.7	9	17.6	16	31.4		Humerus	19	31.1	7	11.5	8	13.1	27	44.3
	Femur	-	-	-	-	-	-	-	-		Femur	16	20.5	39	50.0	15	19.2	8	10.3
1B-IV	Tibia	7	7.6	16	17.4	34	37.0	35	38.0	8C	Tibia	4	4.3	21	22.8	41	44.6	26	28.3
	Radius	3	37.5	3	37.5	1	12.5	1	12.5		Radius	2	15.4	10	76.9	0	0.0	1	7.7
	Ulna	2	8.3	14	58.3	6	25.0	2	8.3		Ulna	5	17.9	14	50.0	6	21.4	3	10.7

Table C.4: Classification results from a linear discriminant function analysis showed in C.1.

	Given group	Classification	Jackknifed
Known Fresh	Fresh	Fresh	unknown
Known Dry	Dry	Dry	unknown
1A-I small	unknown	unknown	unknown
1A-1 Medium	unknown	unknown	Dry
1A-I Large	unknown	Dry	Dry
1A-I Giant	unknown	Fresh	Fresh
1A-I Indet.	unknown	Fresh	Fresh
1A-I ALL	unknown	unknown	Fresh
1A-II small	unknown	Dry	Dry
1A-II medium	unknown	unknown	Dry
1A-II large	unknown	unknown	unknown
1A-II huge	unknown	unknown	unknown
1A-II Indet	unknown	unknown	unknown
1A-II ALL	unknown	unknown	unknown
1A-III small	unknown	unknown	unknown
1A-III medium	unknown	unknown	unknown
1A-III large	unknown	unknown	unknown
1A-III huge	unknown	unknown	unknown
1A-III Indet.	unknown	unknown	unknown
1A-III ALL	unknown	unknown	unknown
1B-IV small	unknown	unknown	Dry
1B-IV Medium	unknown	Dry	Dry
1B-IV huge	unknown	unknown	unknown
1B-IV Indet	unknown	unknown	unknown
1B-IV ALL	unknown	unknown	unknown
6 small	unknown	unknown	Dry
6 medium	unknown	unknown	unknown
6 large	unknown	unknown	unknown
6 Indet.	unknown	unknown	unknown
6 ALL	unknown	unknown	Fresh
8A small	unknown	unknown	unknown
8A medium	unknown	unknown	unknown
8A large	unknown	Dry	Dry
8A Huge	unknown	Dry	Dry
8A Giant	unknown	Dry	Dry
8A Indet.	unknown	unknown	unknown
8A ALL	unknown	unknown	unknown
8B small	unknown	unknown	unknown
8B medium	unknown	Dry	Dry
8B large	unknown	Dry	unknown
8B huge	unknown	Dry	Dry
8B giant	unknown	Dry	unknown
8B Indet.	unknown	unknown	unknown
8B All	unknown	unknown	unknown
8C small	unknown	unknown	unknown
8C medium	unknown	unknown	unknown
8C large	unknown	unknown	unknown
8C Huge	unknown	unknown	unknown
8C giant	unknown	Dry	Dry
8C Indet.	unknown	unknown	unknown
8C ALL	unknown	unknown	unknown

Appendix D

Chapter 6: Bone surface modifications

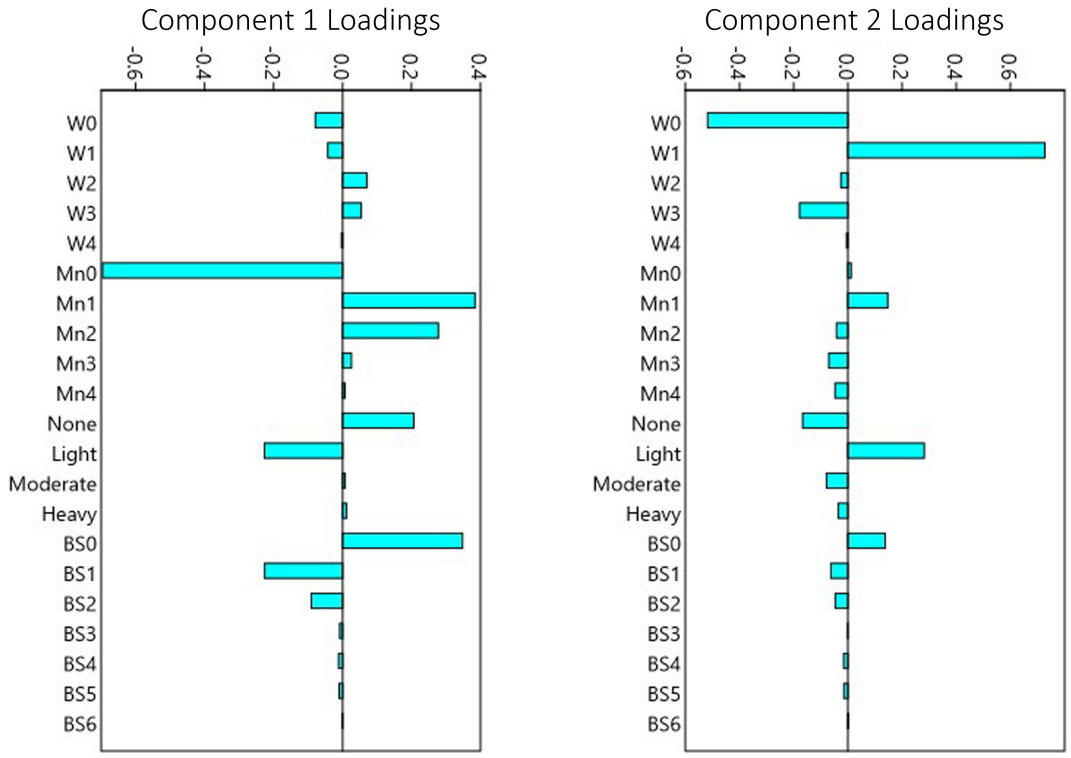

Figure D.1: Loadings contribution of the first and second component to the principal components analysis of post-depositionl values in Figure 6.13.

Appendix E

Chapter 6: High confidence cutmarks and tooth marks

E.0.1 Unit 1A

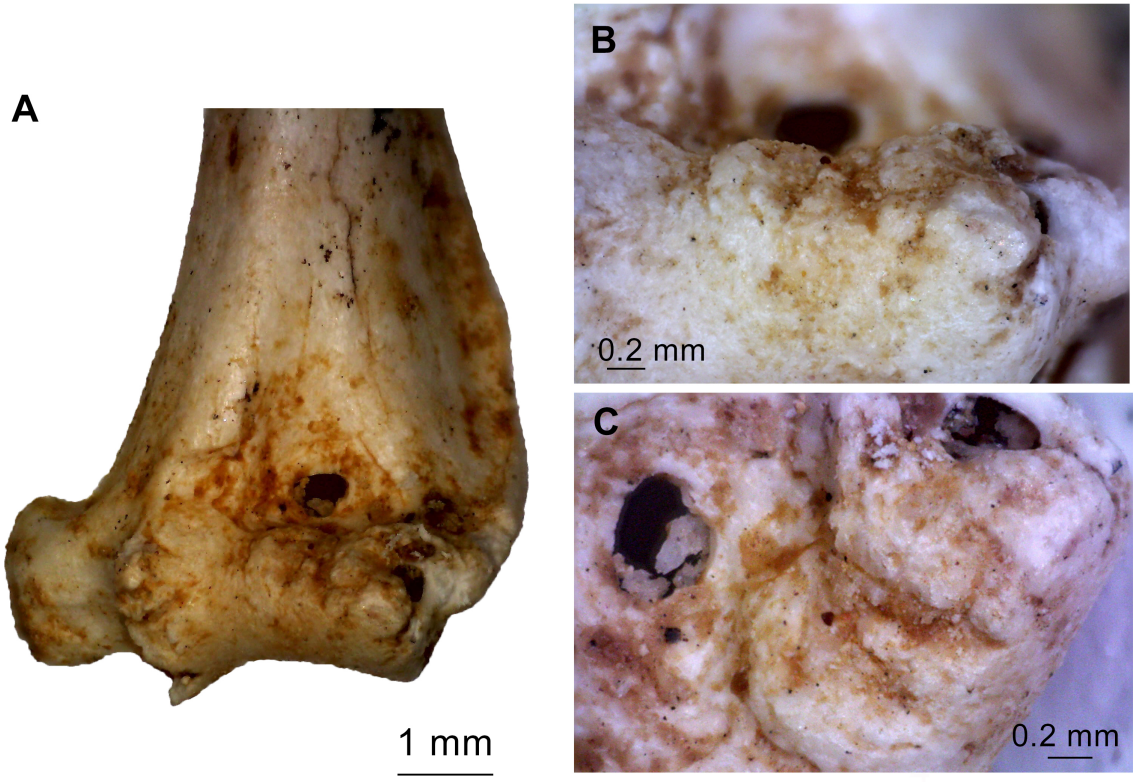

Figure E.1: **Unit:** 1A-I
ID: 480.1-3
Element: Humerus
Spit: 83
Sediment: Brown clay, grey tuff, more humid
BSM: Cutmarks

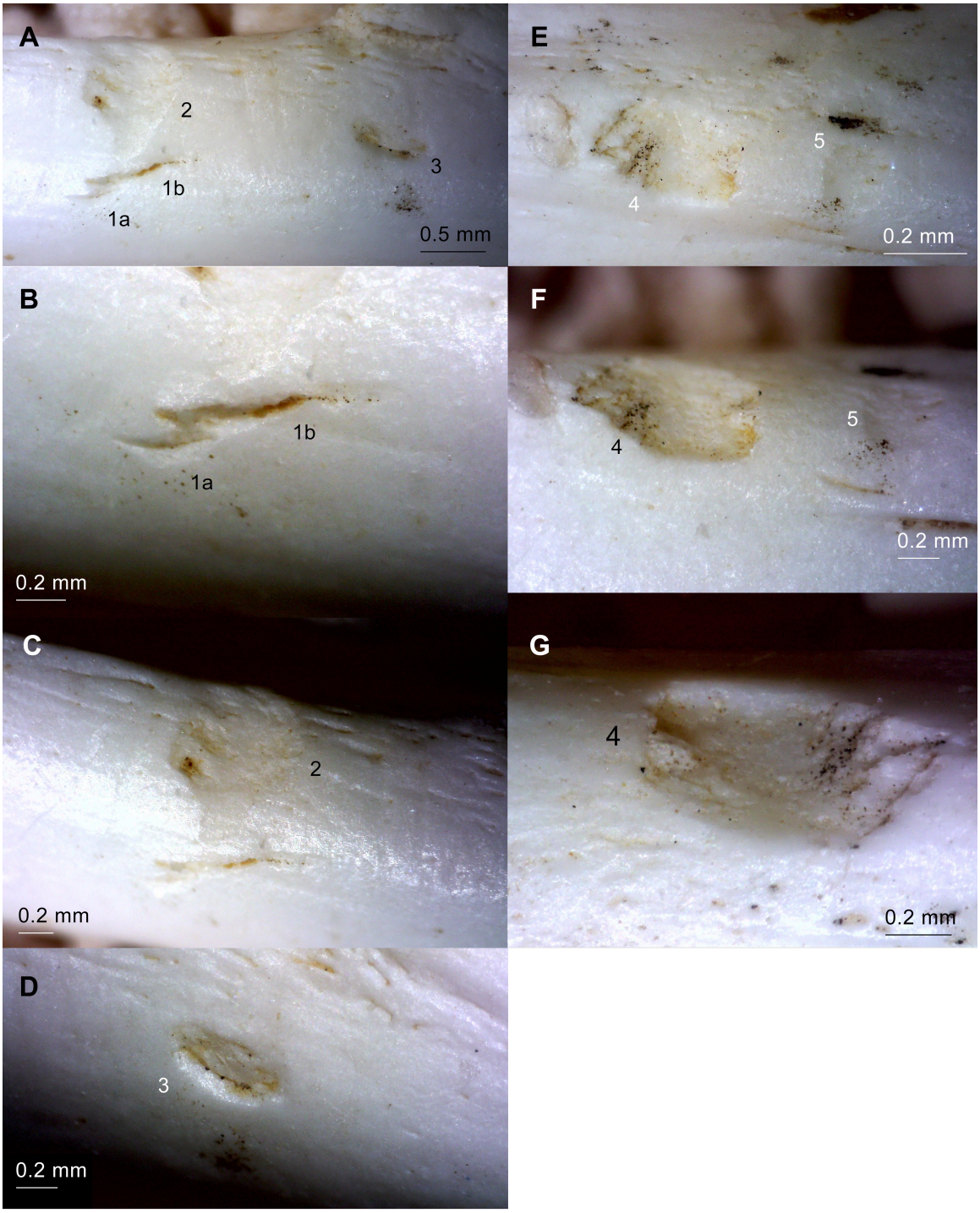

Figure E.2:
Unit: 1A-I
ID: 752.1-6
Element: Tibia
Spit: 79C
Sediment: Brown clay, grey tuff (under conglomerate)
BSM: Hominin tooth marks

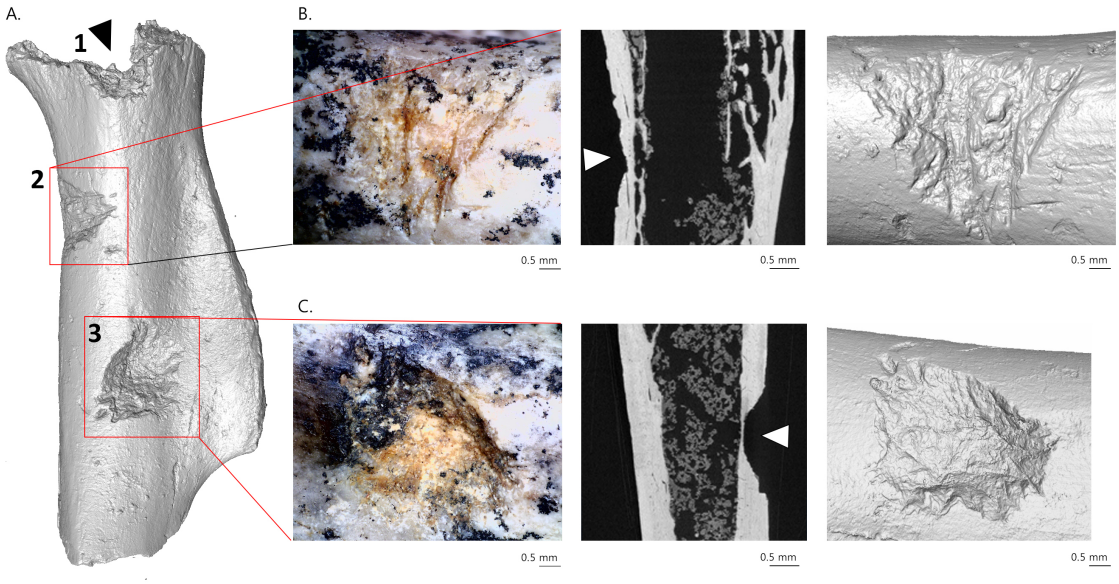

Figure E.3:
Unit: 1A-I
ID: 854.1-2
Element: Humerus
Spit: 78C
Sediment: Brown clay, grey tuff (under conglomerate)
BSM: 1) tooth notch; 2) chop marks; 3) pit

Figure E.4:
Unit: 1A-II
ID: 1091.1
Element: Humerus
Spit: 79B
Sediment: Brown andy clay (Conglomerate)
BSM: Cutmark

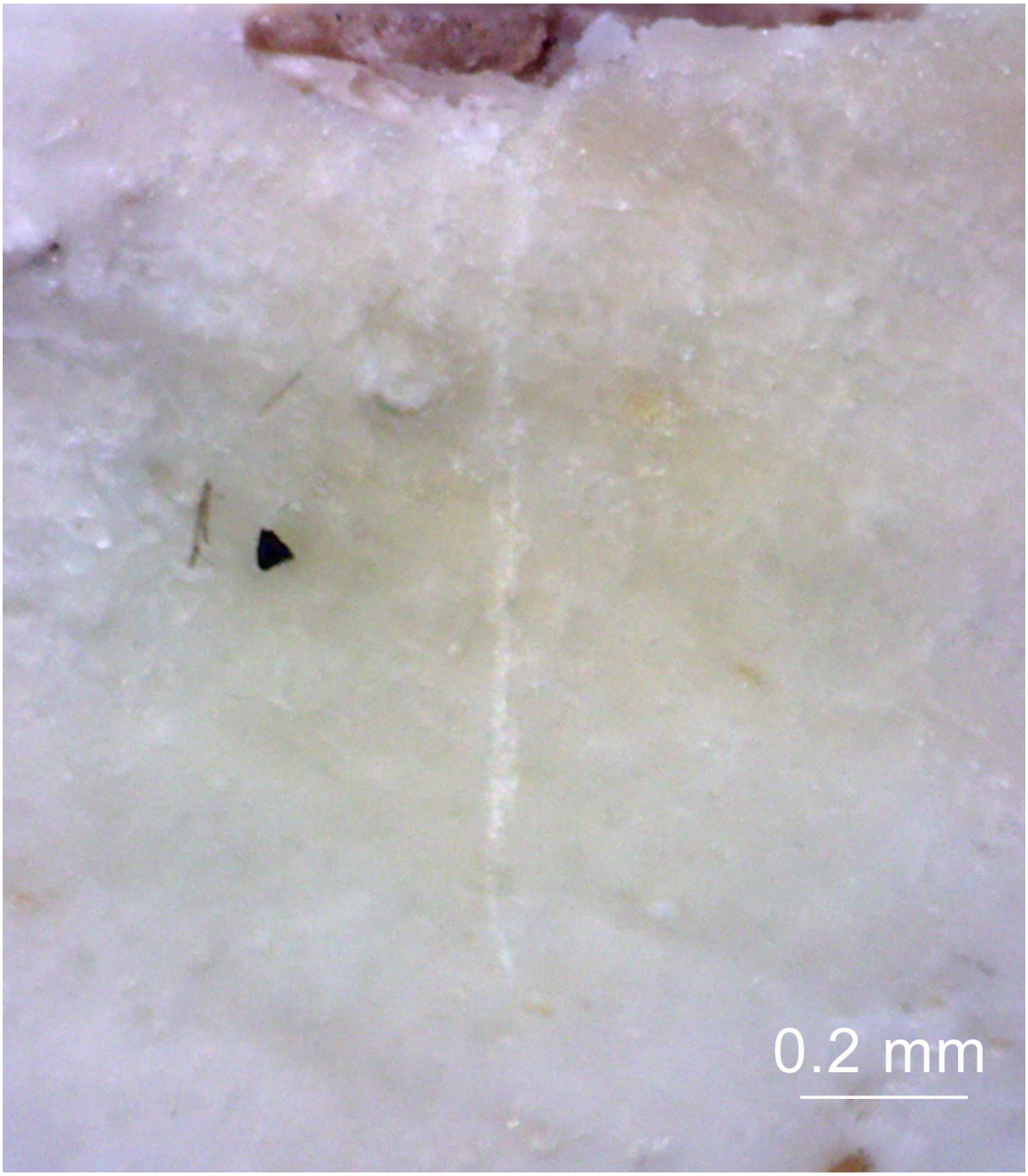

Figure E.5:
Unit: 1A-II
ID: 1091.3
Element: Humerus
Spit: 79B
Sediment: Brown andy clay (Conglomerate)
BSM: Cutmark

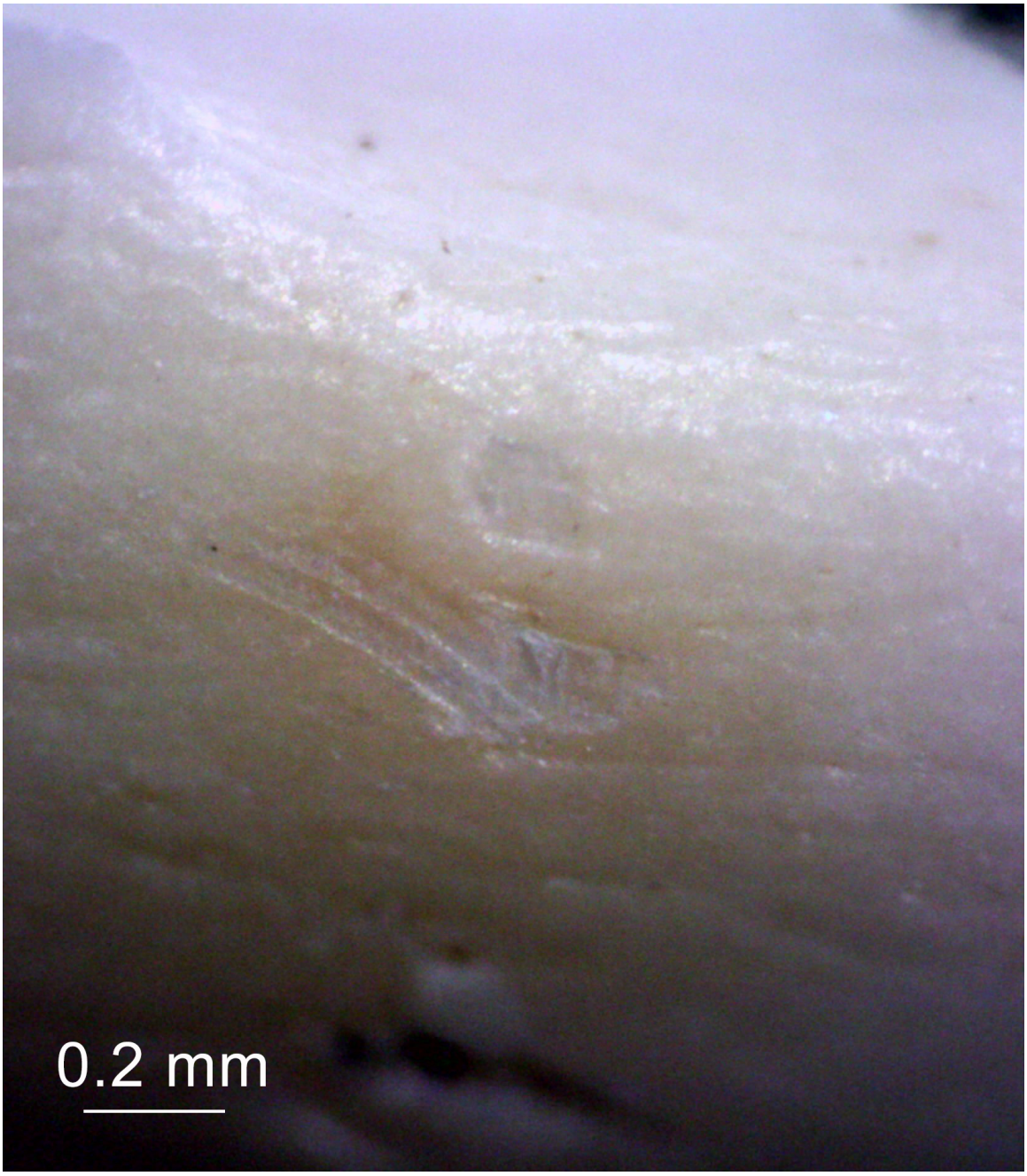

Figure E.6:
Unit: 1A-II
ID: 1098.2
Element: Tibia
Spit: 79B
Sediment: Brown andy clay (Conglomerate)
BSM: Hominin tooth mark

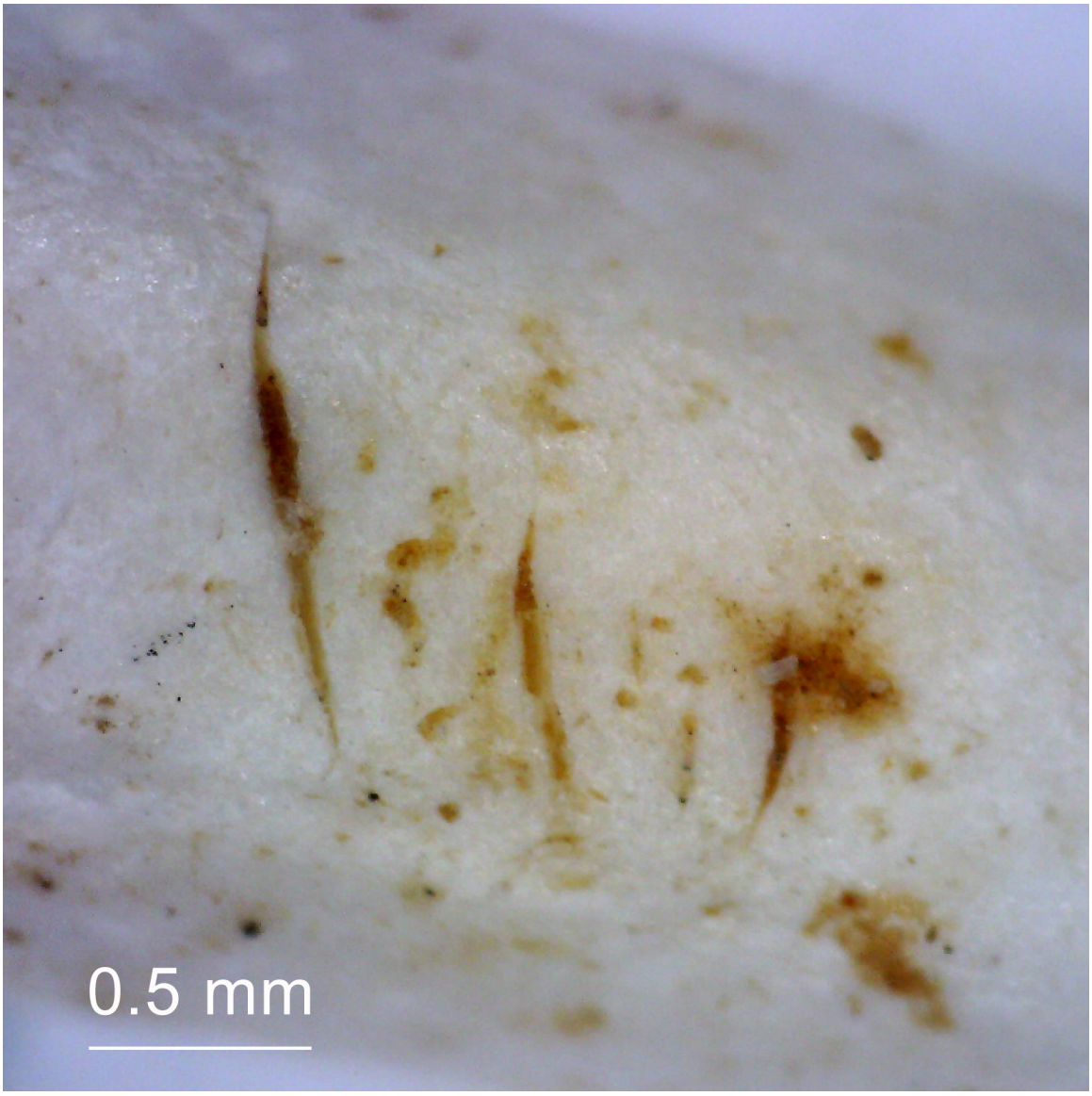

Figure E.7:
Unit: 1A-II
ID: 1260.1-3
Element: Tibia
Spit: 75B
Sediment: NA
BSM: Cutmarks

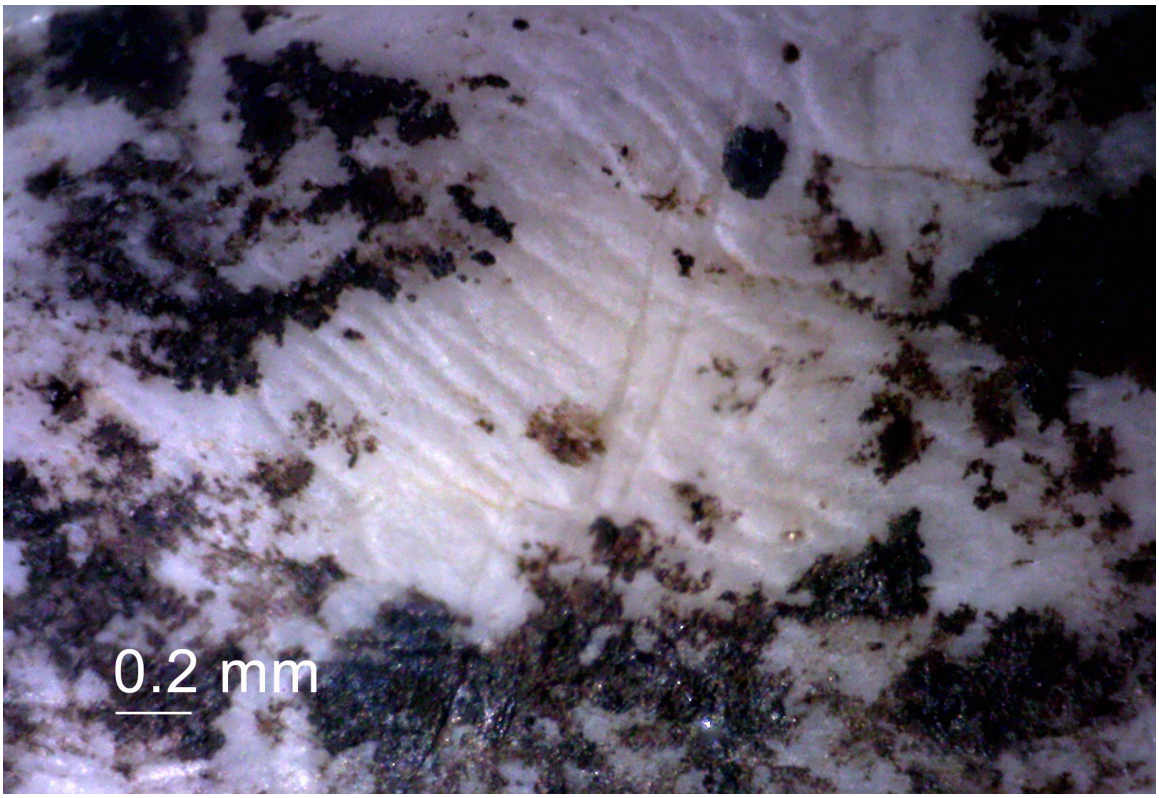

Figure E.8:
Unit: 1A-III
ID: 1473.1-2
Element: Mandible
Spit: 68
Sediment: Brown sandy clay+ grey tuff, hard
BSM: Cutmarks

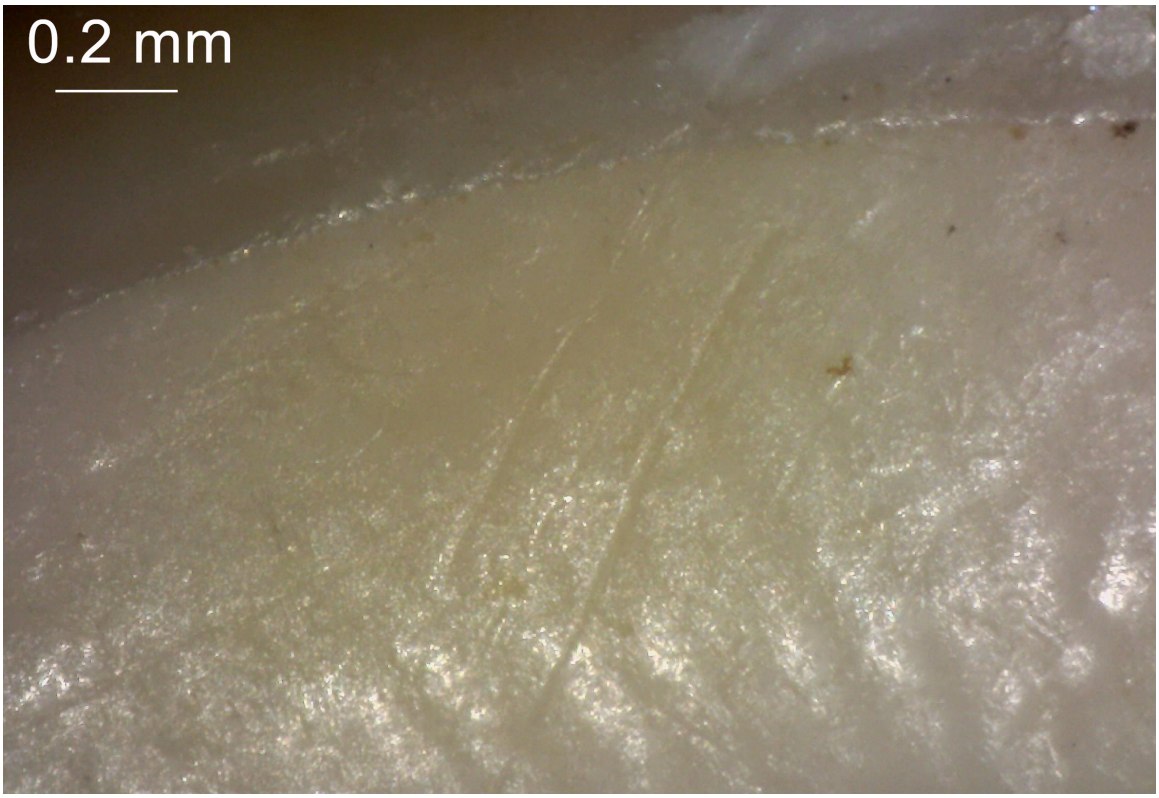

Figure E.9:
Unit: 1A-III
ID: 3836.1-2
Element: Incisor
Spit: 68
Sediment: Brown sandy clay+ grey tuff, hard
BSM: Cutmarks

Figure E.10:
Unit: 1A-III
ID: 3994.1-4
Element: Calcaneus
Spit: 68
Sediment: Brown sandy clay+ grey tuff, hard
BSM: Cutmarks

Figure E.11:
Unit: 1A-III
ID: 4275.1-6
Element: Maxilla
Spit: 68
Sediment: Brown sandy clay+ grey tuff, hard
BSM: Cutmarks

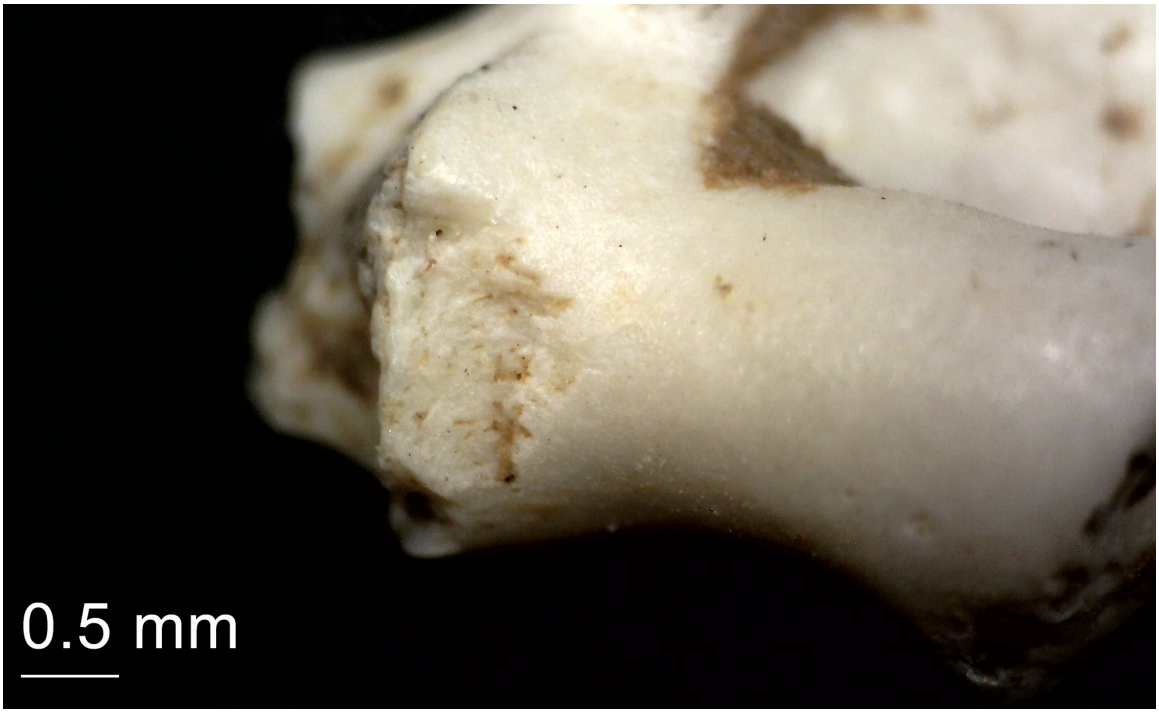

Figure E.12:
Unit: 1A-III
ID: 4363.1
Element: Humerus
Spit: 68
Sediment: Brown sandy clay+ grey tuff, hard
BSM: Tooth scrape

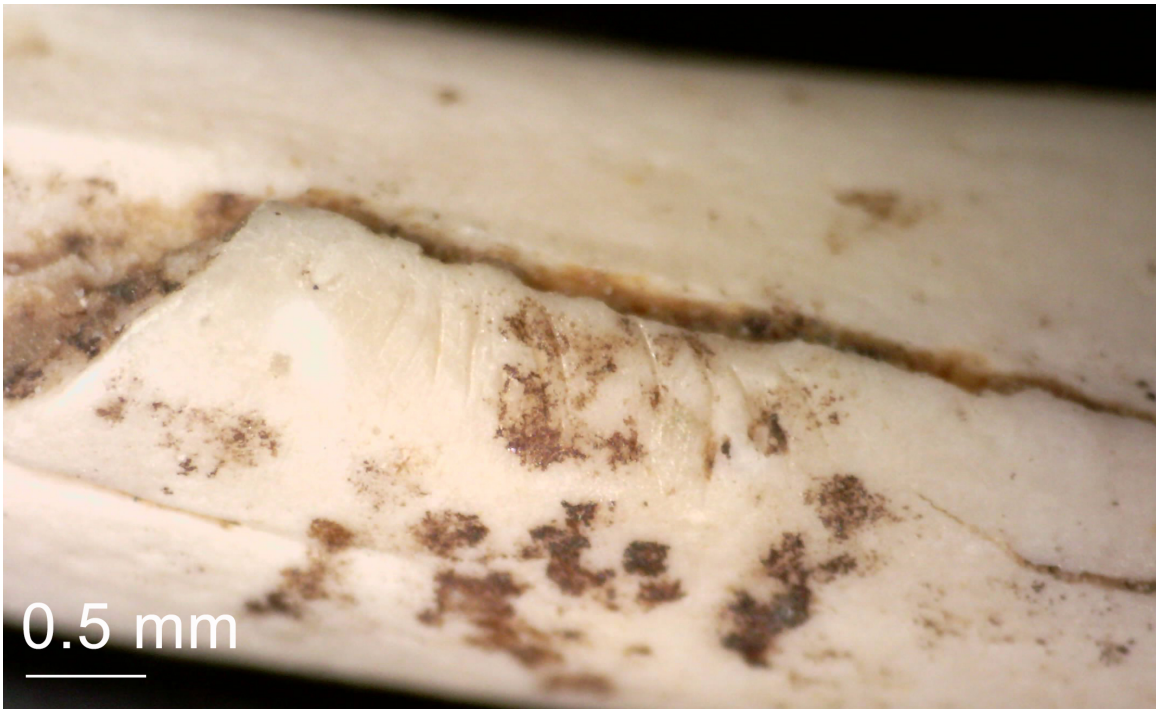

Figure E.13:
Unit: 1A-III
ID: 4723.1-9
Element: Tibia
Spit: 68
Sediment: Brown sandy clay+ grey tuff, hard
BSM: Cutmarks

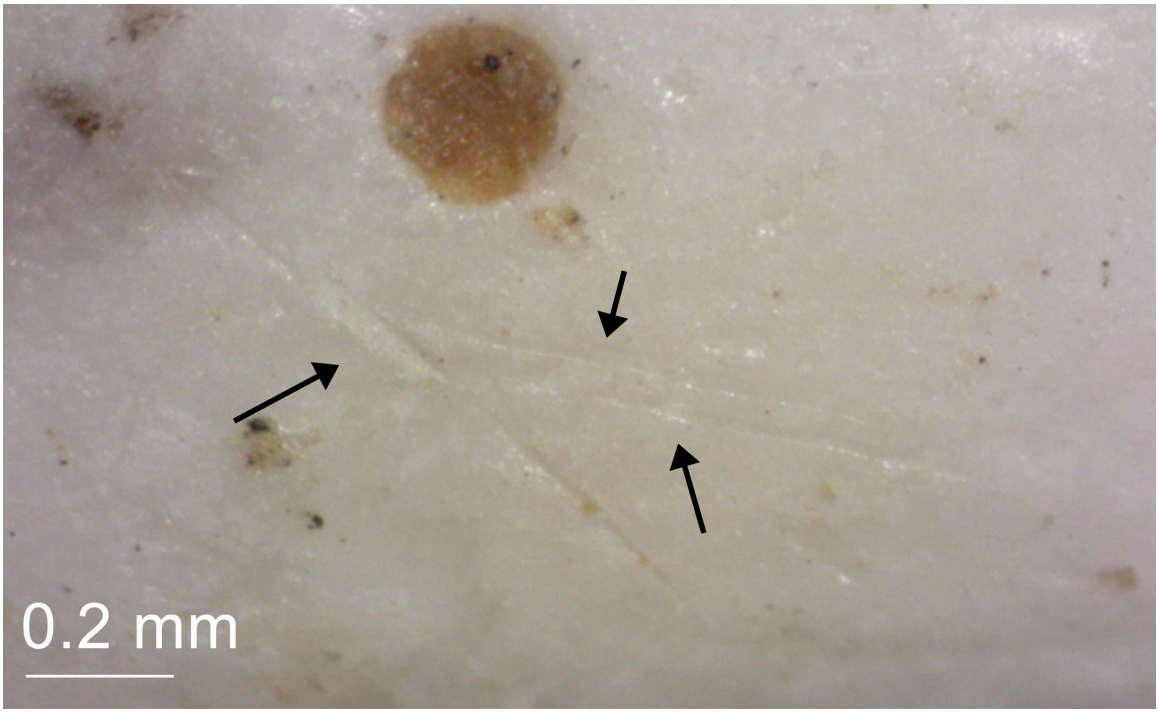

Figure E.14:
Unit: 1A-III
ID: 4747.1-3
Element: Tibia
Spit: 68
Sediment: Brown sandy clay+ grey tuff, hard
BSM: Cutmarks

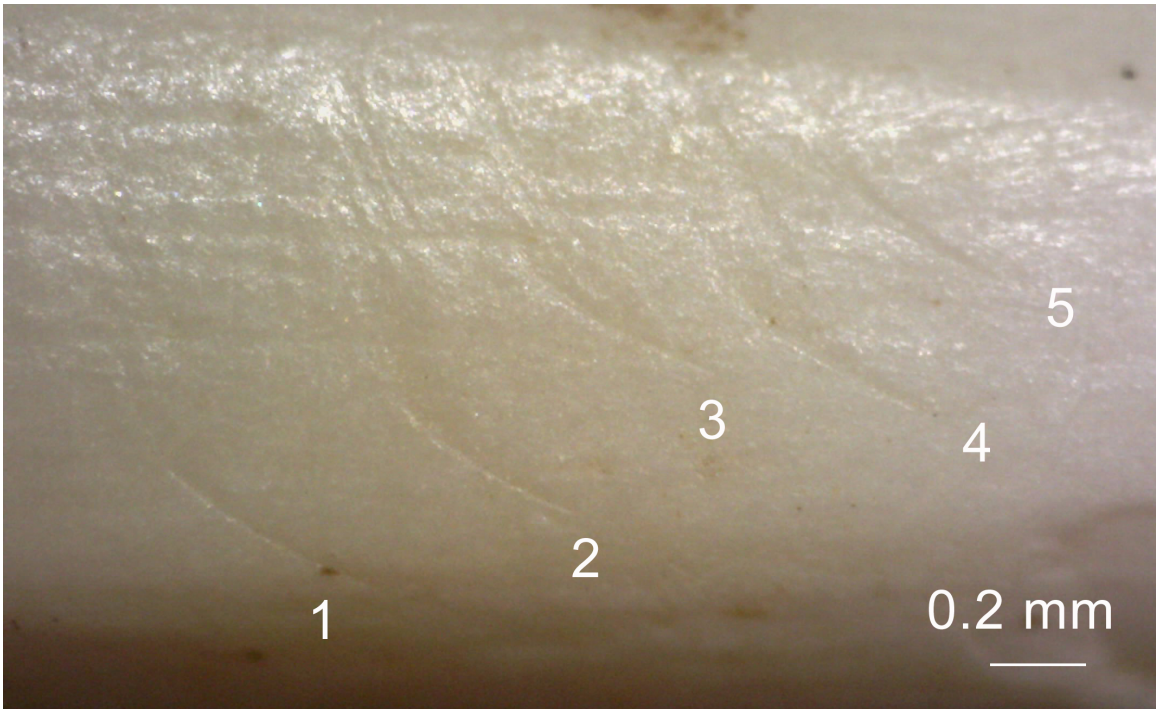

Figure E.15:
Unit: 1A-III
ID: 4826.1-5
Element: Tibia
Spit: 68
Sediment: Brown sandy clay+ grey tuff, hard
BSM: Cutmarks

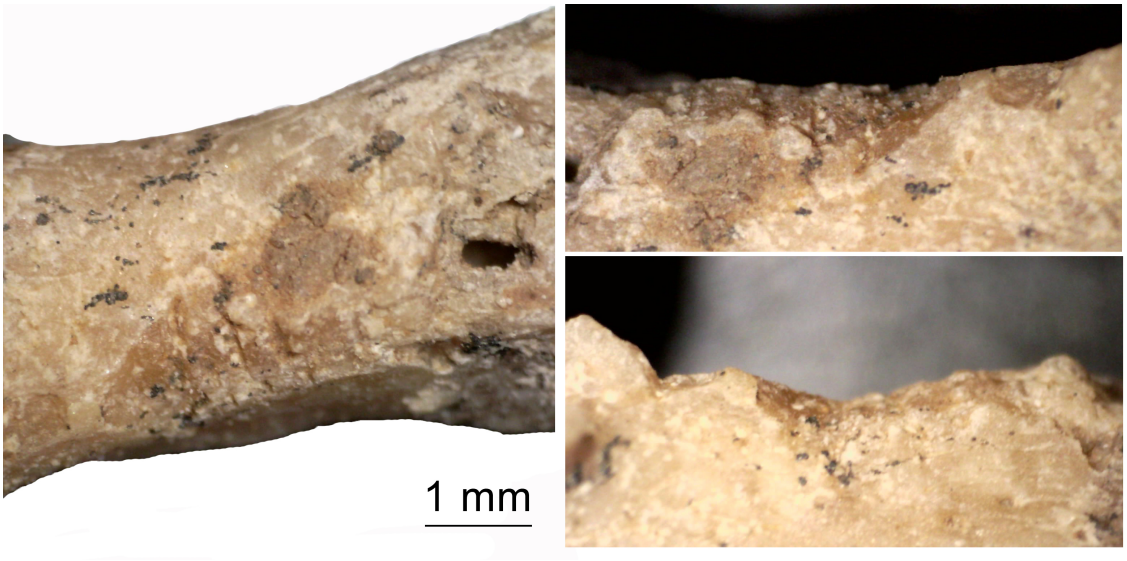

Figure E.16:
Unit: 1A-III
ID: 7722.1
Element: Caudal vertebra
Spit: 74
Sediment: Brown sandy clay+ grey tuff, humid, compact
BSM: Chop marks

E.0.2 Unit 1B

Figure E.17:
Unit: 1B-IV
ID: 7387.1
Element: Innominate
Spit: 55B
Sediment: Brown clay, grey tuff, humid, sticky
BSM: Slice / chop mark

E.0.3 Unit 8A

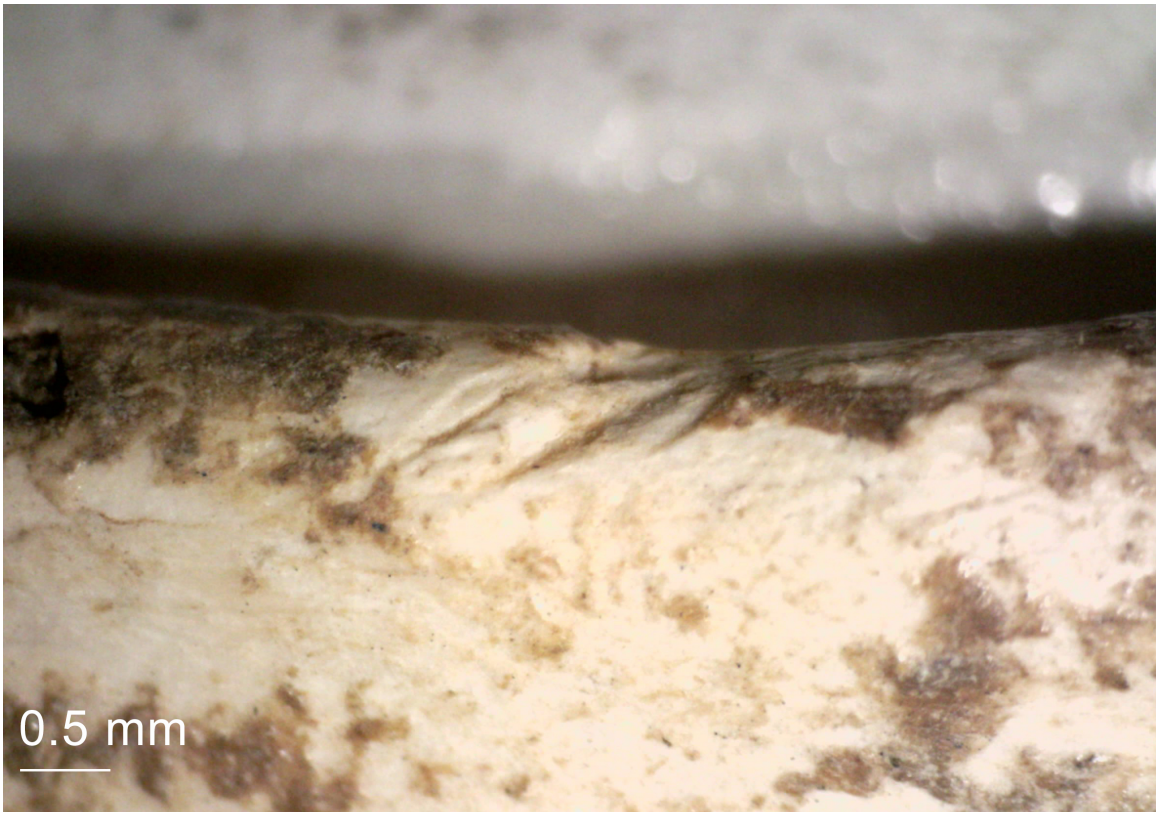

Figure E.18:
Unit: 8A
ID: 5726.1-2
Element: Innominate
Spit: 18
Sediment: NA
BSM: chopped marks

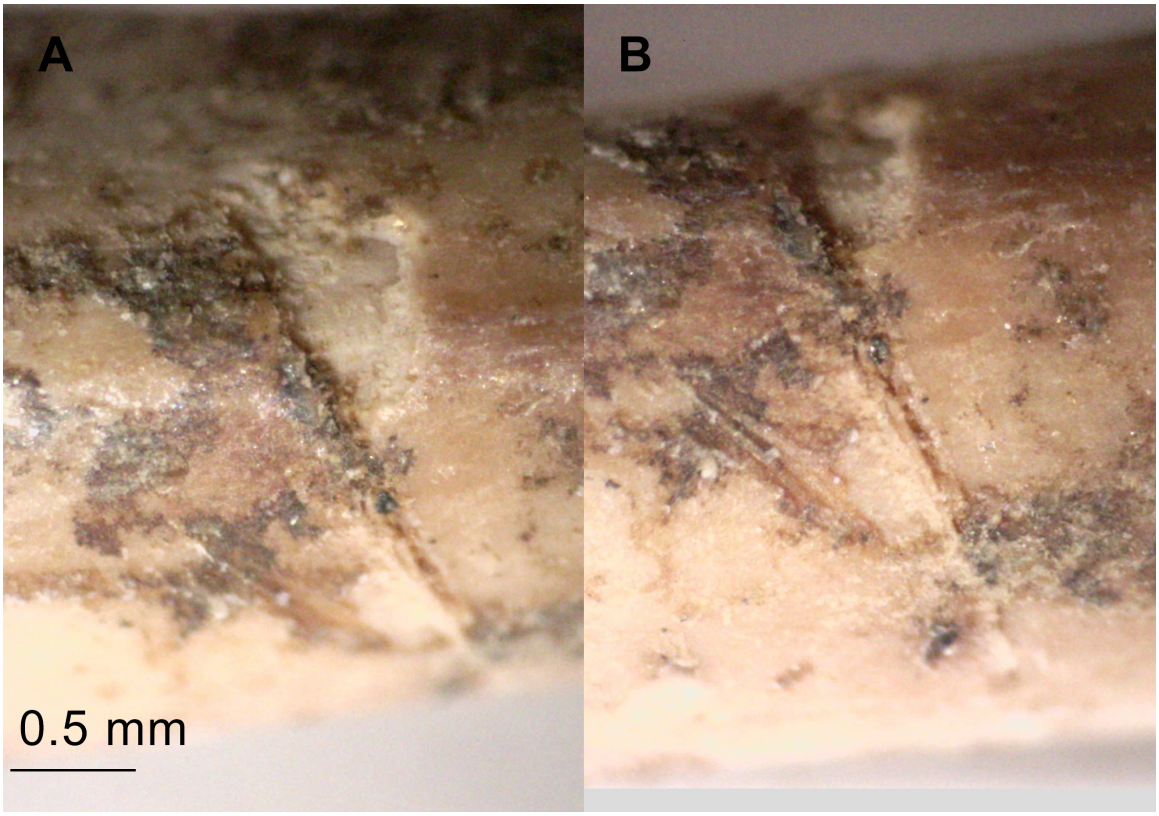

Figure E.19:
Unit: 8A
ID: 5751.1
Element: Tibia
Spit: 18
Sediment: NA
BSM: Cutmark

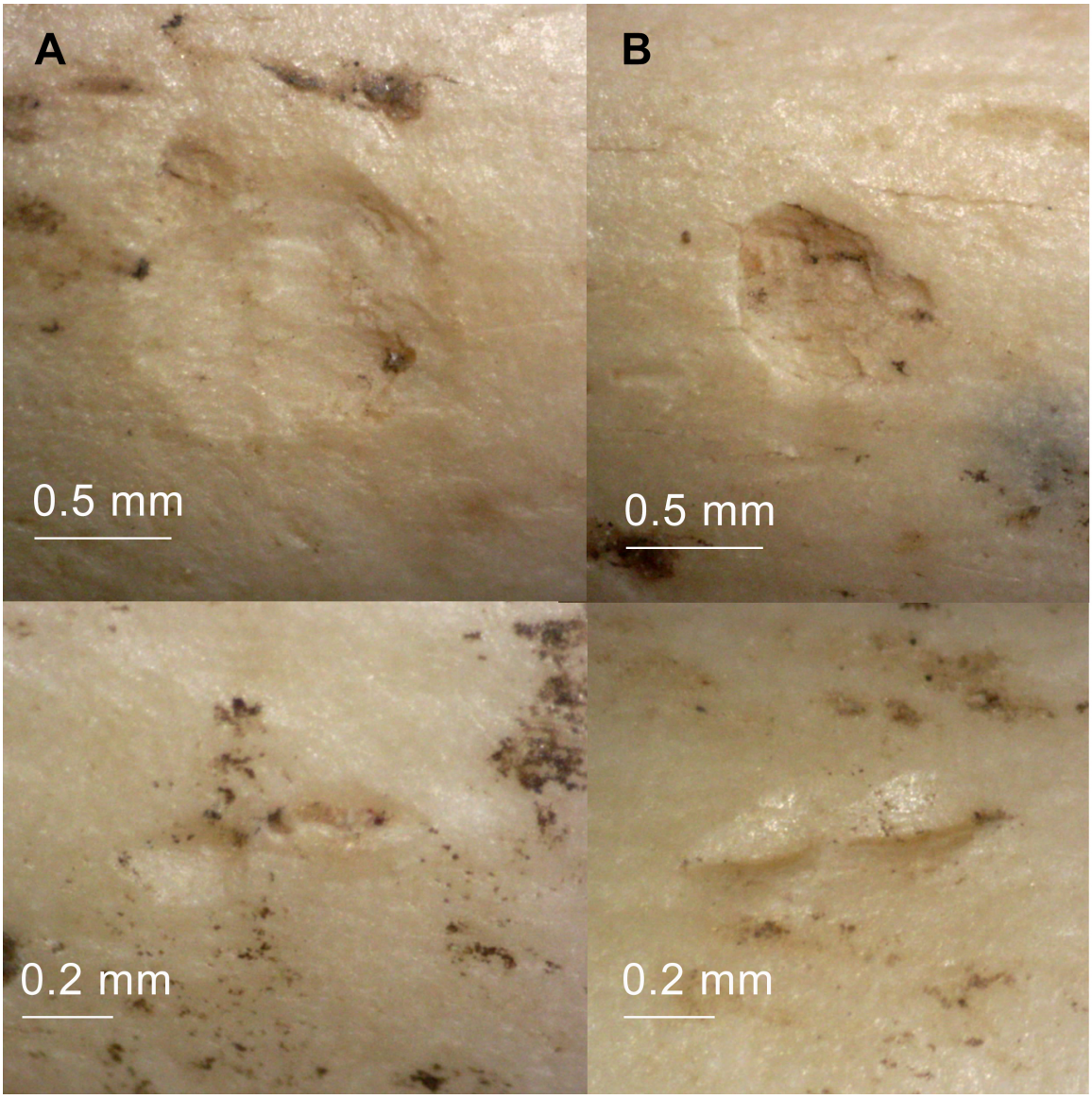

Figure E.20:
Unit: 8A
ID: 5866.1-4
Element: Innominate
Spit: 16
Sediment: NA
BSM: Hominin tooth marks

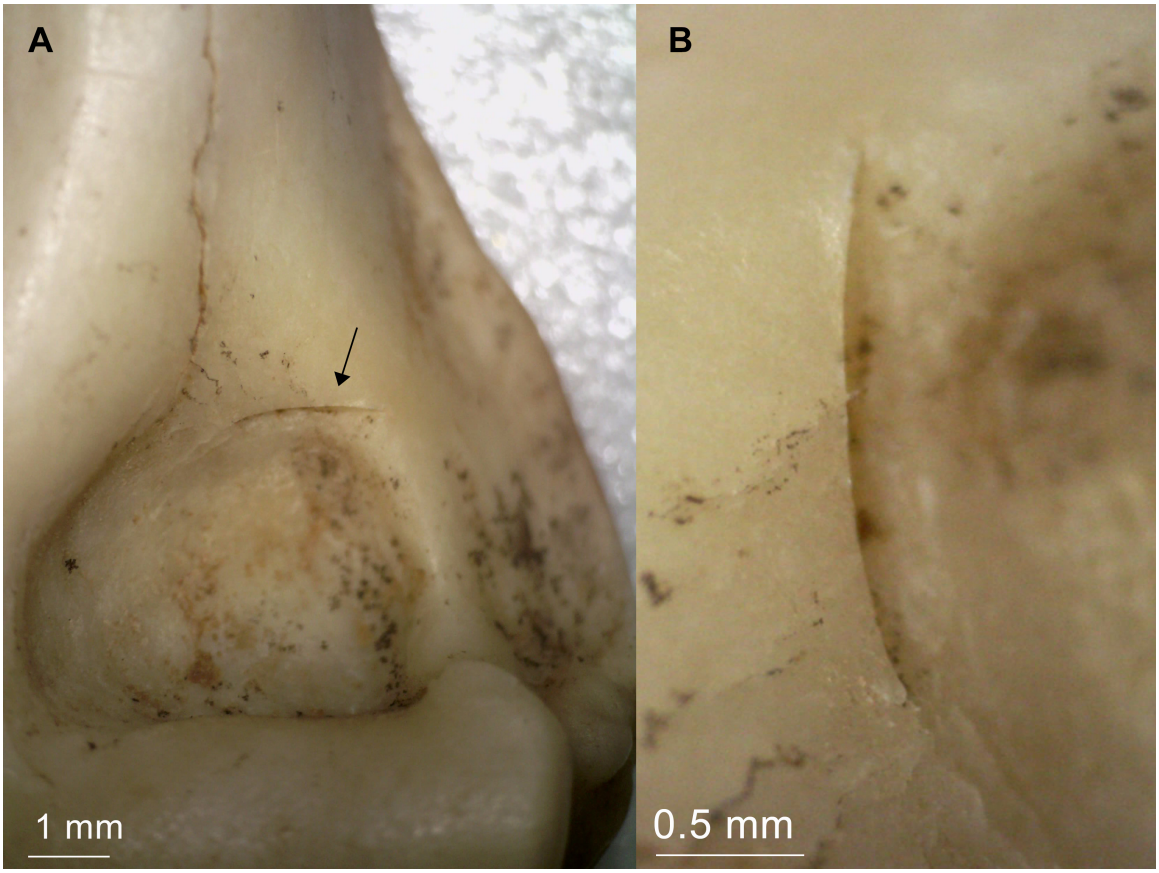

Figure E.21:
Unit: 8A
ID: 6187.1-2
Element: Humerus
Spit: 28
Sediment: NA
BSM: Cutmark

E.0.4 Unit 8B

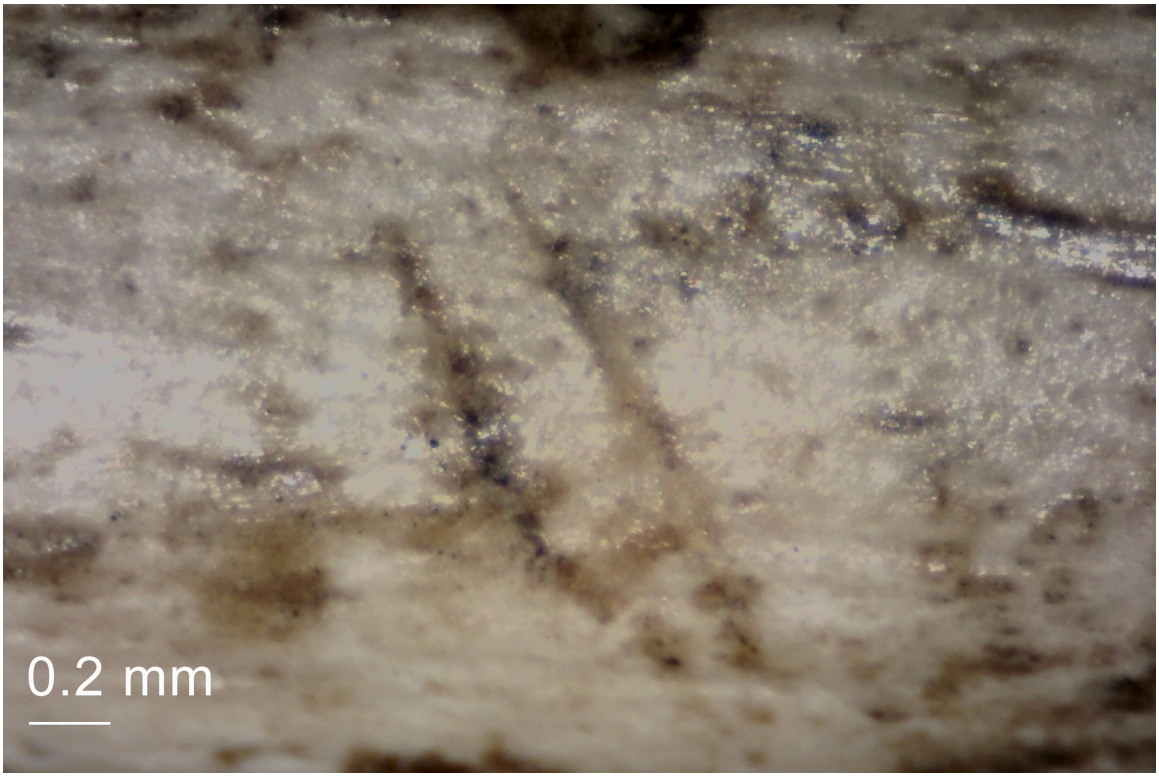

Figure E.22:
Unit: 8B
ID: 3318.1-2
Element: Innominate
Spit: 15
Sediment: NA
BSM: Cutmarks

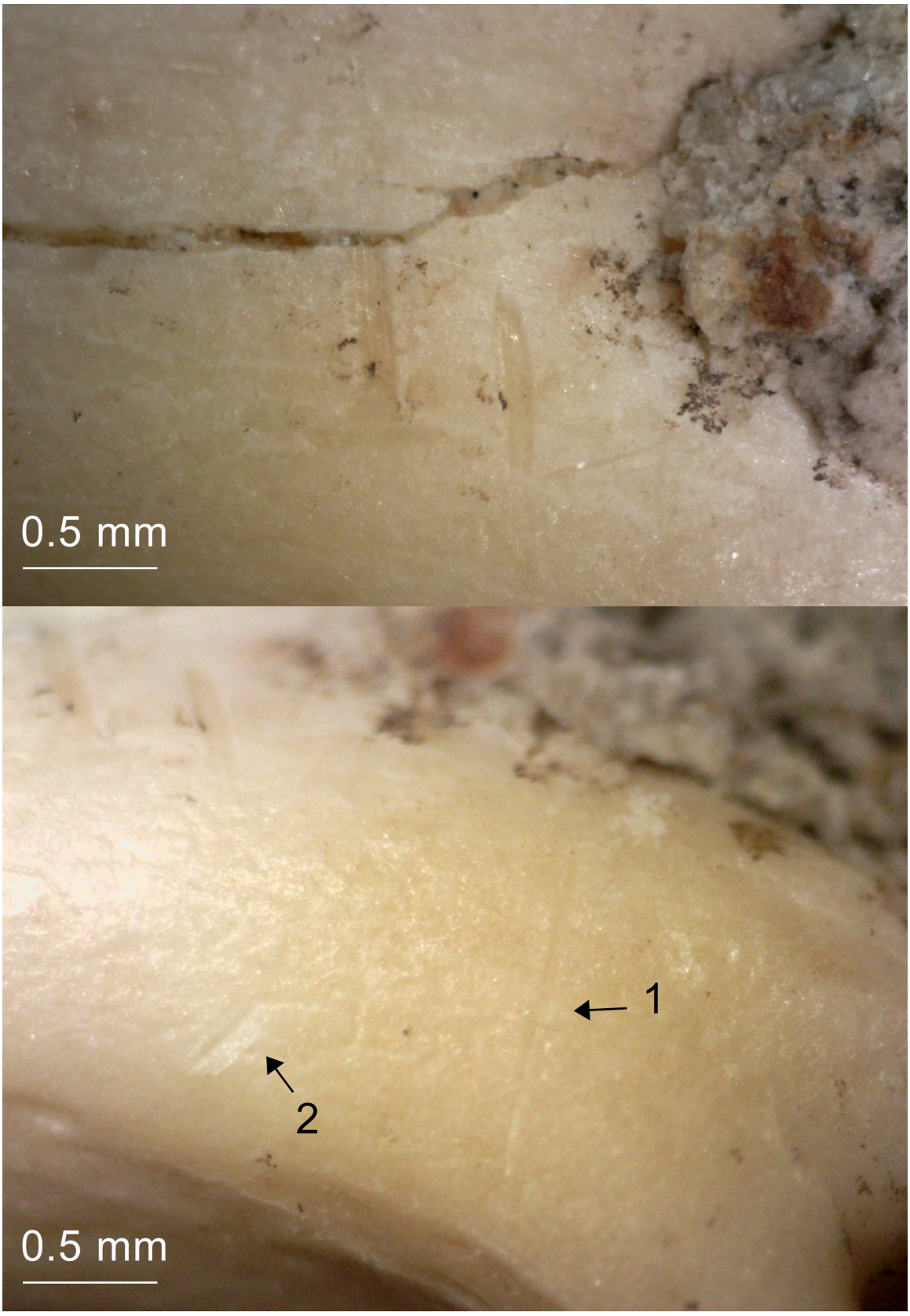

Figure E.23:
Unit: 8B
ID: 3371.1-5
Element: Humerus
Spit: 14
Sediment: NA

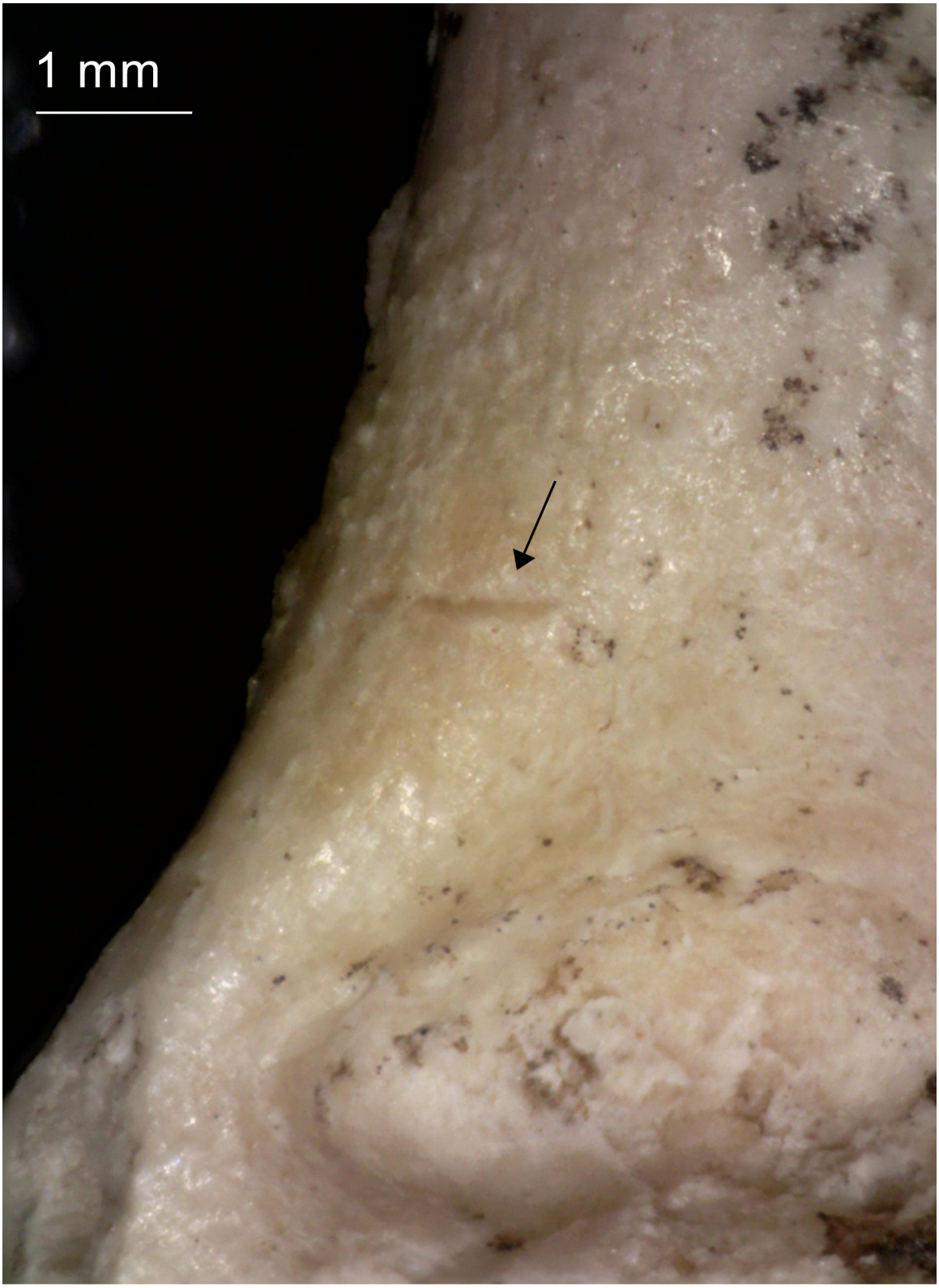

Figure E.24:
Unit: 8B
ID: 3385.1
Element: Humerus
Spit: 14
Sediment: NA
BSM: Cutmark

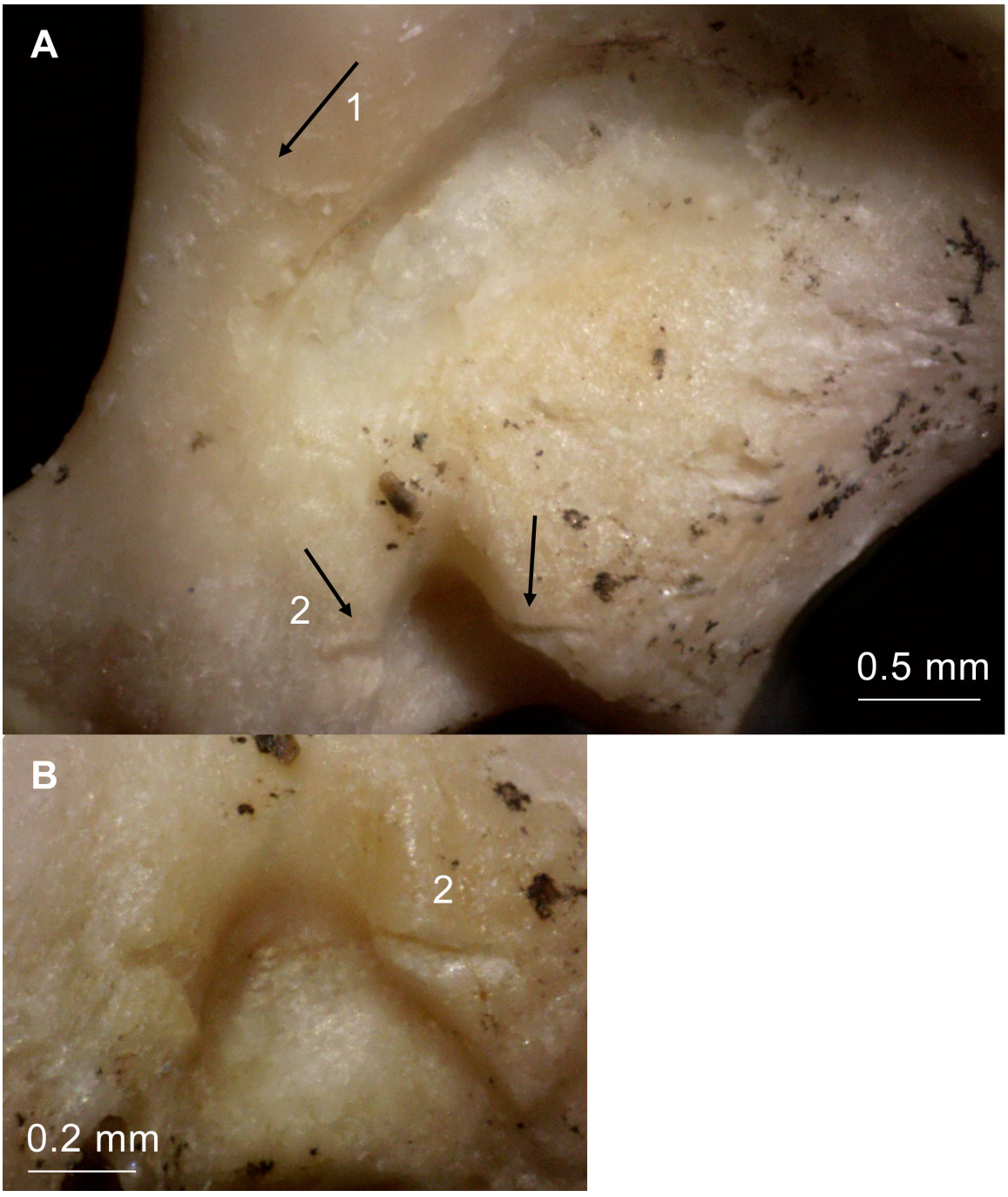

Figure E.25:
Unit: 8B
ID: 3389.1-2
Element: Humerus
Spit: 14
Sediment: NA
BSM: Cutmarks

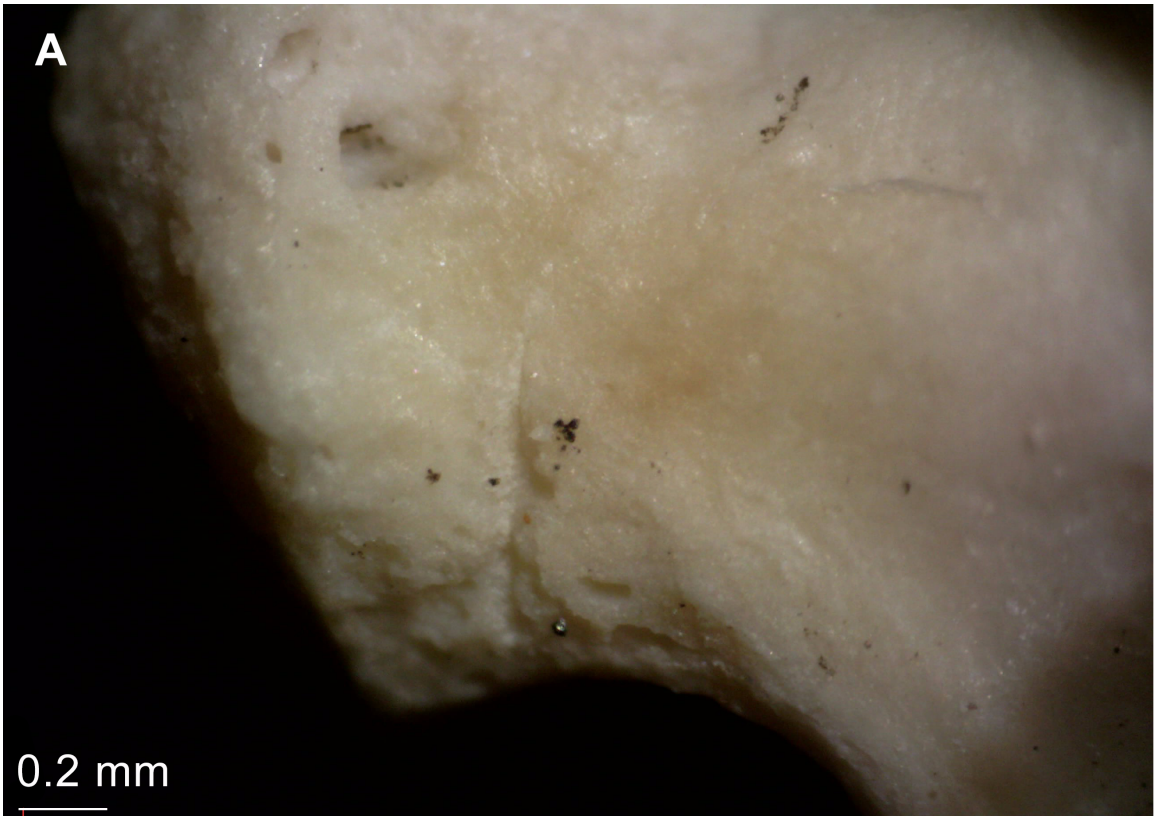

Figure E.26:
Unit: 8B
ID: 3400.1
Element: Femur
Spit: 14
Sediment: NA
BSM: Cutmark

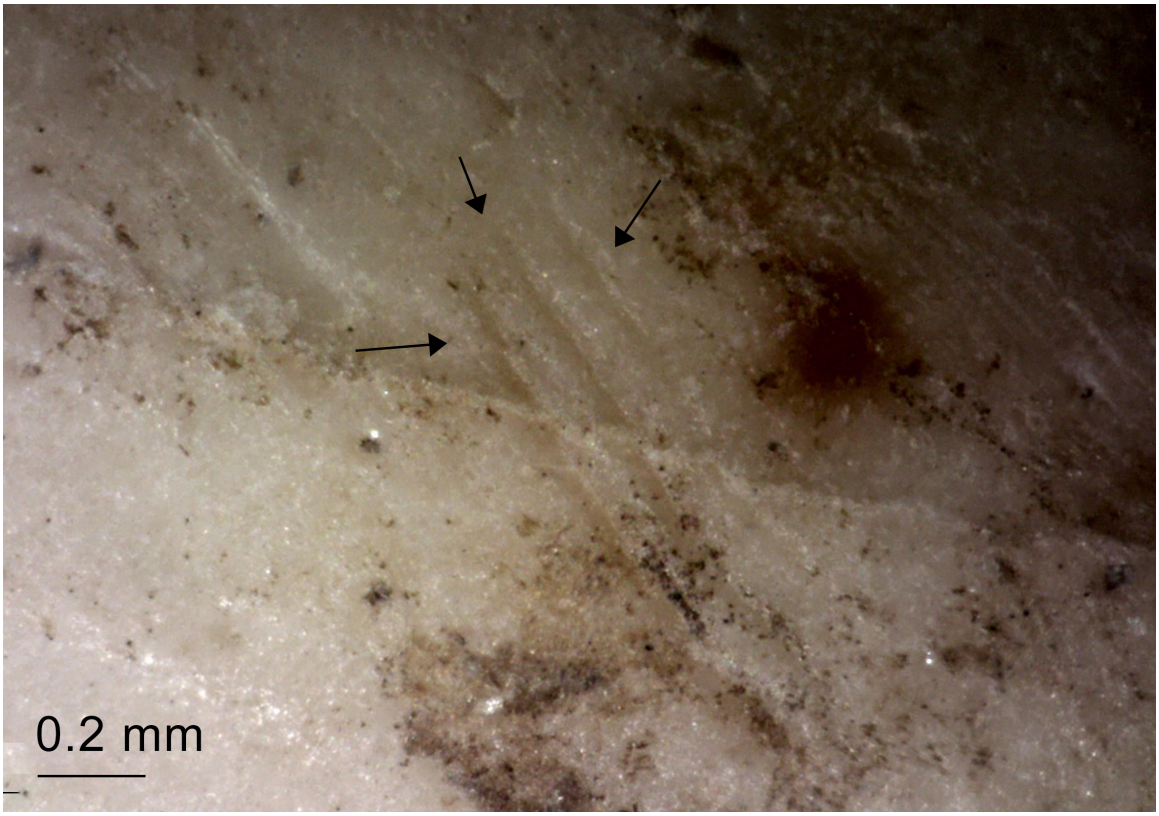

Figure E.27:
Unit: 8B
ID: 3527.1-3
Element: Humerus
Spit: 13
Sediment: NA
BSM: Cutmarks

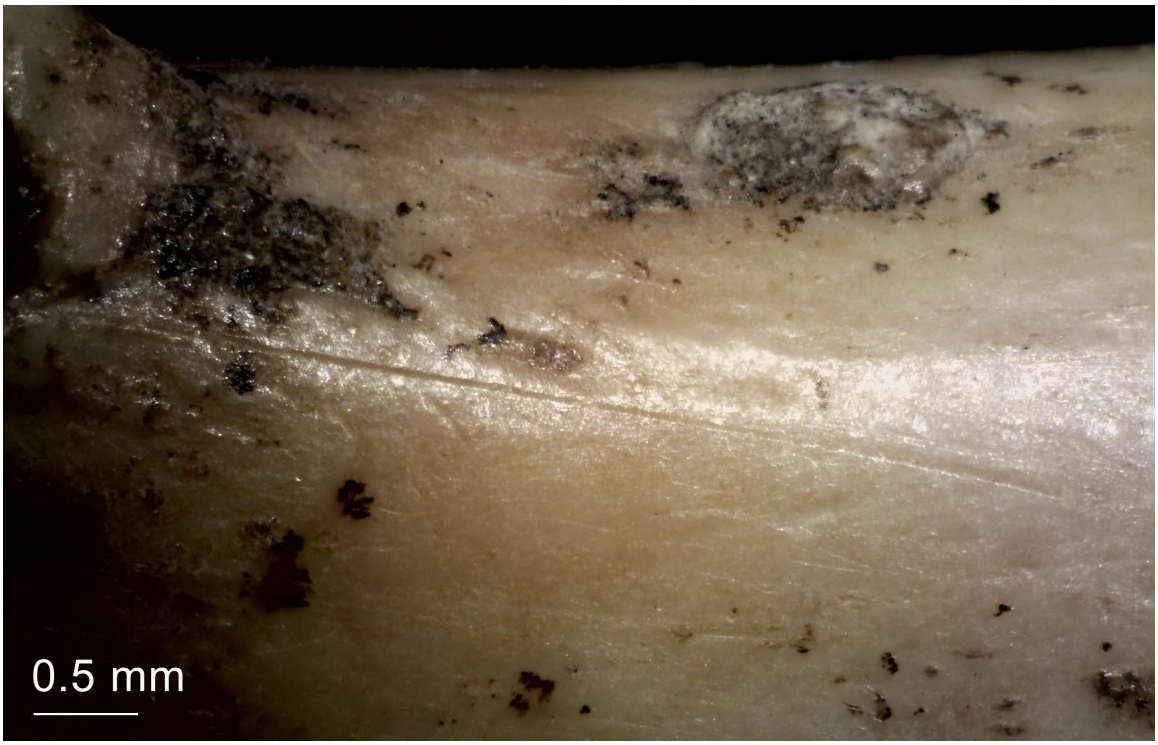

Figure E.28:
Unit: 8B
ID: 3613.1
Element: Femur
Spit: 13
Sediment: NA
BSM: Cutmark

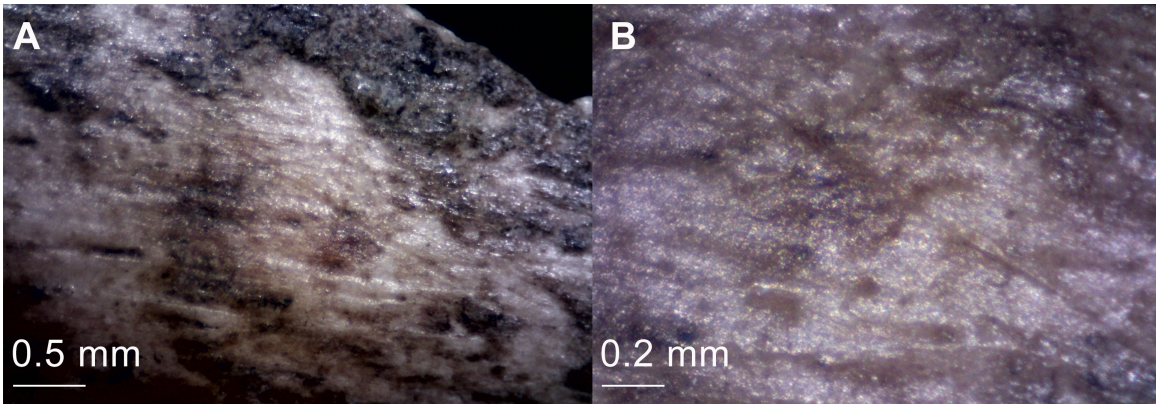

Figure E.29:
Unit: 8B
ID: 3629.1
Element: Tibia
Spit: 13
Sediment: NA
BSM: Cutmark

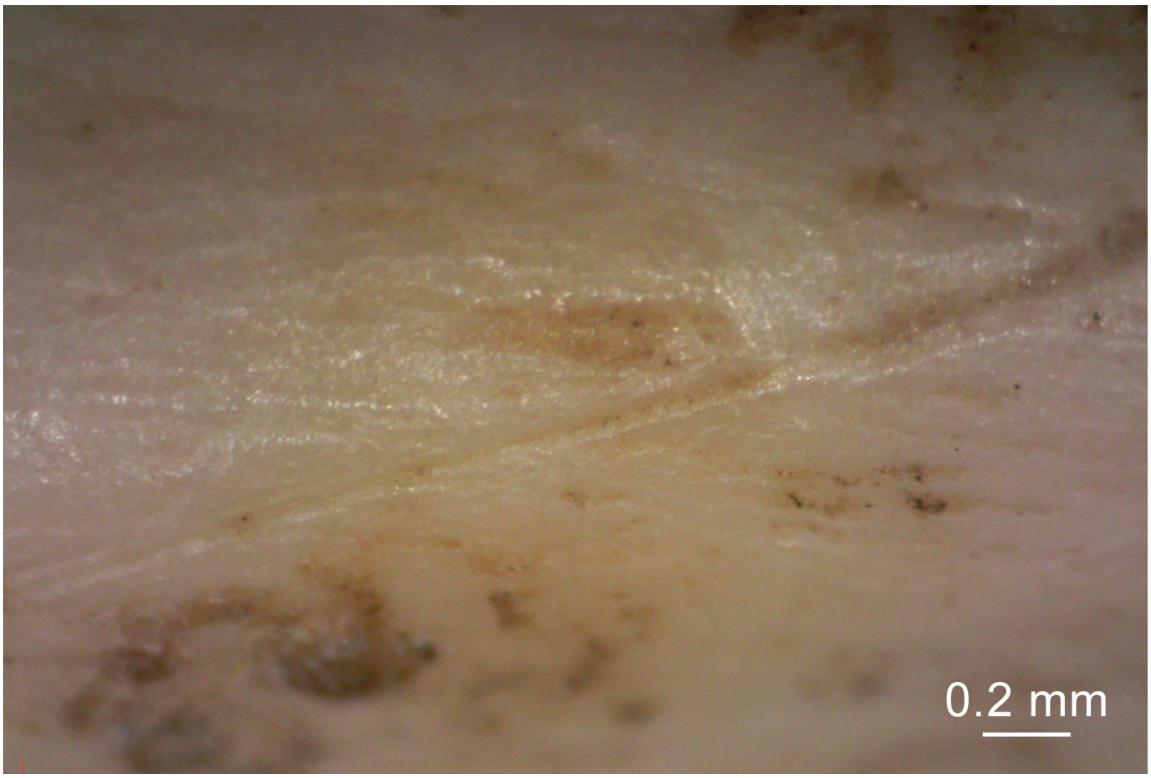

Figure E.30:
Unit: 8B
ID: 3697.1
Element: Innominate
Spit: 13
Sediment: NA
BSM: Cutmark

E.0.5 Unit 8C

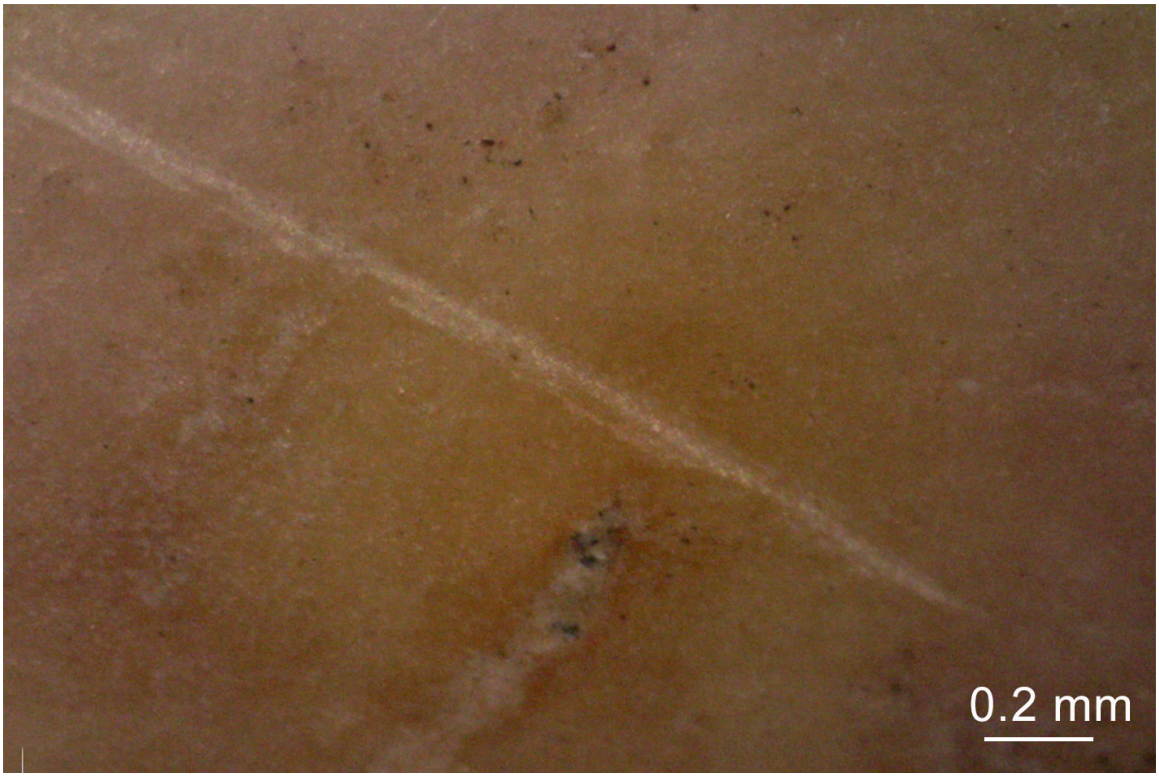

Figure E.31:
Unit: 8C
ID: 5341.1
Element: Femur
Spit: 10
Sediment: NA
BSM: Cutmark

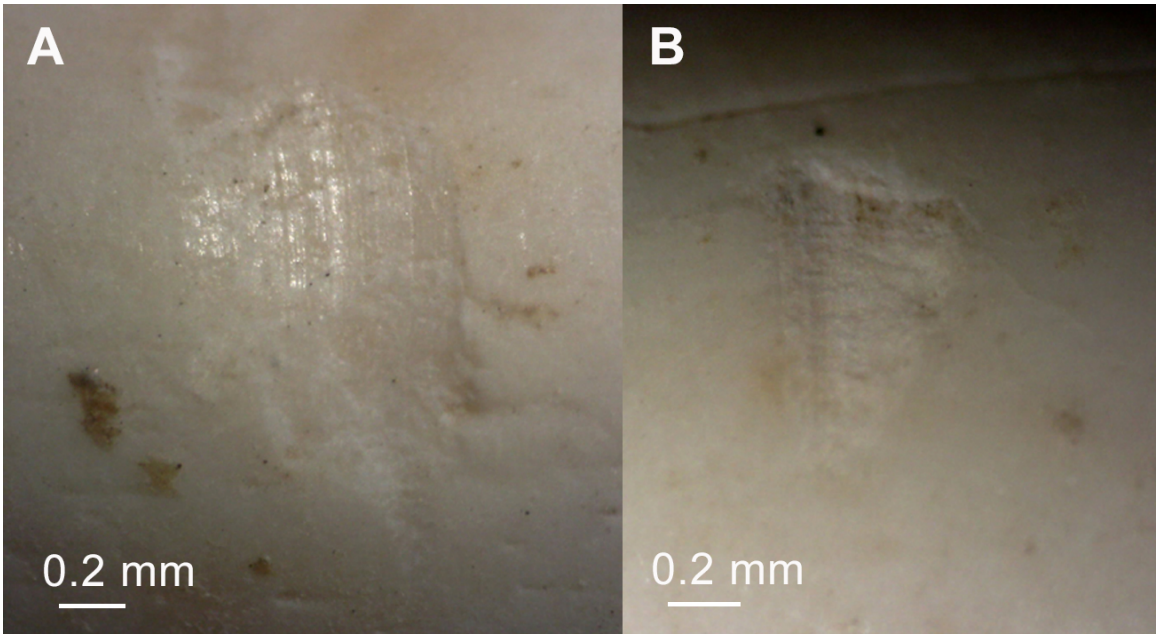

Figure E.32:
Unit: 8C
ID: 5363.1-2
Element: Tibia
Spit: 10
Sediment: NA
BSM: Hominin tooth marks

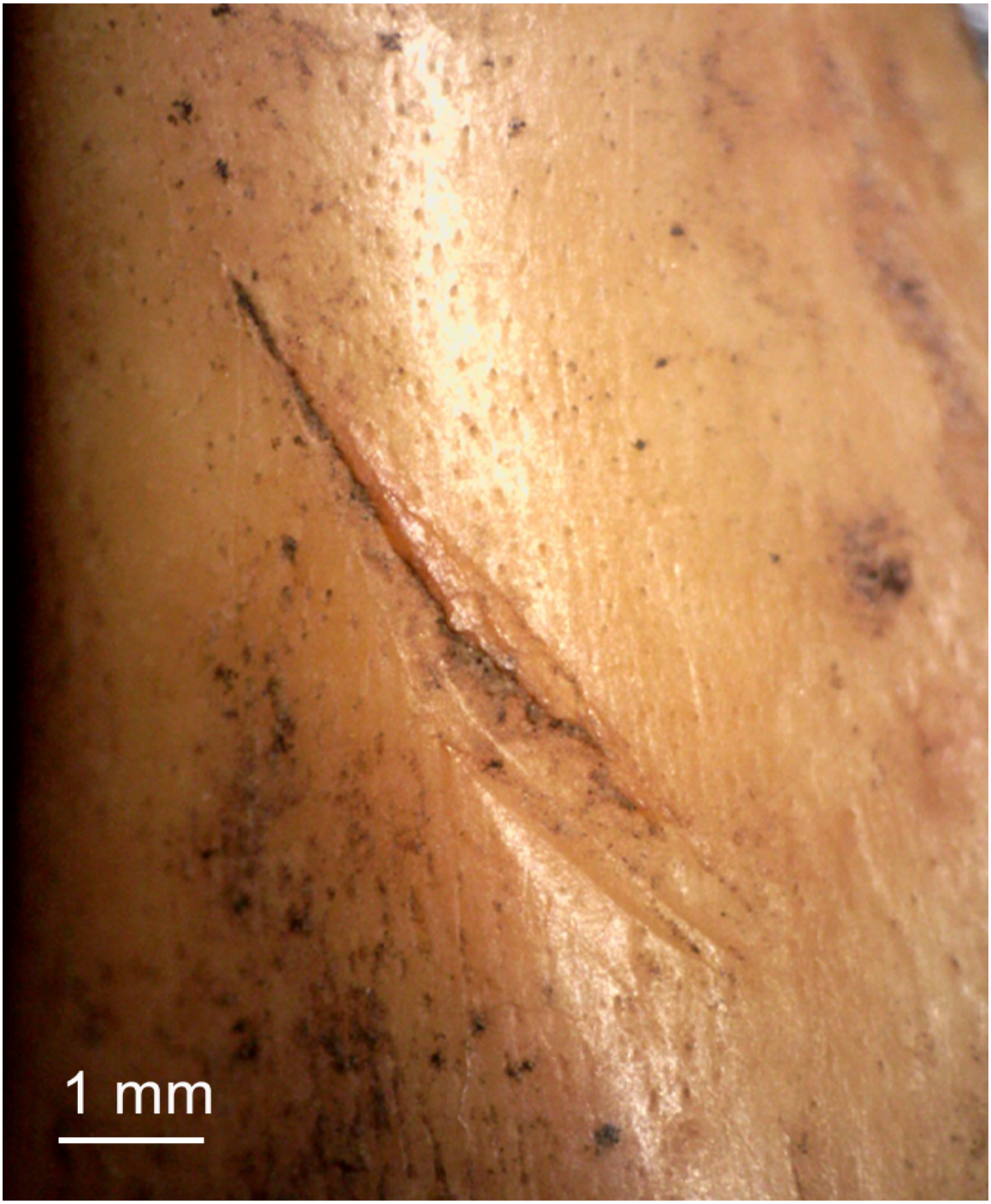

Figure E.33:
Unit: 8C
ID: 5494.1
Element: Femur
Spit: 8
Sediment: NA
BSM: Cutmark

Bibliography

Aiello, L. C. (2010). Five years of *Homo floresiensis*. *American Journal of Physical Anthropology*, 142(2):167–179.

Aiello, L. C. and Wheeler, P. (1995). The Expensive-Tissue Hypothesis: the brain and the digestive-system in human and primate evolution. *Current Anthropology*, 36(2):199–221.

Aigner, J. S. (1981). *Archaeological Remains from Pleistocene China*. München, Verlag C.H. Beck.

Álvarez, M. C., Kaufmann, C. A., Massigoge, A., Gutiérrez, M. A., Rafuse, D. J., Scheifler, N. A., and González, M. E. (2012). Bone modification and destruction patterns of leporid carcasses by Geoffroy's cat (Leopardus geoffroyi): An experimental study. *Quaternary International*, 278:71–80.

Anderson, K. C. (2011). *Stable Carbon And Nitrogen Isotope Analyses Of Subfossil Rats From Liang Bua (flores, Indonesia)*. Masters thesis, University of Central Florida.

Andrade, A. and Fernández, P. M. (2017). Rodent consumption by hunter-gatherers in north Patagonian Andean forests (Argentina): Insights from the small vertebrate taphonomic analysis of two late Holocene archaeological sites. *Journal of Archaeological Science: Reports*, 11:390–399.

Andrews, P. (1990). *Owls, Caves and Fossils: Predation, preservation, and accumulation of small mammal bones in caves, with an analysis of the Pleistocene cave faunas from Westbury-sub-Mendip, Somerset, UK*. University of Chicago Press, Chicago.

Antón, S. C. (2003). Natural History of *Homo erectus*. *Yearbook of Physical Anthropology*, 46:126–169.

Anton, S. C., Potts, R., and Aiello, L. C. (2014). Evolution of early *Homo*: An integrated biological perspective. *Science*, 345:1236828.

Argue, D., Donlon, D., Groves, C., and Wright, R. (2006). *Homo floresiensis*: Microcephalic, pygmoid, *Australopithecus*, or *Homo*? *Journal of Human Evolution*, 51:360–374.

Argue, D., Groves, C. P., Lee, M. S. Y., and Jungers, W. L. (2017). The affinities of *Homo floresiensis* based on phylogenetic analyses of cranial, dental, and postcranial characters. *Journal of Human Evolution*, 107:107–133.

Argue, D., Morwood, M. J., Sutikna, T., Jatmiko, and Saptomo, E. W. (2009). *Homo floresiensis*: a cladistic analysis. *Journal of Human Evolution*, 57(5):623–639.

Armstrong, A. (2016). Eagles, owls, and coyotes (oh my!): Taphonomic analysis of rabbits and guinea pigs fed to captive raptors and coyotes. *Journal of Archaeological Science: Reports*, 5:135–155.

Armstrong, A. and Avery, G. (2014). Taphonomy of Verreaux's Eagle (*Aquila verreauxii*) prey accumulations from the Cape Floral Region, South Africa: Implications for archaeological interpretations. *Journal of Archaeological Science*, 52:163–183.

Armstrong, A. J. (2015). *Small Mammal Taphonomy and Utilization by Middle Stone Age Humans in the Cape Floristic Region of South Africa*. Phd thesis, University of Minnesota.

Avenant, N. (2000). Small mammal community characteristics as indicators of ecological disturbance in the Willem Pretorius Nature Reserve, Free State, South Africa. *South African Journal of Wildlife Research*, 30(1):26–33.

Ayliffe, L. K., Gagan, M. K., Zhao, J. X., Drysdale, R. N., Hellstrom, J. C., Hantoro, W. S., Griffiths, M. L., Scott-Gagan, H., Pierre, E. S., Cowley, J. A., and Suwargadi, B. W. (2013). Rapid interhemispheric climate links via the Australasian monsoon during the last deglaciation. *Nature Communications*, 4:1–6.

Baab, K. L., Brown, P., Falk, D., Richtsmeier, J. T., Hildebolt, C. F., Smith, K., and Jungers, W. (2016). A critical evaluation of the down syndrome diagnosis for LB1, type specimen of *Homo floresiensis*. *PLoS ONE*, 11(6):e0155731.

Baab, K. L. and Mcnulty, K. P. (2009). Size, shape, and asymmetry in fossil hominins: the status of the LB1 cranium based on 3D morphometric analyses. *Journal of Human Evolution*, 57:608–622.

Baab, K. L., Mcnulty, K. P., and Harvati, K. (2013). *Homo floresiensis* Contextualized: A Geometric Morphometric Comparative Analysis of Fossil and Pathological Human Samples. *PLoS ONE*, 8(7):69119.

Balzeau, A. and Charlier, P. (2016). What do cranial bones of LB1 tell us about *Homo floresiensis*? *Journal of Human Evolution*, 93:12–24.

Barham, L., Groves, C., and Thorne, A. (2004). Some initial informal reactions to publication of the discovery of *Homo floresiensis* and replies from Brown and Morwood. *Before Farming*, 2(4):1–7.

Barker, G., Piper, P. J., and Rabett, R. J. (2009). Zooarchaeology at the Niah Caves, Sarawak: Context and Research Issues. *International Journal of Osteoarchaeology*, 463:447–463.

Barr, W. A. and Biernat, M. (2020). Mammal functional diversity and habitat heterogeneity: Implications for hominin habitat reconstruction. *Journal of Human Evolution*, 146:102853.

Bednarik, R. G. (2003). Seafaring in the Pleistocene. *Cambridge Archaeological Journal*, 13(1):41–66.

Bednarik, R. G. (2009). Reviewing the Flores Hobbit Chronicles. *Anthropos*, 104:195–198.

Berger, L. R., Hawks, J., de Ruiter, D. J., Churchill, S. E., Schmid, P., Delezene, L. K., Kivell, T. L., Garvin, H. M., Williams, S. A., DeSilva, J. M., Skinner, M. M., Musiba, C. M., Cameron, N., Holliday, T. W., Harcourt-Smith, W., Ackermann, R. R., Bastir, M., Bogin, B., Bolter, D., Brophy, J., Cofran, Z. D., Congdon, K. A., Deane, A. S., Dembo, M., Drapeau, M., Elliott, M. C., Feuerriegel, E. M., Garcia-Martinez, D., Green, D. J., Gurtov, A., Irish, J. D., Kruger, A., Laird, M. F., Marchi, D., Meyer, M. R., Nalla, S., Negash, E. W., Orr, C. M., Radovcic, D., Schroeder, L., Scott, J. E., Throckmorton, Z., Tocheri, M. W., VanSickle, C., Walker, C. S., Wei, P., and Zipfel, B. (2015). *Homo naledi*, a new species of the genus *Homo* from the Dinaledi Chamber, South Africa. *eLife*, 4:e09560.

Bettinger, R. L., Garvey, R., and Tushingham, S. (2015). *Hunter-Gatherers: Archaeological and Evolutionary Theory*. Springer Science+Business Media, New York, second edition.

Binford, L. R. (1981). *Bones: Ancient Men and Modern Myths*. Academic Press, New York.

Bird, D. W., Bird, R. B., and Codding, B. F. (2009). In Pursuit of Mobile Prey: Martu Hunting Strategies and Archaeofaunal Interpretation. *American Antiquity*, 74(1):3–29.

Bird, D. W., Bird, R. B., and Parker, C. H. (2005a). Aboriginal burning regimes and hunting strategies in australias western desert. *Human Ecology*, 33(4):443–464.

Bird, M. I., Taylor, D., and Hunt, C. (2005b). Palaeoenvironments of insular Southeast Asia during the Last Glacial Period: a savanna corridor in Sundaland? *Quaternary Science Reviews*, 24:2228–2242.

Blasco, R., Rosell, J., Fernández Peris, J., Luis Arsuaga, J., María Bermúdez de Castro, J., and Carbonell, E. (2013). Environmental availability, behavioural diversity and diet: a zooarchaeological approach from the TD10-1 sublevel of Gran Dolina (Sierra de Atapuerca, Burgos, Spain) and Bolomor Cave (Valencia, Spain). *Quaternary Science Reviews*, 70:124–144.

Blasco, R., Rosell, J., Sánchez-Marco, A., Gopher, A., and Barkai, R. (2019). Feathers and food: Human-bird interactions at Middle Pleistocene Qesem Cave, Israel. *Journal of Human Evolution*, 136:102653.

Blumenschine, R. J. (1988). An experimental model of the timing of hominid and carnivore influence on archaeological bone assemblages. *Journal of Archaeological Science*, 15(5):483–502.

Blumenschine, R. J. (1991). Hominid carnivory and foraging strategies, and the socio-economic function of early archaeological sites. *Philosophical Transactions: Biological Sciences*, 334(1270):211–221.

Blumenschine, R. J., Marean, C. W., and Capaldo, S. D. (1996). Blind Tests of Inter-analyst Correspondence and Accuracy in the Identification of Cut Marks,

Percussion Marks, and Carnivore Tooth Marks on Bone Surfaces. *Journal of Archaeological Science*, 23(4):493–507.

Blumenschine, R. J., Whiten, A., and Hawkes, K. (1991). Hominid Carnivory and Foraging Strategies, and the Socio-Economic Function of Early Archaeological Sites [and Discussion]. *Philosophical Transactions of the Royal Society B: Biological Sciences*, 334(1270):211–221.

Bochenski, Z. M., Tomek, T., Tornberg, R., and Wertz, K. (2009). Distinguishing nonhuman predation on birds: pattern of damage done by the white-tailed eagle *Haliaetus albicilla*, with comments on the punctures made by the golden eagle *Aquila chrysaetos*. *Journal of Archaeological Science*, pages 122–129.

Boyd, R., Richerson, P. J., and Henrich, J. (2011). The cultural niche: Why social learning is essential for human adaptation. *Proceedings of the National Academy of Sciences*, 108:10918–10925.

Brain, C. K. (1969). The Contribution of Namib Desert Hottentots to an Understanding of Australopithecine Bone Accumulations. *Scientific Papers of the Namib Desert Research Station*, 39(9):13–22.

Brain, C. K. (1981). *The Hunters or the Hunted? An Introduction to African Cave Taphonomy*. The University of Chicago Press, Chicago.

Braun, D. R., Harris, J. W. K., Levin, N. E., McCoy, J. T., Herries, A. I. R., Bamford, M. K., Bishop, L. C., Richmond, B. G., and Kibunjia, M. (2010). Early hominin diet included diverse terrestrial and aquatic animals 1.95 Ma in East Turkana, Kenya. *Proceedings of the National Academy of Sciences*, 107(22):10002–10007.

Bromham, L. and Cardillo, M. (2007). Primates follow the 'island rule': implications for interpreting *Homo floresiensis*. *Biology Letters*, 3:398–400.

Bronikowski, A. M., Alberts, S. C., Altmann, J., Packer, C., Dee Carey, K., Tatar, M., and Wachter, K. W. (2002). The aging baboon: Comparative demography in a non-human primate. *Proceedings of the National Academy of Sciences*, 99(14):9591–9595.

Bronikowski, A. M., Altmann, J., Brockman, D. K., Cords, M., Fedigan, L. M., Pusey, A., Stoinski, T., Morris, W. F., Strier, K. B., and Alberts, S. C. (2011). Aging in the natural world: Comparative data reveal similar mortality patterns across primates. *Science*, 331(6022):1325–1328.

Broughton, J. M., Cannon, M. D., Bartelink, E. J., Broughton, J. M., Cannon, M. D., and Bartelink, E. J. (2010). Evolutionary ecology, resource depression, and niche construction theory: applications to central California hunter-gatherers and Mimbres-Mogollon agriculturalists. *J Archaeol Method Theory*, 17:371–421.

Broughton, J. M., Cannon, M. D., Bayham, F. E., and Byers, D. A. (2011). Prey body size and ranking in zooarchaeology: Theory, empirical evidence, and applications from the northern Great Basin. *American Antiquity*, 76(3):403–428.

Brown, K., Fa, D. A., Finlayson, G., and Finlayson, C. (2011). Small game and marine resource exploitation by Neanderthals: The evidence from Gibraltar. In Bicho N.F. et al., editor, *Trekking the Shore: Changing Coastlines and the Antiquity of Coastal Settlement, Interdisciplinary Contributions to Archaeology*, chapter 10, pages 247–272. Springer Science+Business Media, LLC.

Brown, P. (2012). LB1 and LB6 *Homo floresiensis* are not modern human (*Homo sapiens*) cretins. *Journal of Human Evolution*, 62(2):201–224.

Brown, P. and Maeda, T. (2009). Liang Bua *Homo floresiensis* mandibles and mandibular teeth: a contribution to the comparative morphology of a new hominin species. *Journal of Human Evolution*, 57:571–596.

Brown, P., Sutikna, T., Morwood, M. J., Soejono, R. P., Jatmiko, Saptomo, E. W., and Due, R. A. (2004). A new small-bodied hominin from the Late Pleistocene of Flores, Indonesia. *Nature*, 431(7012):1055–1061.

Brumm, A., Aziz, F., van den Bergh, G. D., Morwood, M. J., Moore, M. W., Kurniawan, I., Hobbs, D. R., and Fullagar, R. (2006). Early stone technology on Flores and its implications for *Homo floresiensis*. *Nature*, 441(7093):624–628.

Brumm, A., Bergh, G. D. V. D., Storey, M., Kurniawan, I., Brent, V., Setiyabudi, E., Grün, R., and Mark, W. (2016). Age and context of the oldest known hominin fossils from Flores. *Nature*, 534(7606):249–253.

Brumm, A., Jensen, G. M., van den Bergh, G. D., Morwood, M. J., Kurniawan, I., Aziz, F., and Storey, M. (2010). Hominins on Flores, Indonesia, by one million years ago. *Nature*, 464(7289):748–52.

Burger, O., Hamilton, M. J., and Walker, R. (2005). The prey as patch model: optimal handling of resources with diminishing returns. *Journal of Archaeological Science*, 32:114–1158.

Cannon, M. D. (2013). NISP, Bone Fragmentation, and the Measurement of Taxonomic Abundance. *Journal of Archaeological Method and Theory*, 20(3):397–419.

Capaldo, S. D. and Blumenschine, R. J. (1994). A Quantitative Diagnosis of Notches Made by Hammerstone Percussion and Carnivore Gnawing on Bovid Long Bones. *American Antiquity*, 59(4):724–748.

Catón, J. and Tucker, A. S. (2009). Current knowledge of tooth development: patterning and mineralization of the murine dentition. *Journal of Anatomy*, 214:502–515.

Charnov, E. (1976). Optimal foraging: The marginal value theorem. *Theoretical Population Biology*, 9(2):129–136.

Cheng, H., Zhang, H., Spötl, C., Baker, J., Sinha, A., Li, H., Bartolomé, M., Moreno, A., Kathayat, G., Zhao, J., Dong, X., Li, Y., Ning, Y., Jia, X., Zong, B., Brahim, Y. A., Pérez-Mejiás, C., Cai, Y., Novello, V. F., Cruz, F. W., Severinghaus, J. P., An, Z., and Edwards, R. L. (2020). Timing and structure of the Younger Dryas event and its underlying climate dynamics. *Proceedings of the National Academy of Sciences*, 117(38):23408–23417.

Clark, J. L. (2011). The evolution of human culture during the later Pleistocene: Using fauna to test models on the emergence and nature of "modern" human behavior. *Journal of Anthropological Archaeology*, 30(3):273–291.

Cochard, D., Brugal, J. P., Morin, E., and Meignen, L. (2012). Evidence of small fast game exploitation in the Middle Paleolithic of Les Canalettes Aveyron, France. *Quaternary International*, 264:32–51.

Codding, B. F. and Bird, D. W. (2015). Behavioral ecology and the future of archaeological science. *Journal of Archaeological Science*, 56:9–20.

Comay, O. and Dayan, T. (2018). Taphonomic signatures of owls: New insights into micromammal assemblages. *Palaeogeography, Palaeoclimatology, Palaeoecology*, 492:81–91.

Conard, N., Kitagawa, K., Kronneck, P., Bohme, M., and Munzel, S. (2013). The Importance of Fish, Fowl and Small Mammals in the Paleolithic Diet of the Swabian Jura, Southwestern Gernmany. In Clark, J. L. and Speth, J. D., editors, *Zooarchaeology and Modern Human Origins: Human Hunting Behavior during the Later Pleistocene*, chapter 11, pages 209–225. Springer Science+Business Media, Dordrecht.

Cruz-Uribe, K. and Klein, R. G. (1998). Hyrax and Hare Bones from Modern South

African Eagle Roosts and the Detection of Eagle Involvement in Fossil Bone Assemblages. *Journal of Archaeological Science*, 25:135–147.

D'Amore, D. C. and Blumenschine, R. J. (2009). Komodo monitor (*Varanus komodoensis*) feeding behavior and dental function reflected through tooth marks on bone surfaces, and the application to ziphodont paleobiology and the application to ziphodont paleobiology. *Paleobiology*, 35(4):525–552.

Darwin, C. (1871). *The descent of man and selection in relation to sex*. Albermarie Street, London.

Delgado Huertas, A., Iacumin, P., Stenni, B., Sanchez Chillon, B., and Longinelli, A. (1995). Oxygen isotope variations of phosphate in mammalian bone and tooth enamel. *Geochimica et Cosmochimica Acta*, 59(20):4299–4305.

Dembo, M., Matzke, N. J., Mooers, A. Ø., and Collard, M. (2015). Bayesian analysis of a morphological supermatrix sheds light on controversial fossil hominin relationships. *Proceedings of the Royal Society B*, 282(1812):20150943.

Deniro, M. J. (1987). Stable Isotopy and Archaeology. *American Scientist*, 75(2):182–191.

Dennell, R. and Roebroeks, W. (2005). An Asian perspective on early human dispersal from Africa. *Nature*, 438(7071):1099–1104.

Dennell, R. W. (2010). The Colonization of "Savannahstan": Issues of Timing(s) and Patterns of Dispersal Across Asia in the Late Pliocene and Early Pleistocene. In Norton, C. J. and Braun, D. R., editors, *Asian Paleoanthropology*, chapter 2, pages 7–30. Springer, Dordrecht.

Denniston, R. F., Asmerom, Y., Polyak, V. J., Wanamaker, A. D., Ummenhofer, C. C., Humphreys, W. F., Cugley, J., Woods, D., and Lucker, S. (2017). Decoupling

of monsoon activity across the northern and southern Indo-Pacific during the Late Glacial. *Quaternary Science Reviews*, 176:101–105.

Denniston, R. F., Wyrwoll, K. H., Polyak, V. J., Brown, J. R., Asmerom, Y., Wanamaker, A. D., LaPointe, Z., Ellerbroek, R., Barthelmes, M., Cleary, D., Cugley, J., Woods, D., and Humphreys, W. F. (2013). A Stalagmite record of holocene indonesian-australian summer monsoon variability from the australian tropics. *Quaternary Science Reviews*, 78:155–168.

Détroit, F., Salvador Mijares, A., Corny, J., Daver, G., Zanolli, C., Dizon, E., Robles, E., Grün, R., and Piper, P. J. (2019). A new species of *Homo* from the Late Pleistocene of the Philippines. *Nature*, 568:181–186.

Dewar, G., Halkett, D., Hart, T., Orton, J., and Sealy, J. (2006). Implications of a mass kill site of springbok (*Antidorcas marsupialis*) in South Africa: hunting practices, gender relations, and sharing in the Later Stone Age. *Journal of Archaeological Science*, 33(9):1266–1275.

Dodson, P. and Diane, W. (1979). Taphonomic Investigation of Owl Pellets. *Paleobiology*, 5(3):275–284.

Domínguez-Rodrigo, M. (2002). Hunting and scavenging by early humans: the state of the debate. *Journal of World Prehistory*, 16(1):1–54.

Domínguez-Rodrigo, M. and Barba, R. (2006). New estimates of tooth mark and percussion mark frequencies at the FLK Zinj site: the carnivore-hominid-carnivore hypothesis falsified. *Journal of Human Evolution*, 50(2):170–194.

Domínguez-Rodrigo, M., de Juana, S., Galán, A. B., and Rodríguez, M. (2009a). A new protocol to differentiate trampling marks from butchery cut marks. *Journal of Archaeological Science*, 36(12):2643–2654.

Domínguez-Rodrigo, M., Mabulla, A., Bunn, H. T., Barba, R., Diez-Martín, F., Egeland, C. P., Espílez, E., Egeland, A., Yravedra, J., and Sá Nchez, P. (2009b). Unraveling hominin behavior at another anthropogenic site from Olduvai Gorge (Tanzania): new archaeological and taphonomic research at BK, Upper Bed II. *Journal of Human Evolution*, 57:260–283.

Domínguez-Rodrigo, M. and Pickering, T. R. (2017). The meat of the matter: an evolutionary perspective on human carnivory. *Azania: Archaeological Research in Africa*, 52(1):4–32.

Domínguez-Rodrigo, M., Pickering, T. R., and Bunn, H. T. (2012). Experimental study of cut marks made with rocks unmodified by human flaking and its bearing on claims of ∼3.4-million-year-old butchery evidence from Dikika, Ethiopia. *Journal of Archaeological Science*, 39(2):205–214.

Domínguez-Rodrigo, M., Pickering, T. R., Semaw, S., and Rogers, M. J. (2005). Cutmarked bones from Pliocene archaeological sites at Gona, Afar, Ethiopia: implications for the function of the world's oldest stone tools. *Journal of Human Evolution*, 48(2):109–121.

Domínguez-Rodrigo, M. and Piqueras, A. (2003). The use of tooth pits to identify carnivore taxa in tooth-marked archaeofaunas and their relevance to reconstruct hominid carcass processing behaviours. *Journal of Archaeological Science*, 30(11):1385–1391.

Domínguez-Solera, S. and Domínguez-Rodrigo, M. (2011). A taphonomic study of a carcass consumed by griffon vultures (*Gyps fulvus*) and its relevance for the interpretation of bone surface modifications. *Journal of Archaeological and Anthropological Sciences*, 3:385–392.

Du, A., Zipkin, A. M., Hatala, K. G., Renner, E., Baker, J. L., Bianchi, S., Bernal,

K. H., and Wood, B. A. (2018). Pattern and process in hominin brain size evolution are scale-dependent. *Proceedings of the Royal Society B*, 285(1873):1–8.

Dubois, E. (1896). On *Pithecanthropus erectus*: a transitional form between man and the apes. *The Journal of the Anthropological Institute of Great Britain and Ireland*, 25:240–255.

Estioko-Griffin, A. A. and Griffin, P. (1981). Woman the hunter: the Agta. In Dahlberg, F., editor, *Woman the Gatherer*, pages 12–151. Yale University Press, New Haven.

Evans, B. J., Gansauge, M.-T., Tocheri, M. W., Schillaci, M. A., Sutikna, T., Jatmiko, Saptomo, E. W., Klegarth, A., Tosi, A. J., Melnick, D. J., and Meyer, M. (2020). Mitogenomics of macaques (*Macaca*) across Wallace's Line in the context of modern human dispersals. *Journal of Human Evolution*, 146:102852.

Fa, J. E., Stewart, J. R., Lloveras, L., and Vargas, J. M. (2013). Rabbits and hominin survival in Iberia. *Journal of Human Evolution*, 64(4):233–241.

Faith, J. T. (2013). Taphonomic and paleoecological change in the large mammal sequence from Boomplaas Cave, western Cape, South Africa. *Journal of Human Evolution*, 65:715–730.

Faith, J. T., Rowan, J., and Du, A. (2019). Early hominins evolved within non-analog ecosystems. *Proceedings of the National Academy of Sciences*, 116(43):21478–21483.

Falk, D., Hildebolt, C., Smith, K., Morwood, M., Sutikna, T., Brown, P., Jatmiko, Saptomo, W., Brunsden, B., and Prior, F. (2005a). The brain of LB1, *Homo floresiensis*. *Science*, 308(5719):242–245.

Falk, D., Hildebolt, C., Smith, K., Morwood, M. J., Sutikna, T., Saptomo, E. W.,

and Prior, F. (2009). LB1's virtual endocast, microcephaly, and hominin brain evolution. *Journal of Human Evolution*, 57:597–607.

Falk, D., Hildebolt, C., Smith, K., Morwood, M. J., Sutikna, T., Wayhu Saptomo, E., Imhof, H., Seidler, H., and Prior, F. (2007). Brain shape in human microcephalics and *Homo floresiensis*. *Proceedings of the National Academy of Sciences*, 104(7):2513–2518.

Falk, D., Hildebolt, C. F., Smith, K., Morwood, M. J., Sutikna, T., Jatmiko, Saptomo, W. E., Brunsden, B., and Prior, F. (2005b). Response to comment on "The Brain of LB1, *Homo floresiensis*". *Science*, 310:236c.

Fernandez, F. J., Montalvo, C. I., Fernandez-Jalvo, Y., Andrews, P., and Manuel opez, J. L. (2016). A re-evaluation of the taphonomic methodology for the study of small mammal fossil assemblages of South America. *Quaternary Science Reviews*, 155:37–49.

Fernandez-Jalvo, Y. (1995). Small mammal taphonomy at La Trinchera de Atapuerca (Burgos, Spain). A remarkable example of taphonomic criteria used for stratigraphic correlations and palaeoenvironment interpretations. *Palaeo*, 114:167–195.

Fernandez-Jalvo, Y. and Andrews, P. (1992). Small Mammal Taphonomy of Gran Dolina, Atapuerca (Burgos), Spain. *Journal of Archaeological Science*, 19:407–428.

Fernández-Jalvo, Y. and Andrews, P. (2011). When humans chew bones. *Journal of Human Evolution*, 60(1):117–123.

Fernández-Jalvo, Y. and Andrews, P. (2016). *Atlas of Taphonomic Identifications*. Springer Science+Business Media, Dordrecht.

Fernandez-Jalvo, Y., Andrews, P., and Denys, C. (1999). Cut marks on small mammals at Olduvai Gorge Bed-I. *Journal of Human Evolution*, 36(5):587–589.

Fernández-Jalvo, Y., Andrews, P., Denys, C., Sesé, C., Stoetzel, E., Marin-Monfort, D., and Pesquero, D. (2016). Taphonomy for taxonomists: Implications of predation in small mammal studies. *Quaternary Science Reviews*, 139:138–157.

Fernandez-Jalvo, Y. and Avery, D. M. (2015). Pleistocene Micromammals and Their Predators at Wonderwerk Cave, South Africa. *African Archaeological Review*, 32(4):751–791.

Ferraro, J. V., Plummer, T. W., Pobiner, B. L., Oliver, J. S., Bishop, L. C., Braun, D. R., Ditchfield, P. W., Seaman, J. W., Binetti, K. M., Seaman, J. W., Hertel, F., and Potts, R. (2013). Earliest archaeological evidence of persistent hominin carnivory. *PLoS ONE*, 8(4):e62174.

Fiedler, L. (1990). Rodents as a food source. *Proceedings of the Vertebrate Pest Conference*, 14:149–155.

Foster, J. B. (1964). Evolution of mammals on islands. *Nature*, 202(4929):234–235.

Fuentes, A. (2014). The extended evolutionary synthesis, ethnography, and the human niche toward an integrated anthropology. *Current Anthropology*, 57(13):S13–S26.

Fuentes, A. (2015). Integrative Anthropology and the Human Niche: Toward a Contemporary Approach to Human Evolution. *American Anthropologist*, 117(2):302–315.

Fuentes, A. (2017). *The creative spark: How imagination made humans exceptional*. Dutton, New York.

Fuentes, A., Wyczalkowski, M. A., and MacKinnon, K. C. (2010). Niche construction

through cooperation: A nonlinear dynamics contribution to modeling facets of the evolutionary history in the genus *Homo*. *Current Anthropology*, 51(3):435–444.

Gaffney, D. (2021). Pleistocene water crossings and adaptive flexibility within the *Homo* genus. *Journal of Archaeological Research*, 29(2):255–326.

Gaffney, D., Summerhayes, G. R., Luu, S., Menzies, J., Douglass, K., Spitzer, M., and Bulmer, S. (2021). Small game hunting in montane rainforests: Specialised capture and broad spectrum foraging in the Late Pleistocene to Holocene New Guinea Highlands. *Quaternary Science Reviews*, 253:106742.

Galán, A. B., Rodríguez, M., De Juana, S., and Domínguez-Rodrigo, M. (2009). A new experimental study on percussion marks and notches and their bearing on the interpretation of hammerstone-broken faunal assemblages. *Journal of Archaeological Science*, 36:776–784.

Garvie-Lok, S. J., Varney, T. L., and Katzenberg, M. A. (2004). Preparation of bone carbonate for stable isotope analysis: the effects of treatment time and acid concentration. *Journal of Archaeological Science*, 31:763–776.

Gehler, A., Tütken, T., and Pack, A. (2012). Oxygen and Carbon Isotope Variations in a Modern Rodent Community-Implications for Palaeoenvironmental Reconstructions. *PloS ONE*, 7(11):e49531.

Gifford-Gonzalez, D. (1989). Overview - Modern Analogues: Developing an Interpretive Framework. In Bonnichsen, R. and Sorg, M. H., editors, *Bone Modification*, pages 43–52. Center for the Study of the First Americans, Orono, Maine.

Gifford-Gonzalez, D. (1991). Bones are not enough: Analogues, knowledge, and interpretive strategies in zooarchaeology. *Journal of Anthropological Archaeology*, 10(3):215–254.

Gilliam, J. F. and Fraser, D. F. (1987). Habitat Selection Under Predation Hazard: Test of a Model with Foraging Minnows. *Ecology*, 68(6):1856–1862.

Gordon, A. D., Nevell, L., and Wood, B. (2008). The *Homo floresiensis* cranium (LB1): Size, scaling, and early *Homo* affinities. *PNAS*, 105(12):4650–4655.

Grayson, D. K. and Delpech, F. (2003). Ungulates and the Middle-to-Upper Paleolithic transition at Grotte XVI (Dordogne, France). *Journal of Archaeological Science*, 30:1633–1648.

Gremillion, K. J. (2002). Foraging theory and hypothesis testing in archaeology: An exploration of methodological problems and solutions. *Journal of Anthropological Archaeology*, 21:142–164.

Gremillion, K. J., Barton, L., and Piperno, D. R. (2014). Particularism and the retreat from theory in the archaeology of agricultural origins. *Proceedings of the National Academy of Sciences*, 111(17):6171–6177.

Griffiths, M. L., Drysdale, R. N., Gagan, M. K., xin Zhao, J., Hellstrom, J. C., Ayliffe, L. K., and Hantoro, W. S. (2013). Abrupt increase in east Indonesian rainfall from flooding of the Sunda Shelf ∼9500years ago. *Quaternary Science Reviews*, 74:273–279.

Griffiths, M. L., Drysdale, R. N., Gagan, M. K., Zhao, J. X., Ayliffe, L. K., Hellstrom, J. C., Hantoro, W. S., Frisia, S., Feng, Y. X., Cartwright, I., Pierre, E. S., Fischer, M. J., and Suwargadi, B. W. (2009). Increasing Australian-Indonesian monsoon rainfall linked to early Holocene sea-level rise. *Nature Geoscience*, 2(9):636–639.

Gurven, M. and Kaplan, H. S. (2007). Longevity among hunter-gatherers: A cross-cultural examination. *Population and Development Review*, 33(2):321–365.

Hardy, B. L., Moncel, M.-H. H., Daujeard, C., Fernandes, P., Béarez, P., Desclaux, E., Chacon Navarro, M. G., Puaud, S., Gallotti, R., Bearez, P., Desclaux, E., Navarro, M. G. C., Puaud, S., and Gallotti, R. (2013). Impossible Neanderthals? Making string, throwing projectiles and catching small game during Marine Isotope Stage 4 (Abri du Maras, France). *Quaternary Science Reviews*, 82:23–40.

Harrison, R. D., Sreekar, R., Brodie, J. F., Brook, S., Luskin, M., O'Kelly, H., Rao, M., Scheffers, B., and Velho, N. (2016). Impacts of hunting on tropical forests in Southeast Asia. *Conservation Biology*, 30(5):972–981.

Harrison, T., Krigbaum, J., and Manser, J. (2006). Primate Biogeography and Ecology on the Sunda Shelf Islands: A Paleontological and Zooarchaeological Perspective. In Lehman, S. and Fleagle, J. G., editors, *Primate Biogeography*, pages 331–372. Springer, New York.

Hawkes, K. and O'Connell, J. F. (1992). On optimal foraging models and subsistence transitions. *Current Anthropology*, 33:63–65.

Hawkes, K., O'connell, J. F., Blurton Jones, N. G., Oftedal, O. T., and Blumenschine, R. J. (1991). Hunting Income Patterns among the Hadza: Big Game, Common Goods, Foraging Goals and the Evolution of the Human Diet [and Discussion]. *Philosophical Transactions: Biological Sciences*, 334(1270):243–251.

Hawks, J., Elliott, M., Schmid, P., Churchill, S. E., De Ruiter, D. J., Roberts, E. M., Hilbert-Wolf, H., Garvin, H. M., Williams, S. A., Delezene, L. K., Feuerriegel, E. M., Randolph-Quinney, P., Kivell, T. L., Laird, M. F., Tawane, G., Desilva, J. M., Bailey, S. E., Brophy, J. K., Meyer, M. R., Skinner, M. M., Tocheri, M. W., Vansickle, C., Walker, C. S., Campbell, T. L., Kuhn, B., Kruger, A., Tucker, S., Gurtov, A., Hlophe, N., Hunter, R., Morris, H., Peixotto, B., Ramalepa, M., Van Rooyen, D., Tsikoane, M., Boshoff, P., Dirks, P. H., and Berger, L. R. (2017).

New fossil remains of *Homo naledi* from the Lesedi Chamber, South Africa. *eLife*, 6:e24232.

Haws, J. A. and Hockett, B. S. (2004). Theoretical perspectives on the dietary role of small animals in human evolution. In Brugal, J.-P. and Desse, J., editors, *Petits Animaux et Societes Humaines. Du complement alimentaire aux ressources utilitaires*, pages 173–184. APDCA, Antibes.

Heaney, L. R. (1978). Island area and body size of insular mammals: Evidence from the tri-colored squirrel (Callosciurus prevosti) of Southeast Asia. *Evolution*, 32:29–44.

Henneberg, M., Eckhardt, R. B., Chavanaves, S., and Hsü, K. J. (2014). Evolved developmental homeostasis disturbed in LB1 from Flores, Indonesia, denotes Down syndrome and not diagnostic traits of the invalid species *Homo floresiensis*. *Proceedings of the National Academy of Sciences*, 111(33):11967–1972.

Henneberg, M. and Thorne, A. (2004). Flores human may be pathological *Homo sapiens*. *Before Farming*, 4:2–4.

Henshilwood, C. S. (1997). Identifying the Collector: Evidence for Human Processing of the Cape Dune Mole-Rat, *Bathyergus suillus*, from Blombos Cave, Southern Cape, South Africa. *Journal of Archaeological Science*, 24:659–662.

Henshilwood, C. S. and Marean, C. W. (2003). The origin of modern human behavior critique of the models and their test implications. *Current Anthropology*, 44(5):627–651.

Hershkovitz, I., Kornreich, L., and Laron, Z. (2007). Comparative skeletal features between *Homo floresiensis* and patients with primary growth hormone insensitivity (Laron syndrome). *American Journal of Physical Anthropology*, 134:198–208.

Hewlett, B. (1991). Demography and childcare in preindustrial societies. *Journal of Anthropological Research*, 47(1):1–37.

Hill, K., Kaplan, H., Hawkes, K., and Hurtado, A. M. (1987). Foraging decisions among Aché hunter-gatherers: New data and implications for optimal foraging models. *Ethology and Sociobiology*, 8:1–36.

Hill, R. A. and Dunbar, R. I. M. (1998). An evaluation of the roles of predation rate and predation risk as selective pressures on primate grouping behavior. *Behaviour*, 135(4):411–430.

Hockett, B. and Haws, J. a. J. A. (2002). Taphonomic and Methodological Perspectives of Leporid Hunting During the Upper Paleolithic of the Western Mediterranean Basin. *Journal of Archaeological Method and Theory*, 9(3):269–302.

Hockett, B. S. (1996). Corroded, Thinned and Polished Bones Created by Golden Eagles (*Aquila chrysaetos*): Taphonomic Implications for Archaeological Interpretations. *Journal of Archaeological Science*, 23:587–591.

Hockett, B. S. and Ferreira Bicho, N. (2000). The Rabbits of Picareiro Cave: Small Mammal Hunting During the Late Upper Palaeolithic in the Portuguese Estremadura. *Journal of Archaeological Science*, 27:715–723.

Hocknull, S. A., Piper, P. J., Van Den Bergh, G. D., Due Awe, R., Morwood, M. J., and Kurniawan, I. (2009). Dragon's paradise lost: Palaeobiogeography, evolution and extinction of the largest-ever terrestrial lizards (Varanidae). *PLoS ONE*, 4(9):e7241.

Hoek Ostende, L. W. V. D., Berch, G. V. D., and Due, R. A. (2006). First fossil insectivores from Flores. *Hellenic Journal of Geosciences*, 41:67–72.

Hoffecker, J. F. (2009). The spread of modern humans in Europe. *Proceedings of the National Academy of Sciences*, 106(38):16040–16045.

Hoffecker, J. F. and Hoffecker, I. T. (2017). Technological complexity and the global dispersal of modern humans. *Evolutionary Anthropology*, 26(6):285–299.

Holliday, T. W. (2012). Body size, body shape, and the circumscription of the genus *Homo*. *Current Anthropology*, 53:S330–S345.

Hopley, P. J., Latham, A. G., and Marshall, J. D. (2006). Palaeoenvironments and palaeodiets of mid-Pliocene micromammals from Makapansgat Limeworks, South Africa: A stable isotope and dental microwear approach. *Palaeogeography, Palaeoclimatology, Palaeoecology*, 233:235–251.

Hublin, J.-J. (2021). How old are the oldest *Homo sapiens* in Far East Asia? *PNAS*, 118(10):e2101173118.

Isbell, L. A. (1994). Predation on primates: Ecological patterns and evolutionary consequences. *Evolutionary Anthropology*, 3(2):61–71.

Itescu, Y., Karraker, N. E., Raia, P., Pritchard, P. C., and Meiri, S. (2014). Is the island rule general? Turtles disagree. *Global Ecology and Biogeography*, 23(6):689–700.

Jacob, T., Indriati, E., Soejono, R. P., Hsü, K., Frayer, D. W., Eckhardt, R. B., Kuperavage, A. J., Thorne, A., and Henneberg, M. (2006). Pygmoid Australomelanesian *Homo sapiens* skeletal remains from Liang Bua, Flores: Population affinities and pathological abnormalities. *Proceedings of the National Academy of Sciences*, 103(36):13421–13426.

Jeffrey, A., Denys, C., Stoetzel, E., and Lee-Thorp, J. A. (2015). Influences on the stable oxygen and carbon isotopes in gerbillid rodent teeth in semi-arid and

arid environments: Implications for past climate and environmental reconstruction. *Earth and Planetary Science Letters*, 428:84–96.

Jim, S., Ambrose, S. H., and Evershed, R. P. (2004). Stable carbon isotopic evidence for differences in the dietary origin of bone cholesterol, collagen and apatite: Implications for their use in palaeodietary reconstruction. *Geochimica et Cosmochimica Acta*, 68(1):61–72.

Jones, E. L. (2006). Prey choice, mass collecting, and the wild European rabbit (*Oryctolagus cuniculus*). *Journal of Anthropological Archaeology*, 25(3):275–289.

Jones, E. L. and Hurley, D. A. (2017). Beyond depression? A review of the optimal foraging theory literature in zooarchaeology and archaeobotany. *Ethnobiology Letters*, 8(1):35–42.

Jones, N. B. (2016). *Demography and evolutionary ecology of Hadza hunter-gatherers*. Cambridge University Press, Cambridge.

Julianto, A. I., Sutikna, T., Jatmiko, Faith, J. T., and Tocheri, M. W. (2020). The temporal distribution of pottery and aquatic shellfish in the Holocene deposits at Liang Bua indicates major shifts in modern human behaviour through time. In *Canadian Association for Physical Anthropology*.

Jungers, W. L., Harcourt-Smith, W. E. H., Wunderlich, R. E., Tocheri, M. W., and Larson, S. G. (2009a). The foot of *Homo floresiensis*. *Nature*, 459:81–84.

Jungers, W. L., Larson, S., Harcourt-Smith, W., Morwood, M. J., Sutikna, T., Awe Due, R., and Djubiantono, T. (2009b). Descriptions of the lower limb skeleton of *Homo floresiensis*. *Journal of Human Evolution*, 57:538–554.

Kaifu, Y., Baba, H., Kurniawan, I., Sutikna, T., Saptomo, E. W., Awe, R. D., Kaneko, T., Aziz, F., and Djubiantono, T. (2009). Brief Communication: "Pathological"

deformation in the skull of LB1, the type specimen of *Homo floresiensis*. *American Journal of Physical Anthropology*, 140:177–185.

Kaifu, Y., Baba, H., Sutikna, T., Morwood, M. J., Kubo, D., Saptomo, E. W., Due, R., and Djubiantono, T. (2011). Craniofacial morphology of *Homo floresiensis*: Description, taxonomic affinities, and evolutionary implication. *Journal of Human Evolution*, 61:644–682.

Kaifu, Y., Kono, R. T., Sutikna, T., Saptomo, E. W., Jatmiko, Awe Due, R., and Baba, H. (2015a). Descriptions of the dental remains of *Homo floresiensis*. *Anthropological Science*, 123(2):129–145.

Kaifu, Y., Kono, R. T., Sutikna, T., Saptomo, E. W., Jatmiko, and Due Awe, R. (2015b). Unique dental morphology of *Homo floresiensis* and its evolutionary implications. *PLoS ONE*, 10(11):e0141614.

Kaplan, H., Hill, K., Lancaster, J., and Hurtado, a. M. (2000). A theory of human life history evolution: diet, intelligence, and longevity. *Evolutionary Anthropology*, 9:156–185.

Kaplan, H. S., Hooper, P. L., and Gurven, M. (2009). The evolutionary and ecological roots of human social organization. *Philosophical Transactions of the Royal Society B*, 364(1533):3289–3299.

Kelly, R. (1995). *The foraging spectrum: Diversity in hunter-gatherer lifeways*. Cambridge University Press.

Klein, R. G. and Cruz-Uribe, K. (1984). *The Analysis of Animal Bones from Archaeological Sites*. The University of Chicago Press.

Koch, P. L., Tuross, N., and Fogel, M. L. (1997). The Effects of Sample Treatment

and Diagenesis on the Isotopic Integrity of Carbonate in Biogenic Hydroxylapatite. *Journal of Archaeological Science*, 24:417–429.

Kohn, M. J., Schoen1nger, M. J., and Valley, J. W. (1996). Herbivore tooth oxygen isotope compositions: Effects of diet and physiology. *Geochimica et Cosmochimica Acta*, 60(20):3889–3896.

Kubo, D., Kono, R. T., and Kaifu, Y. (2013). Brain size of *Homo floresiensis* and its evolutionary implications. *Proceedings of the Royal Society B*, 280:20130338.

Kurland, J. A. and Beckerman, S. J. (1985). Optimal foraging and hominid evolution: Labor and reciprocity. *American Anthropologist*, 87(1):73–93.

Kusmer, K. D. (1990). Taphonomy of Owl Pellet Deposition. *Journal of Paleontology*, 64(4):629–637.

Laland, K., Matthews, B., and Feldman, M. W. (2016). An introduction to niche construction theory. *Evolutionary Ecology*, 30:191–202.

Laland, K., Uller, T., Feldman, M., Sterelny, K., Muller, G. B., Moczek, A., Jablonka, E., and Odling-Smee, J. (2014). Does evolutionary theory need a rethink? *Nature*, 514:161–164.

Laland, K. N. and O'Brien, M. J. (2010). Niche construction theory and archaeology. *Journal of Archaeological Method and Theory*, 17(4):303–322.

Laland, K. N., Odling-Smee, J., and Feldman, M. W. (2000). Niche construction, biological evolution, and cultural change. *Behavioral and Brain Sciences*, 23:131–175.

Laland, K. N., Uller, T., Feldman, M. W., Sterelny, K., Müller, G. B., Moczek, A., Jablonka, E., and Odling-Smee, J. (2015). The extended evolutionary synthesis:

its structure, assumptions and predictions. *Proceedings of the Royal Society B*, 282:20151019.

Landt, M. J. (2004). *Investigations of human gnawing on small mammal bones: Among contemporary Bofi Foragers of the Central African Republic*. Masters thesis, Washington State University.

Landt, M. J. (2007). Tooth marks and human consumption: ethnoarchaeological mastication research among foragers of the Central African Republic. *Journal of Archaeological Science*, 34(10):1629–1640.

Larson, S. G., Jungers, W. L., Morwood, M. J., Sutikna, T., Wahyu Saptomo, E., Awe Due, R., and Djubiantono, T. (2007). *Homo floresiensis* and the evolution of the hominin shoulder. *Journal of Human Evolution*, 53:718–731.

Larson, S. G., Jungers, W. L., Tocheri, M. W., Orr, C. M., Morwood, M. J., Sutikna, T., Awe, R. D., and Djubiantono, T. (2009). Descriptions of the upper limb skeleton of *Homo floresiensis*. *Journal of Human Evolution*, 57:555–570.

Lebreton, L., Moigne, A. M., Filoux, A., and Perrenoud, C. (2017). A specific small game exploitation for Lower Paleolithic: The beaver (*Castor fiber*) exploitation at the Caune de l'Arago (Pyrénées-Orientales, France). *Journal of Archaeological Science: Reports*, 11:53–58.

Lee-Thorp, J. and Sponheimer, M. (2006). Contributions of Biogeochemistry to Understanding Hominin Dietary Ecology. *Yearbook of Physical Anthropology*, 49:131–148.

Lee-Thorp, J. A. and van der Merwe, N. J. (1987). Carbon isotope analysis of fossil bone apatite. *South African Journal of Science*, 83:71–74.

Lee-Thorp, J. A. and van der Merwe, N. J. (1989). Aspects of chemistry of modern and fossil biological apatites. *Journal of Archaeological Science*, 18:343–354.

Lin, S. C., Julianto, A. I., Ferdianto, A., and Sutikna, T. (2020). Stone artefact assemblage composition as a proxy for changing Holocene land use practices at Liang Bua. In *Canadian Association for Physical Anthropology*.

Lloveras, L., Moreno-García, M., and Nadal, J. (2008a). Taphonomic analysis of leporid remains obtained from modern Iberian lynx (*Lynx pardinus*) scats. *Journal of Archaeological Science*, 35(1):1–13.

Lloveras, L., Moreno-Garcia, M., and Nadal, J. (2008b). Taphonomic study of leporid remains accumulated by the Spanish Imperial Eagle (*Aquila adalberti*). *Geobios*, 41(1):91–100.

Lloveras, L., Moreno-García, M., and Nadal, J. (2009). Butchery, Cooking and Human Consumption Marks on Rabbit (*Oryctolagus cuniculus*) Bones: An Experimental Study. *Journal of Taphonomy*, 7(3):179–201.

Lloveras, L., Moreno-García, M., and Nadal, J. (2012a). Assessing the variability in taphonomic studies of modern leporid remains from Eagle Owl (*Bubo bubo*) nest assemblages: the importance of age of prey. *Journal of Archaeological Science*, 39:3754–3764.

Lloveras, L., Moreno-García, M., and Nadal, J. (2012b). Feeding the Foxes: An Experimental Study to Assess Their Taphonomic Signature on Leporid Remains. *International Journal of Osteoarchaeology*, 22(5):577–590.

Lloveras, L., Moreno-García, M., Nadal, J., Maroto, J., Soler, J., and Soler, N. (2010). The application of actualistic studies to assess the taphonomic origin of Mousterian rabbit accumulations from Arbreda Cave (North-East Iberia). *Archaeofauna*, 19:99–119.

Lloveras, L., Moreno-García, M., Nadal, J., and Zilhão, J. (2011). Who brought in the rabbits? Taphonomical analysis of Mousterian and Solutrean leporid accumulations from Gruta do Caldeirão (Tomar, Portugal). *Journal of Archaeological Science*, 38:2434–2449.

Locatelli, E. (2010). *Insular small mammals from Quaternary deposits of Sicily and Flores*. PhD thesis, Universita degli Studi di Ferrara.

Locatelli, E., Awe Due, R., and van den Hoek Ostende, L. W. (2015). Middle-sized murids from Liang Bua (Flores, Indonesia): insular endemics, human introductions and palaeoenvironment. *Palaeobiodiversity and Palaeoenvironments*, 95:497–512.

Locatelli, E., Due, R. A., van den Bergh, G. D., Van den Hoek Ostende, L. W., Due Awe, R., van den Bergh, G. D., van den Ostende Hoek, L. W., Due, R. A., Bergh, G. D. V. D., and Ostende, L. W. V. D. H. (2012). Pleistocene survivors and Holocene extinctions: The giant rats from Liang Bua (Flores, Indonesia). *Quaternary International*, 281:47–57.

Lomolino, M. V. (1985). Body Size of Mammals on Islands: The Island Rule Reexamined. *The American Naturalist*, 125(2):310–316.

Lomolino, M. V. (2005). Body size evolution in insular vertebrates: Generality of the island rule. *Journal of Biogeography*, 32(10):1683–1699.

Lomolino, M. V., Sax, D. F., Riddle, B. R., and Brown, J. H. (2006). The island rule and a research agenda for studying ecogeographical patterns. *Journal of Biogeography*, 33(9):1503–1510.

Lopez, J. M. (2020). Actualistic taphonomy of barn owl pellet-derived small mammal bone accumulations in arid environments of South America. *Journal of Quaternary Science*, 35(8):1057–1069.

López, J. M. and Chiavazza, H. (2020). From owl prey to human food: taphonomy of archaeological small mammal remains from the late Holocene wetlands of arid environments in Central Western Argentina. *Archaeological and Anthropological Sciences*, 12(276):276.

Louchart, A., Wesselman, H., Blumenschine, R. J., Hlusko, L. J., Njau, J. K., Black, M. T., Asnake, M., and White, T. D. (2009). Taphonomic, avian, and small-vertebrate Indicators of *Ardipithecus ramidus* habitat. *Science*, 326(5949):66–66e4.

Louys, J. and Meijaard, E. (2010). Palaeoecology of Southeast Asian megafauna-bearing sites from the Pleistocene and a review of environmental changes in the region. *Journal of Biogeography*, 37:1432–1449.

Lupo, K. D. (2007). Evolutionary foraging models in zooarchaeological analysis: Recent applications and future challenges. *Journal of Archaeological Research*, 15(2):143–189.

Lupo, K. D. and Schmitt, D. N. (2002). Upper Paleolithic Net-Hunting, Small Prey Exploitation, and Women's Work Effort: A View from the Ethnographic and Ethnoarchaeological Record of the Congo Basin. *Journal of Archaeological Method and Theory*, 9(2):147–179.

Lupo, K. D. and Schmitt, D. N. (2005). Small prey hunting technology and zooarchaeological measures of taxonomic diversity and abundance: Ethnoarchaeological evidence from Central African forest foragers. *Journal of Anthropological Archaeology*, 24(4):335–353.

Lyman, L. R. and Lyman, R. L. (2003). The influence of time averaging and space averaging on the application of foraging theory in zooarchaeology. *Journal of Archaeological Science*, 30(5):595–610.

Lyman, R. L. (1994). Quantitative Units and Terminology in Zooarchaeology. *American Antiquity*, 59(1):36–71.

Lyman, R. L. (2008). *Quantitative paleozoology*. Cambridge University Press, Cambridge.

Lyras, G., van der Geer, A., van der Geer, S., and de Vos, J. (2009). The origin of *Homo floresiensis* and its relation to evolutionary processes under isolation. *Anthropological Science*, 117(1):33–43.

Macarthur, R. H. and Pianka, E. R. (1966). On optimal use of a patchy environment. *The American Naturalist*, 100(916):603–609.

Machovsky-Capuska, G. E., Coogan, S. C., Simpson, S. J., and Raubenheimer, D. (2016). Motive for Killing: What Drives Prey Choice in Wild Predators? *Ethology*, 122(9):703–711.

Madison, P. (2020). Investigating *Homo floresiensis* and the myth of the ebu gogo. *Aeon*.

Marean, C. W. (1991). Measuring the Post-depositional Destruction of Bone in Archaeological Assemblages. *Journal of Archaeological Science*, 18:677–694.

Marean, C. W. and Cleghorn, N. (2003). Large mammal skeletal element transport: Applying foraging theory in a complex taphonomic system. *Journal of Taphonomy*, 1(1):15–42.

Marean, C. W. and Spencer, L. M. (1991). Impact of Carnivore Ravaging on Zooarchaeological Measures of Element Abundance. *American Antiquity*, 56(04):645–658.

Marin-Monfort, M. D., García-Morato, S., Olucha, R., Yravedra, J., Pi, A., Neiro, s., Barja, I., Andrews, P., and Fern Andez-Jalvo, Y. (2019). Wildcat scats: Taphon-

omy of the predator and its micromamal prey. *Quaternary Science Reviews*, 225:106024.

Maringer, J. and Verhoeven, T. (1977). Ein paläolithischer Höhlenfundplatz auf der Insel Flores. *Anthropos*, 72:256–273.

Marti, C. D. (1973). Food Consumption and Pellet Formation Rates in Four Owl Species. *The Wilson Bulletin*, 85(2):178–181.

Matsu'ura, S., Kondo, M., Danhara, T., Sakata, S., Iwano, H., Hirata, T., Kurniawan, I., Setiyabudi, E., Takeshita, Y., Hyodo, M., Kitaba, I., Sudo, M., Danhara, Y., and Aziz, F. (2020). Age control of the first appearance datum for Javanese *Homo erectus* in the Sangiran area. *Science*, 367:210–214.

McPherron, S. P., Alemseged, Z., Marean, C. W., Wynn, J. G., Reed, D., Geraads, D., Bobe, R., and Béarat, H. A. (2010). Evidence for stone-tool-assisted consumption of animal tissues before 3.39 million years ago at Dikika, Ethiopia. *Nature*, 466(7308):857–860.

Medina, M. E., Teta, P., Rivero, Y. D., and Rivero, D. (2012). Burning damage and small-mammal human consumption in Quebrada del Real 1 (Cordoba, Argentina): an experimental approach. *Journal of Archaeological Science*, 39(3):737–743.

Meijer, H. J. M. and Due, R. A. (2010). A new species of giant marabou stork (Aves: Ciconiiformes) from the Pleistocene of Liang Bua, Flores (Indonesia). *Zoological Journal of the Linnean Society*, 160:707–724.

Meijer, H. J. M., Ostende, L. W. V. D. H., Bergh, G. D. V. D., and Vos, J. D. (2010). The fellowship of the hobbit: the fauna surrounding *Homo floresiensis*. *Journal of biogeography*, 37:995–1006.

Meijer, H. J. M., Sutikna, T., Wasisto, S., James, H. F., Morwood, M. J., and Tocheri, M. W. (2013). Late Pleistocene-Holocene non-passerine avifauna of Liang Bua (Flores, Indonesia). *Journal of Vertebrate Paleontology*, 33(4):877–894.

Meiri, S. (2007). Size evolution in island lizards. *Global Ecology and Biogeography*, 16(6):702–708.

Meiri, S., Cooper, N., and Purvis, A. (2008). The island rule: made to be broken? *Proceedings of the Royal Society B*, 275:141–148.

Meyer-Rochow, V. B., Megu, K., and Chakravorty, J. (2015). Rats: If you can't beat them eat them! (Tricks of the trade observed among the Adi and other North-East Indian tribals). *Journal of Ethnobiology and Ethnomedicine*, 11(45):1–11.

Mohlenhoff, K. A., Coltrain, J. B., and Codding, B. F. (2015). Optimal foraging theory and niche-construction theory do not stand in opposition. *Proceedings of the National Academy of Sciences*, 112(24):E3093.

Monahan, C. M. (1996). New zooarchaeological data from Bed II, Olduvai Gorge, Tanzania: Implications for hominid behavior in the Early Pleistocene. *Journal of Human Evolution*, 31(2):93–128.

Moore, M., Sutikna, T., Morwood, M., and Brumm, A. (2009). Continuities in stone flaking technology at Liang Bua, Flores, Indonesia. *Journal of Human Evolution*, 57:503–526.

Moore, M. W. and Brumm, A. (2007). Stone artifacts and hominins in island Southeast Asia: New insights from Flores, eastern Indonesia. *Journal of Human Evolution*, 52:85–102.

Moore, M. W. and Brumm, A. (2008). *Homo floresiensis* and the African Oldowan. In

Hovers, E. and Braun, D. R., editors, *Interdisciplinary Approaches to the Oldowan*, pages 61–69. Springer, Dordrecht.

Morin, E., Meier, J., Guennouni, K. E., Moigne, A.-M., Lebreton, L., Rusch, L., Valensi, P., Conolly, J., and Cochard, D. (2019). New evidence of broader diets for archaic *Homo* populations in the northwestern Mediterranean. *Scientific Advances*, 5:eaav9106.

Morley, M. W., Goldberg, P., Sutikna, T., Tocheri, M. W., Prinsloo, L. C., Jatmiko, Saptomo, E. W., Wasisto, S., and Roberts, R. G. (2017). Initial micromorphological results from Liang Bua, Flores (Indonesia): Site formation processes and hominin activities at the type locality of *Homo floresiensis*. *Journal of Archaeological Science*, 77:125–142.

Morwood, M., O'Sullivan, P., Susanto, E. E., and Aziz, F. (2003). Revised age for Mojokerto 1, an early *Homo erectus* cranium from East Java, Indonesia. *Australian Archaeology*, 57:1–4.

Morwood, M. J., Brown, P., Jatmiko, Sutikna, T., Saptomo, E. W., Westaway, K. E., Due, R. A., Roberts, R. G., Maeda, T., Wasisto, S., and Djubiantono, T. (2005). Further evidence for small-bodied hominins from the Late Pleistocene of Flores, Indonesia. *Nature*, 437(7061):1012–1017.

Morwood, M. J. and Jungers, W. L. (2009). Conclusions: implications of the Liang Bua excavations for hominin evolution and biogeography. *Journal of Human Evolution*, 57:640–648.

Morwood, M. J., Soejono, R. P., Roberts, R. G., Sutikna, T., Turney, C. S. M., Westaway, K. E., Rink, W. J., Zhao, J.-x., van den Bergh, G. D., Rokus Awe Due, Hobbs, D. R., Moore, M. W., Bird, M. I., and Fifield, L. K. (2004). Archaeology

and age of a new hominin from Flores in eastern Indonesia. *Nature*, 431(7012):1087–1091.

Morwood, M. J., Sutikna, T., Saptomo, E. W., Hobbs, D. R., Westaway, K. E., Jatmiko, Hobbs, D. R., and Westaway, K. E. (2009). Preface: research at Liang Bua, Flores, Indonesia. *Journal of Human Evolution*, 57(5):437–449.

Morwood, M. J. M., O'Sullivan, P., Aziz, F., and Raza, A. (1998). Fission-track ages of stone tools and fossils on the east Indonesian island of Flores. *Nature*, 392:173–176.

Munizzi, J. (2013). *Changes In Neolithic Subsistence Patterns On Flores, Indonesia Inferred By Stable Carbon, Nitrogen, And Oxygen Isotope Analyses Of Sus From Liang Bua*. Masters thesis, University of Central Florida.

Munro, N. D. (2004). Zooarchaeological Measures of Hunting Pressure and Occupation Intensity in the Natufian: Implications for Agricultural Origins 1. *Current Anthropology*, 45:S5–S33.

Murray, J. K., Benitez, R. A., and O'Brien, M. J. (2020). The extended evolutionary synthesis and human origins: Archaeological perspectives. *Evolutionary Anthropology*, 30(1):4–7.

Musser, G. G. (1981). *The giant rat of Flores and its relative east of Borneo and Bali*, volume 169. Bulletin of the American Museum of Natural History.

Musser, G. G. and Boeadi (1980). A new genus of Murid rodent from the Komodo islands in Nusatenggara, Indonesia. *Journal of Mammalogy*, 61(4):395–413.

Musser, G. G., van de Weerd, A., and Strasser, E. (1986). Paulamys, a Replacement Name for Floresomys Musser, 1981 (Muridae), and New Material of that Taxon from Flores, Indonesia. *American Museum Novitates*, 2850:1–10.

Nel, T. H., Henshilwood, C. S., Daniau, A., Lechevrel, S., Hanquiez, V., and Haberzettl, T. (2016). The Small Mammal Sequence from the c. 76 – 72 ka Still Bay Levels at Blombos Cave, South Africa – Taphonomic and Palaeoecological Implications for Human Behaviour. *PLoS ONE*, 11(8):e0159817.

Nuzzo, R. (2014). Statistical method: statistical errors. *Nature News*, 506:150–152.

Obendorf, P. J., Oxnard, C. E., and Kefford, B. J. (2008). Are the small human-like fossils found on Flores human endemic cretins? *Proceedings of the Royal Society B*, 275:1287–1296.

O'Brien, M. and Liebert, T. A. (2014). Quantifying the energetic returns for pronghorn: a food utility index of meat and marrow. *Journal of Archaeological Science*, 46:384–392.

O'brien, M. J. and Bentley, R. A. (2020). Genes, culture, and the human niche: An overview. *Evolutionary Anthropology*, pages 1–10.

O'Brien, M. J. and Laland, K. N. (2012). Genes, culture, and agriculture an example of human niche construction. *Current Anthropology*, 53(4):434–470.

Odling-Smee, F., Laland, K. N., and Feldman, M. W. (2003). *Niche construction. The neglected process in evolution.* Princeton University Press, Princeton.

Oliveira, S., Pugach, I., Hubner, A., Essel, E., Hajdinjak, M., Jatmiko, Sutikna, T., Wahyu Saptomo, E., Tocheri, M. W., Meyer, M., and Stoneking, M. (2020). Human genetic variation across the Holocene at Liang Bua. In *Canadian Association for Physical Anthropology.*

Orr, C. M., Tocheri, M. W., Burnett, S. E., Due Awe, R., Wahyu Saptomo, E., Sutikna, T., Wasisto, S., Morwood, M. J., Jungers, W. L., Awe, R. D., Saptomo, E. W., Sutikna, T., Jatmiko, Wasisto, S., Morwood, M. J., and Jungers, W. L.

(2013). New wrist bones of *Homo floresiensis* from Liang Bua (Flores, Indonesia). *Journal of Human Evolution*, 64(2):109–129.

Ouwendijk, E. M., Due, R. A., Locatelli, E., Jatmiko, Ostende, L. W. D. H., and van den Hoek Ostende, L. W. (2014). Bat cave and hobbit hole, microbats of Liang Bua (Flores, Indonesia). *Alcheringa*, 38(3):422–433.

Pante, M. C. (2013). The larger mammal fossil assemblage from JK2, Bed III, Olduvai Gorge, Tanzania: implications for the feeding behavior of Homo erectus. *Journal of Human Evolution*, 64(1):68–82.

Pavao, B. and Stahl, P. W. (1999). Structural Density Assays of Leporid Skeletal Elements with Implications for Taphonomic, Actualistic and Archaeological Research. *Journal of Archaeological Science*, 26:53–66.

Pearce, E., Stringer, C., and Dunbar, R. I. M. (2013). New insights into differences in brain organization between Neanderthals and anatomically modern humans. *Proceedings of the Royal Society B*, 280:20130168.

Pickering, T. R. and Carlson, K. J. (2004). Baboon taphonomy and its relevance to the investigation of large felid involvement in human forensic cases. *Forensic science international*, 144(1):37–44.

Piper, P. J., Rabett, R. J., and Kurui, E. B. (2008). Using community, composition and structural variation in terminal Pleistocene vertebrate assemblages to identify human hunting behavior at the Niah Caves, Borneo. *Indo-Pacific Prehistory Association Bulletin*, 28:88–98.

Pobiner, B. L. (2020). The zooarchaeology and paleoecology of early hominin scavenging. *Evolutionary Anthropology*, 29(2):68–82.

Pobiner, B. L., Desilva, J., Sanders, W. J., and Mitani, J. C. (2007). Taphonomic analysis of skeletal remains from chimpanzee hunts at Ngogo, Kibale National Park, Uganda. *Journal of Human Evolution*, 52:614–636.

Pobiner, B. L., Rogers, M. J., Monahan, C. M., and Harris, J. W. K. (2008). New evidence for hominin carcass processing strategies at 1.5 Ma, Koobi Fora, Kenya. *Journal of Human Evolution*, 55(1):103–130.

Potts, R. B. and Shipman, P. (1981). Cutmarks made by stone tools on bones from Olduvai Gorge, Tanzania. *Nature*, 291(5816):577–580.

Purvis, A., Webster, A., Agapow, P., Jones, K., and Isaac, N. (2003). Primate life histories and phylogeny. In *Primate Life Histories and Socioecology*, pages 25–40. University of Chicago Press, Chicago.

Pyke, G. H. (1984). Optimal foraging theory: a critical review. *Annual Review of Ecology, Evolution and Systematic*, 15(1984):523–575.

Raia, P. and Meiri, S. (2006). The island rule in large mammals: Paleontology meets ecology. *Evolution*, 60(8):1731–1742.

Rayne, T., Domínguez-Rodrigo, M., Heaton, J. L., Yravedra, J., Barba, R., Bunn, H. T., Musiba, C., Baquedano, E., Diez-Martín, F., Mabulla, A., Brain, C. K., Pickering, T. R., Domínguez-Rodrigo, M., Heaton, J. L., Yravedra, J., Barba, R., Bunn, H. T., Musiba, C., Baquedano, E., Diez-Martín, F., Mabulla, A., and Brain, C. K. (2013). Taphonomy of ungulate ribs and the consumption of meat and bone by 1.2-million-year-old hominins at Olduvai Gorge, Tanzania. *Journal of Archaeological Science*, 40(2):1295–1309.

Real, C. (2020). Rabbit: More than the Magdalenian main dish in the Iberian Mediterranean region. New data from Cova de les Cendres (Alicante, Spain). *Journal of Archaeological Science: Reports*, 32:102388.

Reed, D. N. (2003). *Micromammal Paleoecology: Past and present relationships between African small mammals and their habitats*. PhD thesis, Stony Brook University.

Rhodes, S. E., Walker, M. J., López-Jiménez, A., López-Martínez, M., Haber-Uriarte, M., Fernandez-Jalvo, Y., and Chazan, M. (2016). Fire in the Early Palaeolithic: Evidence from burnt small mammal bones at Cueva Negra del Estrecho del Río Quípar, Murcia, Spain. *Journal of Archaeological Science: Reports*, 9:427–436.

Riede, F. (2019). Niche construction theory and human biocultural evolution. In Prentiss, A. M., editor, *Handbook of Evolutionary Research in Archaeology*, pages 337–358. Springer Nature Switzerland, Cham.

Rizal, Y., Westaway, K. E., Zaim, Y., van den Bergh, G. D., Arthur Bettis III, E., Morwood, M. J., Frank Huffman, O., Grün, R., Joannes-Boyau, R., Bailey, R. M., Westaway, M. C., Kurniawan, I., Moore, M. W., Storey, M., Aziz, F., Zhao, J.-x., Sipola, M. E., Larick, R., Zonneveld, J.-P., Scott, R., Putt, S., and Ciochon, R. L. (2020). Last appearance of *Homo erectus* at Ngandong, Java, 117,000-108,000 years ago. *Nature*, 577:381–385.

Roberts, P., Perera, N., Wedage, O., Deraniyagala, S., Perera, J., Eregama, S., Gledhill, A., Petraglia, M. D., and Lee-Thorp, J. A. (2015a). Direct evidnce for human reliance on rainforest resources in late Pleistocene Sri Lanka. *Science*, 347(6227):1246–1250.

Roberts, P., Perera, N., Wedage, O., Deraniyagala, S., Perera, J., Eregama, S., Petraglia, M. D., and Lee-Thorp, J. A. (2017). Fruits of the forest: Human stable isotope ecology and rainforest adaptations in Late Pleistocene and Holocene (36 to 3 ka) Sri Lanka. *Journal of Human Evolution*, 106:102–118.

Roberts, P., Perera, N., Wedge, O., Deraniyagala, S., Perera, J., Eregama, S., Gled-

hill, A., Petraglia, M. D., and Lee-Thorp, J. A. (2015b). Direct evidence for human reliance on rainforest resources in late Pleistocene Sri Lanka. *Science*, 347(6227):1246–1249.

Roberts, P. and Petraglia, M. (2015). Pleistocene rainforests: barriers or attractive environments for early human foragers? *World Archaeology*, 47(5):718–739.

Roberts, P. and Stewart, B. A. (2018). Defining the 'generalist specialist' niche for Pleistocene *Homo sapiens*. *Nature Human Behavior*, 2:542–550.

Roberts, R. G., Westaway, K. E., Zhao, J.-X., Turney, C. S. M., Bird, M. I., Rink, W. J., and Fifield, L. K. (2009). Geochronology of cave deposits at Liang Bua and of adjacent river terraces in the Wae Racang valley, western Flores, Indonesia: a synthesis of age estimates for the type locality of *Homo floresiensis*. *Journal of Human Evolution*, 57:484–502.

Romero, A. J., Carlos Díez, J., Rodríguez, L., and Arceredillo, D. (2015). Anthropic fractures and human tooth marks: An experimental approach to non-technological human action on avian long bones. *Quaternary International*, 421:219–227.

Rosado-Méndez, N. Y., Lloveras, L., García-Argüelles, P., and Nadal, J. (2019). The role of small prey in hunter-gatherer subsistence strategies from the Late Pleistocene-Early Holocene transition site in NE Iberia: the leporid accumulation from the Epipalaeolithic level of Balma del Gai site. *Archaeological and Anthropological Sciences*, 11:2507–2525.

Sathe, V. (2017). Smaller but not Secondary: Evidence of Rodents in Archaeological Context in India. *Ancient Asia*, 8(6):1–20.

Sayers, K., Raghanti, M. A., and Lovejoy, C. O. (2012). Human Evolution and the Chimpanzee Referential Doctrine. *Annu. Rev. Anthropol*, 41:119–38.

Schmitt, D. N. and Lupo, K. D. (2008). Do faunal remains reflect socioeconomic status? An ethnoarchaeological study among Central African farmers in the northern Congo Basin. *Journal of Anthropological Archaeology*, 27:315–325.

Scroxton, N. (2014). *Late Pleistocene Climate and Environment from Speleothems on Flores, Indonesia: Vegetation, Volcanoes and Homo floresiensis*. Phd thesis, Australian National University.

Serra, A. S. and Peris, J. F. (2008). Anthropic processing and consumption of rabbit at the Bolomor Cave (Tavernes de la Valldigna, Valencia). The XVIIc level (ca 350 ka). *Complutum*, 19(1):25–46.

Shen, G., Gao, X., Gao, B., and Granger, D. E. (2009). Age of Zhoukoudian *Homo erectus* determined with 26Al/10Be burial dating. *Nature*, 458(7235):198–200.

Shennan, S. (2004). An evolutionary perspective on agency in archaeology. In Gardner, A., editor, *Agency Uncovered: Archaeological perspectives on social agency, power, and being human*, pages 19–32. UCL Press, London.

Shipman, P. (1981). Applications of scanning electron microscopy to taphonomic problems. *Annals of the New York Academy of Sciences*, 376:357–385.

Shipman, P. (1983). Early Hominid Lifestyle: Hunting and Gathering or Foraging and Scavenging? In Clutton-Brock, J. and Grigson, C., editors, *Animals and Archaeology, Volume 1*, pages 31–49. British Archaeological Reports International Series 163.

Shipman, P. (1986). Scavenging or Hunting in Early Hominids: Theoretical Framework and Tests. *American Anthropologist*, 88(1):27–43.

Shipman, P., Foster, G., and Schoeninger, M. (1984). Burnt Bones and Teeth: an Ex-

perimental Study of Color, Morphology, Crystal Structure and Shrinkage. *Journal of Archaeological Science*, 11:307–325.

Smith, E. A., Bettinger, R. L., Bishop, C. A., Blundell, V., Cashdan, E., Casimir, M. J., Christenson, A. L., Cox, B., Dyson-Hudson, R., Hayden, B., Richerson, P. J., Abella Roth, E., Simms, S. R., Stini, W. A., Roth, E. A., Simms, S. R., Stini, W. A., Abella Roth, E., Simms, S. R., and Stini, W. A. (1983). Anthropological applications of optimal foraging theory: A critical review. *Current Anthropology*, 24(5):625–651.

Sondaar, P. Y. (1977). Insularity and Its Effect on Mammal Evolution. In Hecht, M., Goody, P., and Hecht, B., editors, *Major Patterns in Vertebrate Evolution. NATO Advanced Study Institutes Series (Series A: Life Sciences)*, volume 14, pages 671–707. Springer, Boston.

Speth, J. D. (2010). Big-Game Hunting in Human Evolution: The Traditional View. In *The Paleoanthropology and Archaeology of Big-Game Hunting*, chapter 3, pages 39–44. Springer New York, New York, NY.

Speth, J. D. and Spielmann, K. A. (1983). Energy Source, Protein Metabolism, and Hunter-Gatherer Subsistence Strategies. *Journal of Anthropological Archaeology*, 2:1–31.

Stanford, C. B. (1996). The hunting ecology of wild chimpanzees: Implications for the evolutionary ecology of Pliocene hominids. *American Anthropologist*, 98(1):96.

Stanford, C. B. (2002). Avoiding Predators: Expectations and evidence in primate antipredator behavior. *International Journal of Primatology*, 23(4):741–757.

Stanford, C. B. (2012). Chimpanzees and the Behavior of *Ardipithecus ramidus*. *Annual Review of Anthropology*, 41:139–149.

Stephens, D. W. and Krebs, J. R. (1986). *Foraging Theory*. Princeton University Press, Princeton.

Stiner, M., Munro, N., and Surovell, T. (2000). The tortoise and the hare: Small-Game Use, the Broad-Spectrum Revolution, and Paleolithic Demography. *Current Anthropology*, 41(1):39–79.

Stiner, M. C. (2001). Thirty years on the "Broad Spectrum Revolution" and paleolithic demography. *Proceedings of the National Academy of Sciences*, 98(13):6993–6996.

Stiner, M. C. (2002). On in situ Attrition and Vertebrate Body Part Profiles. *Journal of Archaeological Science*, 29(9):979–991.

Stiner, M. C. (2009). Prey choice, site occupation intensity economic diversity in the Middle-early Upper Paleolithic at the Üçağızlı Caves, Turkey. *Before Farming*, 3:1–20.

Stiner, M. C. (2013). An Unshakable Middle Paleolithic? Trends versus Conservatism in the Predatory Niche and Their Social Ramifications. *Current Anthropology*, 54(8):S288–S304.

Stiner, M. C., Barkai, R., and Gopher, A. (2009). Cooperative hunting and meat sharing 400-200 kya at Qesem Cave, Israel. *Proceedings of the National Academy of Sciences*, 106(32):13207–13212.

Stiner, M. C. and Kuhn, S. L. (2016). Are we missing the "sweet spot" between optimality theory and niche construction theory in archaeology? *Journal of Anthropological Archaeology*, 44:177–184.

Stiner, M. C., Kuhn, S. L., Surovell, T. a., Goldberg, P., Meignen, L., Weiner, S., and

Bar-Yosef, O. (2001). Bone Preservation in Hayonim Cave (Israel): a Macroscopic and Mineralogical Study. *Journal of Archaeological Science*, 28(6):643–659.

Stiner, M. C., Kuhn, S. L., Weiner, S., and Bar-Yosef, O. (1995). Differential Burning, Recrystallization, and Fragmentation of Archaeological Bone. *Journal of Archaeological Science*, 22(2):223–237.

Stiner, M. C., Munro, N. D., Surovell, T. A., Tchernov, E., and Bar-Yosef, O. (1999). Paleolithic population growth pulses evidenced by small animal exploitation. *Science*, 283:190–194.

Stoetzel, E., Marion, L., Nespoulet, R., Abdeljalil, M., Hajraoui, E., and Denys, C. (2011). Taphonomy and palaeoecology of the late Pleistocene to middle Holocene small mammal succession of El Harhoura 2 cave (Rabat-Témara, Morocco). *Journal of Human Evolution*, 60:1–33.

Stringer, C. B. (2014). Human evolution: Small remains still pose big problems. *Nature*, 514:427–429.

Sutikna, T. (2016). *New archaeological research at Liang Bua on the Island of Flores: Implications for the extinction of Homo floresiensis and the arrival of Homo sapiens in Eastern Indonesia*. Phd thesis, University of Wollongong.

Sutikna, T., Faith, J. T., Jatmiko, Saptomo, W. E., and Tocheri, M. W. (2020). Faunal change through the Holocene at Liang Bua: Endemic versus Introduced Mammals. In *Canadian Association for Physical Anthropology*.

Sutikna, T., Tocheri, M. W., Faith, J. T., Jatmiko, Due Awe, R., Meijer, H. J., Wahyu Saptomo, E., and Roberts, R. G. (2018). The spatio-temporal distribution of archaeological and faunal finds at Liang Bua (Flores, Indonesia) in light of the revised chronology for *Homo floresiensis*. *Journal of Human Evolution*, 124:52–74.

Sutikna, T., Tocheri, M. W., Morwood, M. J., Saptomo, W. E., Jatmiko, Awe, R. D., Wasisto, S., Westaway, K. E., Aubert, M., Li, B., Zhao, J.-x., Storey, M., Alloway, B. V., Morley, M. W., Meijer, H. J. M., van den Bergh, G. D., Grun, R., Dosseto, A., Brumm, A., Jungers, W. L., and Roberts, R. G. (2016). Revised stratigraphy and chronology for *Homo floresiensis* at Liang Bua in Indonesia. *Nature*, 532(7599):366–369.

Suwannarong, K. and Chapman, R. S. (2014). Rodent consumption in Khon Kaen Province, Thailand. *Southeast Asian Journal of Tropical Medicine and Public Health*, 45(5):1209–1220.

Suwannarong, K., Chapman, R. S., Lantican, C., Michaelides, T., and Zimicki, S. (2015). Hunting, Food Preparation, and Consumption of Rodents in Lao PDR. *PLoS ONE*, 10(7):e0133150.

Teixeira, J. C., Jacobs, G. S., Stringer, C., Tuke, J., Hudjashov, G., Purnomo, G. A., Sudoyo, H., Cox, M. P., Tobler, R., Turney, C. S. M., Cooper, A., and Helgen, K. M. (2021). Widespread Denisovan ancestry in Island Southeast Asia but no evidence of substantial super-archaic hominin admixture. *Nature Ecology Evolution*, 5(5):616–624.

Thompson, J. C. (2005). The impact of post-depositional processes on bone surface modification frequencies: A corrective strategy and its application to the Loiyangalani site, Serengeti Plain, Tanzania. *Journal of Taphonomy*, 3(2):57–80.

Thompson, J. C., Carvalho, S., Marean, C. W., and Alemseged, Z. (2019). Origins of the Human Predatory Pattern The Transition to Large-Animal Exploitation by Early Hominins. *Current Anthropology*, 60(1):1–23.

Thompson, J. C., Mcpherron, S. P., Bobe, R., Reed, D., Barr, W. A., Wynn, J. G., Marean, C. W., Geraads, D., Alemseged, Z., Bobe, R., Reed, D., Barr, A. W.,

Wynn, J. G., Marean, C. W., Geraads, D., and Alemseged, Z. (2015). Taphonomy of fossils from the hominin-bearing deposits at Dikika, Ethiopia. *Journal of Human Evolution*, 86:112–135.

Thomson, V., Aplin, K. P., Cooper, A., Hisheh, S., Suzuki, H., Maryanto, I., Yap, G., and Donnellan, S. C. (2014). Molecular genetic evidence for the place of origin of the pacific rat, rattus exulans. *PLoS ONE*, 9(3):e91356.

Tocheri, M. W. (2019). Unknown human species found in Asia. *Nature*, 568(7751):176–178.

Tocheri, M. W., Orr, C. M., Larson, S. G., Sutikna, T., Jatmiko, Saptomo, E. W., Awe Due, R., Djubiantono, T., Morwood, M. J., and Jungers, W. L. (2007). The primitive wrist of *Homo floresiensis* and its implications for hominin evolution. *Science*, 317:1743–1745.

Tortosa, J. E. A., Bonilla, V. V., Ripoll, M. P., Valle, R. M., and Guillem Calatayud, P. (2002). Big Game and Small Prey: Paleolithic and Epipaleolithic Economy From Valencia (Spain). *Journal of Archaeological Method and Theory*, 9(3):215–268.

Tucci, S., Vohr, S. H., Mccoy, R. C., Vernot, B., Robinson, M. R., Barbieri, C., Nelson, B. J., Fu, W., Purnomo, G. A., Sudoyo, H., Eichler, E. E., Barbujani, G., Visscher, P. M., Akey, J. M., and Green, R. E. (2018). Evolutionary history and adaptation of a human pygmy population of Flores Island, Indonesia. *Science*, 361:511–516.

Ugan, A. (2005). Does Size Matter? Body Size, Mass Collecting, and Their Implications for Understanding Prehistoric Foraging Behavior. *American Antiquity*, 70(1):75–89.

van den Bergh, G., Awe, R. D., Morwood, M. J., Sutikna, T., Jatmiko, and Wahyu Saptomo, E. (2008). The youngest *Stegodon* remains in Southeast Asia from the

Late Pleistocene archaeological site Liang Bua, Flores, Indonesia. *Quaternary International*, 182(1):16–48.

van den Bergh, G. D., Kaifu, Y., Kurniawan, I., Kono, R. T., Brumm, A., Setiyabudi, E., Aziz, F., Morwood, M. J., Bergh, G. D. V. D., Kaifu, Y., Kurniawan, I., Kono, R. T., Brumm, A., Setiyabudi, E., Aziz, F., and Morwood, M. J. (2016a). *Homo floresiensis*-like fossils from the early Middle Pleistocene of Flores. *Nature*, 534(7606):245–248.

van den Bergh, G. D., Li, B., Brumm, A., Grün, R., Yurnaldi, D., Mark, W., Kurniawan, I., Setiawan, R., Aziz, F., Roberts, R. G., Storey, M., Setiabudi, E., and Morwood, M. J. (2016b). Earliest hominin occupation of Sulawesi, Indonesia. *Nature*, 529:208–211.

van den Bergh, G. D., Meijer, H. J., Due Awe, R., Morwood, M. J., Szabó, K., van den Hoek Ostende, L., Sutikna, T., Saptomo, E. W., Piper, P. J., and Dobney, K. M. (2009). The Liang Bua faunal remains: a 95 k.yr. sequence from Flores, East Indonesia. *Journal of Human Evolution*, 57(5):527–537.

van den Bergh, G. D., Mubroto, B., Aziz, F., Sondaar, P. Y., and de Vos, J. (1996). Did *Homo erectus* reach the island of Flores? *Indo-Pacific Prehistory Association Bulletin*, 1(14):27–36.

van der Geer, A. A. (2020). Size matters: Micro-evolution in Polynesian rats highlights body size changes as initial stage in evolution. *PeerJ*, 8:e9076.

van der Geer, A. A., van den Bergh, G. D., Lyras, G. A., Prasetyo, U. W., Due, R. A., Setiyabudi, E., and Drinia, H. (2016). The effect of area and isolation on insular dwarf proboscideans. *Journal of Biogeography*, 43(8):1656–1666.

Van Heteren, A. H. (2013). Is LB1 diseased or modern? A review of the proposed pathologies. *Gene*, 528:12–20.

Van Valen, L. (1973). Body size and numbers of plants and animals. *Evolution*, 27:27–35.

Vanitha, V. and Kanakasabai, R. (2009). Prey selection by the Barn Owl *Tyto alba* (Scopoli, 1769) in captivity. *Journal of Threatened Taxa*, 1(7):361–365.

VanPool, T. and VanPool, C. (2003). Agency and evolution: The role of intended and unintended consequences of action. In VanPool, T. and VanPool, C., editors, *Essential tensions in archaeological Methods and Theory*, pages 89–114. University of Utah Press, Salt Lake City.

Veatch, E. G. (2014). *A morphological analysis of the humerus and calcaneus of Endemic Rats from Liang Bua, Flores, Indonesia*. Masters thesis, George Washington University.

Veatch, E. G., Tocheri, M. W., Sutikna, T., McGrath, K., Wahyu Saptomo, E., Jatmiko, and Helgen, K. M. (2019). Temporal shifts in the distribution of murine rodent body size classes at Liang Bua (Flores, Indonesia) reveal new insights into the paleoecology of *Homo floresiensis* and associated fauna. *Journal of Human Evolution*, 130:45–60.

Verdolin, J. L. (2006). Meta-analysis of foraging and predation risk trade-offs in terrestrial systems. *Behavioral Ecology and Sociobiology*, 60:457–464.

Villa, P. and Mahieu, E. (1991). Breakage pattern of human long bones. *Journal of Human Evolution*, 21(1):27–48.

Voris, H. K. and Museum, F. (2000). Maps of Pleistocene sea levels in Southeast Asia: shorelines, river systems and time durations. *Journal of Biogeography*, 27:1153–1167.

Wadley, L. (2010). Were snares and traps used in the Middle Stone Age and does it matter? A review and a case study from Sibudu, South Africa. *Journal of Human Evolution*, 58:179–192.

Welch, J. J. (2009). Testing the island rule: primates as a case study. *Proceedings of the Royal Society B*, 276:675–682.

West, J. A. and Louys, J. (2007). Differentiating bamboo from stone tool cut marks in the zooarchaeological record, with a discussion on the use of bamboo knives. *Journal of Archaeological Science*, 34:512–518.

Westaway, K., Sutikna, T., Saptomo, W., Morwood, M., Roberts, R., and Hobbs, D. (2009a). Reconstructing the geomorphic history of Liang Bua, Flores, Indonesia: a stratigraphic interpretation of the occupational environment. *Journal of Human Evolution*, 57:465–483.

Westaway, K. E., Louys, J., Due Awe, R., Morwood, M. J., Price, J., Zhao, J.-x., Aubert, M., Joannes-Boyau, R., Smith, T. M., Skinner, M. M., Compton, T., Bailey, R. M., van den Bergh, D., de Vos, J., Pike, A. W., Stringer, C., Saptomo, E. W., Rizal, Y., Zaim, J., Santoso, W. D., Trihascaryo, A., Kinsley, L., and Sulistyanto, B. (2017). An early modern human presence in Sumatra 73,000-63,000 years ago. *Nature*, 548:322–325.

Westaway, K. E., Morwood, M. J., Roberts, R. G., Zhao, J.-X., Sutikna, T., Saptomo, E. W., and Rink, W. J. (2007a). Establishing the time of initial human occupation of Liang Bua, western Flores, Indonesia. *Quaternary Geochronology*, 2:337–343.

Westaway, K. E., Morwood, M. J., Sutikna, T., Moore, M. W., Rokus, A. D., Van Den Bergh, G. D., Roberts, R. G., and Saptomo, E. W. (2009b). *Homo floresiensis* and the late Pleistocene environments of eastern Indonesia: defining the nature of the relationship. *Quaternary Science Reviews*, 28:2897–2912.

Westaway, K. E., Roberts, R. G., Sutikna, T., Morwood, M. J., Drysdale, R., Zhao, J.-X., and Chivas, A. R. (2009c). The evolving landscape and climate of western Flores: an environmental context for the archaeological site of Liang Bua. *Journal of Human Evolution*, 57:450–464.

Westaway, K. E., Zhao, J.-x., Roberts, R. G., Chivas, A. R., Morwood, M. J., and Sutikna, T. (2007b). Initial speleothem results from western Flores and eastern Java, Indonesia: were climate changes from 47 to 5 ka responsible for the extinction of *Homo floresiensis*? *Journal of Quaternary Science*, 22:429–438.

Wiessner, P. W. (2014). Embers of society: Firelight talk among the Ju/'hoansi Bushmen. *Proceedings of the National Academy of Sciences*, 111(39):14027–14035.

Williams, J. P. (2001). *Small mammal deposits in archaeology: a taphonomic investigation of Tyto alba (barn owl) nesting and roosting sites*. PhD thesis, University of Sheffield.

Winterhalder, B. and Kennett, D. J. (2006). Behavioral Ecology and the Transition from Hunting and Gathering to Agriculture. In Kennett, D. J. and Winterhalder, B., editors, *HBE and the Transition to Agriculture*, pages 1–21. University of California Press, Berkeley.

Winterhalder, B. and Smith, E. A. (2000). Analyzing adaptive strategies: Human behavioral ecology at twenty-five. *Evolutionary Anthropology*, 9(2):51–72.

Wrangham, R. W. (2009). *Catching fire: how cooking made us human*. Basic Books, New York.

Wynn, T. and Coolidge, F. (2008). Why Not Cognition? *Current Anthropology*, 49(5):895–897.

Yeakel, J. D., Bennett, N. C., Koch, P. L., and Dominy, N. J. (2007). The isotopic ecology of African mole rats informs hypotheses on the evolution of human diet. *Proceedings of the Royal Society B*, 274:1723–1730.

Yellen, J. E. (1991a). Small mammals: !Kung San utilization and the production of faunal assemblages. *Journal of Anthropological Archaeology*, 10:1–26.

Yellen, J. E. (1991b). Small Mammals: Post-discard Patterning of !Kung San Fauna Remains. *Journal of Anthropological Archaeology*, 10:152–192.

Yoder, C. J. and Bartelink, E. J. (2010). Effects of different sample preparation methods on stable carbon and oxygen isotope values of bone apatite: A comparison of two treatment protocols. *Archaeometry*, 52(1):115–130.

Zeder, M. A. (2012). The broad spectrum revolution at 40: Resource diversity, intensification, and an alternative to optimal foraging explanations. *Journal of Anthropological Archaeology*, 31(3):241–264.

Zeder, M. A. (2015). Reply to Mohlenhoff et al.: Human behavioral ecology needs a rethink that niche-construction theory can provide. *Proceedings of the National Academy of Sciences*, 112(24):E3094.